Immunological and Electrophysiological Studies of Rat Bone Marrow-Derived Mast Cells

By

Peter Barrie Hill BVSc. MRCVS

A thesis submitted for the degree of
Doctor of Philosophy
in the
Faculty of Veterinary Medicine,
UNIVERSITY OF EDINBURGH

Departments of Preclinical Veterinary Sciences and
Veterinary Clinical Studies,
Royal (Dick) School of Veterinary Studies,
University of Edinburgh

September, 1996

DECLARATION

This thesis has been composed by myself and the work contained herein is my own.

Peter B. Hill BVSc MRCVS

ACKNOWLEDGEMENTS

I am indebted to my joint supervisors, Professor Hugh Miller and Dr. Richard Martin, for their continuous support, advice, encouragement and humour during the course of these studies. Their enthusiasm and depth of knowledge in their respective fields of mast cell biology and electrophysiology have been an inspiration to me.
I would like to thank Dr. Angus MacDonald for his instruction in tissue culture techniques and guidance on setting up the bone marrow cultures. I am particularly grateful to Liz Thornton, Lorraine MacMillan and Jean Vaagenes for their continuous help in feeding the cultures and for general laboratory advice. Thanks also to Dr. Mike Shipston for teaching me the perforated-patch technique.
A special thanks goes to Dr. Cheryl Scudamore for her multi-functional role as advice-giver, computer instructor, worm breeding coordinator, reagent donator, critic and friend, despite having lots of better things to do.
George Newlands kindly provided a number of reagents for the assays in this thesis, and Andrew Sanderson operated the FACscan machine. Bob Munro provided excellent photographic services and Colin Warwick assisted greatly in the preparation of figures and photographic illustrations. Thanks also to Alan Robertson for many fruitful discussions during the course of these studies, and to Dr. Steve Galli for critically reading the Immunology manuscript.
Finally, during the long spells of "patch-clamp-induced depression," it was the smiling faces of Rigsby (RIP) and his successor, Mr. Fish, that kept the show on the road.

This work was funded by the Wellcome Trust

CONTENTS

LIST OF ABBREVIATIONS

α-IgE	goat anti rat IgE
β-hex	β-hexosaminidase
BMMC(s)	bone marrow-derived mast cell(s)
BSA	bovine serum albumin
CTMC	connective tissue mast cell
CRAC	calcium release activated calcium current
DAG	diacylglycerol
DIDS	4,4'-diisothiocyano-2,2'-stilbenedisulfonate
DNP	dinitrophenyl
ELISA	enzyme-linked immunosorbent assay
ELISPOT	enzyme-linked immunospot
FACS	fluorescent-activated cell sorter
FcεRI	high affinity receptor for IgE
FCS	foetal calf serum
FITC	fluorescein isothiocyanate
HBSS	Hank's balanced salt solution
IFN	interferon
Ig	immunoglobulin
IL	interleukin
IMDM	Iscove's modified Dulbecco's medium
IP_3	inositol 1,4,5-trisphosphate
I/V	current/voltage
IR_K	inwardly rectifying potassium current
kDa	kilodaltons
LNCM	lymph node conditioned medium
LT	leukotriene
MMC	mucosal mast cell
MMCP	mouse mast cell protease

MW	molecular weight
NGF	nerve growth factor
NGS	normal goat serum
O.D.	optical density
OR_{Cl}	outwardly rectifying chloride current
PBS	phosphate buffered saline
PLC	phospholipase-C
PKC	protein kinase C
PG	prostaglandin
P/S	penicillin/streptomycin
RBL	rat basophilic leukaemia
RMCP-I	rat mast cell protease-I
RMCP-II	rat mast cell protease-II
RPMC	rat peritoneal mast cell
RT	room temperature
rhSCF	recombinant human stem cell factor
rrSCF	recombinant rat stem cell factor
SCF	stem cell factor
s.d.	standard deviation
s.e.m.	standard error of the mean
TB	Tyrode's buffer
TB^+	Tyrode's buffer + 1 mM Ca^{2+}/1mM Mg^{2+}
TTL	transistor transistor logic
WCR	whole-cell recording

ELECTROPHYSIOLOGICAL TERMS AND UNITS

Current (I) - Amperes (A)

1 mA	1×10^{-3} Amps
1 μA	1×10^{-6} Amps
1 nA	1×10^{-9} Amps
1 pA	1×10^{-12} Amps

Voltage(V) - Volts (V)

1 mV	1×10^{-3} Volts

Resistance (R) - Ohms (Ω)

1 kΩ	1×10^{3} Ohms
1 MΩ	1×10^{6} Ohms
1 GΩ	1×10^{9} Ohms

Conductance (G) - Siemens (S)

1 nS	1×10^{-9} Siemens
1 pS	1×10^{-12} Siemens
1 fS	1×10^{-15} Siemens

Capacitance (C) - Farads (F)

1 pF	1×10^{-12} Farads

Ohm's Law

$V = IxR$ ($1V = 1A \times 1\Omega$)

Relationship between resistance and conductance

$R = 1/G$ ($1\Omega = 1/S$)

The Nernst Equation

Relates the equilibrium potential to the concentration and valence of a particular ion e.g. for potassium ions, $E_K = RT/zF \ln [K]_o/[K]_i$ or $2.303 \times RT/zF \log_{10} [K]_o/[K]_i$ where E = the equilibrium (reversal) potential

R = gas constant

T = absolute temperature

z = valence of ion

$[K]_o$ = concentration of potassium ions outside (extracellular)

$[K]_i$ = concentration of potassium ions inside (intracellular)

RT/F = 25.26 at 20°C, 26.12 at 30°C and 26.73 at 37°C

N.B. For anions such as Cl^- ions, the intracellular concentration is divided by the extracellular concentration.

Current Notations

In this thesis, the standard current notation is adopted i.e. outward currents are displayed upwards and inward currents are displayed downwards. Note that an outward current can be caused by movement of *positive* ions out of the cell, or *negative* ions into the cell.

ABSTRACT

Based on biochemical and functional characteristics, mast cells are broadly classified into mucosal and connective tissue phenotypes. Both types may be effector cells in the pathogenesis of allergic diseases, but intestinal mucosal mast cells (MMCs) are also involved in the immune response against intestinal nematodes. Rat bone marrow-derived mast cells (BMMCs), cultured in the presence of a T lymphocyte conditioned medium, are analogous to MMCs as defined by the granule content of the soluble chymase, rat mast cell protease-II (RMCP-II); by the granule proteoglycan chondroitin sulphate; and by their secretory characteristics. To investigate the secretory response of BMMCs to IgE-dependent stimulation, a sensitive, specific and repeatable enzyme-linked immunospot (ELISPOT) assay was developed to detect the release of RMCP-II from individual cells. Within populations of BMMCs, only 6-24% of the cells responded to challenge with either anti-IgE or specific antigen, leaving a large residual refractory population. Pre-incubation of mature BMMCs with the multi-functional cytokine, stem cell factor (SCF), significantly increased (≈ 2-fold) the proportion of cells responding to IgE-dependent stimulation without directly causing mediator release. Furthermore, SCF enhanced the total percentage release of RMCP-II and β-hexosaminidase from populations of mature BMMCs in association with an increased proportion of cells secreting RMCP-II as detected by ELISPOT. These results suggest that SCF augments IgE-dependent secretion from rat BMMCs primarily by activating previously unresponsive cells.

To further characterise the functional phenotype of rat BMMCs, the electrophysiological properties of the cells were investigated using the whole-cell configuration of the patch-clamp technique. Rat BMMCs had a mean membrane potential of -28.5 mV and a mean whole-cell capacitance of 4.8 pF. With the amphotericin B perforated-patch technique, both inwardly rectifying (IR) and

outwardly rectifying (OR) currents were observed in rat BMMCs. The reversal potential and conductance of the IR current depended on the extracellular K^+ concentration, indicating that the channel was K^+ selective. The OR current was reversibly decreased both by lowering the extracellular Cl^- concentration and by the Cl^- channel blocker DIDS, indicating a Cl^- conductance. The IR_K current could also be detected in the majority of BMMCs using the conventional whole-cell recording technique at room temperature. In contrast, the activity of the OR_{Cl} current was dependent on temperature and the maintenance of cytoplasmic integrity. The OR_{Cl} current may be involved in voltage control of the cell during degranulation. However, in addition, the OR_{Cl} current was influenced by changes in extracellular osmolality, suggesting a possible role in volume control.

These studies provide further insight into the regulation of secretion in rat BMMCs, and therefore suggest mechanisms that may be involved in the modulation of gastrointestinal immune responses.

Chapter 1

GENERAL INTRODUCTION

Mast cells were first observed by Von Recklinghausen in 1863 but were named by the German medical student Paul Ehrlich in 1878 (Foreman, 1993). He called the cells "mastzellan" (well-fed cells) because of the large number of prominent granules in the cytoplasm which he thought represented phagocytosed material. The granules took up blue aniline dyes in histological sections, but stained a pinkish-purplish colour, a process Ehrlich called metachromasia. However, it was subsequently shown that the granules contained stores of inflammatory mediators such as histamine which are released during immunological stimulation of the cells (Riley and West, 1953). This release of inflammatory mediators constitutes the main functional role of the mast cell in inflammation and allergic reactions.

FUNCTIONAL IMPORTANCE OF MAST CELLS

Although a full review of the role of mast cells in physiological and pathological processes is beyond the scope of this introduction, a summary of proposed mast cell functions is provided to emphasise the importance of these cells in immunological responses.

Mast cells are most commonly regarded as key effector cells in the pathogenesis of allergic diseases such as asthma, rhinitis, atopic dermatitis, urticaria, anaphylaxis, and food allergy (Brostoff and Hall, 1993; Miller, 1993b). In these type I hypersensitivity reactions, mast cells are classically activated by cross-linking of receptor-bound IgE by multivalent antigen, resulting in the release of a variety of pre-formed and newly synthesised inflammatory mediators (Table 1.1).

Preformed Granule Mediators

Mediator Type	Mediators	Proposed Functions
Biogenic amines	Histamine Serotonin	Permeabilise venules, dilate arterioles contract bronchial and intestinal smooth muscle, stimulate mucus secretion
Proteoglycans	Heparin Chondroitin sulphate	Anticoagulation, anti-complement, anti-kallikrein, stabilise tryptase, neutralise major basic protein, stabilise the granule matrix, modulate cell adhesion
Neutral Proteases	Tryptase	Degrades fibrinogen, generates C3a from C3, activates collagenase, increases pulmonary smooth muscle response to histamine, degrades VIP
	Chymases	Generate angiotensin, degrade basement membranes, activate IL-1 β precursor, stimulate glandular mucus secretion, degrade substance P

Newly Generated Mediators

Mediator Type	Mediator	Proposed Functions
Leukotrienes	LTC_4	Permeabilises venules, augments mucus secretion, contracts intestinal and bronchial smooth muscle
	LTB_4	Upregulates neutrophil adhesion and chemotaxis, augments mucus secretion, modulates cell growth and differentiation
Prostaglandins	PGD_2	Vasodilation, inhibits platelet aggregation, augments airway reactivity
Phospholipid	PAF	Activation of platelets, activation of neutrophils, contraction of intestinal and bronchial smooth muscle, increases vasopermeability, chemotactic for eosinophils

Table 1.1 - Mast cell-derived mediators and their proposed functions (modified from (Harvima and Schwartz, 1993; Schwartz, 1994). The mediators listed are present to varying extents in mast cells from different species and different locations. For example, the chymases represent a number of distinct serine proteases of which specific types are restricted to certain mast cell subsets (see section on mast cell heterogeneity in this chapter for further details). The proposed functions of the mediators have been largely determined *in vitro*, and in restricted species. VIP = vasoactive intestinal peptide; PAF = platelet activating factor.

An exciting development in the study of mast cell biology was the discovery that mast cells can generate or release various cytokines in addition to the above mediators (Plaut *et al,* 1989; Burd *et al,* 1989; and see Table 1.2). Cytokine synthesis typically occurs hours after mast cell activation in contrast to the release of mediators and the generation of arachidonic acid metabolites, which begin within seconds and last for up to 30 minutes (Harvima and Schwartz, 1993). The production of these cytokines indicates that mast cells are not only stores of inflammatory mediators, but also important regulatory cells in the immune response. Hence, in addition to their role in mediating allergic diseases, mast cell mediators and cytokines are involved in diverse pathophysiological processes such as chronic inflammatory responses, wound healing, fibrosis, and the acute sunburn response (Harvima and Schwartz, 1993; Schwartz, 1994; Gordon *et al,* 1990; Walsh, 1995).

Despite playing a detrimental role in allergic reactions, mast cells have a number of important protective functions. For example, TNF-α production by mast cells was critical for the neutrophilic response and bacterial clearance seen in murine models of septic peritonitis and pneumonia (Echtenacher *et al,* 1996; Malaviya *et al,* 1996). However, perhaps the most important protective role of mast cells is the defence of the host against gastrointestinal nematodes. The epithelial and mucosal changes occurring during intestinal nematode infections have many features that are characteristic of allergic inflammation, including production of IgE, recruitment of mast cells, basophils and eosinophils, and altered epithelial secretion (Miller, 1993a). In rodent models, infection with nematode parasites such as *Nippostrongylus brasiliensis* and *Trichinella spiralis* results in a marked hyperplasia of the intestinal mast cell population, and these cells are functionally active during spontaneous expulsion of *N. brasiliensis* in rats (Woodbury *et al,* 1984). Furthermore, release of inflammatory mediators such as histamine, serotonin, prostaglandins, leukotrienes, platelet-activating factor and chymases have all been quantified during intestinal responses to parasite infections (Miller, 1993a; Moqbel *et al,* 1986; MacDonald,

1994; Miller *et al,* 1983). Hence, in addition to performing a protective role, mast cell responses in the gut represent a model for the study of allergic reactions.

Table 1.2 - Cytokines produced by mast cells

Cytokine Type	Cytokine	Proposed Functions
Interleukins	IL-1*	Lymphocyte activation, macrophage stimulation, increases leukocyte/endothelial adhesion, induces acute phase proteins
	IL-3*	Multilineage (including mast cell) colony stimulating factor
	IL-4*	B cell growth factor, isotype switching to IgE and IgG1, mast cell growth cofactor
	IL-5	B cell growth and differentiation factor, IgA selection, eosinophil differentiation factor
	IL-6*	B cell differentiation, induces acute phase proteins
	IL-8	Chemotactic for neutrophils and basophils
Other factors	TNF-α*	Activation of macrophages, granulocytes and cytotoxic cells, increases leukocyte/endothelial cell adhesion, induction of acute phase proteins, stimulation of angiogenesis, enhanced MHC class I production
	TGF-β	Stimulates connective tissue growth and collagen formation, inhibitory to most immune functions
	GM-CSF	Proliferation of granulocyte and macrophage precursors and activators

Table 1.2 - Cytokine production by rodent mast cells (information derived from (Harvima and Schwartz, 1993; Schwartz, 1994; Gordon *et al,* 1990; Plaut *et al,* 1989; Burd *et al,* 1989; Roitt et al, 1993). The cytokines marked with an asterisk have been demonstrated in protein form. The expression of the other cytokines has only been detected as mRNA. TNF-α and IL-4 production has also been demonstrated in human mast cells.

ORIGIN AND DEVELOPMENT OF MAST CELLS

Mast cells are normal residents of connective tissue and are found in highest numbers in areas of the body that interface with the environment, such as the skin, lung and gastrointestinal tract (Foreman, 1993). However, the origin of mast cells and how they arise in these tissues is a question that has only recently been resolved. Early investigators considered many cell types to be mast cell precursors including fibrocytes, emigrated leukocytes, plasma cells, muscle cells, endothelial cells, degenerate eosinophils or undifferentiated mesenchymal cells (reviewed in Michels, 1963). Subsequent investigators suggested that mast cells might arise from T lymphocytes (Guy-Grand *et al,* 1978; Burnet, 1977). Mast cells also show many similarities to blood basophils (a circulating granulocyte) including the presence of cytoplasmic granules containing histamine and proteoglycan, and the presence of high affinity receptors for IgE on their surfaces. This similarity led to the suggestion that basophils might be the precursor of mast cells. However, mast cells are not identical to basophils and can be distinguished morphologically (Galli, 1990), especially in electron microscopic studies (Dvorak *et al,* 1983). Mast cells also have different immunological surface markers to basophils, showing a profile more similar to macrophages than granulocytes (Valent *et al,* 1990b). In addition, no studies have shown that mature basophils can either proliferate or differentiate into mast cells, and basophils did not lead to mast cell colonies when grown in methylcellulose cultures (Seder *et al,* 1991). It is therefore now generally accepted that basophils are terminally differentiated granulocytes and are not mast cell precursors (Galli, 1990; Kitamura *et al,* 1993).

Evidence that mast cells originated from haematopoietic cells was first provided by studies of beige mice by Kitamura et al. (1977). Beige mice possess two mutant alleles at the *bg* locus and are characterised by the presence of giant granules in various cell types including melanocytes, neutrophils and mast cells (Chi and Lagunoff, 1975). Transplantation of bone marrow cells from 57BL/6-bg^j/bg^j beige

mice to lethally irradiated +/+ mice resulted in the development of mast cells with giant granules in the recipient (Kitamura *et al,* 1977). The haematopoietic cell origin of mast cells was confirmed in a number of other studies in which mast cells were grown in culture from bone marrow using factors derived from T lymphocytes (Nabel *et al,* 1981; Nagao *et al,* 1981; Razin *et al,* 1981; Schrader *et al,* 1981; Tertian *et al,* 1981; Nakahata *et al,* 1982). Mast cells were subsequently shown to originate from multipotential haematopoietic stem cells in studies by Kitamura et al. (1981) and Nakahata and Ogawa (1982) in which colony forming units resulted in the formation of other haematopoietic cells in addition to mast cells.

In contrast to other cells of the haematopoietic stem cell lineage, which differentiate in the bone marrow before being released into the circulation, mast cells do not circulate as mature cells. Morphologically unidentifiable precursors migrate in the blood (Kitamura *et al,* 1979; Sonoda *et al,* 1982; Zucker-Franklin *et al,* 1981) and invade connective or mucosal tissues where they proliferate and differentiate into mature mast cells (Kitamura *et al,* 1979; Kasugai *et al,* 1995). The committed precursor of the mast cell lineage was recently isolated from murine foetal blood and was characterised as a cell possessing Thy-1^{lo} c-kit^{hi} markers, cytoplasmic granules, RNAs encoding mast cell proteases, but lacking expression of the IgE receptor (Rodewald *et al,* 1996). These cells generated functionally competent mast cells in vitro, but lacked developmental potential for other haematopoietic lineages.

Mast Cell Development in Laboratory Animals

1. Non T-cell dependent

The use of mutant mice

The study of mast cell development has been aided by the use of strains of mutant mice, especially the W/W^{v} mutant and the Sl/Sl^{d} mutant. Mice with two mutant alleles at the W locus on chromosome 5 suffer from a combination of defects including macrocytic anaemia, sterility, lack of hair pigmentation and deficiency of

mast cells (Kitamura *et al,* 1978). The same set of defects are seen in mice with a double gene dose of mutant alleles at the *Sl* (steel) locus on chromosome 10 (Kitamura and Go, 1979). The reduction in erythrocytes, germ cells, melanocytes and mast cells in W mutant mice is due to a defect in the cells themselves or their precursors (Kitamura *et al,* 1993). Hence, the number of mast cells in W/W^{v} mice can be normalised by transplanting bone marrow cells from normal (+/+) mice (Kitamura *et al,* 1978; Galli and Kitamura, 1987). In contrast, the precursor cells of Sl/Sl^{d} mice are normal and transplantation of bone marrow cells from Sl/Sl^{d} mice to W/W^{v} mice can also reverse the deficiency in mast cells (Kitamura and Go, 1979), suggesting that the defect in Sl/Sl^{d} mice was a deficiency in a growth factor. When skin from W/W^{v} mice was grafted onto normal (+/+) mice or Sl/Sl^{d} mice, mast cells appeared in the graft suggesting that normal precursor cells from the host had differentiated into mast cells within the graft microenvironment. However, when skin from Sl/Sl^{d} mice was grafted onto normal (+/+) mice or W/W^{v} mice, no mast cells developed in the graft, indicating that the deficiency in mast cells in Sl/Sl^{d} mice was due to a deficiency in the skin microenvironment (Kitamura and Go, 1979; Matsuda and Kitamura, 1981).

Analysis of the W locus

Molecular analysis of the W locus has revealed it to be identical to the *c-kit* proto-oncogene (Chabot *et al,* 1988; Geissler *et al,* 1988) which encodes a transmembrane tyrosine kinase receptor (Chabot *et al,* 1988; Yarden *et al,* 1987). The *c-kit* receptor is structurally similar to the receptors for colony stimulating factor and platelet-derived growth factor, having an extracellular domain with five immunoglobulin-like repeats and a tyrosine kinase split into two domains by an insert sequence of variable length (Yarden *et al,* 1987; Qiu *et al,* 1988; and see Figure 1.1). The rat *c-kit* protein contains a 522 amino acid extracellular domain, a 25 amino acid transmembrane domain, and a 432 amino acid intracellular domain, although the structure and amino acid sequence is well preserved in both rats and humans (Kitamura *et al,* 1993). The

various mutations at the W locus cause a number of abnormalities in the *c-kit* receptor including absence of the transmembrane domain, absence of kinase activity or reduced expression of the extracellular domain (Nocka *et al,* 1990b; Tan *et al,* 1990).

In rats, homozygous mutants at the "white spotting locus" (Ws/Ws) had a similar phenotype to W/W^{v} mice, including anemia and deficiency in mast cells (Niwa *et al,* 1991). Analysis of the Ws locus revealed that the abnormalities were due to a 12 base deletion in the DNA of the *c-kit* gene (Tsujimura *et al,* 1991).

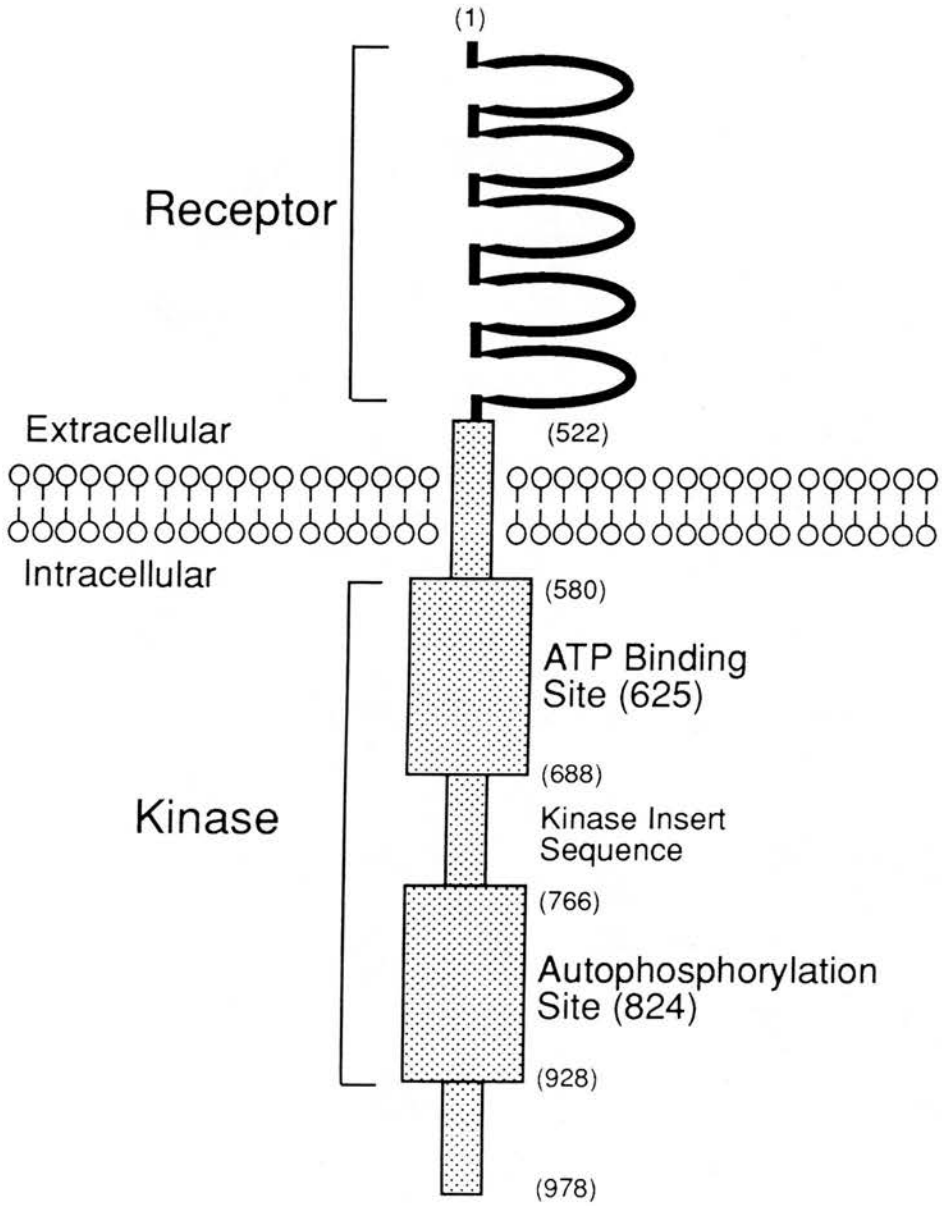

Figure 1.1 - Schematic representation of the rat *c-kit* receptor (modified from (Kitamura *et al*, 1993 and Girault, 1994). The receptor has an extracellular domain with five immunoglobulin-like repeats and an intracellular tyrosine kinase split into two domains by an insert sequence. The numbers in brackets show the amino acid sequence. The autophosphorylation site is a tyrosine residue (amino acid 824).

Analysis of the Sl locus

Molecular analysis has shown that the steel (S*l*) locus encodes the ligand for the *c-kit* tyrosine kinase receptor (Copeland *et al,* 1990; Huang *et al,* 1990; Zsebo *et al,* 1990a) which was variably termed stem cell factor (Zsebo *et al,* 1990b), mast cell growth factor (Williams *et al,* 1990), and kit ligand (Flanagan and Leder, 1990; Huang *et al,* 1990; Nocka *et al,* 1990a) by the investigators who first described it. The ligand is also occasionally referred to as steel factor (Kitamura *et al,* 1993). In this thesis, the currently favoured term, stem cell factor (SCF), is used. The purification of stem cell factor was initially based on its ability to stimulate the growth of mouse bone marrow-derived mast cells (Nocka *et al,* 1990a) and established mast cell lines (Williams *et al,* 1990). It is an extensively and heterogeneously glycosylated protein with a molecular weight of 28 - 35 kDa (Zsebo *et al,* 1990b). Injection of soluble SCF into S*l*/S*l*^{d} mice reversed the characteristic macrocytic anaemia and mast cell deficiency (Zsebo *et al,* 1990a), indicating that these mutants were deficient in active SCF. The main sources of SCF *in vivo* are fibroblasts (Nocka *et al,* 1990a; Flanagan and Leder, 1990) and bone marrow stromal cells (Williams *et al,* 1990), but the molecule has been cloned and exists in membrane bound and soluble forms, both of which are biologically active (Anderson *et al,* 1990). The membrane bound form is produced by alternative splicing and is missing in the S*l*^{d} mutant (Flanagan *et al,* 1991) suggesting that this form may be more important in the intact organism. Hence, analysis of the gene products of the W and S*l* loci has explained the identical clinical syndromes seen in W/W^{v} and S*l*/S*l*^{d} mice, and led to the identification of SCF, a new mast cell growth factor.

Effects of fibroblasts and SCF on mast cell development in vivo

The inter-relationship between fibroblasts and mouse bone marrow-derived mast cells (BMMCs) was demonstrated in studies using diffusion chambers (Ru *et al,* 1990). When BMMCs from normal (+/+) mice were injected into the peritoneal cavity of W/W^{v} mice (which lack *c-kit* but express SCF), the cells survived (Nakano

et al, 1985). In contrast, normal BMMCs injected into the peritoneal cavity in diffusion chambers did not survive in W/W^v mice, suggesting a cell-bound survival factor could not gain access to the cells (Ru *et al,* 1990). When 3T3 fibroblasts were included in the diffusion chambers, the BMMCs proliferated, indicating that the survival factor was present on the surface of the fibroblasts.

Further evidence for the role of SCF in mast cell proliferation was obtained from studies in which the soluble form of the cytokine was injected into normal animals. Subcutaneous injection of recombinant rat SCF^{164} (a biologically active, soluble form of SCF expressed in *E-coli*) into normal mice induced the development of mast cells in the skin, and systemic administration of $rrSCF^{164}$ to rats resulted in a striking expansion of the mast cell population in the skin, lung, liver, spleen, stomach and small intestine (Tsai *et al,* 1991a). A similar, reversible, expansion of the mast cell population was seen in baboons and cynomolgus monkeys after subcutaneous injections with recombinant human SCF (Galli *et al,* 1993), and rhSCF also induced cutaneous mast cell hyperplasia in humans (Costa *et al,* 1996).

SCF/*c-kit* interactions were also shown to contribute to the intestinal mastocytosis that accompanies intestinal nematode infections in laboratory rodents. Treatment of mice with a monoclonal antibody to c-kit (Grencis *et al,* 1993) or SCF (Donaldson *et al,* 1996), or rats with a polyclonal sheep anti rat SCF antibody (Newlands *et al,* 1995) significantly decreased the mast cell hyperplasia in response to infections with *Trichinella spiralis* (Grencis *et al,* 1993; Donaldson *et al,* 1996; Newlands *et al,* 1995) or *Nippostrongylus brasiliensis* (Newlands *et al,* 1995).

Effects of fibroblasts and SCF on mast cell development in vitro

The inter-relationship between fibroblasts and mouse BMMCs was investigated *in vitro* by co-culturing BMMCs from normal (+/+), W/W^v and Sl/Sl^d mice with NIH/3T3 fibroblasts (reviewed in Kitamura *et al,* 1993). The BMMCs from normal

and Sl/Sl^d mice proliferated, but the cells from the W/W^v mice (which lack the *c-kit* receptor) disappeared. In addition, fibroblasts derived from Sl/Sl^d mice (which lack SCF) were unable to support BMMCs from normal mice. These results suggested that interaction between SCF and the *c-kit* receptor was essential for fibroblast-dependent proliferation of BMMCs.

In accord with *in vivo* studies, SCF also promoted the proliferation of both mouse (Tsai *et al,* 1991b; Takagi *et al,* 1992) and rat (Haig *et al,* 1994) BMMCs and peritoneal mast cells *in vitro*. However, when used alone, SCF could not stimulate the development of mast cells from primitive mast cell progenitors, suggesting that its effect was probably dependent both on other cofactors and the degree of maturation of the cells (Rennick *et al,* 1995; Lantz and Huff, 1995a).

In addition to stimulating the development and proliferation of mast cells, SCF also possesses a number of other important functional properties. SCF was shown to be a chemotactic agent for mast cells (Blumejensen *et al,* 1991; Meininger *et al,* 1992), and the interaction between SCF and *c-kit* could regulate the adhesion of mast cells to fibroblasts (Adachi *et al,* 1992) or extracellular matrix components such as fibronectin (Dastych and Metcalfe, 1994; Kinashi and Springer, 1994). These functions could be important for controlling the migration of mast cells into appropriate tissues. Furthermore, recent studies have demonstrated that SCF can also influence the secretory function of mast cells. Treatment with SCF in isolation directly induced mediator release from mouse peritoneal mast cells (Coleman *et al,* 1993), rat peritoneal mast cells (Nakajima *et al,* 1992; Koike *et al,* 1993; Taylor *et al,* 1996), mouse skin mast cells (Wershil *et al,* 1992) and human skin mast cells (Costa *et al,* 1996) without the need for IgE receptor activation. SCF also upregulated IgE-dependent mediator release in a number of connective tissue and mucosal mast cell types. For example, brief preincubations (10 - 15 minutes) with the cytokine enhanced IgE-dependent mediator release from human skin, lung and intestinal mast

cells (Columbo *et al,* 1992; Bischoff and Dahinden, 1992; Bischoff *et al,* 1996). These important observations suggest that SCF may be directly involved in the regulation of immune responses by modulating mast cell secretory function, and will be discussed in more detail in chapter 4.

2. T-cell dependent mast cell development

Infection of normal mice and rats with intestinal nematodes such as *Nippostrongylus brasiliensis* or *Trichinella spiralis* results in a massive hyperplasia of mast cells in the intestinal lamina propria (Miller and Jarrett, 1971; Befus and Bienenstock, 1979). A similar, but reduced, response was also seen in Ws/Ws rats, normally deficient in intestinal mast cells (Arizono *et al,* 1993), although mast cells in connective tissue sites were not increased. This intestinal mastocytosis was shown to be T cell-dependent in studies using congenitally athymic mice (Ruitenberg and Elgersma, 1976), thymectomised rats (Mayrhofer and Fisher, 1979), and adoptive transfer of primed T cells followed by nematode challenge in rats (Nawa and Miller, 1979). The importance of T-cell derived factors for mast cell development was also shown when mast cells were grown in liquid culture from hematopoietic cells of the rat (Haig *et al,* 1982) or mouse (Hasthorpe, 1980; Nabel *et al,* 1981; Nagao *et al,* 1981; Razin *et al,* 1981; Schrader *et al,* 1981; Tertian *et al,* 1981). Five of these six groups used growth factors derived from stimulated T cells, but Nagao et al. used a culture medium from a mouse leukemia cell line (WEHI-3). The mast cell growth factor in WEHI-3 medium was subsequently purified and designated interleukin 3 (IL-3)(Ihle *et al,* 1983). However, other T cell derived cytokines, including IL-4, IL-9 and IL-10, have subsequently been shown to influence mast cell development either *in vivo* and/or *in vitro* (Kitamura *et al,* 1993).

Effects of interleukins on mast cell development in vivo

Repetitive administration of purified IL-3 to nude athymic mice resulted in a 30-fold increase in intestinal mucosal mast cells (Abe *et al,* 1988), and restored the host's ability to develop a mastocytosis in response to the intestinal nematode *Strongyloides ratti* (Abe and Nawa, 1988). In addition, perfusion with IL-3 resulted in the development of mast cells in the skin of W/W^{v} mice (Ody *et al,* 1990). However, as these mice are capable of producing IL-3, the significance of this finding *in vivo* is not known. Further evidence for the role of IL-3, and additionally IL-4, in mast cell development is provided by experiments showing the effect of antibodies directed against the two cytokines on *Nippostrongylus brasiliensis*-induced mastocytosis in mice (Madden *et al,* 1991). Administration of either antibody caused 40-50% inhibition of mast cell numbers, but concurrent administration of both antibodies suppressed the mast cell response by 85-90%, suggesting that the cytokines may act synergistically. A reduced intestinal mast cell response to the nematode *Trichuris muris* was also seen in mice treated with a monoclonal antibody to the IL-4 receptor, again suggesting a role for this cytokine in vivo (Else *et al,* 1994).

Effects of interleukins on mast cell development in vitro

When mouse (Chiu and Burrall, 1990; Razin *et al,* 1984; Ihle *et al,* 1983) or rat (Haig *et al,* 1988) bone marrow cells are cultured in the presence of IL-3, large numbers of mast cells can be generated as virtually a pure population. In both systems, other cell types (neutrophils, eosinophils and macrophages) proliferate initially in response to IL-3, but the response is not sustained and the cells die out (Kitamura *et al,* 1993). IL-3 also supported the survival of mouse peritoneal mast cells in methylcellulose cultures (Tsuji *et al,* 1990) and stimulated the growth of rat peritoneal mast cells (Haig *et al,* 1994). However, IL-3 did not promote mast cell colony formation when used to stimulate highly purified *c-kit*$^{+}$ cells derived from the peritoneal cavity or mesenteric lymph nodes of *Nippostrongylus brasiliensis* infected mice, suggesting

that the effect of the cytokine was dependent on the degree of maturation of the cells (Lantz and Huff, 1995a).

IL-4 did not sustain the long term growth of bone marrow-derived mast cells, but acted synergistically with IL-3 in the stimulation of mouse BMMCs (Schmitt *et al,* 1987), neoplastic mast cell lines (Smith and Renwick, 1986), and peritoneal cells (Tsuji *et al,* 1990). When used in combination with SCF, IL-4 also caused the initiation and proliferation of mast cell colonies from primitive progenitors derived from mesenteric lymph node cells (Rennick *et al,* 1995).

IL-9 prolonged the survival of mouse BMMCs and in conjunction with IL-3, synergistically enhanced the growth of primary bone marrow cultures (Moeller *et al,* 1989) and IL-3 dependent mast cell lines (Hultner *et al,* 1989; Hultner *et al,* 1990).

The effects of IL-10 on mast cell growth were investigated by Thompson-Snipes et al. (1991). IL-10 alone did not support the proliferation of mast cell lines, but it markedly enhanced their growth when used in combination with IL-3 and IL-4. In fact, the combination of IL-10 and IL-4 was as effective at stimulating mast cell growth as IL-3 alone, but optimum conditions were provided by the three cytokines together. When used in combination with SCF, IL-10 was also an efficient differentiation and maturation factor for mast cells derived from primitive progenitors in mesenteric lymph node cells (Rennick *et al,* 1995).

Other factors affecting mast cell development

Another fibroblast-derived factor, nerve growth factor (NGF), was shown to increase the number of mast cells in neonatal rats (Aloe and Levi-Montalcini, 1977), and acted synergistically with IL-3 to stimulate the growth of mouse BMMCs *in vitro* (Matsuda *et al,* 1991). NGF also enhanced the survival of rat peritoneal mast cells placed in culture in the absence of other cytokines (Horigome *et al,* 1994), but did

not lead to proliferation of these cells. Immunoglobulin E (IgE) was also reported to act in combination with IL-3 to promote mast cell differentiation (Kawanashi, 1986), and IgE immune complexes could stimulate the development of mast cell committed progenitors from normal mouse bone marrow (Ashman *et al,* 1991).

Interferon γ (IFN-γ) was shown to inhibit the development of IL-3-stimulated mouse BMMCs, but did not affect the proliferation of mature cells, suggesting an action on mast cell precursors (Nafziger *et al,* 1990). IFN-γ also inhibited the proliferation of mouse peritoneal mast cells in cultures containing IL-3 and IL-4 (Takagi *et al,* 1990). The IL-3-dependent proliferation of mouse BMMCs was also suppressed by transforming growth factor-β1 (Broide *et al,* 1989).

Mast Cell Development in Humans

In the rodent systems described above, both fibroblast-dependent and T-cell dependent mechanisms for stimulating mast cell development were established. In the human system, mast cells (analogous to skin mast cells) developed when umbilical cord blood cells were co-cultured with 3T3 fibroblasts (Furitsu *et al,* 1989). Recombinant human SCF also stimulated the growth of mast cells from their progenitors in human bone marrow (Valent *et al,* 1992; Kirshenbaum *et al,* 1992), peripheral blood (Valent *et al,* 1992), foetal liver (Irani *et al,* 1992), and umbilical cord blood (Mitsui *et al,* 1993). The circulating mast cell progenitor in humans has now been characterised as a c-kit$^+$, CD34$^+$ colony forming cell (Kirshenbaum *et al,* 1991; Agis *et al,* 1993). In addition to SCF, nerve growth factor has also been shown to have mast cell growth promoting properties in human haematopoietic cultures (Matsuda *et al,* 1988a; Matsuda *et al,* 1988b).

In humans, IL-3 appears to be the principal growth factor that induces development of basophils from bone marrow (Kirshenbaum *et al,* 1989; Valent *et al,* 1989), cord

blood (Dvorak *et al,* 1989), or fetal liver cells (Irani *et al,* 1992). In contrast to mice and rats, IL-3 does not promote the development of mast cells from human bone marrow or cord blood (Mitsui *et al,* 1993), although it generally increases the total number of mast cells in cultures stimulated with SCF. However, the proportion of mast cells in IL-3 containing cultures was comparable to that seen with SCF alone, suggesting that the effect is not selective for mast cells (Ishizaka *et al,* 1993). In addition, IL-3 receptors could not be detected on human lung mast cells (Valent *et al,* 1990a).

Yanagida *et al* (1995) examined the effects of T-helper 2-type cytokines on the survival of human mast cells grown to 100% purity from cord blood in the presence of SCF and IL-6 (Yanagida *et al,* 1995). After withdrawal of the cytokines, the mast cells underwent apoptosis within 2 to 6 days. However, addition of SCF, IL-3, IL-4, IL-5 or IL-6 prolonged their survival in a dose-dependent manner, whereas other cytokines such as IL-2, IL-9, IL-10, IL-11, TNF-α, TGF-β1, or NGF had no survival-promoting effect (Yanagida *et al,* 1995). IL-6 was also shown to enhance SCF-dependent growth and maturation of mast cells derived from umbilical cord blood mononuclear cells (Saito *et al,* 1996). In other studies, neither IL-4 nor IL-9 appeared to have any growth promoting activity for human mast cells (Kirshenbaum *et al,* 1989; Valent *et al,* 1992), but IL-4 was shown to down-regulate the *c-kit* receptor on human bone marrow progenitor cells and neoplastic mast cell lines (Sillaber *et al,* 1991).

MAST CELL HETEROGENEITY

It has been increasingly recognised over the last 15-20 years that mast cells from different tissues exhibit considerable variations in their morphological, biochemical and functional characteristics (reviewed in Galli, 1990). This heterogeneity was first observed in the rat in which mast cells of the intestinal mucosa were distinguished

from those in the skin by virtue of their histochemical and secretory properties (Enerback, 1966c; Enerback, 1966b; Enerback, 1966a). This led to the common usage of the terms "mucosal mast cells" (MMCs) and "connective tissue mast cells" (CTMCs) to describe the two subpopulations. Mast cell heterogeneity is now well documented in the rat, mouse, sheep and humans, and is defined in terms of histochemical characteristics, the content of granule mediators, and functional properties (Barrett and Pearce, 1993).

Histochemical characteristics

Enerback (1966) reported that, in contrast to mast cells in rat skin, mast cells in the intestinal mucosa were sensitive to routine formalin fixation and could not be identified in standard histological sections. However, following appropriate fixation and sequential staining with alcian blue and safranin, the MMCs stained blue in comparison to the CTMCs which stained with safranin and were predominantly red (Enerback, 1966b). This staining sequence has been widely used to characterise mast cells from various origins, tissues or species as either mucosal or connective tissue types respectively. Hence, rat BMMCs, rat basophilic leukaemia (RBL-2H3) cells, mouse MMCs, mouse BMMCs and human lung mast cells stain with alcian blue, whereas rat and mouse peritoneal mast cells stain with safranin (Katz *et al,* 1985). Unfortunately, this method is not a totally reliable indicator of mast cell subsets because immature CTMCs stain with alcian blue (Combs *et al,* 1963) and CTMCs from different connective tissue locations in the rat show marked differences in safranin staining depending on the site of origin (Tainsh and Pearce, 1992). Differences in histologic staining characteristics between mast cell subpopulations are also seen with berberine sulphate which forms a strong fluorescent complex with heparin in rat CTMCs, but does not bind to rat MMCs (Enerback, 1974) or rat BMMCs (MacDonald, 1994). This variation in dye binding properties reflects the presence of different proteoglycans in the two subpopulations (see below).

Heterogeneity of Granule Mediators

Proteoglycan heterogeneity

Proteoglycans are a major granular constituent of all mast cells, but the predominant type varies among subpopulations. Each class of proteoglycan has distinctive glycosaminoglycans with characteristic negative-charge densities conferred by the degree of sulphation of the dissacharides. Rat peritoneal and skin mast cells contain heparin (Schiller and Dorfman, 1959; Horner, 1971; Yurt *et al,* 1977), whereas intestinal MMCs (Stevens *et al,* 1986), BMMCs (Broide *et al,* 1988) and rat basophilic leukaemia cells (Seldin *et al,* 1985) contain predominantly chondroitin sulphate di-B. Subsequent work indicated that intestinal MMCs from rats infected with *Nippostrongylus brasiliensis* contained chondroitin sulphate E and dermatan sulphate (Kusche *et al,* 1988). In the mouse, CTMCs contain heparin whereas BMMCs contain chondroitin sulphate E (Razin *et al,* 1982). Mouse intestinal MMCs have not been purified to date, but the non-heparin nature of their proteoglycan has been implied by their inability to stain with berberine sulphate (Nakano *et al,* 1985) and their alcian blue^{+} / safranin^{-} staining characteristics (Crowle and Phillips, 1983). In humans, cutaneous mast cells contain heparin (Metcalfe *et al,* 1980), whereas intestinal mucosal mast cells contain chondroitin sulphate E (Eliakim *et al,* 1986; Gilead *et al,* 1987). Human lung mast cells, considered to be a mucosal phenotype on the basis of their alcian blue and berberine sulphate staining (Flint *et al,* 1985) appear to represent an intermediate form, containing both heparin and chondroitin sulphate E (Stevens *et al,* 1988; Thompson *et al,* 1988).

Protease heterogeneity

Mast cell subpopulations can also be defined on the basis of their content of serine proteases. Two antigenically distinct serine proteases, of chymotryptic specificity, have been isolated from rat mast cells. These chymases have been designated rat mast cell protease I (RMCP-I) and rat mast cell protease II (RMCP-II) (Katanuma *et al,* 1975; Woodbury *et al,* 1978; Woodbury *et al,* 1978a; Woodbury and Neurath,

1980). Although these chymases have similar substrate specificity (Yoshida *et al,* 1980), they can be distinguished on the basis of their physico-chemical and immunological properties (Woodbury *et al,* 1978; Woodbury *et al,* 1978a; Woodbury *et al,* 1978b). In contrast to RMCP-II, which is highly soluble (Woodbury and Neurath, 1980), RMCP-I is insoluble in physiological buffers and remains heparin-bound both in the granule and following secretion (Schwartz *et al,* 1981).

Specific antibodies raised against these enzymes have been used to characterise the protease phenotype of rat mast cells in different locations. Mast cells in the skin, tongue, intestinal serosa and lung parenchyma, which by histochemical techniques have been identified as CTMCs, contained only RMCP-I (Gibson and Miller, 1986). Cells in the jejunal lamina propia and bronchial epithelium, previously classified as MMCs, contained RMCP-II exclusively (Gibson and Miller, 1986). In a more detailed study of the gastrointestinal tract (Gibson *et al,* 1987), the distribution of mast cells staining with alcian blue (MMCs) or safranin (CTMCs) correlated closely with the distribution of cells staining for the presence of RMCP-II or RMCP-I respectively. Hence, the presence of RMCP-II or RMCP-I can be used to identify rat mast cells as either MMCs or CTMCs. However, using paired immunofluorescence, Huntley et al. (1990a) showed that 17 - 23% of the mast cells in the gastric submucosa, liver, and peribronchial regions of the lung were identified as possessing both RMCP-I and RMCP-II, but the significance of this finding was not determined. Rat BMMCs, which can be grown to homogeneity from normal rat bone marrow using an IL-3-rich T cell-conditioned medium (Haig *et al,* 1982; Haig *et al,* 1988), possessed exclusively RMCP-II on immunohistochemical analysis, thus demonstrating their identity with intestinal mucosal mast cells (McMenamin *et al,* 1987). Similarly, RBL-1 cells (an earlier passage of the tumour used to produce RBL-2H3 cells) possessed exclusively RMCP-II, suggesting homology between these cells and rat mucosal mast cells (Seldin *et al,* 1985). Protease heterogeneity in

rat mast cells also extended to tryptase, which was only detected in CTMCs (Chen *et al,* 1993).

In the mouse, five mast cell chymases (MMCP-1, -2, -3, -4, -5), two tryptases (MMCP-6 and -7), and one carboxypeptidase have been reported (Reynolds *et al,* 1990; Schwartz, 1994). MMCPs-3, -4, -5 and -6 and mast cell carboxypeptidase are present in CTMCs, whereas MMCP-1 and -2 are present in MMCs (Schwartz, 1994). However, in contrast to the rat, mouse BMMCs show immunoreactivity to both CTMC and MMC proteases (Newlands *et al,* 1991). They can not, therefore, be definitively categorised as a mucosal phenotype based on protease expression, and may represent the immature stages of both MMCs and CTMCs.

In humans, the differentiation of mast cells into mucosal or connective tissue phenotypes is less clear cut than in rodents. Two mast cell proteases, chymase and tryptase, have been isolated along with a carboxypeptidase and a cathepsin G-like protease (Schwartz, 1994). Schwartz et al. defined two types of human mast cell based on the presence or absence of chymase (Irani *et al,* 1986; Schwartz *et al,* 1987). Cells containing only tryptase (MC_T) were predominant in the lungs, and represented essentially all of the cells in the intestinal mucosa (Irani *et al,* 1986). Mast cells containing both tryptase and chymase, along with carboxypeptidase and cathepsin G-like protease (MC_{TC}), were predominant in the skin and intestinal submucosa (Irani *et al,* 1986; Schwartz, 1994). Mast cells derived from cord blood in the presence of SCF were recently shown to be of the MC_{TC} phenotype (Nilsson *et al,* 1996). Using the rodent classification, MC_T cells could be loosely regarded as MMC phenotype and MC_{TC} cells as CTMC phenotype. However, the notation can not be rigidly applied as shown by the equal numbers of MC_T and MC_{TC} cells found in the nasal mucosa (Schwartz, 1994).

Heterogeneity of other mediators

Variation in the content, or generation, of other mast cell mediators also occurs between the subpopulations. Rat peritoneal mast cells contain, on average, 20 pg histamine per cell, whereas rat cutaneous and intestinal mast cells contain 4 and 1 pg/cell respectively (Barrett *et al,* 1985; Befus *et al,* 1982). Rat BMMCs contained a mean of 2.7 pg histamine per cell (MacDonald, 1994).

The generation of leukotrienes and prostaglandins also vary in CTMCs and MMCs. Following activation with anti-IgE, rat peritoneal mast cells generated exclusively prostaglandin D_2 (PGD_2) (Lewis *et al,* 1982), whereas intestinal MMCs and BMMCs synthesised approximately equal quantities of PGD_2 and leukotriene C_4 (LTC_4) (Heavey *et al,* 1988; Broide *et al,* 1988).

Functional heterogeneity

The most important aspect of mast cell heterogeneity, in terms of clinical relevance, is the variation in functional characteristics seen between mast cell subpopulations. This is manifested experimentally as variations in susceptibility to secretagogues or anti-allergic drugs (Barrett and Pearce, 1993). The first example of functional heterogeneity was provided by Enerback (1966) who found that compound 48/80, a known secretagogue for rat CTMCs, failed to cause degranulation of intestinal MMCs *in situ* (Enerback, 1966a; Enerback, 1974). Subsequent studies confirmed that, in contrast to rat peritoneal CTMCs, neither isolated intestinal rat MMCs (Befus *et al,* 1982) nor rat BMMCs (Broide *et al,* 1988) responded to compound 48/80.

Rat intestinal MMCs also showed a minimal or complete lack of response to a range of neuropeptides including somatostatin, vasoactive intestinal peptide, neurotensin and bradykinin (Shanahan *et al,* 1985). In contrast, these compounds were potent secretagogues for rat peritoneal mast cells. Substance P triggered histamine release from both populations of cells, but the response in MMCs was only 33% of that in

peritoneal mast cells (Shanahan *et al,* 1985). Broide et al. (1988) found that rat BMMCs were unresponsive to both somatostatin and substance P.

Rat intestinal MMCs and peritoneal CTMCs also differ in their response to the anti-allergic drugs disodium cromoglycate and theophylline (Pearce *et al,* 1982). These drugs effectively inhibited IgE-mediated histamine secretion from peritoneal mast cells, but were without effect on isolated intestinal MMCs (Pearce *et al,* 1982). Likewise, disodium cromoglycate failed to inhibit IgE-dependent mediator release from rat BMMCs (Broide *et al,* 1988).

Despite these apparently clear differences in functional characteristics between mucosal and connective tissue type mast cells in the rat, variations occur within subpopulations both in the same animal, and between species. For example, rat cutaneous mast cells were less responsive to compound 48/80 than rat peritoneal mast cells (Barrett *et al,* 1985), and mouse cutaneous mast cells showed different kinetics of histamine release than that of peritoneal mast cells (He *et al,* 1990). Marked differences in the response to secretagogues were also seen when rat CTMCs from various locations (peritoneal cavity, skin, mesentery and lung) were compared (Tainsh and Pearce, 1992). In addition, mouse peritoneal mast cells are less responsive to compound 48/80 than rat peritoneal mast cells (Barrett and Pearce, 1983), and are not stabilised by disodium cromoglycate (Leung *et al,* 1984).

In humans, it is not possible to predict the functional phenotype of a mast cell from its proteoglycan or protease composition. Human skin mast cells (MC_{TC}) respond to compound 48/80 (Lawrence *et al,* 1987; Benyon *et al,* 1989), whereas colonic submucosal mast cells (also MC_{TC}) do not (Rees *et al,* 1988; Liu *et al,* 1990). Similarly, disodium cromoglycate does not inhibit IgE-dependent histamine release from human skin mast cells (Clegg *et al,* 1985; Lowman *et al,* 1988), but has a partial effect on colonic submucosal mast cells (Liu *et al,* 1990).

The functional heterogeneity of rat mast cells also extends to their electrophysiological properties (Lindau and Fernandez, 1986b), but this will be the subject of a more detailed review at the end of this chapter.

Regulation of mast cell phenotypes

The studies described in the previous sections clearly show that proliferation of MMCs is dependent on T cell-derived cytokines and that development of CTMCs requires the interaction between stem cell factor and the *c-kit* receptor. However, this simplistic distinction does not fully explain the derivation of the two phenotypes. W/W^v and Sl/Sl^d mice (which lack the *c-kit* receptor and SCF respectively) lack both CTMCs and MMCs, suggesting that SCF is required for the development of both cell types *in vivo*. In addition, systemic administration of SCF to normal rats resulted in expansion of both the CTMC and MMC populations (Tsai *et al,* 1991a). SCF could also prevent apoptosis of IL-3-dependent mouse mast cells following removal of the IL-3 (Mekori *et al,* 1993). However, pure mast cell populations can be grown from both mouse (Ihle *et al,* 1983)and rat (Haig *et al,* 1988) bone marrow in the presence of IL-3 alone, and systemic administration of IL-3 to W/W^v mice increased the number of cutaneous mast cells (Tsai *et al,* 1991a). Hence, some degree of overlap appears to exist between the two signalling systems, and deficiencies in one can be partially overcome by additional provision of the other, at least in experimental systems.

The mechanisms governing the development of mast cell phenotypes are complex, as highlighted by numerous studies which document the capacity of mouse mast cell populations to change phenotype from MMC to CTMC, or vice versa. When cloned mouse peritoneal mast cells were injected into W/W^v mice, they gave rise to both connective tissue and mucosal mast cells in the appropriate tissue locations (Kobayashi *et al,* 1986). Mouse peritoneal mast cells also produced berberine

sulphate-negative mast cells when cultured in methylcellulose with IL-3 and IL-4, but injection of these "MMCs" back into the peritoneum of W/W^v mice resulted in a reversion to the CTMC phenotype (Kanakura *et al,* 1988). Similarly, when mouse BMMCs were co-cultured with 3T3 fibroblasts, the cells acquired the characteristics of CTMCs including a marked increase in histamine content, *de novo* synthesis of heparin, positive staining with safranin, and an increase in the granule content of carboxypeptidase A (Levi-Schaffer *et al,* 1986; Dayton *et al,* 1988). In addition, injection of IL-3-dependent cultured mouse mast cells into the peritoneal cavity, skin or gastrointestinal mucosa of W/W^v mice replenished both the connective tissue and mucosal mast cell pools (Nakano *et al,* 1985). Mouse BMMCs treated with either nerve growth factor (NGF) (Matsuda *et al,* 1991) or SCF (Tsai *et al,* 1991b) also acquired connective tissue type characteristics such as increased histamine and heparin, and staining with safranin and berberine sulphate. Taken together, these experiments suggested that mouse mast cells could "transdifferentiate" between phenotypes (Barrett and Pearce, 1993). However, as already stated, mouse BMMCs do not have the same protease expression as intestinal MMCs and can not be regarded as mature mucosal mast cells. It is likely, therefore, that mouse BMMCs represent an immature phenotype with the ability to further differentiate into connective tissue or mucosal types if placed in the appropriate microenvironment. Gurish et al. (1995) provided further evidence for tissue regulated differentiation and maturation by injecting *v-abl* immortalized mast cell lines into normal mice. These cells have a protease phenotype analogous to mouse BMMCs, but following infiltration into the liver, spleen and intestine they underwent progressive differentiation and maturation, eventually expressing the same proteases as the indigenous mast cells of the specific organs (Gurish *et al,* 1995).

In contrast to the above studies, rat BMMCs, which on biochemical and functional analysis appear to be identical to rat MMCs, did not develop a CTMC phenotype when co-cultured with 3T3 fibroblasts, as assessed by the levels of RMCP-I and -II

and berberine sulphate staining (MacDonald *et al,* 1996). However, when mast cells were cultured from the bone marrow of Ws/Ws rats in the presence of either SCF alone, or concanavalin A-stimulated spleen cell conditioned medium and fibroblasts, a proportion of the cells developed a mixed phenotype containing both RMCP-I and RMCP-II (Tei *et al,* 1994). Small crystalline structures staining weakly for RMCP-I were also seen when BMMCs derived from normal rats were incubated in the presence of SCF (Haig *et al,* 1994). Hence, in the rat, SCF can induce some characteristics of CTMCs in developing BMMCs, but complete transdifferentiation, as seen in the mouse, does not appear possible.

In human patients with severe immunodeficiency or HIV infection there are markedly decreased numbers of MMCs in the intestinal mucosa, but normal numbers of CTMCs in the submucosa (Irani *et al,* 1987). These observations indicate not only the T-cell dependency of mucosal mast cells, but also suggest that CTMCs in man are terminally differentiated and do not have the capacity to dramatically change phenotype.

STIMULUS-SECRETION COUPLING IN MAST CELLS

The main biological function of mast cells is the release of inflammatory mediators and cytokines. Although this process can be triggered by a variety of immunological and non-immunological stimuli, the most important signalling pathway *in vivo* is by aggregation of surface bound immunoglobulin E (IgE) by specific antigen. In this section, the activation of mast cells via the IgE pathway is reviewed.

The high-affinity IgE receptor

Mast cells and basophils express on their surface a protein that binds the Fc region of IgE with high specificity and affinity (Alber and Metzger, 1993). The IgE receptor, known as FcεR1, is a tetrameric complex of non-covalently attached subunits, consisting of one α (45 kDa), one β (33 kDa) and two γ (9 kDa) subunits, designated $\alpha\beta\gamma_2$ (Alber and Metzger, 1993, and see Figure 1.2A). The genes for the α and γ subunits are situated close together at the distal end of chromosome 1 in mice (Huppi *et al,* 1988; Huppi *et al,* 1989) and humans (LeConiat *et al,* 1990). The gene for the β subunit is located on mouse chromosome 19 (Huppi *et al,* 1989). During assembly, the α subunit associates first with the β subunit, and subsequently with the γ subunits (Alber and Metzger, 1993).

The α subunit contains 245, 250 and 260 amino acids in rat, mouse and human respectively (Kinet *et al,* 1987; Alber and Metzger, 1993). It possesses a single transmembrane domain and an extracellular domain that carries the high-affinity binding site for IgE (Kinet, 1990; Riske *et al,* 1991; Hulett *et al,* 1993). The β subunit of the rat and mouse contains 243 and 235 amino acids respectively (Kinet *et al,* 1988; Ra *et al,* 1989; Alber and Metzger, 1993). It has four transmembrane domains, with both the N- and C- termini protruding into the cytoplasm (Kinet *et al,* 1988). The γ subunit is virtually identical in rat, mice and humans and contains 67 amino acids (Blank *et al,* 1989; Ra *et al,* 1989; Kuster *et al,* 1990). It has a single transmembrane domain, and an extracellular region containing only 5 amino acids.

In the plasma membrane, the γ subunits exist as covalently cross-linked dimers, joined by a disulphide bond (Varin-Blank and Metzger, 1990). In contrast to the α subunit, which is responsible for binding IgE, the β and γ subunits of the IgE receptor are concerned with signal transduction (see below).

Binding of IgE to FcεR1

The IgE receptor can only bind one molecule of IgE at a time (Mendoza and Metzger, 1976) and it does so with an affinity of $\approx 10^{9\text{-}10}$ M^{-1} (Kulczycki and Metzger, 1974). The binding of IgE to FcεR1 can not be inhibited by massive excesses of IgG or other immunoglobulins, so isotype specificity is almost absolute (Alber and Metzger, 1993). Numerous studies have shown that the IgE molecule binds to the α subunit of the IgE receptor via the Cε3 domain in the Fc region of the immunoglobulin heavy chain (Weetall *et al,* 1990; Nissim and Eshhar, 1992; Nissim *et al,* 1991). This results in a bent conformation of the antibody, with the Fab arms projecting up and the Fc region projecting laterally (Figure 1.2B, modified from Baird *et al,* 1989).

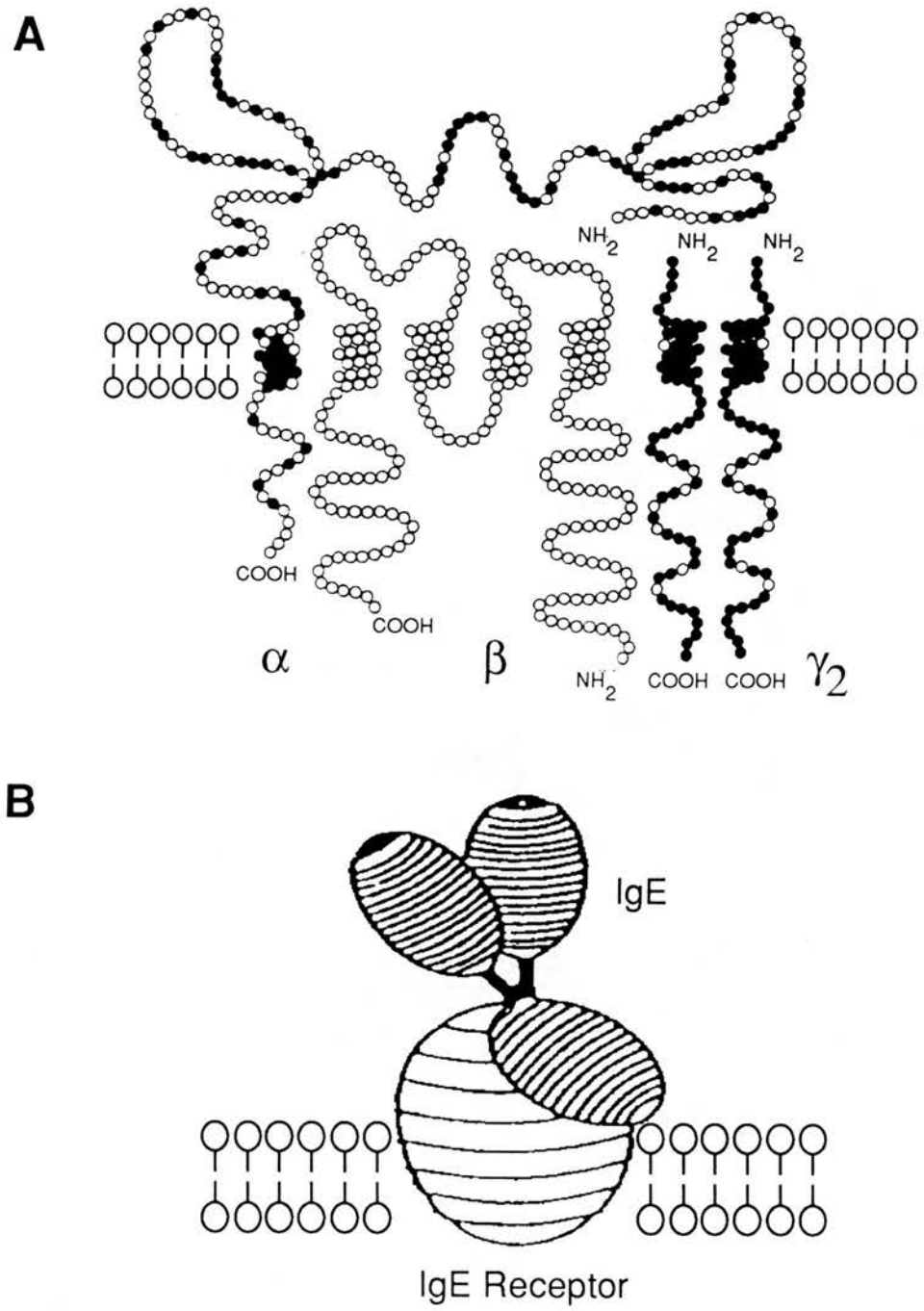

Figure 1.2 - **A**: Schematic representation of the tetrameric IgE receptor (FcεRI, modified from Kinet, 1990). Each circle represents one amino acid residue. The receptor consists of one α chain, one β chain and two γ chains. The large extracellular portion of the α chain contains the IgE binding site. The β subunit possesses four transmembrane domains and, with the γ subunits, is involved in signal transduction. The solid circles show the position of amino acid residues in the α and γ chains that are identical in rat, mouse and human.
B: Model for the binding of IgE to the IgE receptor (modified from Baird *et al,* 1989). The IgE molecule (dark striations) binds via the Cε3 domain in the Fc region of the immunoglobulin heavy chain, resulting in a bent conformation with the Fab arms projecting up and the Fc region projecting laterally.

Aggregation of IgE receptors

It has been known for many years that binding of single IgE molecules to FcεR1 receptors does not lead to activation of the signal transduction pathway. Early studies showed that aggregation of surface bound IgE was required for antigen-induced activation of mast cells (Alber and Metzger, 1993). Subsequent studies revealed that bivalent antibodies to the IgE receptor, but not their monovalent Fab fragments, could trigger mediator release from RBL-2H3 cells, even in the absence of IgE (Ishizaka and Ishizaka, 1978; Isersky *et al,* 1978). These studies demonstrated that aggregation of the receptor itself was the critical stimulus for mast cell activation.

Rat and mouse peritoneal mast cells possess approximately 2-3 x 10^5 IgE receptors per cell (Sterk and Ishizaka, 1982; Conrad *et al,* 1975), whereas RBL-2H3 cells express approximately twice this number (Conrad *et al,* 1975). Rat intestinal mucosal mast cells possessed 3 x 10^4 IgE receptors per cell (Lee *et al,* 1985b), and based on molecular weight, had a different receptor profile than peritoneal mast cells, providing further evidence of heterogeneity (Swieter *et al,* 1989). These receptors diffuse over the surface of the cell like other plasma membrane proteins, but when their bound IgE is aggregated by antigen or anti-IgE, they are rapidly immobilized (Schlessinger *et al,* 1976; Wolf *et al,* 1980; Mao *et al,* 1991; Tamir *et al,* 1996). Immuno-gold labelling studies of IgE receptors demonstrate a change in distribution from a diffuse pattern in resting cells to patched or capped aggregated forms after challenge (Stump *et al,* 1989). Receptor immobilization may occur because of interactions with the underlying cytoskeleton (Mao *et al,* 1991).

Signal transduction

The events following aggregation of FcεR1 receptors that culminate in exocytosis are complex and not fully understood, and the mechanisms underlying this process are a current focus of mast cell research (Beaven and Metzger, 1993). Most of the recent

progress in elucidating these mechanisms has resulted from studies of five main areas: tyrosine kinases; G proteins; the inositol trisphosphate pathway; calcium signalling; and electrophysiology.

Tyrosine kinases

Phosphorylation is a post-translational covalent modification used by cells to regulate the properties of a wide variety of proteins including enzymes, receptors, ion channels and regulatory or structural proteins (Alberts *et al,* 1994). Protein kinases are phosphotransferases which catalyse the transfer of the phosphoryl group of ATP to an amino acid side chain in the presence of Mg^{2+} (Girault, 1994). Phosphoryl acceptors include serine, threonine and the phenol group of tyrosine. Tyrosine kinases exist in two forms: as transmembrane receptors (such as the *c-kit* receptor), and as non-receptor tyrosine kinases (Girault, 1994). The latter group comprises a large number of enzymes includes Src, Yes, Fyn, Lyn, Lck, Blk, Hck, Csk, Tec, Abl, Fes, Fer, Syk, Fak, Tyk and Jak tyrosine kinases. Most, but not all, of these enzymes are characterized by the presence of SH_2 domains which bind to phosphorylated tyrosines and are important regions for protein-protein interactions (Girault, 1994).

At least two families of cytoplasmic tyrosine kinases are activated on cross-linking of FcεRI: the Src family tyrosine kinases c-Src, Lyn and c-Yes (Eiseman and Bolen, 1992); and the syk ($p72^{syc}$) tyrosine kinase (Benhamou *et al,* 1993; Shiue *et al,* 1995). Tyrosine phosphorylation of several proteins is one of the earliest signalling events in mast cells following FcεRI cross-linking (Benhamou *et al,* 1990; Connelly *et al,* 1991; Yu *et al,* 1991; Li *et al,* 1992a; Benhamou *et al,* 1992; Paolini *et al,* 1992; Kawakami *et al,* 1992). Substrates identified to date include the β and γ subunits of the IgE receptor, which are phosphorylated within 5 seconds of receptor aggregation (Paolini *et al,* 1991; Li *et al,* 1992a); phospholipase C-γ1 (Park *et al,* 1991; Schneider *et al,* 1992; Fukamachi *et al,* 1992; Li *et al,* 1992a); a proto-oncogene product p^{95vav} (Margolis *et al,* 1992); a MAP kinase (Fukamachi *et al,*

1993); an SH2 and SH3-containing protein, Nck (Li *et al,* 1992b); and protein SPY75 (Fukamachi *et al,* 1994).

The β and γ subunits of the IgE receptor act as the signalling units between the receptor and cytoplasm (Paolini *et al,* 1991). Recent studies have suggested that triggering of the IgE receptor activates Lyn (already associated with the β subunit) which phosphorylates both the β and γ subunits (Jouvin *et al,* 1994). This induces the activation of Syk which phosphorylates and activates phospholipase C-γ1 (Jouvin *et al,* 1994), an important enzyme in the generation of inositol triphosphate (see below). In this scheme, the β subunit is thought to act as an amplifier of the signal generated by the γ subunit (Lin *et al,* 1996). The critical role of Syk in FcεRI signalling was recently confirmed in a variant of the RBL-2H3 cell line that was deficient in Syk (Zhang *et al,* 1996). In these cells, aggregation of the IgE receptor induced no tyrosine phosphorylation of phospholipase C, no increase in cytosolic Ca^{2+} concentration, and no histamine release. However, following transfection, cloned lines were established with stable expression of Syk, and all these responses were restored (Zhang *et al,* 1996).

The activation of MAP kinases and the *vav* protein by Syk may be involved in the activation of phospholipase A_2 (Hirasawa *et al,* 1995; Hirasawa *et al,* 1995) which contributes to the release of arachidonic acid (Ishimoto *et al,* 1994), whereas activation of the Nck protein may be involved in stimulation of cell activation and growth (Li *et al,* 1992b). Although the function of the SPY75 protein is currently unknown, it contains an SH_3 domain which is a common feature of signalling molecules and cytoskeletal proteins (Fukamachi *et al,* 1994).

The critical role of tyrosine kinases in FcεRI signalling has also been demonstrated using tyrosine kinase inhibitors. A number of inhibitors including genistein (Kawakami *et al,* 1992), lavendustin A (Kawakami *et al,* 1992), methyl 2,5

dihydroxycinnamate (Lavens *et al,* 1992), and piceatannol, a syk-selective inhibitor (Oliver *et al,* 1994), prevented not only tyrosine phosphorylation, but also mediator release.

G-proteins

The second common intracellular mechanism for regulating the function of proteins is the binding and subsequent hydrolysis of GTP (Alberts *et al,* 1994). These so-called G-proteins are activated when bound GDP is exchanged for GTP, and inactivated when the phosphate is removed by hydrolysis (Sagi-Eisenberg, 1993). The similarities between this mechanism and that described above for protein kinases is obvious; both systems rely on the addition and removal of phosphate to modulate protein function. A subfamily of G-proteins called the heterotrimeric G-proteins are involved in transmembrane signalling by coupling receptors to their effector systems (Sagi-Eisenberg, 1993).

The involvement of G-proteins in mast cell activation was first demonstrated when non-hydrolysable analogues of GTP (such as GTP-γ-S) were introduced into the cytoplasm of mast cells that had been temporarily permeabilised with ATP (Gomperts, 1983). These analogues directly activate G-proteins and, in the presence of extracellular Ca^{2+}, caused mast cell degranulation (Gomperts, 1983). Subsequent studies showed that treatment of RBL-2H3 cells with mycophenolic acid, which decreases endogenous GTP levels, resulted in inhibition of IgE receptor-mediated secretion and Ca^{2+} influx, but the response could be restored by replenishing the GTP pool (Wilson *et al,* 1989). In contrast, treatment of RBL-2H3 cells with cholera toxin, which causes prolonged activation of the Gs protein, resulted in enhanced formation of inositol-trisphosphate, Ca^{2+} influx and secretion (Knoop and Thomas, 1984; McCloskey, 1988; Narashimhan *et al,* 1988). Further studies indicated that activation of G-proteins by GTP-γ-S led to a concomitant activation of phospholipase C (Sagi-Eisenberg, 1993). Taken together, the results of these studies suggest that

two main mechanisms are involved in the activation of phospholipase C and the inositol-trisphosphate pathway in mast cells and RBL-2H3 cells: the first is the activation of phospholipase C by tyrosine phosphorylation; and the second involves the coupling of the receptor to the enzyme by G-proteins.

Evidence that a second G-protein may be involved in the direct stimulation of mast cell secretion came from the observation that in patch-clamped or permeabilised cells, GTP-γ-S could elicit degranulation in the absence of Ca^{2+}, and independent of phospholipase C activation (Fernandez *et al,* 1984; Neher, 1988; Barrowman *et al,* 1986). This latter pertussis toxin-sensitive G-protein, termed G_E, is probably responsible for direct triggering of exocytosis following stimulation of the cells with basic secretagogues such as compound 48/80 or substance P (reviewed in Sagi-Eisenberg, 1993). Aridor et al demonstrated that G_E is likely to be the heterotrimeric G-protein $G\alpha i_3$ (Aridor *et al,* 1993). A similar dependency of the secretory response on G-proteins was seen in human and rat cutaneous mast cells stimulated with the peptides mastoparan and neuropeptide Y (Emadikhiav *et al,* 1995). However, the role of this pathway *in vivo* following aggregation of the IgE receptor is not known.

The inositol trisphosphate pathway

Hydrolysis of phosphatidylinositol 4,5-bisphosphate to inositol trisphosphate and diacylglycerol is a universal signal transduction mechanism used for controlling a variety of cellular processes including secretion, metabolism and cell proliferation (reviewed in Berridge and Irvine, 1984). The key enzymes in this reaction are the phospholipase Cs, which can be divided into four types (α, β, γ, and δ) based on their molecular sizes and amino acid sequences (Rhee *et al,* 1989). Each type of phospholipase C comprises a family of isoenzymes such as γ1 and γ2. As discussed earlier, crosslinking of the IgE receptor can lead to activation of phospholipase C-γ1 by both tyrosine phosphorylation and G-protein coupling.

The hydrolysis of phosphatidylinositol 4,5-bisphosphate by phospholipase C yields two intracellular second messengers with different functions (reviewed in Sagi-Eisenberg, 1993). Inositol 1,4,5-trisphosphate (IP_3) triggers the IP_3 receptor on the endoplasmic reticulum, resulting in release of Ca^{2+} from intracellular stores (Streb *et al,* 1983; Spat *et al,* 1986; Spat *et al,* 1986). The other second messenger, diacylglycerol (DAG), activates a family of serine/threonine kinases collectively known as protein kinase C (Dekker and Parker, 1994).

The role of IP_3 and DAG in signal transduction in RBL-2H3 cells was investigated using the phorbol ester 12-O-tetradeconylphorbyl-13-acetate (TPA) (Gat-Yablonski and Sagi-Eisenberg, 1990). TPA blocked the breakdown of phosphatidylinositol 4,5-bisphosphate to IP_3, and also inhibited the rise in intracellular Ca^{2+} induced by antigen (Gat-Yablonski and Sagi-Eisenberg, 1990). However, TPA did not inhibit secretion at concentrations that completely blocked IP_3 formation, suggesting that IP_3 formation was involved in Ca^{2+} mobilization, but was not essential for exocytosis. More recent studies have suggested that the IP_3 signal induced by FcεRI crosslinking is not sufficient to explain the Ca^{2+} signal in RBL-2H3 cells, and that sphingosine-1-phosphate, an alternative second messenger for intracellular mobilization, is more important (Choi *et al,* 1996).

A number of studies have documented the importance of protein kinase C in the secretory process and proliferation of mast cells (Ozawa *et al,* 1993a; Ozawa *et al,* 1993b; Barane and Razin, 1991; Chaikin *et al,* 1994). Secretion in RBL-2H3 cells could be abolished by inhibiting protein kinase C, but the response was restored by addition of the β and δ isoenzymes, suggesting that these were critical for exocytosis (Ozawa *et al,* 1993a; Ozawa *et al,* 1993b). One possible substrate for protein kinase C in RBL-2H3 cells is myosin (Ludowyke *et al,* 1989). Both myosin light and heavy chains were phosphorylated by protein kinase C in RBL-2H3 cells *in vivo*, and the

time course and extent of the reaction were correlated with histamine secretion (Ludowyke *et al,* 1989).

Ca^{2+} signalling

It has been known for many years that Ca^{2+} plays an important role in exocytosis in mast cells. Foreman and coworkers showed that external Ca^{2+} was essential for secretion (Foreman and Mongar, 1972), that calcium ionophores could elevate intracellular Ca^{2+} and evoke a secretory response (Foreman *et al,* 1973), and that IgE-mediated secretion was accompanied by an uptake of $^{45}Ca^{2+}$ into the cells (Foreman *et al,* 1977). Although secretion in mast cells can be triggered under certain experimental conditions without an increase in intracellular Ca^{2+} (such as internal application of GTP-γ-S or artificial activation of protein kinase C) it seems that under physiological conditions, a rise in intracellular Ca^{2+} is crucial for exocytosis.

The rise in intracellular Ca^{2+} in mast cells arises from two sources. The initial rise that follows crosslinking of the IgE receptor results from Ca^{2+} release from the endoplasmic reticulum. As discussed above, this is triggered by IP_3 (Sagi-Eisenberg, 1993) and sphingosine-1-phosphate (Choi *et al,* 1996). The second source of Ca^{2+} is an influx from the extracellular milieu, and this important pathway will be discussed in more detail in the electrophysiology section of this review.

The effects of the rise in intracellular free Ca^{2+} may be manifested through the calcium binding protein calmodulin. Calmodulin has been detected in association with the granules of rat peritoneal mast cells (Chock and Schmauderchock, 1992), and it may play a critical role in the regulation of intracellular enzymes and cytoskeletal proteins, both of which may be involved in the release process.

Exocytosis

Exocytosis is the last stage in the secretory pathway and involves fusion of the granule membranes with those of the plasma membrane. Although the precise mechanisms by which this occurs are not known, it is likely to involve the cytoskeleton, fusion proteins, and granule swelling. Mast cells possess actin filaments that are located predominantly in a cortical distribution below the plasma membrane (Rohlich, 1975). Following activation of the IgE receptor, the actin filaments are extensively reorganised (Nielsen *et al,* 1989; Nielsen, 1990; Koffer *et al,* 1990), with a centripetal redistribution of F-actin from the periphery to the cell interior (Norman *et al,* 1994). The disassembly of F-actin at the cortex was dependent on a heterotrimeric G-protein, whereas the appearance of actin filaments in the interior was dependent on two small GTPases, rho and rac. Rho was responsible for de novo actin polymerization, whereas rac was required for entrapment of the released cortical filaments (Norman *et al,* 1994). This redistribution of the actin cytoskeleton may facilitate the translocation of granules from the cell interior to the plasma membrane. Contact of the granule membrane with the plasma membrane may be facilitated by Ca^{2+}-dependent fusion proteins such as SNAPS and SNARES (reviewed in Edwardson and Marciniak, 1995), although these mechanisms have not yet been established in mast cells.

A second factor involved in exocytosis may be granule swelling. In one hypothesis, the signal transduction pathways result in an influx of water into the granule whilst it is still inside the cell (Chock and Schmauderchock, 1992). This not only causes granule swelling, which brings the granule membrane closer to the plasma membrane, but also activation of granule enzymes, an osmotic pressure surge, a pH shift and activation of the arachidonic acid cascade (Chock and Schmauderchock, 1992). However, more definitive studies concluded that swelling of the mast cell granule occurred after membrane fusion, resulting from an influx of water through the fusion pore (Zimmerberg *et al,* 1987). In this model, the fusion pore then dilates,

probably due to tension in the secretory granule membrane, and releases the granule contents into the extracellular medium (Monck *et al,* 1991).

A summary of the factors that may be involved in the secretory response of mast cells is shown in Figure 1.3.

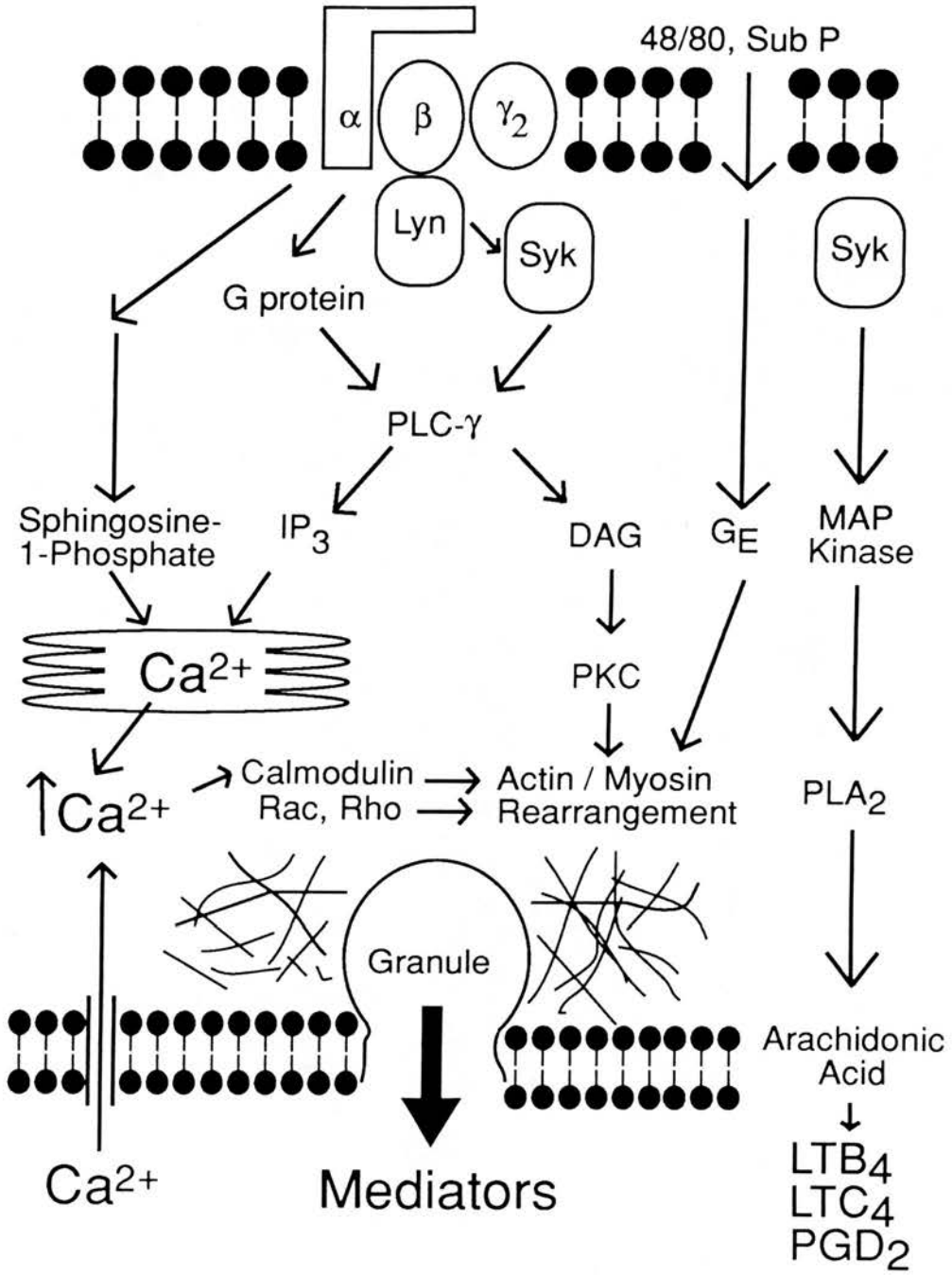

Figure 1.3 - Possible signalling pathways in stimulus-secretion coupling in mast cells. Activation of the IgE receptor subunits ($\alpha\beta\gamma_2$) leads to phosphorylation and activation of Lyn and Syk tyrosine kinases and activation of G proteins. Both pathways can activate phospholipase C-γ (PLC) which leads to the formation of inositol trisphosphate (IP_3) and diacylglycerol (DAG). IP_3, and sphingosine-1-phosphate, liberate Ca^{2+} from intracellular stores which activates the Ca^{2+} influx pathway, whereas DAG activates protein kinase C (PKC). The release of granule mediators may arise due to a rearrangement in the actin/myosin cytoskeleton, brought about by the rise in intracellular Ca^{2+}, PKC and the small G proteins Rac and Rho. The heterotrimeric G protein (G_E) may act in a similar way, possibly by-passing the IgE receptor. The Syk tyrosine kinase also activates a MAP kinase which activates phospholipase A_2 (PLA_2), resulting in the generation of leukotrienes B_4 (LTB_4), C_4 (LTC_4) and prostaglandin D_2 (PGD_2) from arachidonic acid.

ELECTROPHYSIOLOGICAL PROPERTIES OF MAST CELLS

In recent years, the electrophysiological properties of many isolated mammalian cells have been studied using the tight-seal whole-cell recording configuration of the patch-clamp technique (Hamill *et al,* 1981). Mast cells have been a common subject for such studies for two reasons. First, because mast cells are a valuable model for studying the basic mechanisms involved in cellular secretion; and second because the ion channels and ionic fluxes across the plasma membrane are critically involved in the process of degranulation, the principle effector function of mast cells. Hence, a knowledge of the ionic conductances in mast cells may ultimately lead to new anti-allergic drugs that specifically target ion channels.

Recent electrophysiological studies have identified a number of different ion channels in mast cells. The presence or absence of these currents depended on the phenotype of the mast cell (connective tissue or mucosal), the species from which the cells were derived, and whether the cells were in the resting state or stimulated with second messengers or secretagogues.

Ionic Conductances in Resting Mast Cells

In three recent studies, rat mast cells derived from bone marrow stimulated with recombinant IL-3 (McCloskey and Qian, 1994) and RBL-2H3 cells (Lindau and Fernandez, 1986b; Qian and McCloskey, 1993), both mucosal phenotypes, possessed only an inwardly rectifying K^+ (IR_K) current in the resting state. This current was shown to set the resting membrane potential of RBL-2H3 cells at about -90 mV. In contrast, rat peritoneal mast cells, a connective tissue phenotype, had no significant membrane currents in the resting state, and had a membrane potential close to zero (Lindau and Fernandez, 1986b; McCloskey and Qian, 1994). Mouse bone marrow-derived mast cells (BMMCs), which can potentially differentiate into both mucosal and connective tissue phenotypes, possessed two different currents (Kuno *et al,* 1995). A K^+ selective inwardly rectifying current was present in 36% of the cells, and

an outwardly rectifying Cl^- (OR_{Cl}) current was present in 46% of cells (Kuno *et al,* 1995). In individual cells, the two currents could be observed either concurrently or individually, but some cells (40%) appeared electrically quiescent, displaying neither the IR_K nor the OR_{Cl} current. In the mouse system, both the IR_K and the OR_{Cl} currents were involved in regulation of the resting membrane potential, which ranged from -66 to +6.4 mV with a mean and s.d. of -23 ± 25 mV (Kuno *et al,* 1995).

Ionic Conductances in Stimulated Mast Cells

Other membrane currents have been described in rat mast cells but only when the cells were stimulated with secretagogues or if various second messengers were included in the pipette solution. These messenger or ligand activated channels include: Ca^{2+} permeable channels; cation-selective channels; outwardly rectifying chloride channels; and outwardly rectifying K^+ channels.

Ca^{2+} permeable channels

Elevation of cytoplasmic free calcium ($[Ca^{2+}]_i$) is considered to play an important role in stimulus-secretion coupling in mast cells (Foreman *et al,* 1973; Ishizaka *et al,* 1979; Ishizaka *et al,* 1980; White *et al,* 1984; Millard *et al,* 1988; Gericke *et al,* 1995; Habara and Kanno, 1996). Although the initial rise in $[Ca^{2+}]_i$ occurs via release from intracellular stores (Neher and Almers, 1986; Millard *et al,* 1989), entry of Ca^{2+} through the plasma membrane is required to initiate secretion (MacGlashan and Botana, 1993; Williams *et al,* 1990). In early studies, changes in membrane conductance that might account for the Ca^{2+} influx pathway could not be identified when rat peritoneal mast cells (Lindau and Fernandez, 1986b; Lindau and Fernandez, 1986a) or RBL-2H3 cells (Lindau and Fernandez, 1986b) were stimulated with antigen. However, in recent patch-clamp studies, a specific Ca^{2+} influx-pathway was activated in rat peritoneal mast cells when the cells were stimulated with intracellular inositol 1,4,5-trisphosphate (IP_3) or extracellular agonists such as compound 48/80 or substance P (Kuno *et al,* 1989; Matthews *et al,* 1989b). In contrast to electrical

excitable cells such as bovine chromaffin cells (Penner and Neher, 1988), the Ca^{2+} influx in mast cells was not activated by depolarization but was increased by hyperpolarization (Matthews *et al,* 1989b; Kuno *et al,* 1989).

The Ca^{2+}-selective entry pathway was subsequently shown to be activated by depletion of intracellular Ca^{2+} stores (Hoth and Penner, 1992; Hoth and Penner, 1993) and termed I_{CRAC} (for calcium release-activated calcium current). The link between the filling state of the intracellular Ca^{2+} stores and the Ca^{2+} channels in the plasma membrane has not yet been elucidated (Fasolato *et al,* 1994). However, the activation mechanism of I_{CRAC} appears to involve a diffusible cytosolic factor (Fasolato *et al,* 1993; Innocenti *et al,* 1996), a monomeric (Fasolato *et al,* 1993) or heterotrimeric (Xu *et al,* 1995) GTP-binding protein (Fasolato *et al,* 1993), and it can be inhibited by protein kinase C (Parekh and Penner, 1995) and ADP (Innocenti *et al,* 1996). It appears that the Ca^{2+} influx factor (CIF) described by Randriamampita and Tsien (1993) does not activate I_{CRAC} (Penner, personal communication). Under experimental conditions closely approximating physiological (perforated-patch technique at 37°C), the I_{CRAC} could also be activated by crosslinking of the IgE receptor, demonstrating its importance in stimulus-secretion coupling (Zhang and McCloskey, 1995).

The single channel conductance of the Ca^{2+} release activated channel is extremely small and could not be measured in mast cells using variance analysis, although it was estimated to be well below 1 pS (Hoth and Penner, 1993). In Jurkat T-lymphocytes, which also possess I_{CRAC}, the single channel conductance was only 9 fS in an extracellular solution containing 2 mM Ca^{2+} (Zweifach and Lewis, 1993). Recent studies have suggested that proteins encoded by the *trp* homologue genes in mice might represent functional subunits of the Ca^{2+} release activated Ca^{2+} channel, not unlike those of classical voltage-gated ion channels (Zhu *et al,* 1996).

Cation selective channels

In addition to the specific Ca^{2+} permeable channels described above, mast cells also possess a second pathway through which Ca^{2+} may enter the cell. Stimulation of rat peritoneal mast cells with compound 48/80 (Matthews *et al,* 1989b; Kuno *et al,* 1989; Fasolato *et al,* 1993) or intracellular guanosine 5'-O-3-thiotriphosphate (GTP-γ-S) (Matthews *et al,* 1989b) activated a large-conductance cation channel with a conductance of 50 pS. Although these channels had a much larger conductance than the Ca^{2+} permeable channels described above, they only partially contributed to the plateau phase of elevated $[Ca^{2+}]_i$ occurring after stimulation, probably due to low specificity (Fasolato *et al,* 1993). However, because they are inhibited by $[Ca^{2+}]_i$, they may play a greater role under conditions of low $[Ca^{2+}]_i$ (Matthews *et al,* 1989b).

Outwardly rectifying chloride channels

In contrast to mouse bone marrow-derived mast cells, outwardly rectifying Cl^- currents have only been described in rat mast cells following stimulation with secretagogues or intracellular messengers. In rat peritoneal mast cells, external stimulation with compound 48/80 (Matthews *et al,* 1989a) or substance P (Matthews *et al,* 1989a; Janiszewski *et al,* 1994), or internally applied cyclic AMP (Matthews *et al,* 1989a; Dietrich and Lindau, 1994) or GTP-γ-S (Matthews *et al,* 1989a) resulted in the slow development of an outwardly rectifying Ca^{2+}-dependent Cl^- current. The channel had a unitary conductance of 1-2 pS (estimated from noise analysis) and could be blocked by the chloride channel blockers 4,4'-diisothiocyano-2,2'-stilbenedisulfonate (DIDS) (Matthews *et al,* 1989a; Dietrich and Lindau, 1994) and 5-nitro-2-(3-phenylpropylamino) benzoic acid (NPPB) (Janiszewski *et al,* 1994).

A single channel study of cell-attached patches of RBL-2H3 cells also revealed a slowly activating Cl^- channel with a conductance of 32 pS and an increasing open-state probability with increasing depolarization (Romanin *et al,* 1991). This channel could be activated by stimulating the cell-attached patches with antigen or a

monoclonal antibody specific for the FcεR1 receptor. In addition, inhibition of the Cl^- channel with NPPB or the anti-allergic drug disodium cromoglycate also inhibited serotonin secretion, suggesting that the current was involved in stimulus-secretion coupling. The difference in the two single channel conductances described above has yet to be explained, although the possibility exists that more than one type of Cl^- channel is present in mast cells.

The outwardly rectifying Cl^- current may play a role in regulation of the membrane potential during degranulation (Matthews *et al,* 1989a). In the absence of any other conductance, activation of the Ca^{2+} influx pathways described above would tend to depolarise the cell (Penner *et al,* 1988). The membrane potential would then approach the reversal potentials of the respective agonist-activated conductances i.e. positive values for the calcium specific pathway or close to 0 mV for the non-selective cation conductance (Penner *et al,* 1988). However, activation of the Cl^- current resulted in hyperpolarization of rat peritoneal mast cells to about -40 mV, a value probably in the region of the Cl^- reversal potential (Penner *et al,* 1988). This would tend to clamp the membrane potential at a sufficiently negative value to support the hyperpolarization-driven Ca^{2+} influx (Matthews *et al,* 1989a; Penner *et al,* 1988). Further evidence for this hypothesis was provided by studies demonstrating $^{36}Cl^-$ influx during antigen stimulated degranulation (Glenert *et al,* 1993; Friis *et al,* 1994).

Outwardly rectifying K^+ channels

An outwardly rectifying K^+ current was recently described in RBL-2H3 cells (Qian and McCloskey, 1993) and rat BMMCs grown in the presence of rat recombinant IL-3 (McCloskey and Qian, 1994). This current was not observed in rat peritoneal mast cells, providing a further indication of heterogeneity. Unlike the K^+ selective inwardly rectifying current, which was constitutively active, the outwardly rectifying K^+ current was activated by intracellularly applied GTP-γ-S or extracellularly applied

adenosine 5'-[β-thio]diphosphate (ADP) or adenosine 5'[β,γ-methylene]triphosphate (ATP). Activation of this current was inhibited by pertussis toxin, implicating mediation by a G protein. Once activated, the current passed outward current at depolarised potentials and could therefore counteract the depolarising Ca^{2+} currents described above in a similar way to that proposed for the outwardly rectifying Cl^- channel. It was concluded that adenosine nucleotides released at sites of inflammation by platelets, endothelial cells or injured tissue might modulate the mast cell response by inducing the outwardly rectifying K^+ current, thus contributing to the negative membrane potential required for exocytosis.

Volume-activated Cl^- channels

A volume-activated Cl^- current was recently described in RBL-2H3 cells (Nilius *et al,* 1994). The current was outwardly rectifying and could be induced by placing the cells in a hyposmotic extracellular solution. At positive potentials, a large outward current was passed, but there was virtually no current activation at negative voltages. The current showed rapid run-down suggesting a dependency on an intracellular factor. The single channel conductance of the volume-activated Cl^- channels was approximately 6 pS, and they were blocked by 5-nitro-2-(3-phenylpropylamino)-benzoic acid (NPPB). It was hypothesised that, as in other cell types, the current was activated by stretching of the membrane, and probably played a role in the regulation of cell volume (Nilius *et al,* 1994).

BACKGROUND TO THESE STUDIES

The role of mucosal mast cells in intestinal immune responses

Previous work in this laboratory and others has focused on the immune responses to gastrointestinal helminths, with particular emphasis on the role of the intestinal mucosal mast cell (MMC). As described earlier in this chapter, intestinal MMCs

represent a distinct subpopulation of cells with specific functional and biochemical characteristics. For example, MMCs differ from connective tissue mast cells in their T cell dependency (Nawa and Miller, 1979), response to secretagogues (Befus *et al,* 1982), and in their content of proteoglycans (Enerback, 1987) and granule proteases (Gibson and Miller, 1986). Unlike rat connective tissue mast cells (such as peritoneal and cutaneous mast cells) which contain RMCP-I, rat MMCs contain the highly soluble granule chymase RMCP-II (Gibson and Miller, 1986).

The importance of MMCs in intestinal immune responses was suggested by *in vivo* studies in which infection of normal mice and rats with intestinal nematodes such as *Nippostrongylus brasiliensis* or *Trichinella spiralis* induced a marked mastocytosis in the intestinal lamina propria (Miller and Jarrett, 1971; Befus and Bienenstock, 1979; Nawa and Miller, 1979). Furthermore, histological and ultrastructural changes indicative of mast cell discharge were observed during expulsion of *N brasiliensis* in rats (Miller, 1971). Subsequent studies demonstrated that rat intestinal MMCs were functionally active during nematode expulsion, releasing RMCP-II into both the gut lumen and the systemic circulation (Miller *et al,* 1983; Woodbury *et al,* 1984). Systemic release of mouse mast cell protease-I (Tuohy *et al,* 1990; Huntley *et al,* 1990b) and sheep mast cell protease (Huntley *et al,* 1987) was also observed following activation of the intestinal mucosal mast cell population by nematode infections in the respective species. Using an *ex vivo* perfusion model, Scudamore et al. (1995a) demonstrated basal secretion and anaphylactic release of RMCP-II into the rat jejunal lumen before and after challenge with *N. brasiliensis* worm antigen. Furthermore, RMCP-II release during anaphylaxis was associated with the rapid development of paracellular permeability to macromolecules, suggesting a specific functional role for the protease *in vivo* (Scudamore *et al,* 1995b). Hence, the release of RMCP-II is a physiologically relevant marker for mucosal mast cell activation *in vivo*, and can therefore be used to monitor mast cell secretory function *in vitro*.

Characterisation of MMC and BMMC function *in vitro*

The initial characterisation of the properties of intestinal MMCs was based on *in vitro* studies, using mast cells isolated from the rat intestinal mucosa (Befus *et al,* 1982; Pearce *et al,* 1982; Lee *et al,* 1985a). However, the techniques used for isolation and purification of mast cells from the gut are laborious, and can give variable results (Befus *et al,* 1982; Lee *et al,* 1985a). In contrast, the *in vitro* study of MMC function was greatly facilitated when techniques were developed to culture mast cells to homogeneity from rat bone marrow using cytokines derived from T lymphocytes of *Nippostrongylus brasiliensis* infected rats (Haig *et al,* 1982; Haig *et al,* 1988). These bone marrow-derived mast cells (BMMCs) have been extensively characterised, and in all respects so far studied, they are identical to rat intestinal MMCs. For example, like MMCs, they possess the MMC protease rat mast cell protease-II (RMCP-II). They also contain a predominantly non-heparin proteoglycan and low levels of histamine (McMenamin *et al,* 1987; Ortega *et al,* 1988; Broide *et al,* 1988). In addition, they share similar functional characteristics including the release of RMCP-II and β-hexosaminidase following challenge with anti-IgE or specific antigen (Broide *et al,* 1988; MacDonald *et al,* 1989), but are resistant to the effects of compound 48/80 (Broide *et al,* 1988; Befus *et al,* 1982). Hence, functional and biochemical characterisation of rat BMMCs has demonstrated that they are useful models for studying MMCs *in vitro*. Such studies are important for elucidating the mechanisms that might be involved in gastrointestinal immune responses; they contribute to the growing body of knowledge on mast cell heterogeneity; and they can provide an insight into the role of MMCs in various disease states in the gut or other tissues.

Aims of this study

Despite the advances made in the above studies, a number of important aspects of BMMC function have yet to be explored. For example, the cytokine regulation of IgE-dependent secretion of RMCP-II by BMMCs is currently poorly understood. As

described earlier, many aspects of mast cell function are influenced by SCF, the ligand for the *c-kit* tyrosine receptor. Rat intestinal MMCs proliferate in response to systemic injections of SCF (Tsai *et al,* 1991a), and SCF contributes to the MMC hyperplasia seen in rats infected with *Nippostrongylus brasiliensis* and *Trichinella spiralis* (Newlands *et al,* 1995). In addition, SCF vigorously promotes the *in vitro* growth of rat BMMCs over a period of 7 - 14 days (Haig *et al,* 1994; Tei *et al,* 1994). Furthermore, in addition to its effects on growth and development, SCF can influence the serine protease expression by rat peritoneal mast cells and BMMCs *in vitro* (Haig *et al,* 1994), prevent apoptosis in IL-3- (Mekori *et al,* 1993; Iemura *et al,* 1994) or SCF- (Iemura *et al,* 1994) dependent mast cells, and induce or enhance mediator release from a variety of mast cell types including mouse and human skin, mouse and rat peritoneal, and human lung and intestinal mast cells (Wershil *et al,* 1992; Columbo *et al,* 1992; Coleman *et al,* 1993; Nakajima *et al,* 1992; Bischoff and Dahinden, 1992; Bischoff *et al,* 1996). One of the aims of this study, therefore, was to further characterise the IgE-dependent release of RMCP-II from rat BMMCs, and to determine the effect of SCF on their secretory response. This was achieved using a combination of conventional mediator release assays, and a novel enzyme-linked immunospot (ELISPOT) assay, developed to detect the release of RMCP-II from individual BMMCs (these experiments are described in chapters 3 and 4).

A second aspect of BMMC function that has not been investigated is their electrophysiological properties. As described earlier, the ionic conductances of mast cells are important both in the resting state, and following activation of the IgE receptor. Also, the presence of ionic conductances in mast cells depends on their phenotype, providing further evidence of heterogeneity. However, the studies of mucosal type mast cells to date have used either the neoplastic RBL-2H3 cell line (Lindau and Fernandez, 1986b; Qian and McCloskey, 1993) or rat BMMCs grown in rat recombinant IL-3 (McCloskey and Qian, 1994). RBL-2H3 cells are not true functional analogues of intestinal MMCs, and the recombinant IL-3 culture system

has not been extensively characterised in the rat. Hence, neither of these cell types are ideal for investigating the function of intestinal MMCs. Furthermore, most of the electrophysiological studies of mast cells have been performed using the conventional whole-cell recording technique (Hamill *et al,* 1981). This method causes "washout" of the cytoplasm which could prevent the detection of messenger-dependent currents (Horn and Marty, 1988). Hence, a second aim of these studies was to characterise the electrophysiological properties of rat BMMCs using the amphotericin B perforated-patch technique (Rae *et al,* 1991). This technique preserves the cell's cytoplasm, thus allowing a full complement of second messengers and enzymes to be retained (Horn and Marty, 1988). Therefore, the results obtained with this method, and in rat BMMCs, should be more analogous to the electrophysiological properties of rat intestinal MMCs than those obtained in previous studies (these experiments are described in chapter 5).

Chapter 2

MATERIALS AND METHODS

CULTURE AND ISOLATION OF MAST CELLS

2.1 - Reagents and Solutions

The following solutions were obtained from Gibco-BRL Life Technologies, Paisley, UK: Iscove's modified Dulbecco's medium, without supplements, with L-glutamine (IMDM); RPMI 1640 medium with 20 mM HEPES buffer (RPMI); Hanks balanced salt solution, without calcium, magnesium, phenol red (HBSS); 10 x Hanks balanced salt solution without calcium, magnesium, with phenol red (x10 HBSS). A batch of heat-inactivated horse serum (HS) previously shown to support mast cell growth was obtained from Advanced Protein Products, Brierly Hill, UK. Foetal calf serum (FCS) was batch tested and subsequently purchased from either Serotec, Oxford, UK or Gibco-BRL. Penicillin 10,000 units/ml and Streptomycin 10,000 μg/ml (P/S) was obtained from Gibco-BRL and used at dilution of 1:100 unless stated otherwise. Percoll was obtained from Pharmacia, St. Albans, UK. Phosphate buffered saline (PBS) was prepared as described in Appendix 1.

2.2 - Cell Culture

Unless stated otherwise, all cells were cultured in plastic tissue-culture treated flasks with vented caps. 175 cm^2 flasks were obtained from Nunclon, Gibco-BRL, and 162 cm^2, 75 cm^2, and 25 cm^2 flasks were obtained from Costar, Cambridge, MA, USA. Cells were cultured in a CO_2 incubator at 37°C in a humidified atmosphere of 5% CO_2 in air.

2.3 - Cell handling and washing

For washing and other manipulations, cells were decanted into 50 ml or 15 ml plastic centrifuge tubes (Costar). Cells were washed by centrifugation at 200 x g for 7

minutes at room temperature (18 - 20°C) followed by resuspension in the appropriate medium (see specific sections). Unless stated otherwise, this procedure was repeated three times.

2.4 - Cell counting and viability

Cells were counted in an improved Neubauer haemocytometer after mixing 10 µl of cell suspension with an equivalent volume of 0.2% nigrosine. Viability was assessed based on nigrosine exclusion. For initial counts of nucleated bone marrow cells, 10 µl of cell suspension was also diluted 50:50 in white blood cell counting fluid (0.01% Gentian violet in 3% acetic acid in distilled water).

2.5 - Cytospin and Staining

To determine the percentage of mast cells in either bone marrow cultures or peritoneal cell preparations, 100µl of a cell suspension containing approximately 2 - 5 x 10^5 cells/ml was centrifuged for 5 minutes at 600 rpm onto a glass slide in a cytocentrifuge (Shandon Cytospin 2, Southern Instruments LTD., Runcorn, UK). After air drying, the slides were stained with 100% Leishman's solution for two minutes followed by 50% Leishman's solution for a further six minutes (obtained by adding an equal volume of distilled water to the slide). The slides were then well rinsed in tap water, air dried and mounted with DPX mountant (BDH, Poole, UK). This procedure stained mast cell granules purple allowing easy discrimination from contaminating cells. The percentage of mast cells on each slide was determined by counting 400 cells in randomly chosen high power fields.

2.6 - Experimental Animals

Male Wistar rats were obtained from either Bantam and Kingman Universal, Hull, UK or the Moredun Research Institute, Edinburgh, UK and were fed a standard pelleted diet and given water *ad libitum*. For collection of bone marrow, peritoneal washes or for preparation of lymph node conditioned medium, rats weighing between

150g and 250g were deeply anaesthetised in an induction chamber containing 4% halothane (Rhone Merieux, Dublin, Ireland) and killed by exsanguination followed by cervical dislocation.

2.7 - *Nippostrongylus Brasiliensis* Larval Culture

A larval culture of the intestinal nematode *Nippostrongylus brasiliensis* was maintained throughout these studies. To perpetuate the culture, lightly anaesthetised rats were infected with 3000 - 4000 third stage larvae by subcutaneous injection in the neck. On day six of infection, the rats were transferred to cages containing grids overlying moist paper towels. After 24 hours, the faecal pellets were collected and an egg count was performed. 3g of faeces was mixed with 45 ml of saturated NaCl and the resulting suspension was added to a McMaster counting chamber. A good infection normally yielded 50,000 eggs per gram. The remaining faeces were mixed with distilled water to form a slurry, and charcoal granules (Fisons, Loughborough, UK) were gradually added until a black, semi-moist consistency was formed. Small, compact mounds of the charcoal/faeces mixture were placed onto the centre of moistened, round, 5.5 cm diameter filter papers (No. 1, Whatman International, Maidstone, UK) in the base of petri dishes and incubated in a sealed, humid chamber at 26°C. The larvae hatched within a few days and were viable for 4 - 8 weeks.

2.8 - Infection of Rats with *Nippostrongylus brasiliensis*

Infective third stage larvae (≥ 7 days old) were obtained by adding drops of a 0.9% NaCl solution at 37°C to the charcoal/faecal mounds until a small quantity of solution collected at the bottom of the petri dishes. The solution containing the larvae was aspirated and filtered through a single layer of paper towel (Kimwipes, Kimberley Clark Corp., Clwyd, UK) supported by a sieve into a funnel filled with additional NaCl solution. The larvae gravitated to the bottom of the funnel and accumulated in a clamped silicone tube. The clamp was then released and the larvae were transferred to a 15ml centrifuge tube. The larvae were washed twice by

removing the supernatant and resuspending in fresh NaCl solution. The number of live larvae in 20μl of solution was counted under a dissecting microscope and the volume of the remaining solution was adjusted to give a final density of 6000 larvae per ml. Rats were infected with 3000 - 4000 larvae as described above.

2.9 - Preparation of lymph node conditioned medium

Lymph node conditioned medium (LNCM) was prepared using 8 to 15 rats on day 15 of a primary infection with *Nippostrongylus brasiliensis*. The mesenteric lymph nodes were excised and placed in sterile RPMI containing 5% FCS and P/S. After removing excess fat under sterile conditions, the nodes were finely chopped with scissors and transferred to a sterile stomacher bag (Seward Medical, London, UK) in about 15 ml of the above medium. The lymphocytes were mechanically dispersed using a stomacher (Seward Medical) at high speed for approximately two minutes. The resulting cell suspension was filtered through two layers of sterile lens tissue into 50ml centrifuge tubes, and washed four times in the above medium. The lymphocytes were counted and resuspended in serumless IMDM (Appendix 1) at a concentration of 4 x 10^6 viable cells/ml and stimulated with 3μg/ml concanavalin A. After incubating at 37°C for 48 - 72 hours, the supernatant was separated from the cells by centrifugation and stored at -20°C until used.

Batches of LNCM were initially tested for their ability to stimulate the growth of mast cells from rat bone marrow in 12 well tissue culture plates (Costar). The cells were stimulated with 10, 20 or 30% v/v LNCM, and batches supporting the growth of 10 - 30% mast cells by day 7 were considered acceptable. These batches were then used in bone marrow mast cell cultures (see below - 2.10) at an optimum concentration of 15 - 25%. Twenty two batches of LNCM were prepared during the course of these studies, of which 19 were used. Nine batches supported excellent mast cell growth, whereas the others were either poor (n=5) or totally ineffective (n=5), usually resulting in cultures containing only macrophages. The source of this

variation was never determined but it probably reflected variation in the content of cytokines in the LNCM such as IL-3, IFN-γ or GM-CSF.

2.10 - Culture of bone marrow-derived mast cells (BMMCs)

The hindlimbs of a non-infected rat were dissected to expose the femurs. The cartilaginous growth plates above the stifle joints were disarticulated and the bones were removed close to the hip joint using bone forceps. A 5ml syringe containing IMDM, 20% HS, and P/S was attached to a 19 gauge needle and used to flush the bone marrow out of the bone lumen into a universal container. The cell suspension was mixed by repeated aspiration and filtered through two layers of sterile lens tissue into a 50ml centrifuge tube. The cells were washed three times in the above medium, and counted and assessed for viability as described earlier (section 2.4). The cells were initially cultured at 2.5 x 10^5 viable cells/ml with 15 - 25% batch-tested LNCM for the first 5 days. They were then resuspended at 5 x 10^5 cells/ml in fresh medium containing 10 -25% LNCM every 2 - 5 days depending on cell density and pH of the medium (as assessed by the colour of the phenol red).

Thirty seven BMMC cultures were set up during the course of these studies. Twenty cultures progressed to maturity, containing virtually homogeneous populations of mast cells. The other cultures failed to develop, probably due to deficiencies in the LNCM (see section 2.9). Figure 2.1 shows Leishman-stained cytospin preparations from a successful bone marrow culture at 0, 4, 11 and 15 days after addition of LNCM. At day 0, the expected mixture of bone marrow cells is present including neutrophils, monocytes, lymphocytes and megakaryocytes (Figure 2.1A). At day 4, a small number of granulated mast cells have developed (Figure 2.1B arrows), and these proliferate to form clumps by day 11 (Figure 2.1C). At day 15, the culture contains predominantly mast cells that possess large numbers of purple-staining granules (Figure 2.1D). The growth characteristics of six representative successful cultures, and the accumulation of the mucosal mast cell specific granule chymase, rat

mast cell protease II (RMCP-II), are shown in Figure 2.2. The mast cells developed rapidly initially, representing approximately 85% of the total cells by days 10 - 15 of culture. After this, the percentage of BMMCs increased slowly to almost 100%. The cultures survived for up to 30 - 40 days, depending on cell usage, but were not viable after this time. The concentration of granule RMCP-II in developing BMMCs, measured by ELISA of freeze-thawed cell pellets (see sections 2.17 and 2.18 below), increased from 3.4 ± 0.3 pg/cell at day 4 to 30.4 ± 3 pg/cell at day 28 (Figure 2.2 - data points represent the mean ± s.e.m. of 12 - 24 cell pellet assays from two cultures).

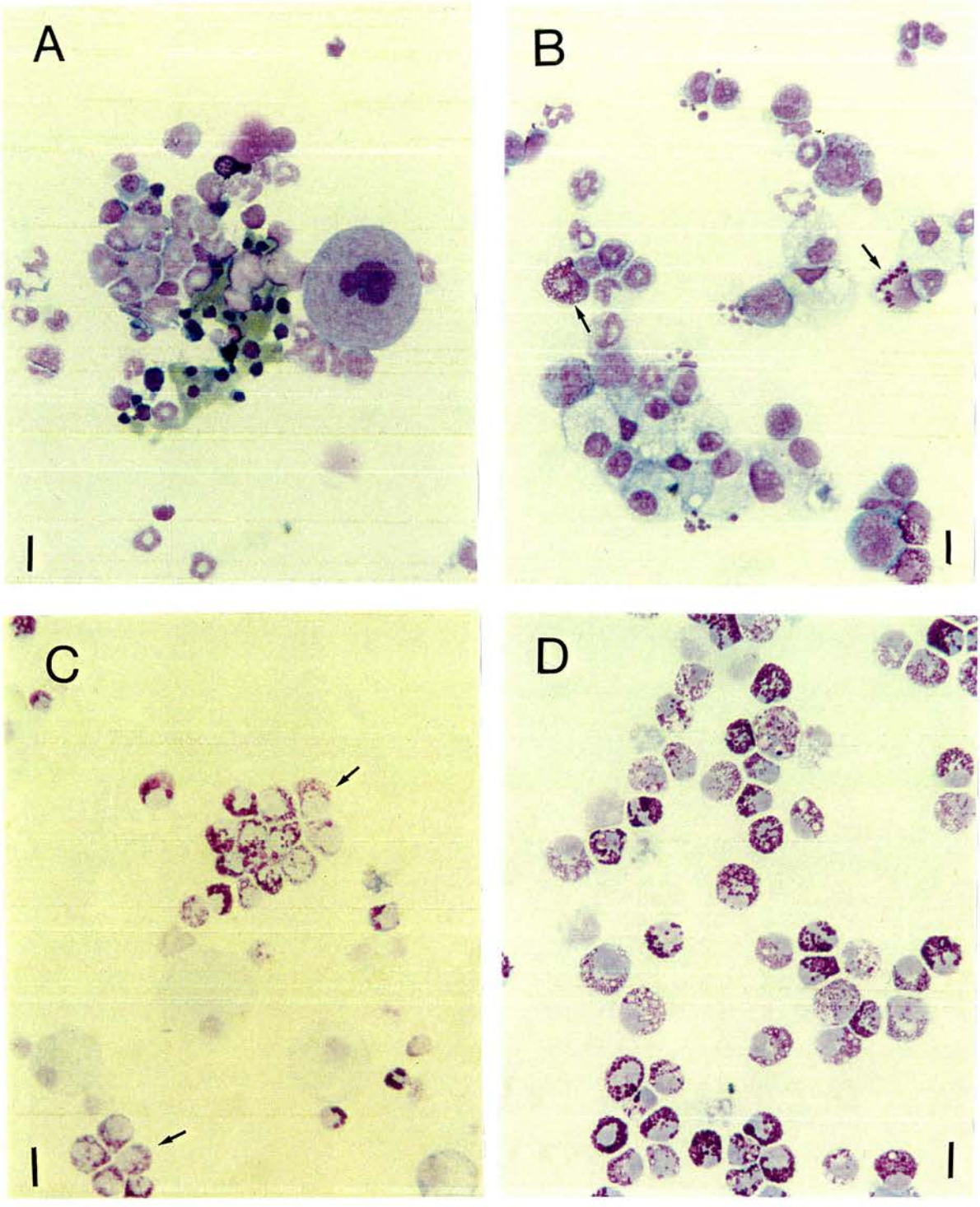

Figure 2.1 - Leishman's-stained cytospin preparations of a representative rat bone marrow culture.
A: Day 0, before addition of the lymph node conditioned medium (LNCM).
B: Day 4 of culture. Two developing mast cells are marked by arrows.
C: Day 11 of culture. Individual mast cells are present in addition to two mast cell colonies (arrows).
D: Day 15 of culture. The culture contains predominantly mast cells, with a few residual monocytes. Scale bars = 10 μm.

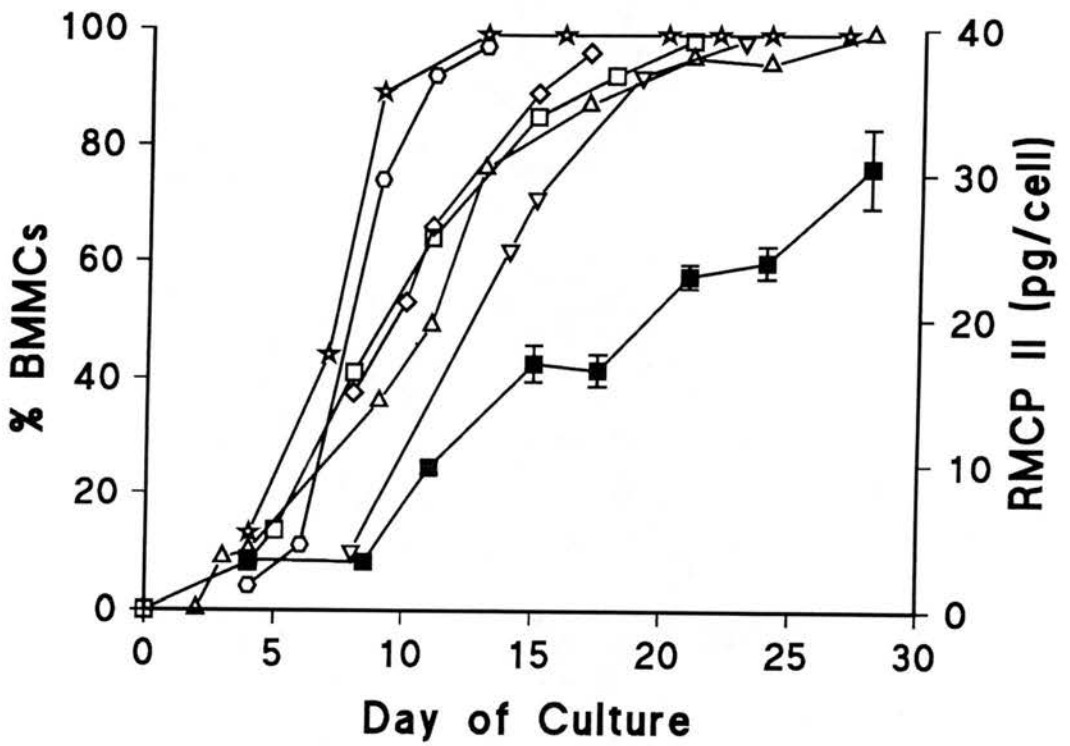

Figure 2.2 - Development of six successful rat bone marrow cultures showing the typical kinetics of BMMC growth (left axis and open symbols). The percentage of BMMCs increases rapidly until the cultures contain approximately 85% BMMCs. After this, the number of BMMCs increases more slowly until the cultures contain virtually 100% mast cells. The cultures lasted for up to 30 - 40 days. Mean RMCP-II concentration in individual mast cells (right axis and solid squares) was determined by ELISA of freeze-thawed cell pellets. The data from two cultures has been combined so that each data point represents the mean ± s.e.m. of 12 - 24 cell pellet assays from one, or both, of the cultures.

2.11- Isolation and purification of rat peritoneal mast cells

Peritoneal mast cells were collected by injecting 20ml of HBSS containing 2% FCS, penicillin/streptomycin and 10 units/ml heparin into the abdominal cavity. After gentle massage, the abdomen was carefully opened and the fluid containing 5 - 10 % mast cells was collected using a sterile pastette (Figure 2.3A). The cells were washed twice in the above solution and resuspended in 1ml of 30% Percoll. The mast cells were then purified using a two stage Percoll density step gradient consisting of 4ml of 1.09 g/ml layered on top of 2ml of 1.1 g/ml. After centrifugation at 500 x g for 20 minutes, the Percoll was removed and a pellet containing > 95% mast cells was obtained (Figure 2.3B). The cells were washed three times in HBSS to remove residual Percoll and finally resuspended at a concentration of 2 - 4 x 10^5 cells/ml in RPMI containing 10% FCS and P/S. This medium was chosen because IMDM, as used for the BMMC cultures, appeared to be cytotoxic to rat peritoneal mast cells (experimental evidence for this is presented in appendix 2). A direct comparison of the morphology of rat peritoneal mast cells and rat BMMCs is shown in Figure 2.3 (C and D respectively). Rat BMMCs were slightly smaller than rat peritoneal mast cells, and were more sparsely granulated.

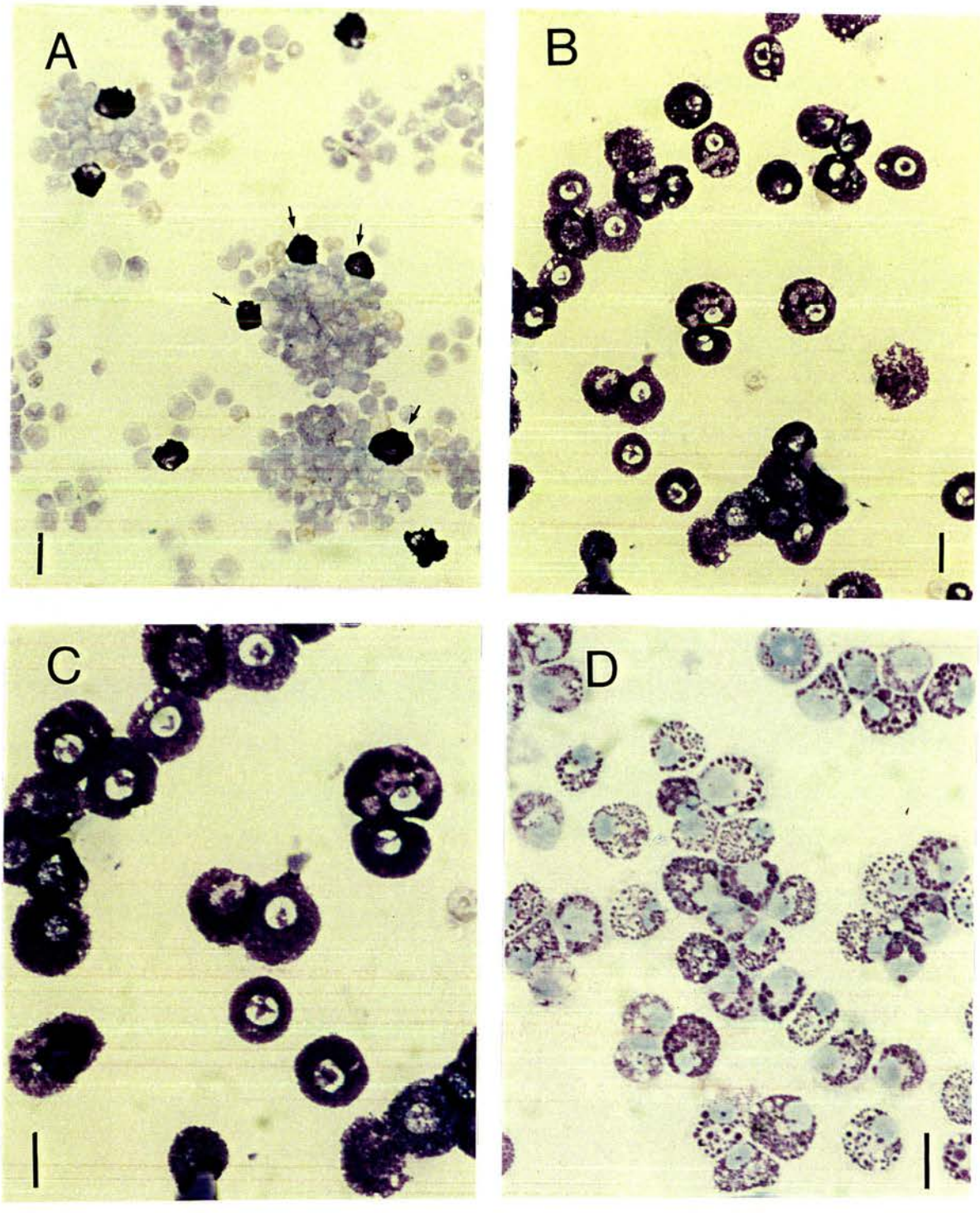

Figure 2.3 - **A**: Leishman's-stained cytospin preparation of rat peritoneal lavage fluid. 20 ml of HBSS/2%FCS/PS/Heparin was injected into the abdominal cavity. After gentle massage, the fluid was collected using a sterile pastette. The preparation contains 5-10% mast cells (arrows).
B: Leishman's-stained cytospin preparation of Percoll purified rat peritoneal mast cells (see text for details). The preparation contains >95% mast cells.
C and **D**: A comparison of the morphology of rat peritoneal mast cells (C) and rat BMMCs (D). The BMMCs are more sparsely granulated and slightly smaller.
Scale bars = 10 μm.

IMMUNOLOGICAL STUDIES

2.12 - Reagents and Solutions

The following solutions were used for immunological studies. Chemicals were obtained from BDH, and bovine serum albumin (BSA) was obtained from Sigma, Poole, UK. Foetal calf serum (FCS) for use in flow cytometry buffer (section 2.13) was purchased from either Serotec, Oxford, UK or Gibco-BRL.

Tyrode's Buffer (TB)	Tyrode's Buffer/Ca^{2+}/Mg^{2+} (TB^{+})	Tyrode's Buffer/EDTA (TB/EDTA)
137 mM NaCl	137 mM NaCl	137 mM NaCl
2.7 mM KCl	2.7 mM KCl	2.7 mM KCl
0.4 mM NaH_2PO_4	0.4 mM NaH_2PO_4	0.4 mM NaH_2PO_4
5.6 mM glucose	5.6 mM glucose	5.6 mM glucose
0.25% w/v BSA	0.25% w/v BSA	0.25% w/v BSA
10 mM HEPES	10 mM HEPES	10 mM HEPES
pH 7.25 - 7.35	**1 mM $CaCl_2$**	**4 mM EDTA**
	1 mM $MgCl_2$	pH 7.25 - 7.35
	pH 7.25 - 7.35	

2.13 - Analysis of surface bound IgE by flow cytometry

BMMCs were labelled with fluorescein isothiocyanate (FITC) -conjugated anti-rat IgE (Mare-1-FITC, Serotec, Oxford, UK) or, following sensitisation with mouse IgE anti-DNP (SPE-7, Sigma), rat anti-mouse IgE-FITC (LO-ME-3, Serotec) as described in detail in chapter 3 (section 3.1). The labelled cells were examined by flow cytometry which was performed by Mr. Andrew Sanderson, Institute of Cell, Animal and Population Biology, Department of Biological sciences, University of Edinburgh using a FACscan (Becton Dickinson, Oxford, UK). The machine was set for the population of cells to be analysed by ensuring that forward scatter, side scatter

and fluorescence fell within the analytical range of the instrument. The same settings were used for each analysis, allowing comparisons between different cell populations. The machine was gated so that cellular debris and red blood cells were not registered. In addition, a further gate was applied after the experimental run to exclude extreme outliers and possible dying cells from the analysis (Figure 2.4). Each population of cells from each culture tested comprised 10^5-10^6 cells and each flow cytometric analysis was based on 10^4 cells. Results were displayed as histograms with log fluorescence intensity along the *x*-axis (arbitrary units) and number of cells on the *y*-axis.

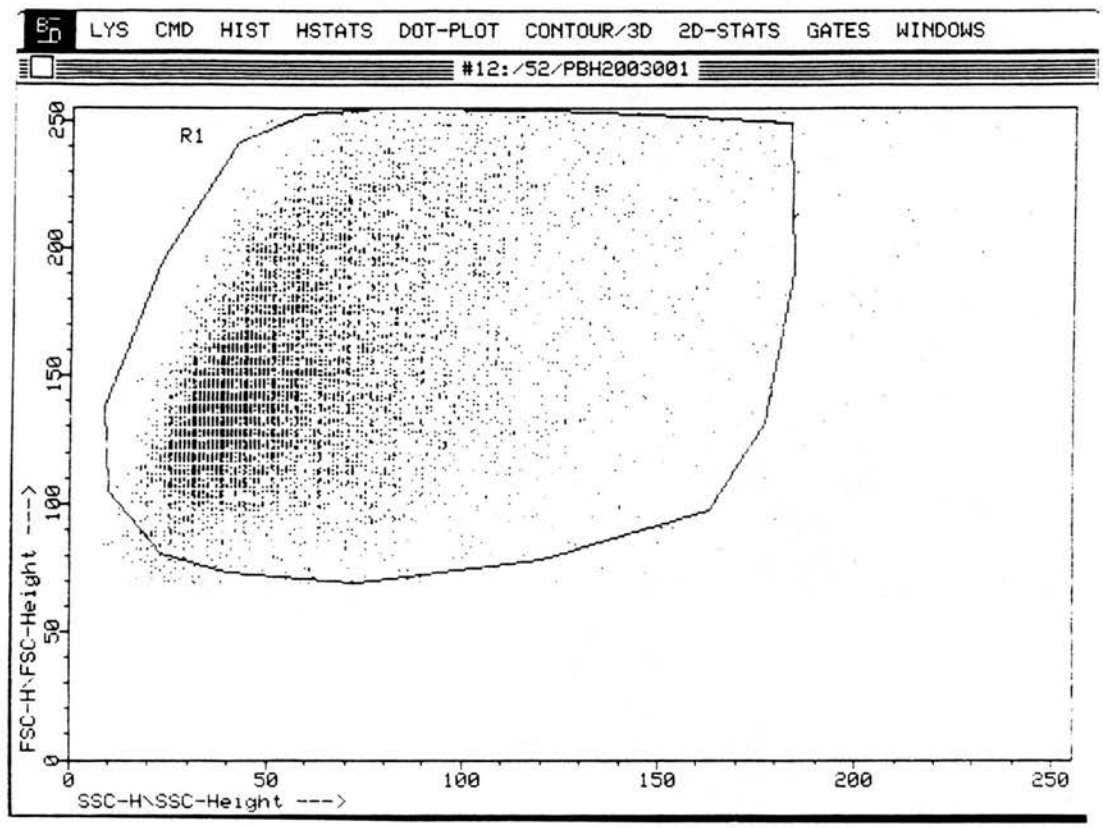

Figure 2.4 - Flow cytometric analysis of rat BMMCs showing the gating procedure. The machine (FACScan, Becton Dickinson) was gated so that cellular debris and red blood cells were not registered. In addition, a further gate was applied (black line) after the experimental run to exclude extreme outliers and possible dying cells from the analysis. Each population of cells from each culture tested comprised 10^5-10^6 cells and each flow cytometric analysis was based on 10^4 cells.

2.14 - Preparation of cell suspensions for mediator release assays

Before use in mediator release experiments, BMMCs were centrifuged at 200 x g for 7 min at room temperature and resuspended in Tyrode's buffer (TB). After two further washes, the cells were resuspended in TB^+ which included 1 mM Ca^{2+} and 1 mM Mg^{2+} to support mediator release. Cells were then counted and assessed for viability, and the percentage of mast cells was determined in Leishman's stained cytospin preparations.

2.15 - Sensitisation of BMMCs with mouse IgE anti-DNP for mediator release assays

In some mediator release experiments, BMMCs were sensitised with exogenous mouse monoclonal IgE anti-DNP (SPE-7, Sigma) to increase the amount of IgE bound to each cell. The validity of this method is demonstrated in chapter 3 (section 3.1). After washing three times in TB, a suspension of BMMCs was resuspended in TB/EDTA and incubated with 10 μg IgE/10^6 cells for 1 hour at 37°C, with gentle periodic inversion to ensure mixing. The cells were then washed again three times in TB to remove unbound IgE, counted, and assessed for viability and the percentage of mast cells.

2.16 - Immunological Stimulation of mediator release from BMMCs

In some experiments, unsensitised BMMCs were challenged directly with goat anti-rat IgE (anti-IgE provided by Dr. E. Hall, Glasgow Veterinary School, UK) with normal goat serum (NGS) as a control stimulus. Both reagents were stored at -70°C and used at an optimal dilution of 1:250 (MacDonald. 1994). In other experiments, cells were sensitised with exogenous IgE anti-DNP, and DNP-BSA (Calbiochem, Nottingham, UK) was used as the secretagogue with TB^+ as a control stimulus. DNP-BSA was stored at -70°C as a 10 mg/ml stock solution. The dilution of DNP-BSA that induced maximal mediator release was determined by assaying the release

of β hexosaminidase from populations of BMMCs stimulated with concentrations ranging from 1 mg/ml to 0.1 μg/ml (see chapter 3, section 3.2 for details).

2.17 - Assays of mediator release from BMMC populations

Triplicate or quadruplicate aliquots (0.5ml in Eppendorf tubes) of 0.8 - 1 x 10^6 BMMCs suspended in TB^+ were incubated with 0.5ml of appropriately diluted stimulant (anti-IgE or DNP-BSA) or control (NGS or buffer) at 37°C for 30 min in a shaking water bath, with occasional gentle mixing. Previous studies had shown that the IgE-mediated release of RMCP-II and β hexosaminidase was maximal by 30 min (MacDonald. 1994). The activation reaction was stopped by centrifugation of the tubes at 12,000 x g for 4 min at 4°C to pellet the cells, after which the tubes were transferred to an iced water bath. After collection of the supernatants, the cell pellets were resuspended in 1ml TB^+ and both pellets and supernatants were stored at -70°C until assayed for RMCP-II or β hexosaminidase.

To extract the granule contents, the tubes containing the cell pellets (and the supernatants for controls) were subjected to three freeze/thaw cycles to fracture plasma membranes and release remaining mediators (MacDonald, 1994). This was achieved by alternating the tubes between a methanol/dry ice bath and a water bath at 37°C. After the contents had thawed for the third time, the tubes were returned to an iced water bath. The tubes were then centrifuged again at 12,000 x g for 4 min at 4° C to pellet the membranous debris. The supernatants and pellet supernatants were assayed for RMCP II or β hexosaminidase as described below.

2.18 - RMCP-II ELISA

Purified RMCP-II, murine monoclonal anti-RMCP-II and sheep anti-RMCP-II for use in ELISA assays were prepared as described (Huntley *et al,* 1990a) and provided by Mr. G.F.J. Newlands, Moredun Research Institute, Edinburgh, UK. 96 well plates (M129B, Dynatech, Billinghurst, UK) were coated with 50 μl of a 1 μg/ml solution

of affinity purified mouse monoclonal anti-RMCP-II in sodium carbonate buffer (pH 9.6) and incubated overnight at 4°C. After washing 6 times in PBS/ 0.05% Tween 20 (PBS/T20), remaining binding sites were blocked by adding 50µl/well 4% BSA in PBS/T20 and incubating for 1 - 2 hours at room temperature (RT, 18 - 22°C). The plate was washed once in PBS/T20 and 50 µl of appropriately diluted samples in 4% BSA in PBS/T20 were added to the wells in duplicate and incubated for 1.5 hours at RT. A standard curve was generated by assaying purified RMCP-II at concentrations of 5, 4, 2, 1.5, 1.0, 0.75, 0.5 and 0.25 ng/ml. After washing 6 times in PBS/T20, 50 µl of a 1/200 dilution of affinity purified polyclonal sheep anti-RMCP-II conjugated to horseradish peroxidase was added to the wells and incubated at RT for 1 hour. The plate was then washed 6 times in PBS/T20 and 50 µl of 3,3',5,5'-tetramethylbenzidine peroxidase substrate was added to each well. The colour development was monitored in each well, and the reaction was stopped with 0.18M H_2SO_4 when colour first appeared in the standard with the lowest concentration. Plates were read at 450 nm in a Dynatech MR7000 ELISA reader and RMCP-II concentrations were calculated automatically from the standard curve by the built-in software. The concentration of RMCP-II in supernatants was then expressed as a percentage of the total RMCP-II in both supernatants and pellets to give the percentage release.

2.19 - β Hexosaminidase assay

The preparation of the sodium citrate (pH 4.5) and 0.2 M glycine-NaOH (pH 10.7) buffers is described in appendix 1. 1.7 mg of β Hexosaminidase substrate (p Nitrophenyl N-acetyl β-D-Glucosaminide, Sigma) was added per 1 ml of sodium citrate buffer and sonicated in an ultrasonic water bath until dissolved. 30 µl of each sample was added to the wells of a 96 well ELISA plate followed by 60 µl of the substrate/citrate buffer solution. After incubating for 45 minutes at 37°C, the reaction was stopped by adding 150 µl /well of glycine buffer and the plates were read at 405 nm in a Dynatech ELISA plate reader. The percentage release of β

hexosaminidase was calculated by expressing the O.D. values of the supernatants as a percentage of the sum of the O.D. values for the pellets and supernatants.

2.20 - Statistical Analysis

Statistical analysis of immunological studies was performed using Minitab statistical software. Treatment groups were compared by one way analysis of variance (ANOVA) and unpaired Student's t tests. Results are reported as mean ± s.d. or s.e.m. as described in the appropriate sections.

2.21 - Development of an RMCP-II ELISPOT assay

Part of these studies involved developing an enzyme-linked immunospot assay (ELISPOT) that detects release of RMCP-II from individual BMMCs. The methodology and validation of the assay are described in Chapter 3 (section 3.3 - 3.6).

ELECTROPHYSIOLOGICAL STUDIES

2.22 - Solutions

The following solutions were prepared using chemicals obtained from either BDH or Sigma. Prior to use, mast cell Ringers and pipette solutions were filtered through 0.2 μm filters (Whatman Cellulose Nitrate Filters, Maidstone, UK).

Extracellular solutions

Standard Mast Cell Ringer	Modified Mast Cell Ringer
137 mM NaCl	137 mM NaCl
2.7 mM KCl	2.7 mM KCl
1 mM $CaCl_2$	**2 mM $CaCl_2$**
1 mM $MgCl_2$	**5 mM $MgCl_2$**
5.6 mM glucose	5.6 mM glucose
10 mM HEPES	10 mM HEPES
pH to 7.3 with M NaOH	pH to 7.3 with M NaOH

High K^+ extracellular solutions for ion substitution experiments (pH 7.3)

10 mM $[K^+]$	50 mM $[K^+]$	90 mM $[K^+]$	137 mM $[K^+]$	165 mM $[K^+]$
10 mM KCl	50 mM KCl	90 mM KCl	137 mM KCl	165 mM KCl
129.7 mM NaCl	89.7 mM NaCl	49.7 mM NaCl	2.7 mM NaCl	2.7 mM NaCl
1 mM $CaCl_2$	1 mM $CaCl_2$	1 mM $CaCl_2$	1 mM $CaCl_2$	1 mM $CaCl_2$
1 mM $MgCl_2$	1 mM $MgCl_2$	1 mM $MgCl_2$	1 mM $MgCl_2$	1 mM $MgCl_2$
10 mM HEPES	10 mM HEPES	10 mM HEPES	10 mM HEPES	10 mM HEPES

Low Cl^- extracellular solutions for ion substitution experiments (pH 7.3)

14 mM [Cl^-]	51 mM [Cl^-]	114 mM [Cl^-]	16.7 mM [Cl^-]
140 mM Na-acetate	100 mM Na-acetate	47 mM Na-acetate	137 mM Na-isethionate
	37 mM NaCl	90 mM NaCl	
2.7 mM K-acetate	2.7 mM K-acetate	2.7 mM K-acetate	2.7 mM KCl
2 mM $CaCl_2$	2 mM $CaCl_2$	2 mM $CaCl_2$	2 mM $CaCl_2$
5 mM $MgCl_2$	5 mM $MgCl_2$	5 mM $MgCl_2$	5 mM $MgCl_2$
10 mM HEPES	10 mM HEPES	10 mM HEPES	10 mM HEPES
5.6 mM glucose	5.6 mM glucose	5.6 mM glucose	5.6 mM glucose

Pipette Solutions for conventional whole cell recordings (pH 7.3)

Standard	Modified
137 mM KCl	137 mM K-methane sulfonate
2.7 mM NaCl	2.7 mM NaCl
0.1 mM $CaCl_2$	0.1 mM $CaCl_2$
1 mM $MgCl_2$	1 mM $MgCl_2$
10 mM HEPES	10 mM HEPES
1 mM EGTA	1 mM EGTA

Pipette solutions for amphotericin B perforated patch recordings (pH 7.3)

Standard	Modified
137 mM KCl	137 mM K-methane sulfonate
2.7 mM NaCl	2.7 mM NaCl
1 mM $CaCl_2$	1 mM $CaCl_2$
3 mM $MgCl_2$	3 mM $MgCl_2$
10 mM HEPES	10 mM HEPES

2.23 - Ion Channel Blockers

The channel blockers 4,4' -diisothiocyano-2,2' -stilbenedisulfonate (DIDS), 4-aminopyridine and tetraethylammonium chloride (TEA) were obtained from Sigma. Anthracene-9-carboxylic acid was obtained from Aldrich Chemical Co., Gillingham, UK.

2.24 - Whole-cell recording

The components of the recording setup are shown diagrammatically below and described in detail in the subsequent text. The solid thin lines indicate voltage pulses produced by the stimulator or the CED software. The solid bold lines indicate the path taken by the evoked whole cell currents. The dashed lines represent a TTL pulse produced by the stimulator to trigger the CED software.

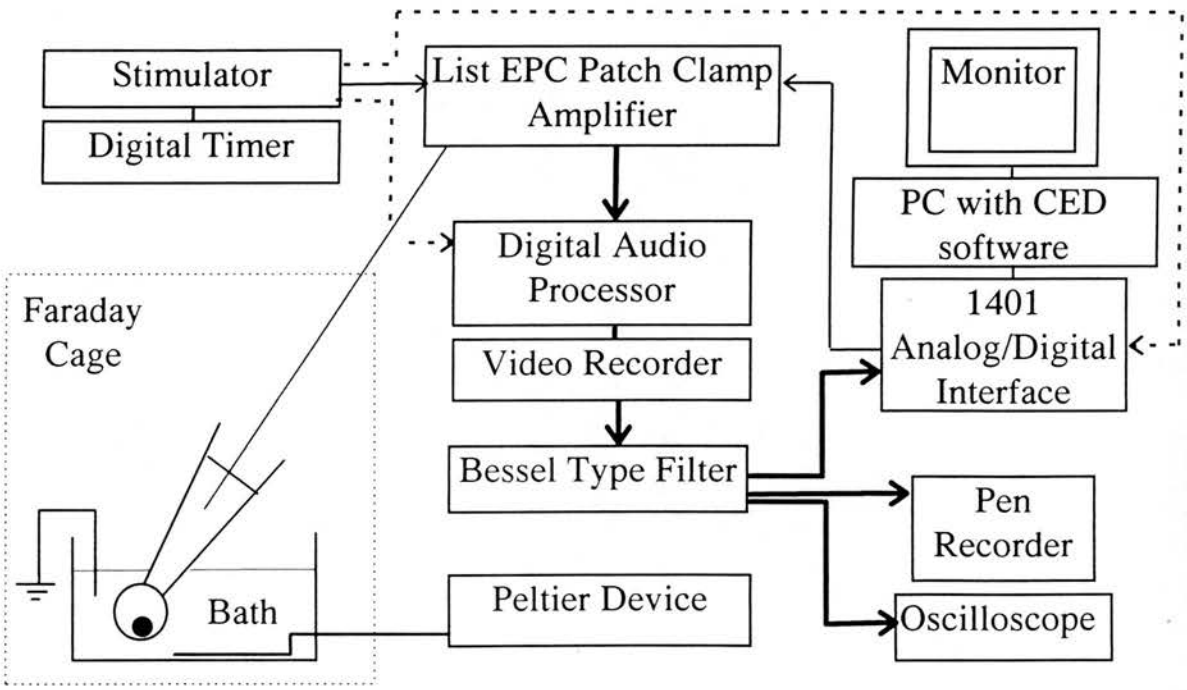

2.25 - Recording Station

The microscope, micromanipulator, bath and perfusion system were mounted inside an aluminium Faraday cage on an anti-vibration table (Micro-g, Technical

Manufacturing Corporation, MA, USA). Cells were observed with an inverted microscope (Microstar, Reichert Jung, Germany) powered by a DC power supply (Weir 761, RS Components LTD, UK) located outside the Faraday cage to avoid mains interference. The headstage of the patch clamp amplifier (EPC-7, List, Germany) was mounted on a 3-dimensional oil filled hydraulic micromanipulator (Narishige, Japan).

2.26 - Recording Bath

The recording bath was made from 8 mm perspex sheet and had a chamber volume of 4 ml (Figure 2.5). To improve optical resolution, cells were viewed through a rectangular hole in the base of the bath covered with a 48 x 64 mm glass coverslip. Solution exchanges were made by a gravity-feed perfusion system comprising a 20 ml reservoir connected to the bath by fine bore tubing. The perfusion rate was controlled by a screw valve allowing solution exchange in 30s to 2 min, depending on flow rate. Excess solution was removed by a continuous aspiration tube connected to a vacuum pump (Hy-Flo Model B, Potters Bar, UK). The temperature of the bath was measured and controlled using a temperature probe and Peltier device (Firbank Electronics, Norwich, UK) with each 5°C temperature rise taking approximately 2 min. However, rapid cooling of the bath was not possible because of the size of the heat sink on the Peltier element. During solution exchanges, the perfusate passed over the activated Peltier element before reaching the cells, thus minimising temperature changes The bath temperature typically decreased by 2-3°C during this time but this did not affect the current recordings described here.

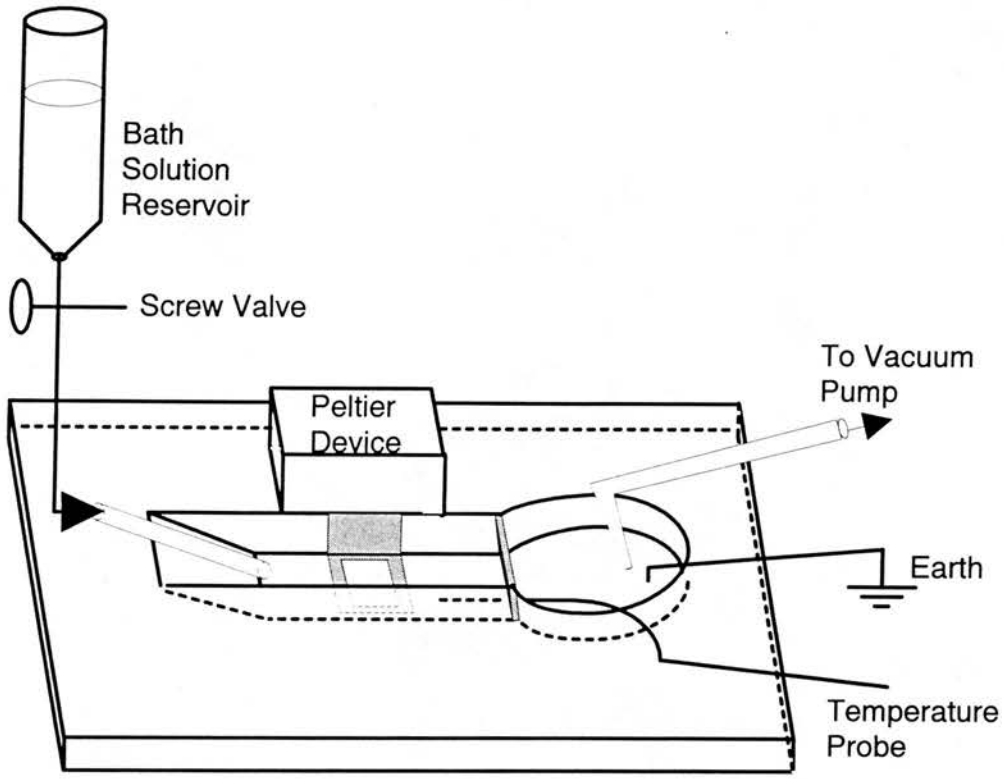

Figure 2.5 - The electrophysiological recording chamber. The bath was fabricated from 8 mm perspex sheet. The base of the bath comprised a 48 x 64 mm glass coverslip which was sealed to the perspex with Sylgard (Dow Corning, MI, USA). Solution exchanges were made by a gravity-feed perfusion system from a solution reservoir, and excess solution was removed by a continuous aspiration tube connected to a vacuum pump. The perfusion rate was controlled using a screw valve. The temperature of the bath was controlled using a Peltier device, and the round coverslip supporting the cells was placed in the square hole in the centre of the Peltier element (shaded).

2.27 - Reference electrodes and agar bridges

The pipette and ground electrodes were formed from silver wires which were coated with molten AgCl (Sigma). In most experiments (including all ion substitution experiments), the ground electrode was connected to the bath through an agar bridge consisting of a short length of silicone tubing containing 150 mM KCl in 5% agar. In control experiments, exchange of mast cell ringer for either high K^+ or low Cl^- solutions produced junctional potentials which were less than 1 mV; hence, no corrections were made. When the KCl in the pipette solution was replaced with KCH_3SO_4, large junctional potentials developed at the pipette solution/pipette electrode interface. These could not be cancelled using the pipette offset potential circuitry on the amplifier. This problem was overcome by placing a fine tube containing 150 mM KCl in 5% agar over the pipette electrode which acted as an agar bridge between the electrode and the pipette solution (modified from Bormann *et al,* 1990).

2.28 - Preparation of cells for whole-cell recordings

For electrophysiological recordings, bone marrow-derived mast cells (BMMCs) or peritoneal mast cells were resuspended in mast cell Ringer and plated onto 10 mm diameter circular glass cover slips (No. 1, Chance propper Ltd., Warley, UK) in petri dishes. Both BMMCs and peritoneal mast cells adhered to untreated glass without the need for further immobilisation. After incubating at 37°C without CO_2 for up to seven hours, the coverslips were transferred from the petri dish to the recording bath containing mast cell Ringer. The cells were washed by rapid perfusion of fresh mast cell Ringer, which also removed non-immobilised cells. Any contaminating macrophages in the preparation could be discerned by their large size and lack of cytoplasmic granularity.

2.29 - Preparation of Patch Pipettes

Pipettes were pulled from borosilicate capillary glass with an internal diameter of 1.15 mm and an external diameter of 1.55 mm (7052, Garner Glass Company, CA, USA) using a two-stage vertical micropipette puller (PB-7, Narishige, Japan). For perforated-patch recordings, the pipette geometry was crucial for success of the technique. Pipettes were pulled to have short, blunt tips with a rapidly widening shaft (see Figure 2.6 in section 2.31 - amphotericin B perforated-patch recording). For conventional whole-cell recordings, the tip geometry was less important and pipettes were usually longer and thinner. Pipettes were coated to near their tips with Sylgard (Sylgard 184, Dow Corning, MI, USA) to reduce capacitance transients evoked by voltage pulses. Immediately prior to use, pipettes were heat polished by micromanipulating the tip close to a heated platinum wire. They were then filled with pipette solution (see below), connected to the pipette holder on the headstage of the amplifier and lowered into the bath.

2.30 - Obtaining seals

The development of pipette/membrane seals in the GΩ range (gigaseals) was observed by monitoring the currents evoked by repetitive voltage pulses transmitted to the pipette (Hamill *et al,* 1981). Voltage pulses for sealing were generated in two ways. In some experiments, a precision delay digital timer was used to trigger an isolated stimulator (equipment produced in the departmental electronics workshop). However, in the majority of experiments, voltage pulses were generated by CED patch-clamp software (Cambridge Electronic Design Ltd., Cambridge, UK) on a personal computer (DCS 286) connected to an intelligent interface (CED, 1401). With both systems, 1V pulses of 10 ms duration were applied every 300 ms to the input of the patch clamp amplifier (EPC-7, List). The signal was scaled to 1 mV and the evoked currents were displayed on an oscilloscope (5103N, Tektronix, Guernsey, UK). The pipette resistance was determined from the quotient of the voltage and current amplitudes (pipettes were heat polished to yield resistances of 0.5 - 2.5 MΩ

for perforated patch recordings and 2 - 5 MΩ for conventional whole-cell recordings). Before formation of the gigaseal, the current output signal of the amplifier was set to zero. The pipette tip was then placed against the cell surface until a noticeable increase in resistance was observed. Gentle oral suction was applied to the pipette until the resistance increased to a minimum of 1 GΩ. Any fast capacitance transients were cancelled using the capacitive cancellation circuitry on the amplifier. In most experiments, BMMCs were then lifted off the coverslip and suspended in the bath solution to minimize the risk of breakdown due to drift or solution exchange. However, peritoneal mast cells adhered more tightly to the glass and this was not always possible.

2.31 - Recording configurations

Conventional whole-cell voltage-clamp recordings (Hamill *et al,* 1981).

For whole-cell voltage-clamp recordings, pipettes were filled by dipping the tip in pipette solution followed by back-filling. Any excess solution was vapourised by placing the base of the pipette in an alcohol flame. After formation of the gigaseal, the amplifier was placed in voltage-clamp mode at a holding potential of -40 mV and further suction was applied to the pipette to break down the membrane patch within the tip. Successful break-in was revealed by the sudden appearance of large capacitance transients. These were cancelled using the slow capacitance and series conductance cancellation dials on the amplifier. The readings on the dials correspond to the cell capacitance (a measure of the membrane surface area) and the series conductance. The reciprocal of the latter value yields the access resistance which comprises both the pipette resistance and the resistance through the broken membrane patch.

Perforated-patch recordings (Rae *et al,* 1991)

Perforated-patch recordings were performed using amphotericin B (Calbiochem, Nottingham, UK) to permeabilise the membrane patch in the pipette tip. A 50 mg/ml

stock solution of amphotericin B was prepared by dissolving 5 mg amphotericin B powder in 100μl tissue culture grade DMSO (Sigma). This was stored at -20°C for up to a week. A working solution containing 200 μg/ml amphotericin B was prepared by adding 2μl of the stock solution to 0.5 ml of pipette solution and sonicating for 20 min in an ultrasonic water bath. This ensured that the poorly soluble amphotericin particles were micronised. The working solution was kept in the dark at room temperature and was stable for 2 - 3 hours. Because the presence of amphotericin B at the tip inhibits sealing, pipettes were first filled to a length of ≈ 150 μm with pipette solution free of amphotericin B. This was achieved by briefly dipping (< 1s) the tip in clean pipette solution. The pipettes were then back-filled with the amphotericin B/pipette solution before being used immediately to obtain a gigaseal as described above.

The initial application of the amphotericin B perforated-patch technique to rat BMMCs posed a number of technical problems and the following summary indicates the measures that had to be taken to enable success. Without adhering strictly to all the points listed below, the technique (as described above) did not work.

1) The amphotericin B had to be fresh. After the bottle of amphotericin was opened, it was stored at 4°C in a sealed container containing a dessicant for up to 3 months. However, the stability was variable, so if successful perforations did not occur a new batch of amphotericin was purchased. The amphotericin B stock solution, made up in DMSO, was stored at -20°C for up to 7 days after which it was discarded. The working solution, comprising 200 μg/ml amphotericin B in pipette solution, was only stable for 2-3 hours and had to be protected from light. As some experiments could last for 1 hour, the amphotericin solution was not used if it was more than 2 hours old.

2) The amphotericin B was dissolved in tissue-culture grade DMSO which was obtained in 5ml sterile vials. The DMSO was dispensed into 1ml aliquots and stored in Eppendorf tubes. Occasionally, the amphotericin B did not dissolve in the DMSO and appeared to form an emulsion. This resulted in a bright yellow opaque suspension instead of the usual translucent caramel coloured solution. This occurrence could be minimised by ensuring that the amphotericin B powder was warmed to room temperature before the bottle was opened, thus reducing the possibility of condensation.

3) Amphotericin B is not soluble in electrolyte solutions. When it is added to the pipette solution, a suspension of particles results which can be easily visualised under a microscope. The working solution was therefore micronised in an ultrasonic water bath for 20 min before use. If re-examined microscopically, the reduction in particle size could be clearly demonstrated. This procedure was performed by placing 0.5ml of pipette solution/amphotericin B in an Eppendorf tube which was allowed to float free in the bath.

4) The shape of the pipettes was crucial to the success of the perforated patch technique. If the tips were slightly too long, perforation was either very slow and incomplete, or did not occur at all. The electrode puller was therefore set up to produce pipettes with a short, rapidly tapering tip (Figure 2.6). However, analysis of the tip geometry was somewhat subjective, despite attempts to quantify it with a graticule, and day to day variation could result in failure of the technique. It was therefore important to avoid altering the settings on the pipette puller, as correct readjustment could be very time consuming.

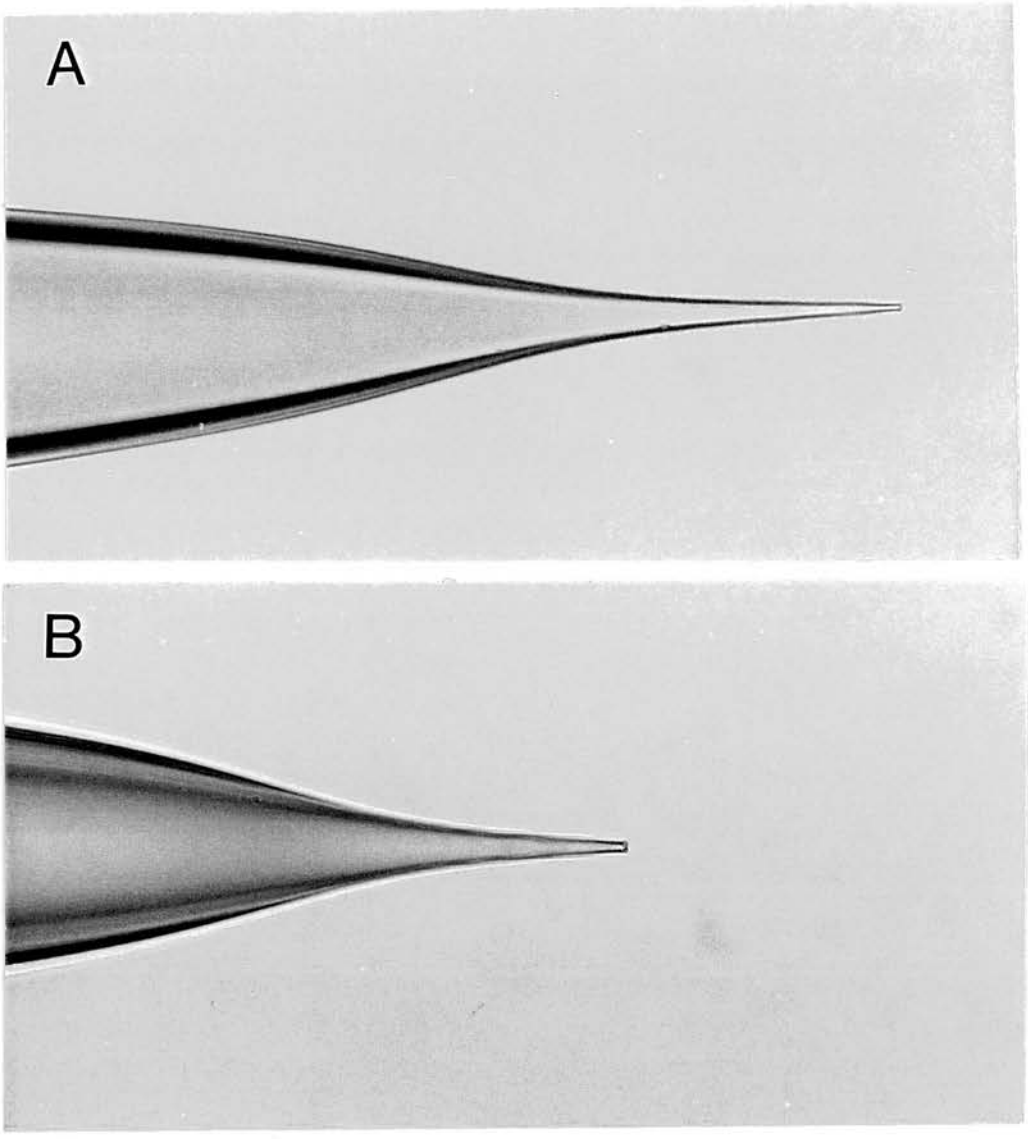

Figure 2.6 - Patch pipettes for conventional whole-cell recordings (**A**) and amphotericin B perforated-patch recordings (**B**). For conventional whole-cell recordings, long, thin pipettes were acceptable. For perforated-patch recordings, the tip geometry was crucial and short, blunt tips with a rapidly widening shaft were required.

5) The presence of amphotericin B at the pipette tip inhibits sealing. This was overcome by briefly dipping the pipettes in pipette solution free of amphotericin B before back-filling. The length to which the pipettes were filled was also critical to the success of the technique. It was found that filling to a length of ≈ 150 μm produced reasonably consistent results. If pipettes were filled beyond this, perforation was very slow or did not occur. If pipettes were not filled to this level, the chances of obtaining a seal were reduced.

If the above measures were adopted, perforation of the membrane patch was revealed by the gradual appearance of capacitance transients in response to the command pulse. These were cancelled using the capacitance cancellation circuitry on the amplifier to yield the cell capacitance and the access resistance. With optimal tip geometry and filling, the access resistance decreased rapidly within 5-25 min and continued to fall for up to 2 hours.

2.32 - Measurement of Membrane Potential

The membrane potential of rat BMMCs was measured with the conventional whole-cell configuration using the current clamp mode of the patch clamp amplifier. Immediately following break-in, the amplifier was switched to current clamp and the displayed voltage was recorded. If the voltage fluctuated, the range was noted and the median value was taken as the resting membrane potential.

2.33 - Voltage Pulse Protocols

Voltage pulses for detection of whole-cell currents were generated by the CED voltage-clamp software as described earlier. In all experiments, 5 or 10 mV voltage steps of 200 ms duration were applied every second from a holding potential of -40 mV. Four different voltage step ranges were used throughout the course of these studies: -80 mV to +50 mV; -100 mV to + 40 mV; -140 mV to + 40 mV; and -140 mV to + 100 mV. The range used for each particular cell is given in the results and

in appendix 4. The voltage pulse protocols were either triggered internally by the program, or externally by repetitive 5 V TTL pulses at 1 Hz generated by the isolated stimulator.

2.34 - Data Storage

The voltage pulses and the evoked whole-cell membrane currents were stored in three different ways allowing flexibility in data acquisition and analysis.

1. Video tape

The whole-cell currents first passed from the current output of the amplifier to a digital audio processor (Pulse code modulation-701ES, Sony Corporation, Japan) and were recorded digitally on a video cassette recorder (Betamax SL-HF100E, Sony) along with the voltage steps. To allow the recorded data to be subsequently handled directly by the CED software, the 5 V TTL triggering pulses were also recorded on the videotape using an additional input channel (modification by Electronics Department, Cambridge University, UK). The recorded pulse was then used to trigger the CED software during playback.

2. Computer Disk

After passing through the digital audio processor, the membrane currents were filtered at 2 kHz by an 8 pole Bessel type filter (Department of Preclinical Veterinary Sciences Electronic Workshop, University of Edinburgh), passed to the input of the analogue-digital interface (CED 1401), and displayed with the voltage steps in real time on the computer monitor. The current and voltage traces could be saved to the hard drive (DCS 286) during experiments and subsequently downloaded onto diskettes for later analysis. However, due to limitations in memory, entire experiments could not be recorded in this way. Hence, only important sections of the experiment were saved to disk and if additional analysis was required, the relevant periods of the experiment were replayed into the computer from video tape.

3. Pen Recorder

The currents and voltage steps were also displayed in real time on a 2 channel continuous pen recorder (Electromed MX 216, Devices LTD, Welwyn Garden City, UK).

2.35 - Calibration

Electronic instruments were calibrated by the manufacturers. The magnitude of voltage pulses generated by the stimulator or the CED software was verified on an oscilloscope before and after scaling. Current responses during sealing and voltage pulse protocols were verified by applying voltage steps to a model cell (Model circuit MC-7, List) and recording the evoked currents on an oscilloscope and pen recorder.

2.36 - Data analysis

1. Generation of current/voltage (I/V) relationships

Current/voltage relationships were generated and analysed with the CED voltage-clamp software. The currents elicited by each voltage pulse were sampled at 1 kHz and averaged over a 20 ms period. In most cases, the currents were sampled in the middle of the 200 ms pulse. However, if there was evidence of time-dependent inactivation, the currents were sampled in the region of the peak. To generate the I/V plot, the sampled currents were plotted against the corresponding voltage steps. Although the software-generated I/V plots can be printed, the figures presented in chapter 5 were produced by transferring the current and voltage cursor values to a separate graphics program (Cricket Graph).

2. Leak Subtraction

Leak currents were identified as the data points in the linear (ohmic) region of the I/V plot (Martin *et al,* 1992). Before calculating slope conductances, the slope of this region was subtracted using the leak subtraction program of the of the CED voltage-

clamp software. The following arbitrary example illustrates how the program calculates a leak current that is subtracted from all the events in the I/V curve

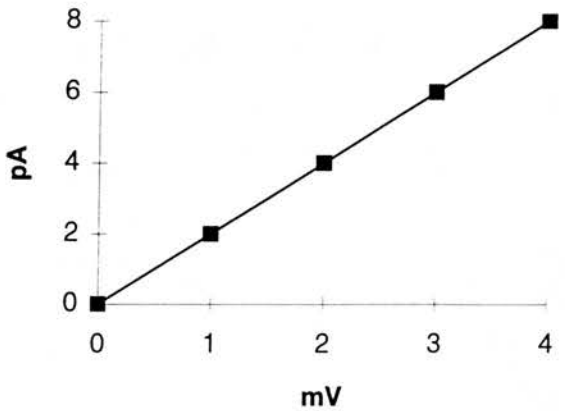

In the above I/V plot, the five data points represent an ohmic leak conductance. After leak subtraction, the slope of this line should be reduced to zero. The program performs the calculation by summing both the current steps (i.e. 20 pA) and voltage steps (i.e. 10 mV) from the five data points chosen as leak. The current subtracted from each event in the curve is the ratio of the summed currents and summed voltages (i.e. 20 pA/10 mV) multiplied by the voltage step for each particular event. In this case, the current subtracted from each event is the voltage at each event multiplied by 2. Therefore, at the 1 mV step, a current of 2 pA is subtracted; at the 2 mV step, a current of 4 pA is subtracted, and so on. As can be seen from this example, the calculation has the desired effect of reducing the slope of the line to zero.

3. Slope Conductance

Slope conductances were calculated by the CED software using a least squares fit to data points on the I/V curve between set voltage ranges. In most cases these were -140 mV to -100 mV for inward currents and +80 mV to +100 mV for outward

currents. In some cases (e.g. when recordings were made in high [K^+] buffers), the conductance was calculated in the range -100 mV to -80 mV.

2.37 - Statistical Analysis

Statistical analysis of electrophysiological studies was performed using Minitab statistical software and Microsoft Excel 5.0. Comparisons between normally distributed conductances in different treatment groups were made by ANOVA. Individual groups were compared by unpaired Student's t tests. When recordings were made on the same cell under different conditions, paired Students t tests were used for comparison. Comparisons between groups with non parametric distributions were made by Kruskal Wallis and Mann-Whitney tests. Whole-cell conductances are expressed as mean ± s.d.

Chapter 3

CHARACTERISATION OF IGE-DEPENDENT SECRETION IN RAT BONE MARROW-DERIVED MAST CELLS USING A NOVEL ENZYME-LINKED IMMUNOSPOT (ELISPOT) ASSAY TO DETECT THE RELEASE OF RMCP-II

INTRODUCTION

The secretory function of many mast cell types has been studied extensively *in vitro* in an attempt to further understand the pathogenesis of allergic diseases (Paterson *et al,* 1976; Flint *et al,* 1985; Lawrence *et al,* 1987; Benyon *et al,* 1989) or gastointestinal immune responses (Befus *et al,* 1982; Rees *et al,* 1988). Many of these studies are designed to investigate the release of particular mediators in response to challenge with various secretagogues. Hence, the responses of numerous mast cell types to compound 48/80 (Befus *et al,* 1982; Broide *et al,* 1988; Barrett *et al,* 1985), substance P (Shanahan *et al,* 1985; Broide *et al,* 1988), GTP-γ-S (Gomperts, 1983), and Ca^{2+} (Foreman *et al,* 1973) have all been investigated (see chapter 1 for details). However, activation of mast cells via the IgE receptor provides a more physiological stimulus that is analogous to the response seen *in vivo* during allergic reactions.

In experimental protocols, the IgE receptor can be aggregated in three ways. Firstly, by using divalent antibodies directed against the receptor itself (Ishizaka and Ishizaka, 1978; Isersky *et al,* 1978). Secondly, by using anti-IgE antibodies to cross-link receptor bound IgE (Lawrence *et al,* 1987; Levi-Schaffer *et al,* 1987a; MacDonald *et al,* 1989). And thirdly, by sensitising the receptors with IgE specific for a particular antigen, and challenging the cell with the antigen (Broide *et al,* 1988). The last method most commonly involves IgE antibodies raised against the multivalent hapten dinitrophenyl-bovine serum albumin (DNP-BSA).

Cultured rat BMMCs stimulated with lymph node conditioned medium (LNCM) are ordinarily exposed to 1 - 2 μg of rat IgE per ml, most likely derived from B cells in the Con A-stimulated mesenteric lymph node cell cultures (Haig *et al,* 1983). This endogenous IgE binds to the BMMCs via the FcεRI receptors, allowing anti-rat IgE to be used as a secretagogue in studies of these cells (MacDonald, 1994). MacDonald (1994) demonstrated the presence of this surface bound IgE by flow cytometry, but also showed that the level of IgE binding could be increased by sensitising the cells with IR162 rat myeloma IgE (Experimental Immunology Unit, Faculty of Medicine, University of Louvain, Belgium). However, this sensitisation regime resulted in high background mediator release (15-20%), probably due to activation of the IgE receptors by aggregated IgE molecules (MacDonald, 1994). Attempts to remove these aggregates by ultracentrifugation and gel filtration were only partially successful. Therefore, in this study, it was decided to adapt the IgE anti-DNP system to rat BMMCs. This would allow the secretory responses of "unsensitised" and "IgE-sensitised" cells to be compared.

In studies of mast cell function, the effects of immunological or non-immunological stimuli are usually measured in terms of *percentage* release of various mediators. Typically, secretagogue-activated mast cell populations specifically release 10-50% of the stored mediators present in the cells (White and Pearce, 1982; Pearce *et al,* 1982; Razin *et al,* 1983; Levi-Schaffer *et al,* 1987a; Kaplan *et al,* 1991; Lavens *et al,* 1992; Swieter *et al,* 1993; Shalit *et al,* 1993; Jaffar and Pearce, 1993). Similar studies with rat BMMCs showed that, under optimum conditions, 16% of the RMCP-II (MacDonald *et al,* 1989) and 16-26% of β-hexosaminidase (Broide *et al,* 1988; MacDonald *et al,* 1989) was released following IgE-mediated stimulation. An important question relevant to the control of mediator secretion is how these values for specific mediator release might reflect the extent to which *individual* BMMCs within the population respond to stimulation. For example, 20% RMCP-II release

from a population of cells could entail:- 1) all the cells releasing 20% of their contents; 2) 20% of the cells releasing all their contents; or 3) variable proportions of cells releasing variable quantities of RMCP-II. This question could have important implications for the mechanisms involved in regulating mast cell function. For example, factors that upregulate mast cell secretion could do so either by increasing the proportion of cells that respond to stimulation, or by increasing the quantity of mediator released from each cell. It would therefore be useful to develop a technique that allowed mediator release to be detected from individual BMMCs within the population.

Two techniques have been used previously to detect secretion from single mast cells: whole-cell capacitance measurements (Fernandez *et al,* 1984; Lindau and Neher, 1988) and fast voltammetry using carbon fibre electrodes (Tatham *et al,* 1991). However, these techniques do not allow the responses of single cells to be compared to the response of the whole population. Hide et al. (1993) used flow cytometry to monitor degranulation of individual rat peritoneal mast cells by relating the reduction in 90° side scatter to the loss of cytoplasmic granules. In a similar technique, MacGlashan (1995) used both the reduction in forward scatter and the loss of granules stained with acridine orange as measures of degranulation in human basophils following challenge with secretagogues. However, flow cytometry does not provide a direct measure of mediator release from mast cells, making comparisons with conventional secretion assays more difficult.

Sedgwick and Holt (1983) introduced an alternative technique for monitoring secretion from individual cells. They developed a solid phase immunoenzymatic method to detect secretion of specific antibodies from individual lymphocytes. This technique, subsequently named the enzyme-linked immunospot (ELISPOT) assay (Czerkinsky *et al,* 1983), relies on the binding of secreted cellular products to a capture antibody bound to the base of plastic wells. The secreted product binds in a

small zone surrounding each cell so that, following the addition of an enzyme-labelled antibody and subsequent enzymatic development, a grossly visible spot appears at the site of secretion. To date, ELISPOT assays have been restricted to the detection of immunoglobulins and cytokines, including immunoglobulins A (Feltelius *et al,* 1991), G (Tarkowski *et al,* 1984), M (Nick *et al,* 1987), and E (Thomas and Przybilla, 1992), and various cytokines including IL-2, IL-4 and IL-6 (Fujihashi *et al,* 1993), and IL-5 and IFN-γ (Taguchi *et al,* 1990; Sedgwick and Czerkinsky, 1992).

Previous studies in this laboratory had suggested that a similar assay could possibly be developed to monitor secretion in rat BMMCs. For example, when activated immunologically, rat BMMCs secrete RMCP-II in a dose- and time-dependent manner, and this correlates significantly with the release of the granule mediators β hexosaminidase and histamine (MacDonald *et al,* 1989; MacDonald, 1994). Furthermore, a highly specific enzyme-linked immunosorbent assay (ELISA) has been developed to measure RMCP-II in tissues and cell supernatants (Huntley *et al,* 1990a). Hence, the monoclonal anti-RMCP-II antibody used in the ELISA could potentially be used as a capture antibody in an ELISPOT assay.

The initial aims in this part of the study were to further characterise IgE-dependent secretion in rat BMMCs, with particular emphasis on how individual cells within the population respond to stimulation. The specific aims were:-

1) To determine if an IgE anti-DNP sensitisation protocol could be used in rat BMMCs.

2) To develop and validate an ELISPOT assay that could detect the release of RMCP-II from individual rat bone marrow-derived mast cells (BMMCs).

3) To use the ELISPOT assay to determine how individual BMMCs within the population respond to IgE-mediated stimulation. This might provide important clues as to how rat BMMC secretory function is modulated.

EXPERIMENTAL METHODS AND RESULTS

3.1 - Flow cytometric analysis of surface bound IgE on rat BMMCs

Aims

The initial aim of these experiments was to determine if an IgE anti-DNP sensitisation protocol could be used in rat BMMCs. Unfortunately, a rat IgE anti-DNP reagent was not available for these studies, but previous investigators have demonstrated that mouse IgE binds equally well to the rat FcεRI receptor (Sterk and Ishizaka, 1982). Therefore, to determine the feasibility of using mouse IgE anti-DNP to sensitise rat BMMCs, flow cytometry was used to compare cells possessing endogenous IgE to cells passively sensitised with mouse monoclonal IgE anti-DNP (SPE-7, Sigma).

Methods

The BMMCs in these and subsequent experiments were cultured, washed, identified, counted and assessed for viability as described in detail in chapter 2 (sections 2.1 - 2.9). A suspension of cells was removed from each of three different bone marrow cultures containing 19%, 80% and 93% BMMCs respectively (all ≥ 98% viability). The cells were washed three times and resuspended in flow cytometry buffer (FCB, comprising PBS with 0.1% NaN_3 and 3% v/v FCS). Half the cells from each culture were incubated with 10μg mouse IgE anti-DNP / 10^6 cells for 1 hour at 37°C; the other half were incubated with buffer alone. After washing a further three times in FCB to remove unbound IgE, cells from each group were incubated for 1 hour at 4°C with one of the following labels:-

1) A 1/200 dilution of fluorescein isothiocyanate (FITC) conjugated mouse monoclonal IgG_1 anti-rat IgE (Mare-1- FITC, Serotec, Oxford, UK) to detect endogenous IgE. Previous studies using an irrelevant monoclonal mouse IgG_1 specific for a viral protein (VPM-FITC provided by G. Entrican, Moredun Research Institute, Edinburgh) showed that this class of antibody did not bind non-specifically to BMMCs (MacDonald, 1994).

2) A 1/100 dilution of rat monoclonal IgG_1 anti-mouse IgE-FITC conjugate (LO-ME-3, Serotec) to detect bound mouse IgE.

3) Buffer alone.

After labelling, the cells were washed three times in FCB, fixed in 2% paraformaldehyde and stored in 15 ml centrifuge tubes at 4°C in the dark until analysed by flow cytometry (described in chapter 2, section 2.13). Each population of cells from each culture comprised 10^5-10^6 cells and each flow cytometric analysis was based on 10^4 cells.

Results

The binding of the endogenous IgE derived from the LNCM, and of the added IgE in the cultures containing 19%, 80% or 93% BMMCs is shown in figures 3.1 to 3.3 and summarised in table 3.1. Within the three cultures, 11%, 70% and 71% of the unsensitised cells respectively were labelled with anti-rat IgE. Similar figures were obtained for the cells sensitised with mouse IgE, indicating that the anti-rat IgE did not cross-react with the mouse IgE. However, in the mature culture containing 93% BMMCs, 14% of the cells appeared to fluoresce after labelling with buffer only (see Figure 3.3). This apparently high background fluorescence may represent autofluorescent cells, and does not necessarily indicate that the percentage of cells labelled with anti-rat IgE or anti-mouse IgE in this culture is artificially high. However, the proportion of cells labelled with anti-rat IgE did not increase between the 80% and 93% cultures, and if this high background fluorescence is subtracted, the percentage of cells labelled with anti-rat IgE is less in the culture containing 93% BMMCs than that containing 80%. In addition, the mean fluorescence intensity (proportional to the number of IgE molecules per cell) is higher in the fluorescing cells from the culture containing 19% BMMCs than in either of the more mature cultures (Table 3.2). These results suggest that the proportion of BMMCs bearing

endogenous IgE, and the occupancy of the IgE receptors on each BMMC, might actually decrease as the cultures reach maturity.

After sensitisation with monoclonal mouse IgE anti-DNP, 33%, 76% and 95% of the cells from the same cultures were positively labelled with rat anti-mouse IgE (Table 3.1), demonstrating that the mouse IgE had bound to the rat IgE receptor. However, 24, 21 and 25% of the cells respectively from the unsensitised groups were also labelled by the rat anti-mouse IgE, suggesting that this reagent might be cross-reacting with rat IgE and/or binding non-specifically to other cell types. The latter conclusion was also suggested by the finding that 33% of the cells fluoresced in the culture that only contained 19% BMMCs. However, when cells from cultures containing 80% and 93% BMMCs were sensitised with IgE and labelled with anti-mouse IgE, the fluorescence histograms shifted to the right (Figures 3.2 and 3.3), demonstrating both an increase in the proportion of fluorescing cells and an increase in mean fluorescence (Table 3.2). Taken together, these results suggest that the binding of endogenous IgE to BMMCs may decrease throughout culture, but the proportion of cells with surface-bound IgE, and the occupancy of the IgE receptors on each cell, can be increased by passive sensitisation with mouse IgE anti-DNP.

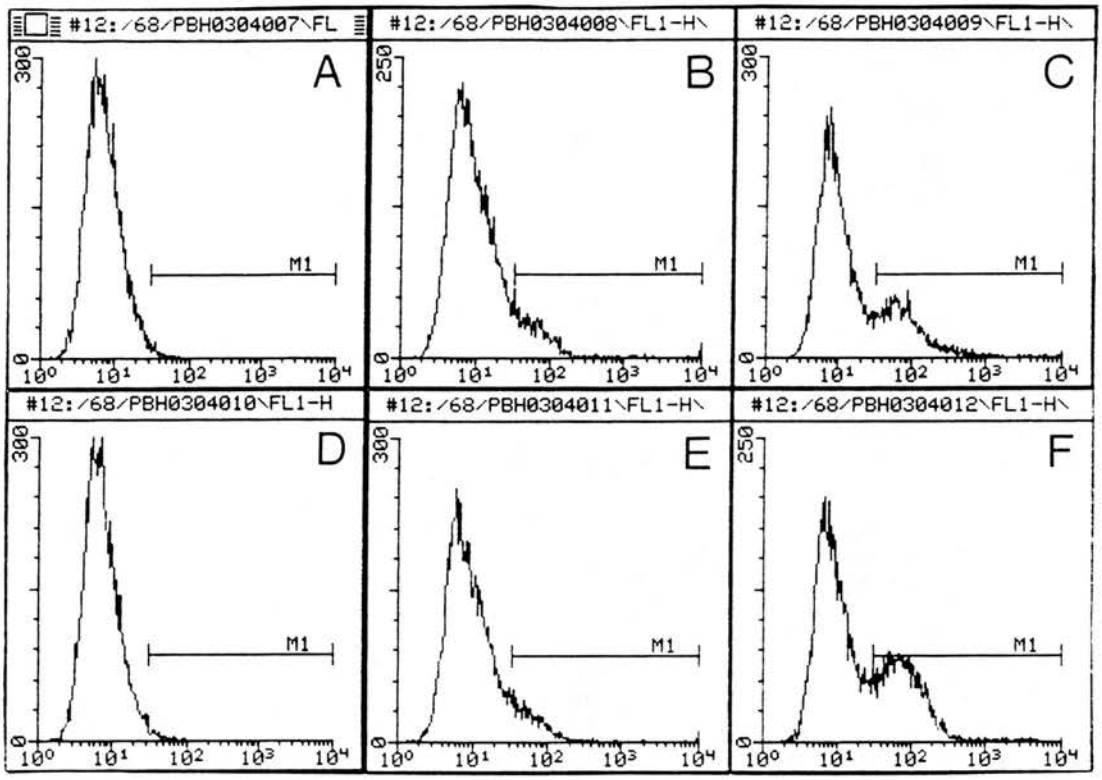

Figure 3.1 - Flow cytometric analysis of rat BMMC culture containing 19% mast cells. Cells were either unsensitised (A,B,C) or sensitised with mouse IgE anti-DNP (D,E,F). Cells from both groups were then labelled with either buffer alone (A and D), mouse anti-rat IgE-FITC conjugate (B and E), or rat anti-mouse IgE-FITC conjugate (C and F). A bi-modal distribution with a small peak to the right appears in the cells labelled with anti-rat IgE or anti-mouse IgE, indicating the subpopulation of cells with bound IgE (see text for details).
x-axis = log units of fluorescence; y-axis = number of cells; M1 marker placed at the right border of the negative control histogram (A, cells labelled with buffer only).

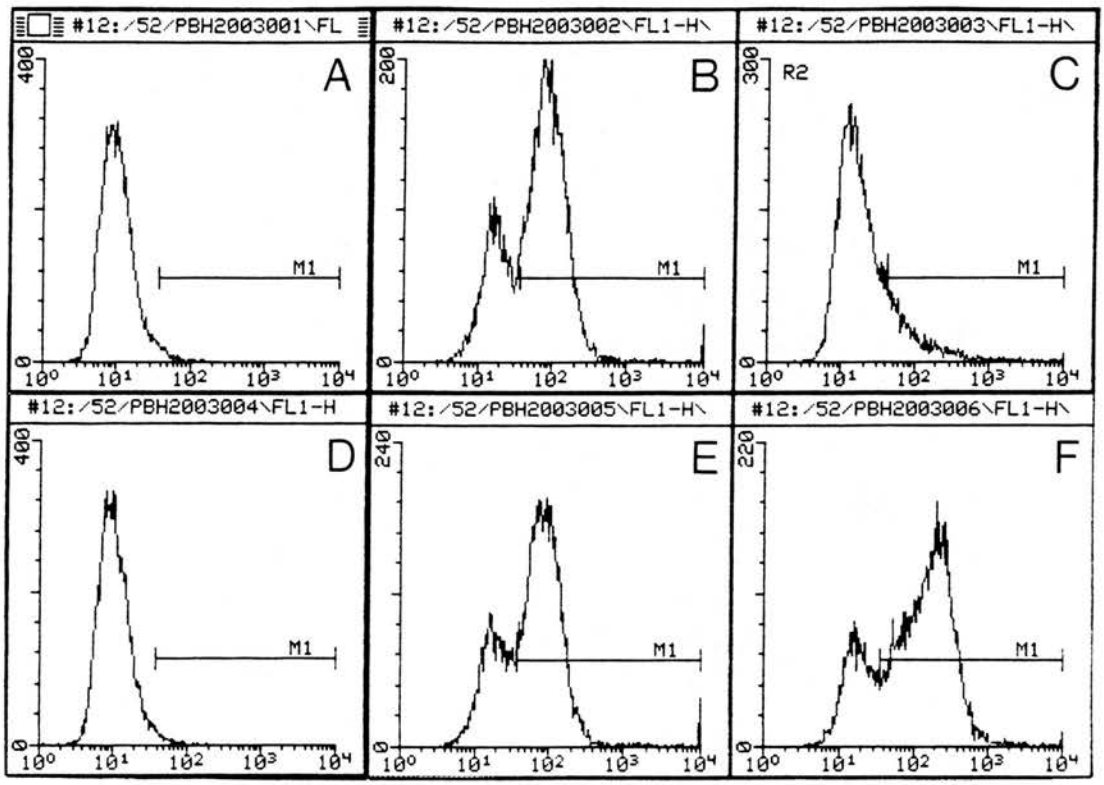

Figure 3.2 - Flow cytometric analysis of rat BMMC culture containing 80% mast cells. Cells were either unsensitised (A,B,C) or sensitised with mouse IgE anti-DNP (D,E,F). Cells from both groups were then labelled with either buffer alone (A and D), mouse anti-rat IgE-FITC conjugate (B and E), or rat anti-mouse IgE-FITC conjugate (C and F). A bi-modal distribution with a large peak to the right appears in cells labelled with anti-rat IgE or anti-mouse IgE, but cells labelled with anti-mouse IgE have a higher mean fluorescence (see text for details).
Axes and M1 marker as in Figure 3.1.

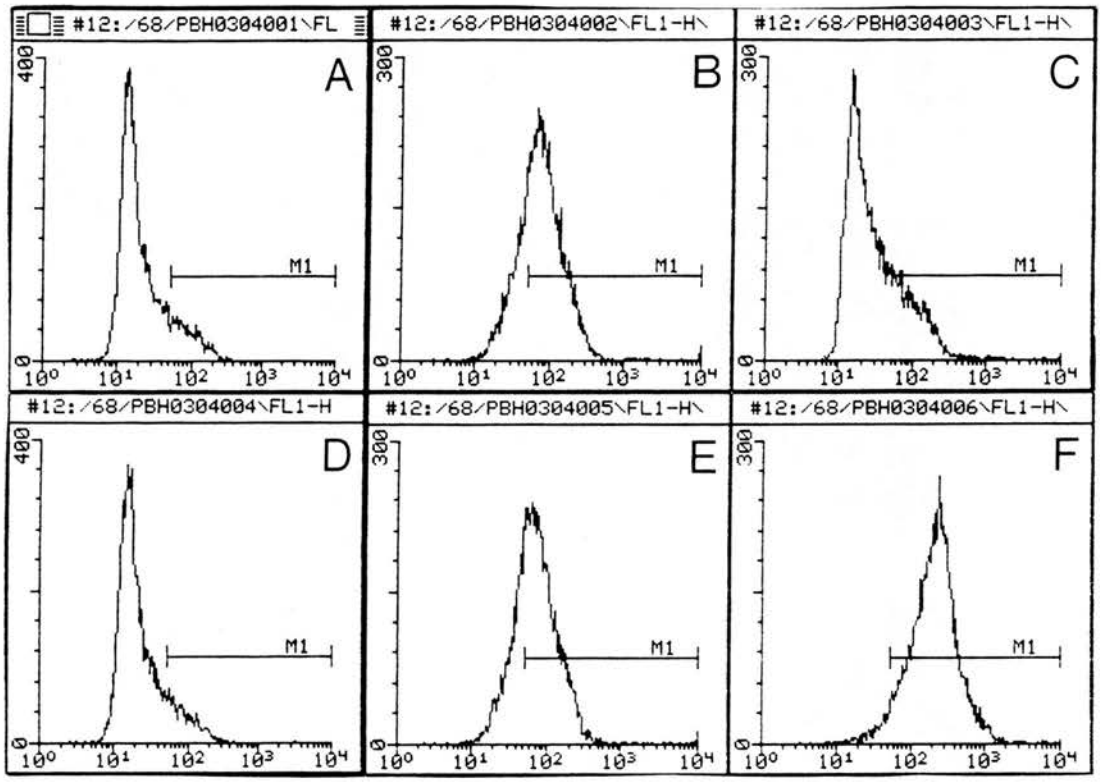

Figure 3.3 - Flow cytometric analysis of rat BMMC culture containing 93% mast cells. Cells were either unsensitised (A,B,C) or sensitised with mouse IgE anti-DNP (D,E,F). Cells from both groups were then labelled with either buffer alone (A and D), mouse anti-rat IgE-FITC conjugate (B and E), or rat anti-mouse IgE-FITC conjugate (C and F). Cells labelled with either anti-rat IgE or anti-mouse IgE are labelled as a normal distribution, with no second peak. The proportion of cells labelled with anti-mouse IgE is higher than those labelled with anti-rat IgE, and they have a higher mean fluorescence.
Axes as in Figure 3.1. The M1 marker was placed at the start of the tail on the right border of the negative control histogram (A, cells labelled with buffer only). This region was excluded because it may contain autofluorescent cells.

Table 3.1 - Percentage of BMMCs labelled with anti-IgE

Treatment	Label	Maturity of Culture		
		19% BMMCs	80% BMMCs	93% BMMCs
Unsensitised	Buffer	0.8%	2%	14%
	α rat IgE	11%	70%	71%
	α mouse IgE	24%	21%	25%
Sensitised	Buffer	0.9%	1.7%	14%
	α rat IgE	11%	70%	69%
	α mouse IgE	33%	76%	95%

Table 3.2 - Mean log fluorescence of labelled cells

Treatment	Label	Maturity of Culture		
		19% BMMCs	80% BMMCs	93% BMMCs
Unsensitised	Buffer	39	51	101
	α rat IgE	205	146	134
	α mouse IgE	160	201	158
Sensitised	Buffer	43	52	102
	α rat IgE	166	166	136
	α mouse IgE	124	234	282

Tables 3.1 and 3.2 - Detection of surface bound endogenous or exogenous IgE by flow cytometry in three different bone marrow cultures containing 19%, 80% and 93% BMMCs. Cells from each culture were either unsensitised or sensitised with mouse IgE anti-DNP. Cells from both groups were then labelled with either buffer alone, mouse anti-rat IgE-FITC conjugate or rat anti-mouse IgE-FITC conjugate.
Table 3.1 - The figures indicate the percentage of total cells labelled.
Table 3.2 - The figures indicate the mean log fluorescence of the labelled cells (arbitrary units).

3.2 - Activation of BMMC secretion by challenging IgE-sensitised cells with DNP-BSA

Aims

The flow cytometry analysis showed that i) mouse IgE anti-DNP could bind to rat BMMCs, and ii) that passive sensitisation with mouse IgE could increase both the proportion of cells binding IgE, and the amount bound. However, it was important to demonstrate that DNP-BSA could trigger mediator release from IgE-sensitised BMMCs. The following preliminary experiment was designed to compare the responses of sensitised BMMCs to a range of DNP-BSA concentrations with those of unsensitised BMMCs to an optimal dilution of anti-IgE.

Methods

A suspension of BMMCs from a culture containing 98% mast cells (100% viability) was washed three times in Tyrodes buffer/EDTA (TB/EDTA, chapter 2, section 2.12) and divided into two aliquots. One aliquot was sensitised with mouse monoclonal IgE anti-DNP as described in chapter 2 (section 2.15) and the other aliquot was incubated with buffer alone. After three further washes in TB to remove unbound IgE, the cells were resuspended in TB/Ca^{2+}/Mg^{2+} (TB^{+}) and divided into 14 treatment groups as shown overleaf. Each group comprised a suspension of 0.9×10^{6} cells in a volume of 0.5 ml TB^{+}. The BMMCs were challenged with various concentrations of DNP-BSA or anti-IgE as described in chapter 2 (sections 2.16 - 2.17), and the pellets and supernatants were assayed for β hexosaminidase as described in section 2.19.

Experimental Design

IgE-Sensitised Cells			Unsensitised Cells		
Tube	Secretagogue	Dilution	Tube	Secretagogue	Dilution
1.	DNP-BSA	1/10 (1mg/ml)	9.	Goat anti-rat IgE	1/250
2.	DNP-BSA	1/100	10.	Goat anti-rat IgE	1/250
3.	DNP-BSA	1/1000			
4.	DNP-BSA	1/10,000	11.	DNP-BSA	1/100
5.	DNP-BSA	1/100,000	12.	DNP-BSA	1/100,000
6.	Tyrode's Buffer		13.	Normal goat serum	1/250
7.	Tyrode's Buffer		14.	Normal goat serum	1/250
8.	Tyrode's Buffer				

Results

The percentage release of β hexosaminidase from BMMCs in each treatment group is shown in Figure 3.4. As described in previous studies (MacDonald, 1994), goat anti-rat IgE triggered the release of β hexosaminidase from BMMCs without the need for prior sensitisation with IgE (11% release for anti-IgE vs. 0.5% in response to NGS, or 1.2% in response to DNP-BSA, mean of 2 tubes). DNP-BSA stimulated β hexosaminidase release from IgE-sensitised cells at all dilutions tested, but dilutions of 1/1000 or less were required for optimum secretion (14.3% at 1/1000 vs. 0.4% in response to buffer alone, Figure 3.4). In subsequent secretion assays, DNP-BSA was therefore used at a final dilution of 1/1000 (10μg/ml). These assays, and the statistical analysis of the effects of anti-IgE and DNP-BSA on BMMC secretion, are described in the remainder of this chapter, and in chapter 4.

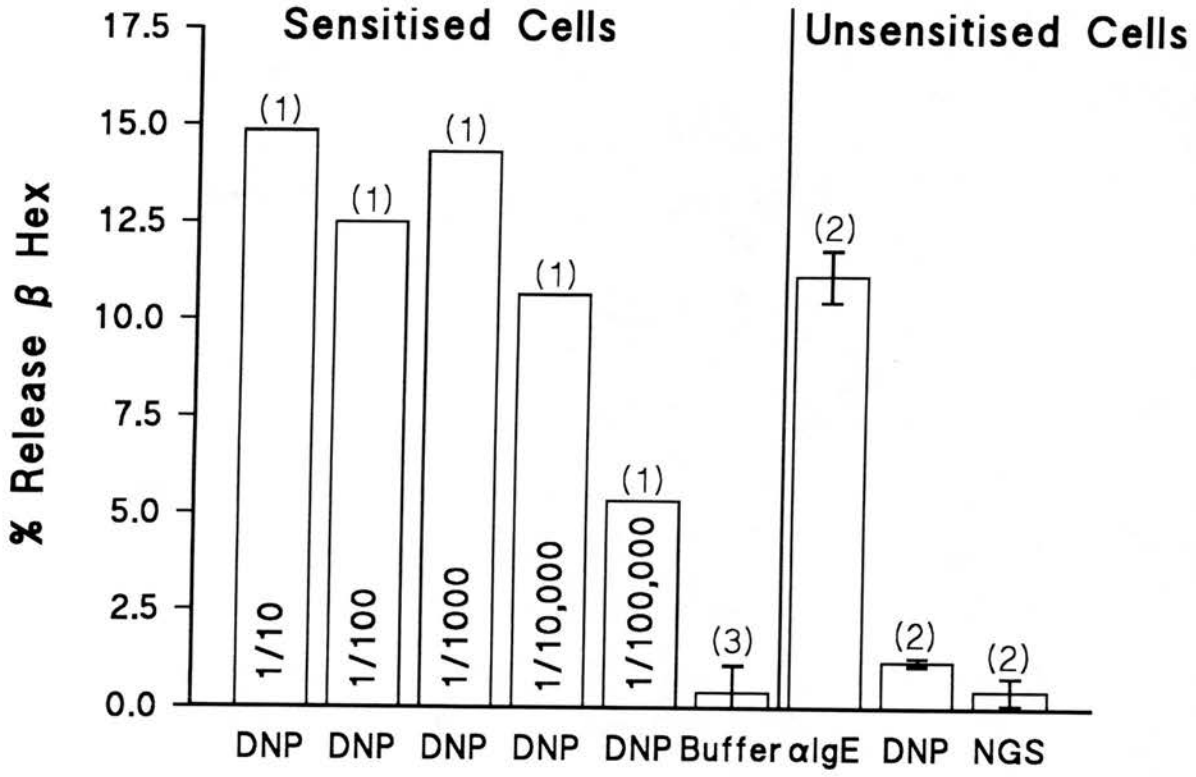

Figure 3.4 - Preliminary experiment showing the percentage release of β hexosaminidase from BMMCs in response to IgE-dependent stimulation. BMMCs from a culture containing 98% mast cells were either sensitised with mouse IgE anti-DNP or incubated with buffer alone. The sensitised cells were challenged with concentrations of DNP-BSA ranging from 1 mg/ml (1/10) to 10 ng/ml (1/100,000), and the unsensitised cells were challenged with goat anti-rat IgE at an optimal dilution of 1/250. The number above each bar represents the number of tubes, each containing 0.9 x 10^6 cells, that received each stimulus. For replicate tubes, the range is shown. DNP = DNP-BSA, Buffer = Tyrode's buffer/Ca^{2+}/Mg^{2+}, αIgE = goat anti-rat IgE, NGS = normal goat serum.

3.3 - Development of an enzyme-linked immunospot (ELISPOT) assay for the detection of IgE-dependent RMCP-II release from individual BMMCs

Aims

The aim of this section was to determine the feasibility of detecting RMCP-II release from individual cells using an ELISPOT method.

Methods

The mouse monoclonal anti-RMCP-II and the affinity-purified polyclonal sheep anti-RMCP-II for use in the ELISPOT assay was kindly provided by Mr. G.F.J. Newlands, Moredun Research Institute, Edinburgh, UK. The purified RMCP-II was provided by Mr. G.F.J. Newlands and Dr. C.L. Scudamore, Royal (Dick) School of Veterinary Studies, University of Edinburgh, UK. The preparation of these reagents has been described (Huntley *et al,* 1990a).

The ELISPOT assay methodology was a modification of the solid-phase immuno-enzymatic technique introduced by Sedgwick and Holt (1983). The principle of the assay is shown in Figure 3.5 and described below. 48 well cell culture plates (Costar, Cambridge, MA, USA) were incubated overnight at 4°C with 150 µl/well mouse monoclonal anti-RMCP II (1µg/ml) in PBS, pH 7.5. After washing twice with PBS/0.05% tween 20 (PBS/T20), remaining binding sites were blocked by adding 200µl of 1% non fat milk (Marvel, Premier Brands, Stafford, UK) in PBS to each well and incubating for 1 hour at 37°C. The plate was then washed 4 times in PBS and a known number of BMMCs suspended in 125 µl of TB^+ was added to each well. Cells were usually diluted to provide between 100 and 400 cells/well using the following dilution factor:

$$\text{Dilution factor} = \frac{\text{Number of BMMCs/µl}}{\text{Number of BMMCs/well}} \times 125$$

Hence, with a typical initial cell density of 5 x 10^5 BMMCs/ml (500/μl), a dilution of 1:625 would provide 100 cells per well. The presence of a single cell suspension was confirmed by examination of the wells under a phase contrast microscope. RMCP II (125μl at 50ng/ml) was added to one or two wells as a positive control, and wells containing buffer but no cells were included as negative controls. The cells were challenged with 125 μl of appropriately diluted secretagogue (anti-IgE or DNP-BSA) or control stimulus (NGS or TB^+) and incubated for 30 min at 37°C. The wells were washed four times in PBS/T20 to remove the cells, and bound RMCP-II was detected by sequentially incubating the plate with 150μl/well 1:1000 sheep anti-RMCP-II and 150μl/well 1:10,000 donkey anti-sheep IgG-alkaline phosphatase conjugate (Sigma), both diluted in PBS/T20/4% BSA. Incubations were for one hour at 37°C and plates were washed four times after each incubation in PBS/T20. The substrate solution was prepared as described (see appendix 1 and Sedgwick & Holt, 1983) and comprised 1 mg/ml 5-bromo-4-chloro-3-indoyl phosphate (BCIP, Sigma) dissolved in AMP buffer (1.0 M 2-amino-2-methyl-1-propanol (Sigma), 0.7mM $MgCl_2$ and 0.01% v/v Triton-X-405, pH 10.25). This solution was heated to 40°C and mixed with an agarose solution (Type 1, Sigma) at 60°C to yield a final concentration of 0.6% w/v agarose. 200μl of the substrate/agarose mixture was added immediately to each well, and the plate was left overnight at room temperature (18 - 20°C) to allow colour development.

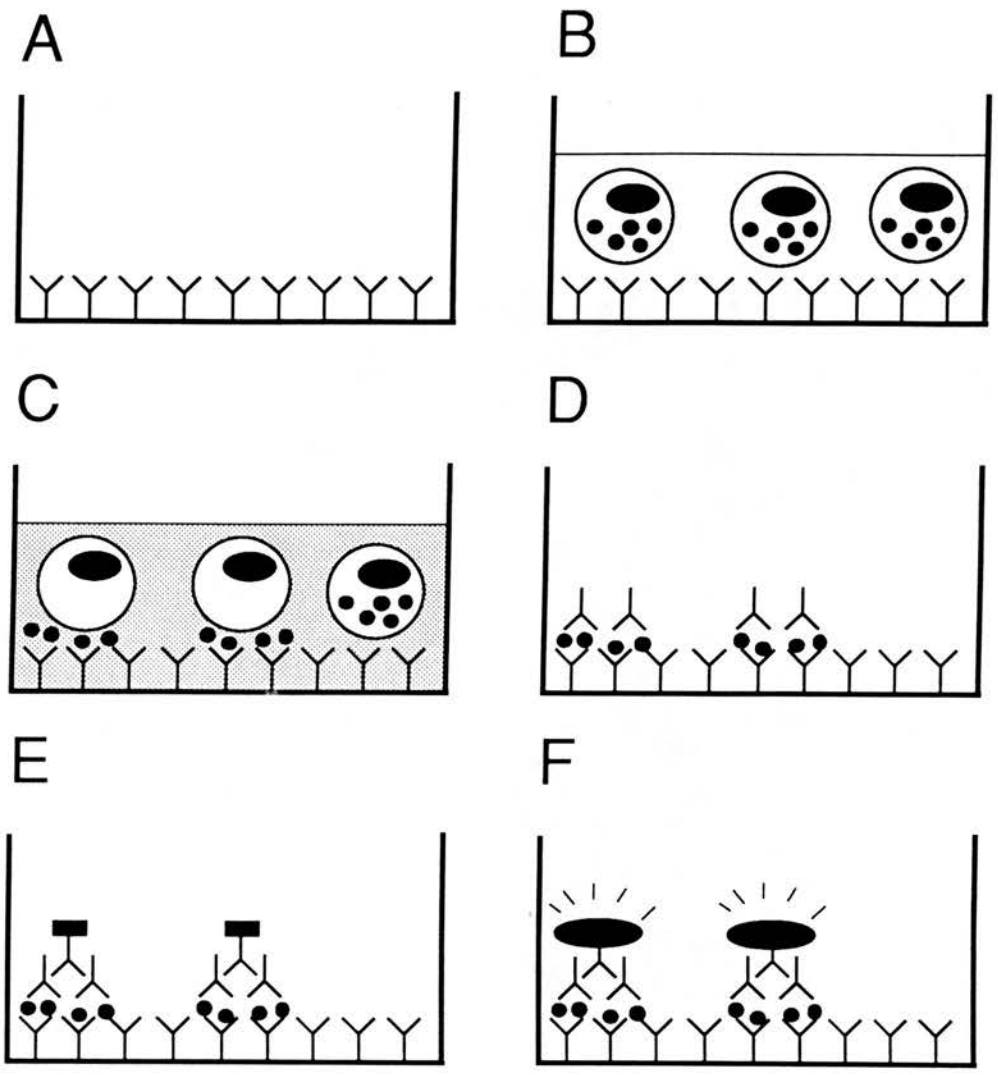

Figure 3.5 - Principle of the ELISPOT assay. **A** - Wells are coated with mouse monoclonal anti-RMCP-II. **B** - A known number of BMMCs are added to each well. **C** - The cells are challenged with a secretagogue causing mediator release by a proportion of the cells. The granule chymase RMCP-II binds to the capture antibody in a focal spot surrounding each cell. **D** - The cells are washed away and the bound RMCP-II is detected with a polyclonal sheep anti-RMCP-II antibody. **E** - The sheep anti RMCP-II is recognised by a donkey anti-sheep IgG-alkaline phosphatase conjugate. **F** - A substrate for alkaline phosphatase is added resulting in colour development at the site of the focal spot of bound RMCP-II (see text for details).

Results

The results of a typical ELISPOT assay are shown in Figure 3.6 (The plate map for this and subsequent ELISPOT assays, along with the spot counts, are shown in appendix 3). For this assay, a suspension of BMMCs from a culture containing 92% mast cells (viability 100%) was washed three times in TB/EDTA and sensitised with IgE as described in chapter 2 (section 2.15). The cells were then diluted to yield 134 BMMCs (150 cells) per well, which were added to columns 1 - 7 of the plate. Column 8 contained buffer but no cells, and well F8 contained 50 ng/ml RMCP-II as a positive control (Figure 3.6). The cells in rows A to E were challenged with DNP-BSA, and those in row F were challenged with TB^+ to detect spontaneous release.

During development of the plate, discrete blue spots started to appear within 10 min of addition of the substrate, but complete development took a number of hours. The plates were therefore left overnight before the number of spots was assessed (Figure 3.6). The spots reveal sites at which individual BMMCs had degranulated, releasing RMCP-II which bound to the capture antibody. The spots could be counted under a bright light without magnification, although they were more clearly visualised with a 6.4 x dissecting microscope (Figure 3.6). Examination of wells at higher magnification was unhelpful because pin-point foci of substrate became visible, even in the negative control wells. The size of the spots was not measured objectively, although variation was observed in all assays, as can be seen in Figure 3.6. An attractive feature of the assay was that the coloured spots of substrate were fixed in the solidified agarose matrix, allowing plates to be kept for a number of weeks without deterioration.

The wells in which BMMCs were challenged with DNP-BSA contained 18 ± 5 spots (mean $\pm$ s.d., n=35), which was significantly greater those challenged with Tyrode's buffer (2 ± 1 spots, n=7, $p < 0.0001$). As would be expected with any biological system, the number of spots varied from well to well, and this variability is addressed

in detail in section 3.6 of this chapter. The positive control well (F8, 50 ng/ml RMCP-II) and the negative (no cells) control wells (A8 to E8) were diffusely blue and clear respectively (Figure 3.6). However, in some assays, spots were occasionally observed in the negative control wells (see appendix 3). In this case, the spot counts were averaged and subtracted from the spot counts in treatment wells before statistical analysis.

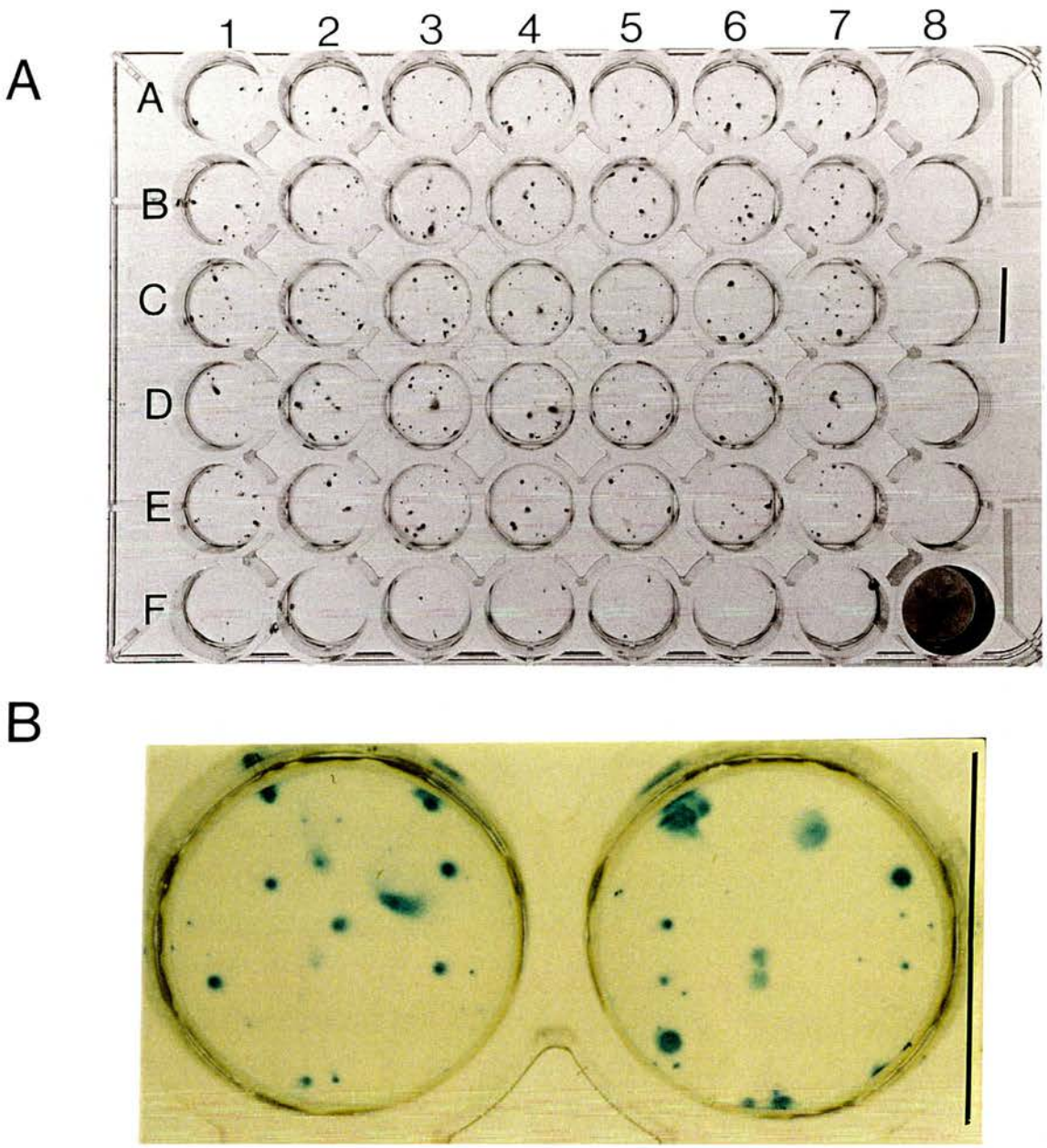

Figure 3.6 - A: 48 well plate showing the typical appearance of an ELISPOT assay. 134 IgE-sensitised BMMCs were added to columns 1 - 7. Column 8 contained buffer but no cells as a negative control, and well F8 contained 50 ng/ml RMCP-II as a positive control. Rows A to E were challenged with DNP-BSA, and row F was challenged with Tyrode's buffer/Ca^{2+}/Mg^{2+}. The spots represent sites at which individual BMMCs had degranulated, releasing RMCP-II which bound to the capture antibody. The bound RMCP-II was detected by an immuno-enzymatic method (see text for details). Scale marker = 1 cm.

B: Magnified wells showing the discrete blue spots that can be easily visualised and counted. Scale marker = 1 cm.

3.4 - Sensitivity and specificity of the ELISPOT assay

Aims

The previous experiment demonstrated that the ELISPOT assay could detect RMCP-II release from IgE-sensitised BMMCs challenged with DNP-BSA. However, at this stage it was not known whether the assay was sufficiently sensitive to detect RMCP-II release from all the cells. For example, a mean of 18 spots appeared in the antigen-stimulated wells, although these wells contained 134 BMMCs. This might occur if the assay could only detect RMCP-II release from a proportion of larger cells with the most RMCP-II. Hence, if conclusions were to be drawn about the proportion of BMMCs within the population that responded to IgE-mediated stimulation, it was important to determine the sensitivity of the assay. In addition, it was important to determine that the released RMCP-II was binding specifically to the capture antibody rather than non-specifically to the plate.

Methods

To determine if the ELISPOT assay was sufficiently sensitive to detect the release of RMCP-II from individual cells, the lowest concentration of purified RMCP-II that could be detected in 1μl droplets was measured. The droplets were added to the anti-RMCP-II antibody-coated plates using a 1μl pipette in an attempt to reproduce the small quantities of RMCP-II released from BMMCs during degranulation. Four separate experiments were performed in which twofold serial dilutions of RMCP-II from 500 pg/μl to 0.03 pg/μl were added to wells. 1μl droplets containing only buffer were added to three wells as controls. The plates were wrapped in clingfilm to prevent evaporative losses and incubated for 30 min at 37°C in a humidified incubator. The droplets had not dried out when the plates were removed from the incubator and were still clearly visible. After the plates were washed to remove the droplets, they were developed as described above (section 3.3).

To ensure that RMCP-II was binding specifically to antibody coated wells, a similar experiment was performed in which serial dilutions of RMCP-II in 1μl droplets were added to wells coated with PBS, rabbit polyclonal anti-RMCP-I, or mouse monoclonal anti-RMCP-II.

Results

Figure 3.7 shows one of four similar experiments in which serial dilutions of RMCP-II were added to anti-RMCP-II-coated plates in the form of 1μl droplets (4 droplets per well). The plate is divided into three regions comprising the upper two, middle two and lower two rows. The serial dilutions ranging from 500 pg/μl to 0.03 pg/μl run from left to right, with droplets in wells B8 and D8 containing only buffer and well F8 containing 50 ng/ml RMCP-II. The limit of detection was taken as the last well in which four distinct spots could be clearly visualised (arrows). In this assay, spots were visible at a concentration of 0.24 pg/μl, but in three similar experiments the end points were 0.98 pg/μl, 1.95 pg/μl, and 3.9 pg/μl yielding a mean theoretical sensitivity of 1.8 ± 1.6 pg RMCP-II/μl (mean ± s.d., n=4).

The mean RMCP-II concentration in individual mast cells, determined by ELISA of freeze/thawed cell pellets, increased from 3.4 ± 0.3 pg/cell at day 4 to 30.4 ± 3 pg/cell at day 28 (see chapter 2, Figure 2.2). Thus, the ELISPOT assay could theoretically detect a mature mast cell that released ≈ 6% of its RMCP-II, and a developing BMMC at day 4 that released ≈ 50% of its RMCP-II. However, the size of the applied droplets was inevitably much larger than the diffusional area of RMCP-II released from a cell, resulting in a wider spread of the applied protease over the base of the well than would occur following degranulation (compare the spot sizes in Figures 3.7 and 3.6). It is likely, therefore, that the observed limit of detection of 1.8 pg RMCP-II/μl is an under-estimate of the true sensitivity of the assay. Despite this, these results demonstrate that the ELISPOT assay is sufficiently sensitive to detect RMCP-II release from the vast majority of BMMCs, with the

possible exception of extremely immature cells that release less than 50% of their RMCP-II.

In a similar experiment to that described above, RMCP-II only bound to wells coated with anti RMCP-II, and no spots developed in wells coated with PBS or anti-RMCP-I (not shown), thus confirming that the binding of RMCP-II represented a specific antibody-antigen interaction.

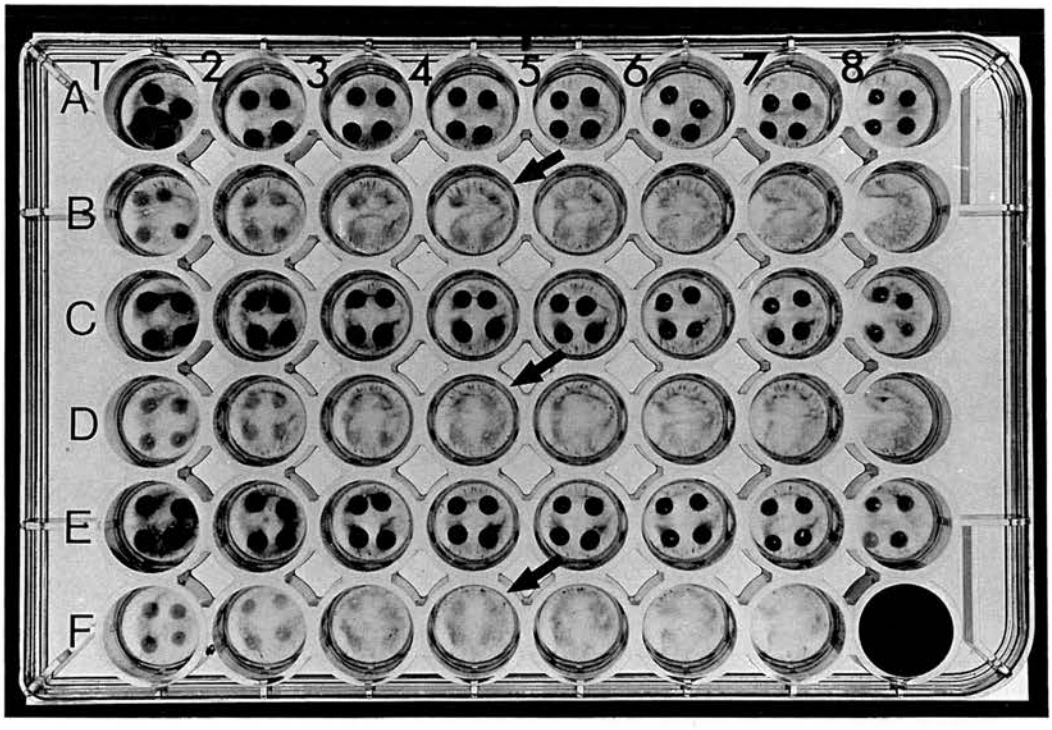

Figure 3.7 - Sensitivity of the ELISPOT assay. The 48 well plate was coated with anti-RMCP-II and is divided into three regions: upper two (A and B), middle two (C and D) and lower two rows (E and F). Serial dilutions of RMCP-II running from left to right and ranging from 500 pg/μl (wells A1, C1, E1)to 0.03 pg/μl (wells B7, D7, F7) were added to the wells as 1μl droplets (4 per well). Wells B8 and D8 contained droplets of buffer only, and well F8 contained 50 ng/ml RMCP-II as a positive control. The limit of detection was taken as the last well in which four distinct spots could be clearly visualised (arrows, 0.24 pg/μl).

3.5 - Correlation between cell density and the number of spots per well in ELISPOT assays

Aims

The previous experiments demonstrated that the ELISPOT assay could detect RMCP-II release from individual BMMCs. However, for accurate interpretation of ELISPOT assays, it was important to demonstrate that the number of spots appearing in each well correlated with the number of cells placed in each well, even if only a proportion of the BMMCs responded to stimulation.

Methods

Four similar ELISPOT assays were performed in which cell suspensions from cultures containing different proportions of BMMCs were serially diluted to yield 400, 200, 100, 50, 25, 12 and 6 cells per well. The estimated number of BMMCs per well in each experiment is shown below, with the number of replicate wells in brackets.

	Percentage of BMMCs in each culture			
	38%	53%	95%	97%
Total cells per well	Approximate number of BMMCs per well			
400	150 (5)	210 (2)	380 (8)	390 (8)
200	75 (5)	105 (2)	190 (8)	195 (8)
100	38 (5)	52 (2)	95 (8)	98 (8)
50	19 (5)	26 (2)	48 (8)	49 (8)
25	9 (5)	13 (2)	24 (8)	25 (8)
12	5 (3)	7 (2)	12 (8)	12 (8)
6	2 (3)	3 (2)	6 (8)	6 (8)

The cells from cultures containing 38% and 53% BMMCs were challenged with goat anti-rat IgE and those from cultures containing 95% and 97% BMMCs were sensitised with mouse IgE and challenged with DNP-BSA (described in chapter 2,

sections 2.14-2.16). Normal goat serum (NGS) and TB^+ were used as negative controls as described previously. The number of spots that developed in each well was then counted and compared to the estimated number of BMMCs in each well.

Results

The relationship between cell density and number of spots per well in the four experiments is shown in Figure 3.8. In all assays, the number of spots in wells challenged with either anti-IgE or DNP-BSA increased linearly with increasing cell density (solid circle, $r=0.99$ in each case, $p<0.001$). The slope of the lines therefore indicates the proportion of BMMCs that responded to stimulation. Hence, 21% and 16% of the BMMCs from the cultures containing 38% and 53% mast cells respectively detectably released RMCP-II in response to anti-IgE. The spontaneous degranulation of BMMCs from these cultures was extremely low, with spot counts amounting to 1.1% of the BMMC counts in both cases (Figure 3.8 A and B, solid triangles). In the cultures containing 95% and 97% mast cells, 16% and 15% of the BMMCs respectively released RMCP-II in response to DNP-BSA. However, the spontaneous release from BMMCs challenged with buffer alone was higher than in the immature cultures (3.9% in both cases), and again, cell density correlated closely with the number of spots counted (Figure 3.8 C and D, solid triangles, $r=0.99$, $p<0.001$).

These results demonstrate that the spots developing in ELISPOT assays are closely correlated with the number of BMMCs placed in each well. They also indicate that only 12 - 15% of BMMCs within the population specifically responded to challenge with either anti-rat IgE or DNP-BSA. This phenomenon is discussed further in section 3.7 of this chapter.

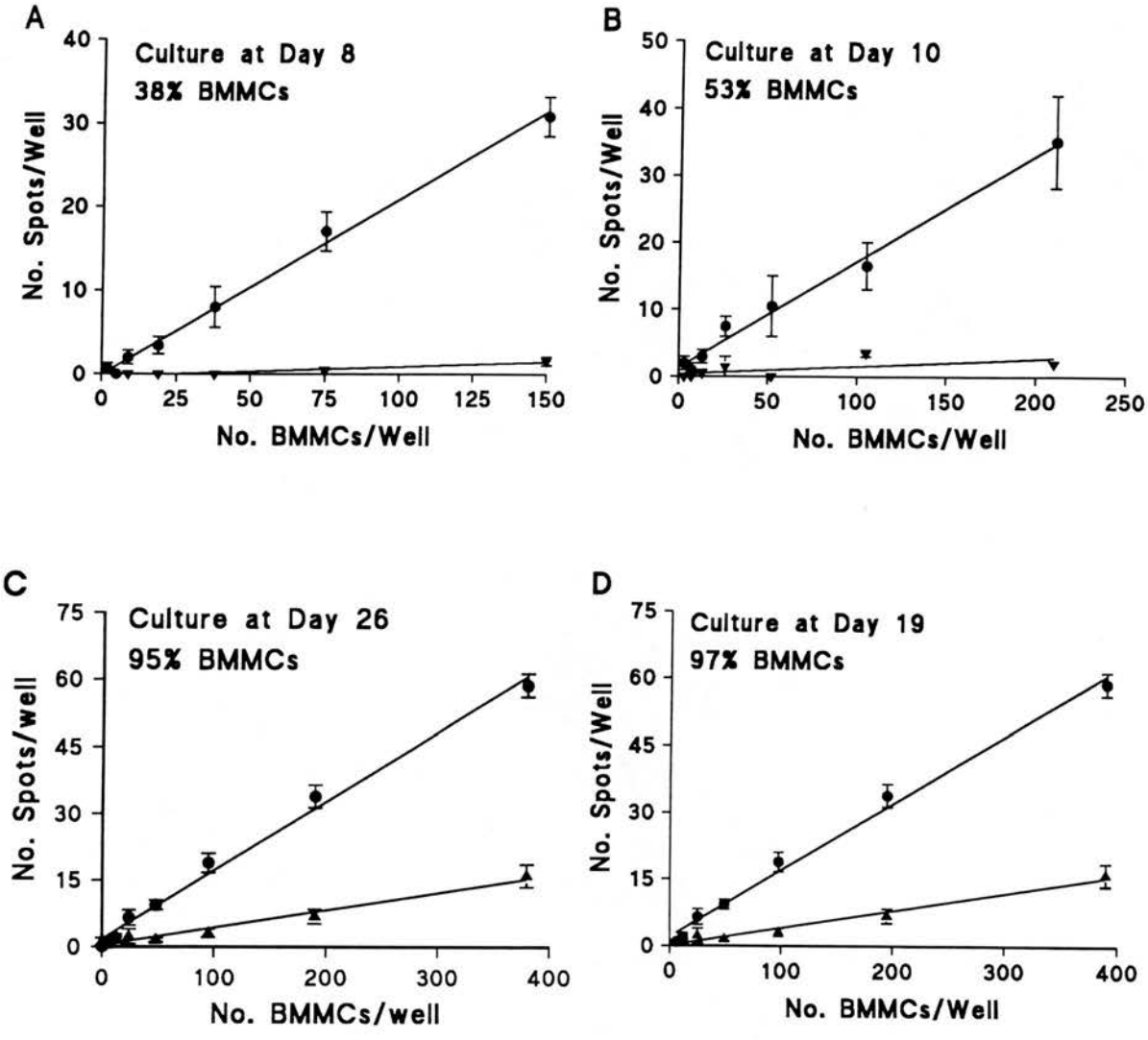

Figure 3.8 - The relationship between density of BMMCs and the number of spots per well in ELISPOT assays. BMMCs were serially diluted as described in the text. BMMCs from cultures containing 38% (**A**) and 53% (**B**) mast cells were challenged with goat anti-rat IgE (**A** and **B** solid circles) or normal goat serum (solid triangles). BMMCs from cultures containing 95% (**C**) and 97% (**D**) mast cells were sensitised with mouse IgE anti-DNP and challenged with DNP-BSA (**C** and **D** solid circles) or Tyrode's buffer (solid triangles). Each point represents the mean ± s.e.m. of individual spot counts from the number of wells indicated in the text. Correlation coefficients for all lines = 0.99, $p<0.001$, except for the groups challenged with normal goat serum in A and B (A, $r = 0.97$, $p<0.01$; B, $r = 0.64$, $p = 0.12$).

3.6 - Repeatability and statistical analysis of the ELISPOT assay

Aims

The variability of other immunological assays such as ELISAs and radioimmunoassays (RIAs) depends chiefly on physico-chemical factors such as pipetting, dilutions, antibody coating, antibody/antigen interactions and enzyme kinetics. However, in the case of the ELISPOT assay, an additional source of variation is the biological responses seen in a population of cells (see the variation in the number of spots per well in Figure 3.5). Hence, it was important to characterise this variation to allow correct statistical analysis of ELISPOT data.

Methods

A suspension of IgE-sensitised BMMCs from a culture containing 98% mast cells (100% viability) was diluted to provide 100 BMMCs/well. The cells were added to 42 wells of 5 separate 48 well plates. Cells in 28 wells in each plate were challenged with DNP-BSA and the cells in 14 wells were challenged with TB^+. The remaining 6 wells contained buffer but no cells, and comprised the positive and negative controls (Figure 3.9).

DNP-BSA	100	100	100	100	100	100	100	-
	100	100	100	100	100	100	100	-
	100	100	100	100	100	100	100	-
	100	100	100	100	100	100	100	-
Buffer	100	100	100	100	100	100	100	-
	100	100	100	100	100	100	100	⊕

Figure 3.9 - Plate map for the above experiment. Five identical plates were prepared in which 100 BMMCs were placed in each well marked 100. - = negative control (no cells), ⊕ = 50 ng/ml RMCP-II. The top four rows were challenged with DNP-BSA, the lower two with Tyrode's buffer/Ca^{2+}/Mg^{2+}.

Results

The spot counts from the five replicate plates are shown below.

1

7	12	16	11	10	16	5	0
5	13	20	11	15	5	26	0
8	15	11	16	17	23	12	0
9	13	9	21	18	18	17	0
2	2	3	2	1	3	2	0
3	1	1	1	2	6	0	+

2

17	6	13	13	6	9	11	0
11	5	21	12	18	12	16	0
11	11	14	7	19	20	15	0
17	12	13	8	11	16	13	0
0	1	1	5	1	4	2	0
1	1	1	4	2	1	5	+

3

9	15	14	7	13	8	11	0
8	12	13	9	23	8	14	0
11	14	11	17	17	8	14	0
8	22	14	12	22	22	12	0
1	3	4	2	1	2	3	0
2	1	0	3	1	1	1	+

4

18	11	13	10	12	13	12	0
10	18	26	14	25	13	10	0
7	17	16	16	24	33	17	0
9	16	12	20	20	16	25	1
3	3	2	5	1	1	1	0
3	1	1	2	1	0	0	+

5

14	16	12	11	9	9	10	0
15	12	17	19	25	11	16	0
14	14	17	17	27	20	14	0
12	16	18	20	11	27	11	0
4	3	2	4	2	0	0	0
0	2	1	3	2	2	3	+

The spot counts in each of the five replicate ELISPOT assays from both the DNP-BSA treated cells and the buffer-treated cells were normally distributed as assessed by the Ryan-Joiner test (Minitab Statistical Software). The data was therefore

suitable for analysis by parametric tests. The proportions of BMMCs releasing RMCP-II following challenge with DNP-BSA or buffer are shown below (means ± s.d. to nearest whole number):

Plate Number	DNP-BSA	Buffer
1	14 ± 5%	2 ± 1%
2	13 ± 4%	2 ± 2%
3	13 ± 5%	2 ± 1%
4	16 ± 6%	2 ± 1%
5	16 ± 5%	2 ± 1%

The well to well coefficients of variation for the five plates (based on the 28 DNP-BSA challenged wells) were 40%, 33%, 36%, 38% and 32%, yielding a mean well to well coefficient of variation of 36 ± 3%. This relatively high figure represents the biological variation within the cell population, and has an important bearing on the performance of the ELISPOT assay. Clearly, experiments involving the comparison of individual wells would be unacceptable. Hence, it was important to determine how many wells would be required for meaningful comparisons to be made between different treatment groups. Put differently, how many wells in the above experiment would need to be compared to yield an acceptable (≈ 10-15%) coefficient of variation? This problem was addressed by assigning the 28 DNP-BSA-stimulated wells in the above experiment to arbitrary treatment groups, allowing the inter-plate coefficient of variation to be calculated using different numbers of wells per group (see Figure 3.9).

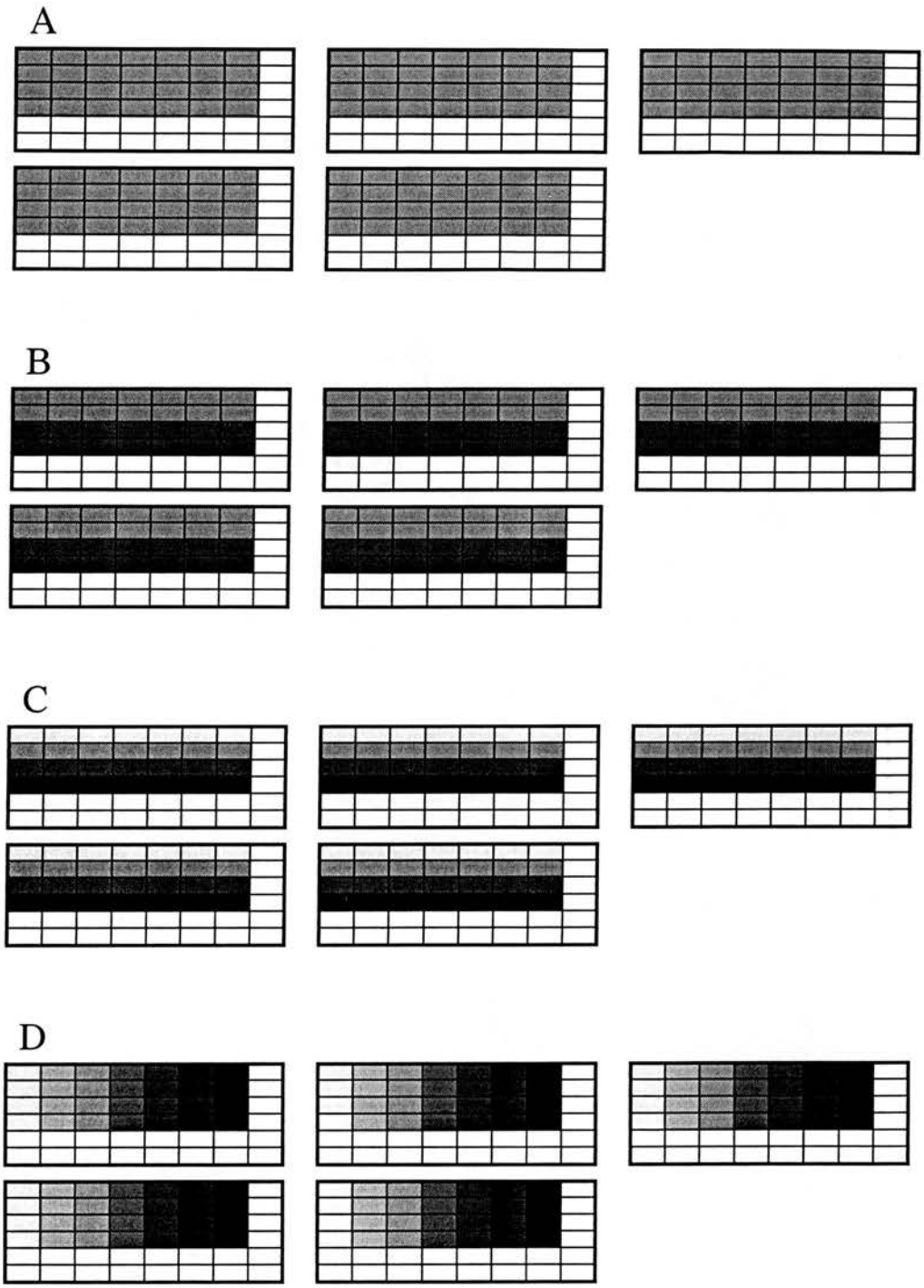

Figure 3.9 - Comparison of different numbers of wells for determination of the inter-plate coefficient of variation (c.v. = s.d.÷mean x100%). The shaded regions represent corresponding wells in which the cells are regarded as one group. In A, the spot counts from the 28 wells in each plate are regarded as one treatment group and averaged. The inter-plate c.v. is then based on the mean and s.d. of the 5 averages. In B, C, and D the mean and s.d. of the 5 average spot counts from 14, 7, or 4 corresponding wells are compared. The coefficients of variation for each calculation are 10.6% (A), 10.9% (B, mean of 2), 11.5% (C, mean of 4) and 17.5% (D, mean of 7). See text for details.

The inter-plate coefficient of variation was calculated by comparing spot counts from either 4, 7, 14 or 28 corresponding wells from the 5 plates (Figure 3.9). If the spot counts in the 28 wells were averaged and regarded as one treatment group, the coefficient of variation between the 5 plates was 10.6%. If 14 corresponding wells per plate were regarded as separate treatment groups, the mean coefficient of variation was 10.9 ± 1% (n=2). When 7 wells per plate were compared, the mean coefficient of variation was 11.5 ± 4% (n=4), and this increased to 17.5 ± 6% (n=7) when 4 corresponding wells were compared. As expected, these results indicate that the larger the treatment group (in terms of the number of wells counted), the lower the variability. However, they suggest that treatment groups studied in the ELISPOT assay should preferably comprise at least seven wells to avoid excessive inter-assay variation.

A further question regarding the analysis of data from ELISPOT assays concerns the use of statistical tests. As the data is normally distributed, parametric tests such as one way analysis of variance (ANOVA) and Student's t test should be appropriate for comparing treatment groups. However, when the spot counts in the 28 identically treated DNP-BSA-challenged wells from the 5 plates were compared by ANOVA, the mean spot counts were marginally different at a significance level of 0.05 ($p=0.047$). Hence, when using parametric tests such as ANOVA, a significance level of 0.01 would be more appropriate for analysis of ELISPOT data. When the 28 wells from the 5 plates were compared by the non-parametric Kruskal Wallis test (which is more robust against outliers), the spot counts were not significantly different ($p=0.113$). In summary, these results suggest that if spot counts from different treatment groups are compared using ANOVA, a significance level of 0.05 might reflect assay variation. Therefore, treatment groups should be compared at a significance level of 0.01, or alternatively, non parametric statistical tests should be used.

3.7 - Characterisation of IgE-mediated RMCP-II release by BMMCs at various stages of culture

Aims

This section provides a summary of all the ELISPOT assays performed to date in which BMMCs were challenged with either anti-IgE or DNP-BSA. Some of the assays were described earlier in this chapter, and the remainder represent controls for experiments described in chapter 4. The purpose of this section is to allow a comparison between the effects of anti-rat IgE on unsensitised BMMCs at various stages of culture, and DNP-BSA on BMMCs sensitised with mouse IgE anti-DNP.

Methods

To characterise the response of BMMCs to anti-IgE during various stages of maturation, a series of 16 ELISPOT assays was performed on cells taken at intervals throughout the growth of 3 different cultures (summarised in Table 3.3). In addition, a further 7 ELISPOT assays were performed using IgE-sensitised BMMCs from mature cultures (Table 3.3). The cells were prepared, diluted and stimulated as described in chapter 2 (sections 2.10, 2.14-2.16) and the ELISPOT assays were performed as described in section 3.3.

Results

The results of the 22 ELISPOT assays are summarised in Table 3.3 (and shown in appendix 3). Overall, 7 ± 7% of unsensitised BMMCs specifically released RMCP-II in response to challenge with anti rat IgE (calculated by subtracting the percentage of BMMCs that released RMCP-II in response to NGS). However, this response was dependent on the stage of culture from which the BMMCs were derived. In eight experiments performed using cultures containing 8, 36, 38, 41, 53, 64, 66% or 85% BMMCs, a highly significant ($p<0.001$) proportion of BMMCs responded to anti-IgE when compared to NGS controls, with a mean specific response of 13 ± 7%. By contrast, in eight experiments performed using cultures containing 87, 89, 92, 95, 95,

96, 98 or 99% mast cells, only 1.8 ± 1% of the BMMCs specifically responded to anti-IgE.

To determine if the poor specific response in mature cultures was related to the level of IgE binding, BMMCs from four different mature cultures were sensitised with mouse IgE anti-DNP IgE and challenged with DNP-BSA. In seven experiments performed using cultures containing 92, 95, 97, 98, 98, 99, or >99% mast cells, a mean of 12 ± 2% of BMMCs specifically released RMCP-II in response to DNP-BSA (Table 3.3)

The explanation for the poor specific response to anti-IgE in the mature cultures did not appear to be related to higher spontaneous release from these cells. Although the spontaneous release of RMCP-II was higher in the BMMCs showing a poor specific response (11 ± 10%) than those showing a significant specific response (2.4 ± 0.8%), the difference was not significant. Likewise, the poor response of the mature BMMCs to anti-IgE did not seem to be related to poor cell viability, although in one experiment, a viability of only 77% resulted in spontaneous release of RMCP-II from 34% of the cells (see Table 3.3).

These results, together with the flow cytometry analysis, strongly suggest that the level of endogenous IgE binding may be deficient in mature BMMC cultures, resulting in a sub-optimal response to challenge with anti-IgE. However, more interestingly, even when BMMCs were passively sensitised with exogenous IgE, only 12% of the cells apparently degranulated. This suggests that, under our experimental conditions, a large proportion of the BMMC population was refractory to IgE-dependent stimulation.

A - Response of BMMCs to anti-IgE

Culture	Day of Culture	% BMMCs	% Viability	Response to α-IgE (%)	Spontaneous release (%)	Specific response (%)	No. Wells Counted	Details of Experiment
1	8	38	92	21[a]	1.1[a]	20*	31	Section 3.5
	10	53	97	16[a]	1.1[a]	15*	14	Section 3.5
	11	66	97	15.8 ± 4.5	3.2 ± 2.7	16*	8	Section 3.7
	15	89	98	2.8 ± 0.5	1.5 ± 0.4	1	9	Section 3.7
	17	96	99	3.1 ± 0.4	2 ± 1.2	2	9	Section 4.2
2	4	8	>99	26.8 ± 6.8	2.4 ± 2.7	24*	18	Section 4.4
	8	41	>99	8.1 ± 1.9	2.5 ± 1.3	6*	18	Section 4.4
	11	64	97	10.6 ± 3	2.2 ± 1.2	8*	18	Section 4.4
	15	85	96	9.9 ± 1.9	3.1 ± 1.6	7*	18	Section 4.4
	18	92	96	12.5 ± 4.2	10.2 ± 2.6	2	18	Section 4.4
	21	98	93	20.5 ± 5.3	20.5 ± 5.9	0	18	Section 4.4
3	9	36	98	8.9 ± 3.2	2.9 ± 1.2	6*	18	Section 4.4
	17	87	98	9.5 ± 5.7	6.4 ± 3.7	3	18	Section 4.4
	21	95	96	9.4 ± 3.3	7.6 ± 2.4	2	18	Section 4.4
	24	95	92	9.1 ± 3.7	6.5 ± 2.8	3	18	Section 4.4
	28	99	77	35.3 ± 9.3	34 ± 8.9	1	18	Section 4.4

B - Response of IgE-Sensitised BMMCs to DNP-BSA

Culture	Day of Culture	% BMMCs	% Viability	Response to DNP (%)	Spontaneous release (%)	Specific response (%)	No. Wells Counted	Details of Experiment
4	16	98	100	12.7 ± 1.7	3.4 ± 3	9*	9	Section 4.5
	17	99	100	14.7 ± 4.9	1.9 ± 1.5	13*	9	Section 4.5
	22	>99	100	9.7 ± 3.6	3.1 ± 1.3	6.6*	8	Section 4.3
5	19	92	100	13.7 ± 5	1.6 ± 1.2	12*	35	Section 3.3
	26	95	100	16[a]	3.9[a]	12*	56	Section 3.5
6	19	97	100	15[a]	3.9[a]	11*	56	Section 3.5
7	23	98	100	14.5 ± 5	1.9 ± 1.4	13*	140	Section 3.6

Table 3.3 - Proportion of BMMCs that responded to anti-IgE or DNP-BSA, calculated by expressing spot counts in ELISPOT assays as a percentage of the number of BMMCs per well. BMMCs from immature cultures (<85% BMMCs) show a significant response to anti-IgE, but a poor response is seen in cells from mature cultures. The response can be restored by sensitising the BMMCs with IgE anti-DNP and challenging with DNP-BSA. [a] = values determined from the slope of regression lines (see section 3.5); * = significant difference between challenged and spontaneous release ($p<0.001$).

DISCUSSION

In this chapter, the development of a novel enzyme-linked immunospot (ELISPOT) assay to detect RMCP-II release from individual BMMCs is described. This technique has proved remarkably successful, allowing basic questions concerning the regulation of IgE-dependent mediator release in rat BMMCs to be addressed. The technique is also the first to quantify the release of a specific mediator from individual mast cells of any type.

The assay was based on the detection of rat mast cell protease-II (RMCP-II), a granule chymase specific to rat intestinal mucosal mast cells and rat bone marrow-derived mast cells (BMMCs) (Gibson and Miller, 1986; McMenamin *et al,* 1987). Release of RMCP-II from BMMCs correlates closely with the release of other preformed granule mediators such as β hexosaminidase and generation of membrane-derived lipid mediators such as leukotriene C_4 (MacDonald *et al,* 1989). Detection of RMCP-II release is therefore a useful marker of secretion in these cells. In addition, RMCP-II is released by rat intestinal mucosal mast cells both constitutively and following IgE-mediated activation, and is thought to play an important role in the expulsion of gastro-intestinal nematodes (Miller *et al,* 1983; Woodbury *et al,* 1984; Scudamore *et al,* 1995b). Thus, detection of RMCP-II release by BMMCs in the ELISPOT assay *in vitro* has great relevance *in vivo*, and provides an insight into the regulation of mast cell responses in the gut.

As with any new biological assay, specificity, sensitivity and reproducibility are important considerations. The assay was developed using reagents that are highly specific for RMCP-II (Huntley *et al,* 1990a), and the protease was shown to bind specifically to wells coated with anti-RMCP-II antibodies. More importantly, the assay was shown to be sufficiently sensitive to detect RMCP-II release from individual cells, allowing the proportion of responding BMMCs within a population to be determined. In terms of repeatability, the mean intra-assay (well to well)

coefficient of variation in the ELISPOT assay (36%) was much higher than that accepted for ELISAs or RIAs (Kemeny, 1991). However, this would be expected because the ELISPOT assay relies on biological responses which inevitably introduce more variation than physico-chemical factors such as antibody binding and enzyme kinetics. This problem could be overcome by increasing the number of wells per treatment group. For example, if 7 replicate wells were compared between two plates, the inter-assay coefficient of variation was an acceptable 11.5%. The well to well variation in the ELISPOT assay also influences the use of statistical tests. As the spot counts in replicate wells were normally distributed, the use of parametric tests is appropriate. However, the inter-plate variability between 5 replicate plates introduced sufficient variation to yield a significant difference when spot counts from 28 wells were compared by ANOVA ($p = 0.047$). Hence, statistical comparisons between treatment groups in different plates should be interpreted with caution, preferably at a significance level of 0.01 or less.

Possible explanations for the variation in spot size noted in the ELISPOT wells (Figure 3.6) include variation in RMCP-II content per cell, wider diffusion of RMCP-II from cells degranulating more rapidly after addition of the secretagogue, and mediator release from a cluster of cells. Clustering of cells was considered unlikely because, in order to reduce the cell density from 5×10^5 /ml to a few hundred cells/well, three dilution steps were performed which completely separated clumps of cells. In addition, examination of wells under phase contrast microscopy revealed single cell suspensions. The actual area of the spots could therefore be used to estimate the quantity of RMCP-II released from each cell. Although spot size was not quantified in this study, it could possibly be measured in future studies using computerised digital imaging.

The initial reason for developing an ELISPOT assay was to determine how individual BMMCs within the population responded to stimulation. The assay was

therefore used to investigate the responses of rat BMMCs to two IgE-mediated stimulation protocols. Surprisingly, only 6-24% of the BMMCs within a population appeared to respond to stimulation by either anti-IgE or specific antigen (Table 3.3). When compared to previous studies, which showed 10-25% mediator release from populations of BMMCs (Broide *et al,* 1988; MacDonald *et al,* 1989; and Figure 3.4), these results suggest that the behaviour of the cells under these experimental conditions approached that described in the introduction under hypothesis 2, i.e. the total mediators released by a population of BMMCs arise from a group of cells that release most, if not all, their stored mediators ("all-or-none" mode of secretion). However, although the total number of BMMCs per well correlated closely with the number of spots per well (Figure 3.8), the detection of responding cells could be artifactually decreased if all the BMMCs were not in contact with the base of the well. For example, if a number of BMMCs degranulated whilst in suspension, the released RMCP-II would not result in a spot. Although examination of the wells under phase contrast microscopy revealed that the majority of cells were in contact with the base of the well, this could not be quantified due to the low cell densities. A potential solution to the problem in future studies would be to develop a stimulation protocol that results in 100% mediator release from rat BMMCs, but this has not yet been achieved. Hence, at this stage, the above figures can not be interpreted as direct evidence for an "all-or-none" mode of secretion in rat BMMCs.

Despite this, the above problem was not of a sufficient magnitude to explain the large refractory population of BMMCs that failed to respond to IgE-mediated stimulation (75-90% of the cells). This phenomenon could result from a deficiency in individual cells at any stage of the signal transduction pathway including: inadequate FcεR1 expression; insufficient IgE; lack of intracellular transduction proteins; reduced intracellular calcium stores; and/or reduced ion channel expression. In mouse bone marrow-derived mast cells, expression of FcεR1 coincides with granule formation, suggesting that cultured mast cells possess IgE receptors at the onset of maturation

(Lantz and Huff, 1995b). In addition, flow cytometry demonstrated that rat BMMCs have surface bound endogenous IgE throughout culture, and therefore FcεR1 receptors, although this appeared to be sub-optimal for stimulation in cells from mature cultures. However, when cells were passively sensitised with exogenous mouse IgE, which increased occupancy of the IgE receptors, a refractory population of BMMCs still remained indicating that failure to respond was not purely related to the degree of IgE binding. In rat basophil leukaemia (RBL-2H3) cells (Millard *et al,* 1988; Millard *et al,* 1989), and human basophils and mast cells (MacGlashan and Guo, 1991; MacGlashan and Botana, 1993), stimulation of populations of cells via the FcεR1 resulted in variable intracellular calcium fluxes and oscillations. Correlation of intracellular calcium fluxes with mediator release from individual cells indicated that a sustained rise in intracellular calcium, seen only in a proportion of the cells, was required to initiate secretion (Kim, T.D., personal communication). Although calcium responses have not been imaged in rat BMMCs, a similar heterogeneity of intracellular calcium responses could explain the large proportion of BMMCs that failed to respond to immunological stimulation in this study.

The ELISPOT assay therefore proved to be a useful method for analysing the secretory responses of individual rat BMMCs. However, the assay also possessed a number of features that offer potential for other areas of mast cell research. First, it was simpler and more economical to perform than conventional mediator release assays. The latter assays require populations of cells to be stimulated and then separated from their supernatants. Remaining mediators have to be extracted from the cell pellets, and then both supernatants and cell pellets have to be assayed for mediator levels, typically using ELISA or radioimmunoassays. With the ELISPOT assay, the release of RMCP-II is detected directly so the results are obtained with a single assay.

A second advantage of the ELISPOT assay is that mast cell secretion can be studied using far fewer cells than previously possible. Conventional mediator release assays require 10^4 - 10^6 cells per treatment group so that sufficient mediator is released to be detectable by conventional assays such as ELISA or RIA. In general, mast cells in sufficient numbers for these experiments can only be obtained in four ways. Firstly, by using tumour cell lines such as the rat basophilic leukaemia cell (RBL-2H3) which is an analogue of mucosal mast cells (Barsumian *et al,* 1981; Crews *et al,* 1981); secondly, by growing mast cells in culture by stimulating bone marrow or umbilical cord blood with various cytokines (Razin *et al,* 1983; Haig *et al,* 1988; Mitsui *et al,* 1993); thirdly, by isolation and purification of mast cells from laboratory rodents, such as rat peritoneal mast cells or intestinal mucosal mast cells (White and Pearce, 1982; Befus *et al,* 1982); and finally by isolation and purification of mast cells from pathological specimens such as human lungs, skin, nasal polyps, or intestines (Paterson *et al,* 1976; Schulman *et al,* 1982; Lawrence *et al,* 1987; Finotto *et al,* 1994; Bischoff *et al,* 1996). Unfortunately, the study of mast cell activation in other species, or in clinical cases of allergic disease, has been limited because it is not feasible to obtain mast cells in such high numbers. For example, samples of broncho-alveolar lavage fluid (Flint *et al,* 1985) or skin biopsies from atopic patients would not be amenable to such large-scale studies, even though the mast cells in these disease states may have distinctive and interesting properties. However, if the ELISPOT methodology was modified to detect mediator release from human mast cells, statistically quantifiable results could be obtained with as few as 5000 cells per assay. Such an assay could be a valuable tool in the investigation of allergic diseases, and could potentially be used for diagnostic purposes to determine if mast cells were sensitised to specific antigens.

In summary, the results in this chapter show that mediator release from individual mast cells can be detected with a sensitive and repeatable RMCP-II ELISPOT assay. The assay was used to characterise IgE-mediated secretion from rat BMMCs at

various stages of culture and showed that only 6-24% of BMMCs within a population responded to stimulation, leaving a large residual refractory population. If a similar assay was developed for other species, it could be very valuable for studying mast cell secretion in various allergic states such as asthma or atopic dermatitis.

Chapter 4

EFFECTS OF STEM CELL FACTOR ON IGE-DEPENDENT MEDIATOR RELEASE FROM RAT BONE MARROW-DERIVED MAST CELLS

INTRODUCTION

In the previous chapter, the IgE-dependent release of rat mast cell protease-II from rat BMMCs was investigated using a novel ELISPOT assay. In this chapter, the effect of the multi-functional cytokine stem cell factor (SCF) on IgE-dependent mediator release from BMMCs is investigated using both the ELISPOT assay and conventional mediator release assays.

As described in detail in chapter 1, SCF has a wide range of effects on mast cell function both *in vivo* and *in vitro*. Hence, an absolute or partial deficiency in SCF or its receptor, *c-kit*, results in greatly reduced mast cell numbers in Sl/Sl^d (Kitamura and Go, 1979) or W/W^v (Kitamura *et al,* 1978) mice respectively. Injection of soluble SCF into Sl^d/Sl^d mice reversed the mast cell deficiency (Zsebo *et al,* 1990a), and in normal rats caused a marked increase in the numbers of both connective tissue and mucosal mast cells (Tsai *et al,* 1991a). In addition, SCF contributed to the mucosal mast cell hyperplasia seen in response to infection with the parasites *Nippostrongylus brasiliensis* and *Trichinella spiralis* (Newlands *et al,* 1995; Donaldson *et al,* 1996), and stimulated the expansion of lymph node conditioned medium-dependent rat BMMCs *in vitro* (Haig *et al,* 1994). Furthermore, SCF enhanced the survival of mast cells by preventing apoptosis (Mekori *et al,* 1993; Iemura *et al,* 1994). SCF was also shown to be a chemotactic agent for mast cells (Blumejensen *et al,* 1991; Meininger *et al,* 1992), and regulated the adhesion of mast

cells to fibroblasts (Adachi *et al,* 1992) or extracellular matrix components such as fibronectin (Dastych and Metcalfe, 1994; Kinashi and Springer, 1994).

In addition to these roles in chemotaxis, adhesion, proliferation, differentiation, maturation and survival, recent studies have shown that SCF can also influence mediator release from a number of mast cell types. Treatment with SCF in isolation directly induced mediator release from mouse peritoneal mast cells (Coleman *et al,* 1993), rat peritoneal mast cells (Nakajima *et al,* 1992; Koike *et al,* 1993; Taylor *et al,* 1996), mouse skin mast cells (Wershil *et al,* 1992) and human skin mast cells (Costa *et al,* 1996) without the need for IgE receptor activation. In these connective tissue phenotype mast cells, SCF acted as a secretagogue at concentrations ranging from 20 - 500 ng/ml. However, SCF can also act as a *potentiator* of IgE-dependent mediator release in both connective tissue and mucosal mast cells. For example, brief preincubations (10 - 15 minutes) with the cytokine (100 ng/ml) enhanced IgE-dependent mediator release from human skin, lung and intestinal mast cells (Columbo *et al,* 1992; Bischoff and Dahinden, 1992; Bischoff *et al,* 1996). In the latter two studies, involving mucosal mast cells from the lung and intestine, SCF had no significant secretagogue effect *per se*, but it augmented the release of histamine by 226% (lung) and 46% (intestine) following activation of the cells with an antibody to the IgE receptor (Bischoff and Dahinden, 1992; Bischoff *et al,* 1996). Taken together, these studies provide evidence that SCF may be directly involved in the regulation of immune responses by modulating the secretory function of mast cells.

Similar studies have not been performed on mast cells isolated from the intestinal tract of the rat. However, earlier work by MacDonald (1994) showed that SCF was not a secretagogue for rat BMMCs, but it enhanced IgE-dependent mediator release from these cells in a concentration and time-dependent manner. Preincubation of BMMCs with 10, 100 and 1000 ng/ml SCF for 15 minutes significantly increased β

hexosaminidase release from populations of BMMCs stimulated with anti-IgE, but concentrations of 0.001 to 1 ng/ml had no effect (see Figure 1 in Hill *et al*, 1996 at the back of this thesis). When mature BMMCs were incubated with SCF (50 ng/ml) for 5, 15, or 60 minutes, or 3 or 24 hours before challenge with anti-IgE, maximal enhancement of RMCP-II and β hexosaminidase occurred after a 5 minute preincubation, but the effect declined thereafter and was not statistically significant in cells treated with the cytokine for 3 or 24 hours (see Figure 2 in Hill *et al*, 1996). Hence, as in the studies of other mast cell types, these preliminary results suggested that SCF may play a critical role in the regulation of secretory responses in rat BMMCs.

The main aim in this chapter was to further characterise the role of SCF in modulating the secretory function of rat BMMCs. The specific aims were:-

1) To confirm and extend the results of MacDonald (1994) by investigating the effects of SCF on IgE-mediated secretion from unsensitised BMMCs, and BMMCs sensitised with mouse IgE anti-DNP.

2) To determine whether SCF-dependent enhancement in IgE-mediated secretion from BMMCs reflected individual cells releasing more mediator, or increased numbers of cells responding to stimulation. This question could have important implications for the regulation of mast cell secretory function *in vivo*. Therefore, the effects of SCF on IgE-dependent mediator release were re-examined using conventional mediator release assays and the RMCP-II ELISPOT assay described in the previous chapter.

EXPERIMENTAL METHODS AND RESULTS

4.1 - The effect of SCF on IgE-dependent mediator release from BMMC populations

Aims

The aim of this initial experiment was to confirm the results of MacDonald (1994) using the present BMMC cultures and the mouse IgE anti-DNP sensitisation regime.

Methods

Stem cell factor (recombinant rat SCF^{164}, 2.2 mg/ml) was kindly provided by Dr. Keith Langley of Amgen Inc., Thousands Oaks, CA. It was stored in aliquots at -70°C and was thawed once before use. For secretion experiments, SCF was diluted in Tyrodes buffer/Ca^{2+} /Mg^{2+} (TB^+) and TB^+ was used as a control (see chapter 2, section 2.12).

The BMMCs for this and subsequent experiments were cultured, washed, identified and assessed for viability as described in chapter 2 (sections 2.1-2.9). A suspension of cells from a culture containing 96% BMMCs (100% viability) was washed three times in TB/EDTA and divided into two aliquots. One aliquot was sensitised with mouse IgE anti-DNP (section 2.15) and the other was incubated with buffer alone. After three further washes in TB to remove unbound IgE, the cells were resuspended in TB^+ and divided into 8 treatment groups as shown overleaf. Each group comprised triplicate tubes containing 10^6 viable BMMCs in a volume of 0.5 ml TB^+. To determine the effect of SCF on BMMC secretion, SCF (or TB^+ as a control) was added to the Eppendorf tubes in a volume of 55µl at a concentration of 500 ng/ml to give the required concentration (50 ng/ml) when the cells were added. The cells were then incubated in the presence or absence of SCF for 5 min at 37°C in a shaking water bath.

Experimental Design

IgE-Sensitised Cells			Unsensitised Cells		
Group	Secretagogue	Dilution	Group	Secretagogue	Dilution
1.	DNP-BSA	1/1000	5.	Anti-IgE	1/250
2.	TB^+	-	6.	NGS	1/250
3.	SCF + DNP-BSA	1/1000	7.	SCF + Anti-IgE	1/250
4.	SCF + TB^+	-	8.	SCF + NGS	1/250

The cells were challenged with DNP-BSA, TB^+, anti-IgE or NGS as described in chapter 2 (sections 2.16-2.17) and the pellets and supernatants were assayed for β hexosaminidase as described in section 2.19. The percentage release of β-hexosaminidase in the various treatment groups was compared by ANOVA and Student's t test, and the results are reported as mean ± s.e.m.

Results

Challenge of both the sensitised or unsensitised groups of BMMCs with DNP-BSA or anti-IgE respectively induced significant release of β hexosaminidase in this experiment (16.1 ± 0.4% for DNP-BSA vs. 1.3 ± 0.2% for buffer, $p<0.001$; 10.4 ± 0% for anti-IgE vs. 1.2 ± 0.02% for NGS, $p<0.001$, Figure 4.1). However, as described in previous reports (MacDonald, 1994), preincubation of unsensitised rat BMMCs with 50 ng/ml SCF for 5 minutes before challenge with anti-IgE significantly increased the release of β hexosaminidase to 22 ± 0.2% ($p<0.001$, Figure 4.1). A similar effect was seen following challenge of IgE-sensitised cells with DNP-BSA, with the release of β hexosaminidase increasing significantly to 30.6 ± 0.3% ($p<0.001$) after a 5 min preincubation with SCF. In addition, the responses of the BMMCs to DNP-BSA alone, or SCF/DNP-BSA, were both significantly higher than those seen in the corresponding groups challenged with anti-IgE, or SCF/anti-IgE ($p<0.001$ for either comparison, Figure 4.1). This would be expected because the levels of endogenous IgE are likely to be sub-optimal in mature cultures (see chapter 3). However, SCF increased the percentage release of β hexosaminidase

approximately two-fold in both groups, suggesting that the specific effect of the cytokine was not dependent on the degree of IgE binding. In agreement with previous reports (MacDonald, 1994), incubation of BMMCs with SCF did not cause significant release of β hexosaminidase in the absence of DNP-BSA or anti-IgE (1.5 ± 0.2% for SCF/TB^+ vs. 1.3 ± 0.2% for TB^+, p=0.35; 1.2 ± 0.02 % for SCF/NGS vs. 1 ± 0.05% for NGS, p=0.074). These results confirm that, in isolation, SCF was not a significant secretagogue for these cells.

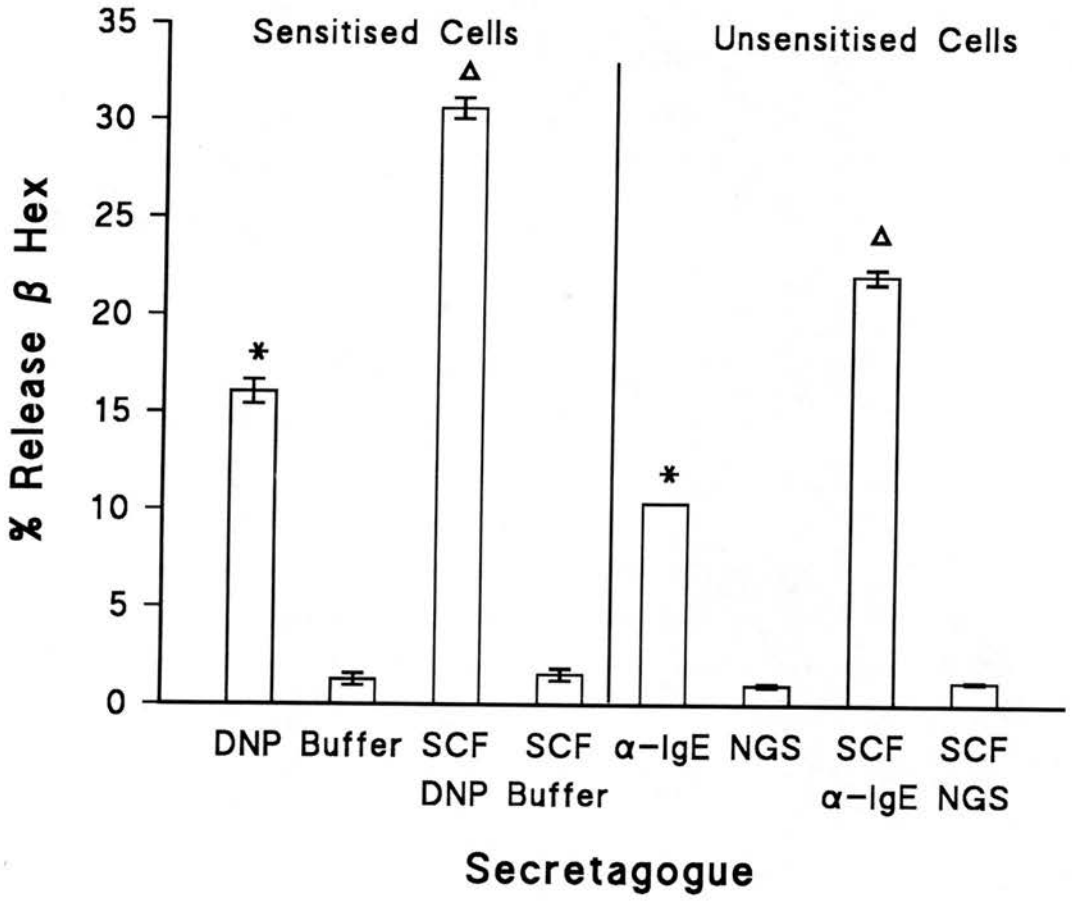

Figure 4.1 - Effect of SCF on the percentage release of β hexosaminidase from IgE-sensitised or unsensitised BMMCs in response to challenge with DNP-BSA or anti-IgE. The BMMCs (10^6 per tube) were preincubated with 50 ng/ml SCF or buffer alone for 5 min, followed by DNP-BSA (DNP, 1/1000), Tyrode's buffer/Ca^{2+}/Mg^{2+} (TB^+), goat anti-rat IgE (α IgE, 1/250), or normal goat serum (NGS, 1/250) for a further 30 min. Each bar represents the mean ± s.e.m. of triplicate release assay tubes. * = significant difference from negative control ($p<0.001$), Δ = significant difference from challenge with DNP-BSA or anti-IgE ($p<0.001$).

4.2 - The effect of SCF on the proportion of BMMCs that release RMCP-II in response to anti-IgE

Aims

The previous experiment confirmed that SCF augments the secretory response of rat BMMCs resulting in an increase in total mediator release from the population of cells. The RMCP-II ELISPOT assay was then used to determine whether pre-incubation with SCF altered the *proportion* of BMMCs within the population that responded to stimulation with anti-IgE.

Methods

BMMCs from a culture containing 96% mast cells (99% viability) were washed and diluted to yield 400, 200 and 100 cells per triplicate well (384, 192 and 96 BMMCs per well) as shown in the plate map in appendix 3. The cells were preincubated with 50 ng/ml SCF or buffer alone for 5 min before addition of anti-IgE or NGS. The plates were developed and the spots counted as described previously (chapter 3, section 3.3). To facilitate statistical analysis of the data, the spot counts in each well were expressed as a percentage of the number of BMMCs per well, and the results from the 9 wells in each treatment group were compared by ANOVA and Student's t test. The results are reported as mean ± s.e.m. In a second (dose response) experiment, BMMCs from a culture containing >99% mast cells (100% viability) were diluted to yield 100 BMMCs per quadruplicate well, and were preincubated with concentrations of SCF ranging from 400 ng/ml to 1.56 ng/ml (or buffer alone) before addition of anti-IgE.

Results

The spot counts from BMMCs releasing RMCP-II in response to anti-IgE in the presence or absence of 50 ng/ml SCF are shown in Figure 4.2. The proportion of BMMCs responding to SCF/anti-IgE was significantly higher than in BMMCs challenged with anti-IgE alone (7.2 ± 0.8% vs. 3 ± 0.7%, $p<0.005$, $n=9$).

Interestingly, the proportion of responding cells was increased approximately two-fold by preincubation with SCF, as occurred in the previous conventional mediator release assay (section 4.1). The proportion of BMMCs responding to anti-IgE alone (3 ± 0.7%) was not significantly different from that of cells challenged with NGS (2 ± 0.6%), probably due to sub-optimal IgE binding. As in the previous experiment, SCF had no significant direct secretagogue effect on rat BMMCs (1.6 ± 0.6%, $p>0.5$ vs. NGS alone).

The effect of SCF was dependent on concentration as shown in Figure 4.3. Preincubation with concentrations of 50 or 25 ng/ml SCF resulted in the highest proportion of BMMCs responding to anti-IgE (35 ± 5% or 36 ± 3% respectively, n=4), compared to 4 ± 0.7% of cells treated with anti-IgE alone or 4.5 ± 1% of cells treated with buffer alone. These results are in agreement with those of MacDonald (1994) who showed that concentrations of >10 ng/ml SCF were optimal for enhancing IgE-dependent mediator release from BMMCs. Therefore, in subsequent secretion assays in these studies, a SCF concentration of 50 ng/ml was used.

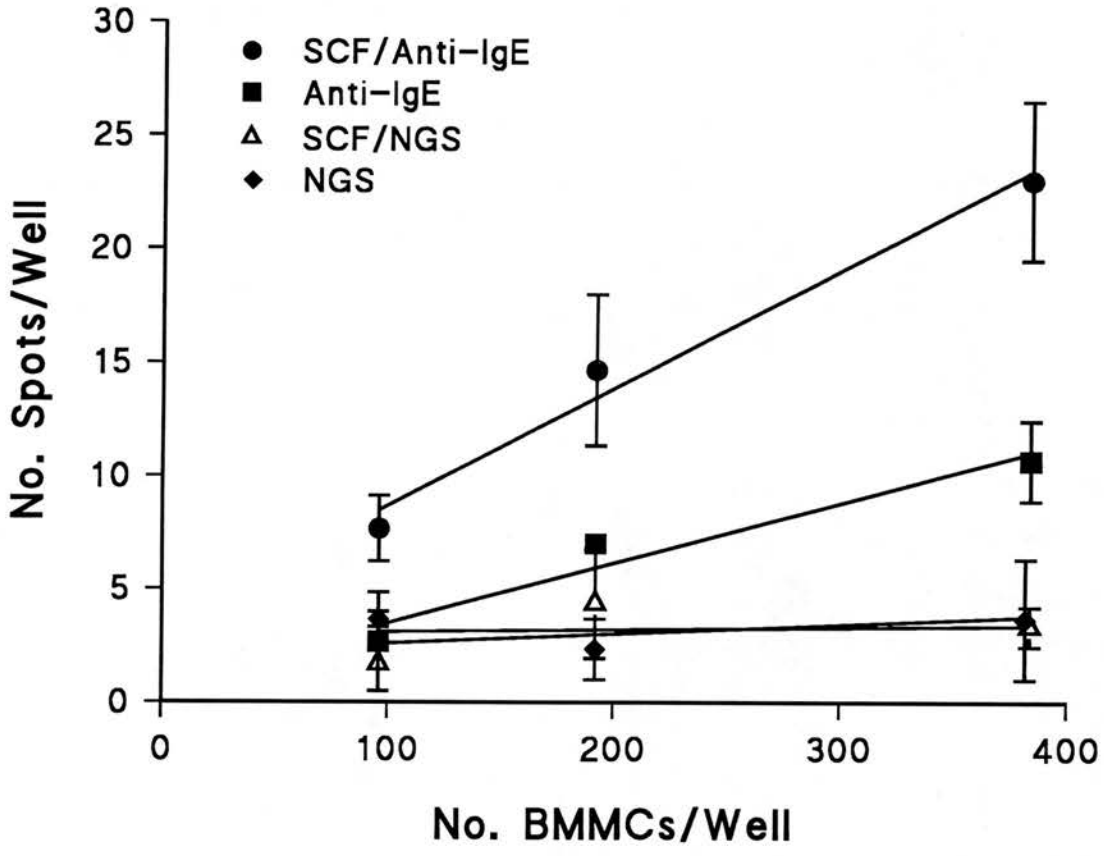

Figure 4.2 - Effect of SCF on the proportion of BMMCs responding to challenge with anti-IgE as determined by ELISPOT assay. BMMCs from a culture containing 96% mast cells were diluted to yield 384, 192 and 96 BMMCs per triplicate well. The cells were preincubated with 50 ng/ml SCF or buffer alone for 5 min, followed by challenge with goat anti-rat IgE or NGS (both at 1/250) for a further 30 min. Each point represents the mean ± s.e.m. of spot counts from triplicate wells, and the points are joined by regression lines (r=0.99 for SCF/anti-IgE; r= 0.97 for anti-IgE). For statistical analysis, the spot counts in each well were expressed as a percentage of the number of BMMCs per well, and the results from the 9 wells in each treatment group were compared by ANOVA and Student's *t* test (see text for results).

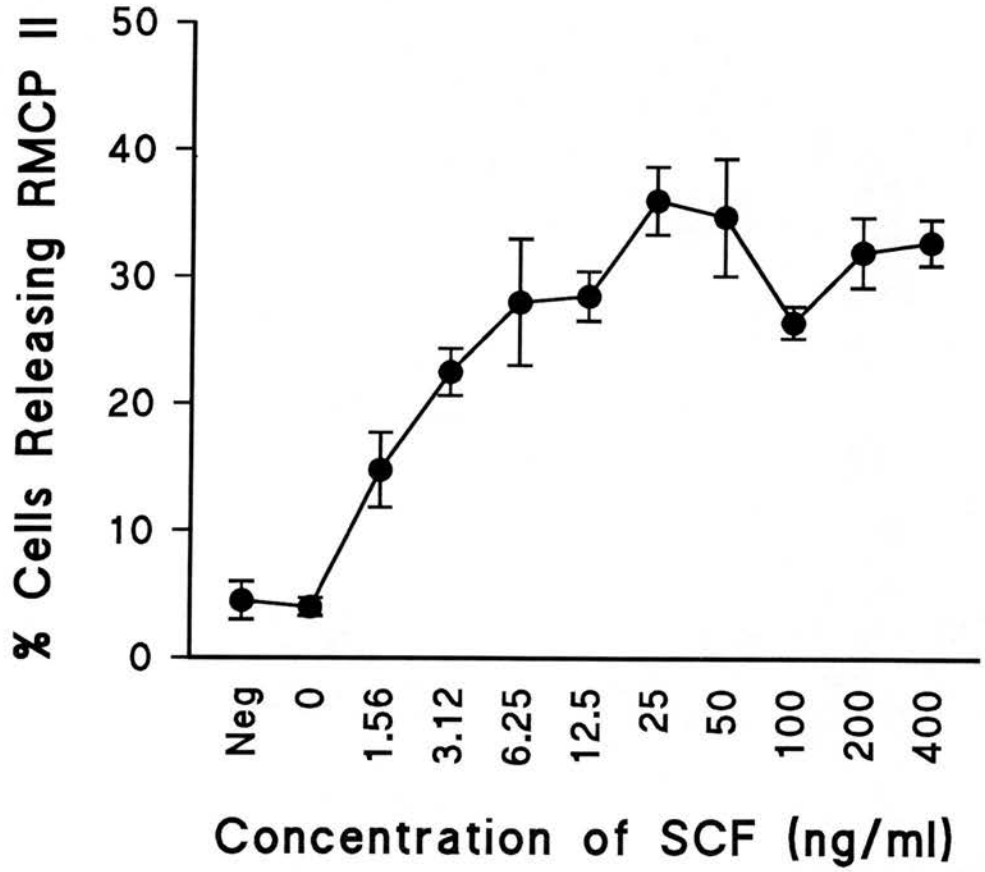

Figure 4.3 - Effect of SCF concentration on the proportion of BMMCs responding to challenge with anti-IgE as determined by ELISPOT assay. BMMCs from a culture containing >99% mast cells were diluted to yield 100 BMMCs per quadruplicate well. The cells were preincubated with various concentrations of SCF or buffer alone for 5 min before challenge with goat anti-rat IgE or NGS (both at 1/250) for a further 30 min. Each point represents the mean ± s.e.m. of spot counts from quadruplicate wells. Neg = cells not challenged with SCF or anti-IgE.

4.3 - Time course of the SCF effect

Aims

The previous experiments demonstrated that SCF enhanced both the total release of β-hexosaminidase from populations of BMMCs (section 4.1) and the proportion of BMMCs that responded to challenge with anti-IgE (section 4.2). In previous studies, the effect of SCF on IgE-dependent mediator release from BMMCs was maximal after short (5 min) preincubations (MacDonald, 1994). In this section, the time course of the SCF effect was investigated in both ELISPOT and conventional mediator release assays.

Methods

In an initial ELISPOT assay, BMMCs from a culture containing 99% mast cells (100% viability) were diluted to yield 200 BMMCs per well, with each treatment group comprising 6 wells. The cells were then preincubated with 50 ng/ml SCF for 5, 15, 30, 60, or 120 min, or with buffer alone for 120 min, before challenge with anti-IgE or NGS. In a second experiment, BMMCs from a culture containing >99% mast cells (100% viability) were sensitised with mouse IgE anti-DNP as described previously (section 2.15). After washing, the cells were divided into 5 treatment groups, each containing 3 x 10^6 BMMCs. The cells in three of the groups were incubated with 50 ng/ml SCF for 5, 15, or 30 min respectively, and in the remaining two groups with buffer only. The cells were then washed twice in TB/EDTA to remove the SCF. Cells from each group were either added to triplicate release assay tubes (0.6 x10^6 cells per tube) as described in section 2.17, or diluted to yield 200 BMMCs per well in an ELISPOT plate (8 wells per treatment group). The cells were challenged with DNP-BSA or TB^+ as shown overleaf.

Experimental Design

Group	SCF incubation	Secretagogue	No. of Replicate Tubes	No. of Replicate Wells
1.	5 min	DNP-BSA	3	8
2.	15 min	DNP-BSA	3	8
3.	30 min	DNP-BSA	3	8
4.	No SCF	DNP-BSA	3	8
5.	No SCF	Tyrode's Buffer	3	8

Results

In the initial ELISPOT assay, preincubation of BMMCs with SCF for 30 min before challenge with anti-IgE resulted in the highest proportion of cells releasing RMCP II (34 ± 2%, n=6), but this was not significantly different from the results obtained after a 5 min incubation (26 ± 3%, Figure 4.4). Both values were significant when compared to results for cells treated with anti-IgE alone (8 ± 1%, n=6, $p<0.01$ for either comparison).

The results of the combined ELISPOT/conventional release assay are shown in Figure 4.5. In the conventional release assay, the percentage release of β-hexosaminidase from the cells incubated with SCF for 5 min (12.3 ± 0.3%), 15 min (11.1 ± 0.5%) or 30 min (9.2 ± 0.2%) was significantly higher than the cells challenged with DNP-BSA alone (8.2 ± 0.2%, $p<0.05$ for each comparison). In addition, the response of cells incubated with SCF for 5 min was significantly higher than those incubated with the cytokine for 30 min ($P<0.05$). An almost identical trend was observed in the ELISPOT assay, with the shortest SCF incubation time causing the greatest proportion of BMMCs to release RMCP-II in response to challenge with DNP-BSA (Figure 4.5). However, in the ELISPOT assay, the difference between the responses of cells incubated in the presence or absence of

SCF did not reach statistical significance, probably due to the larger variation seen in this experiment.

Taken together, these results indicate that short preincubations with SCF (5-30 min) increase both total mediator release from a population of BMMCs and the proportion of cells responding to IgE-dependent challenge. Hence, for all subsequent secretion assays, BMMCs were incubated with SCF for 5 min before addition of the secretagogue (anti-IgE or DNP-BSA) or control.

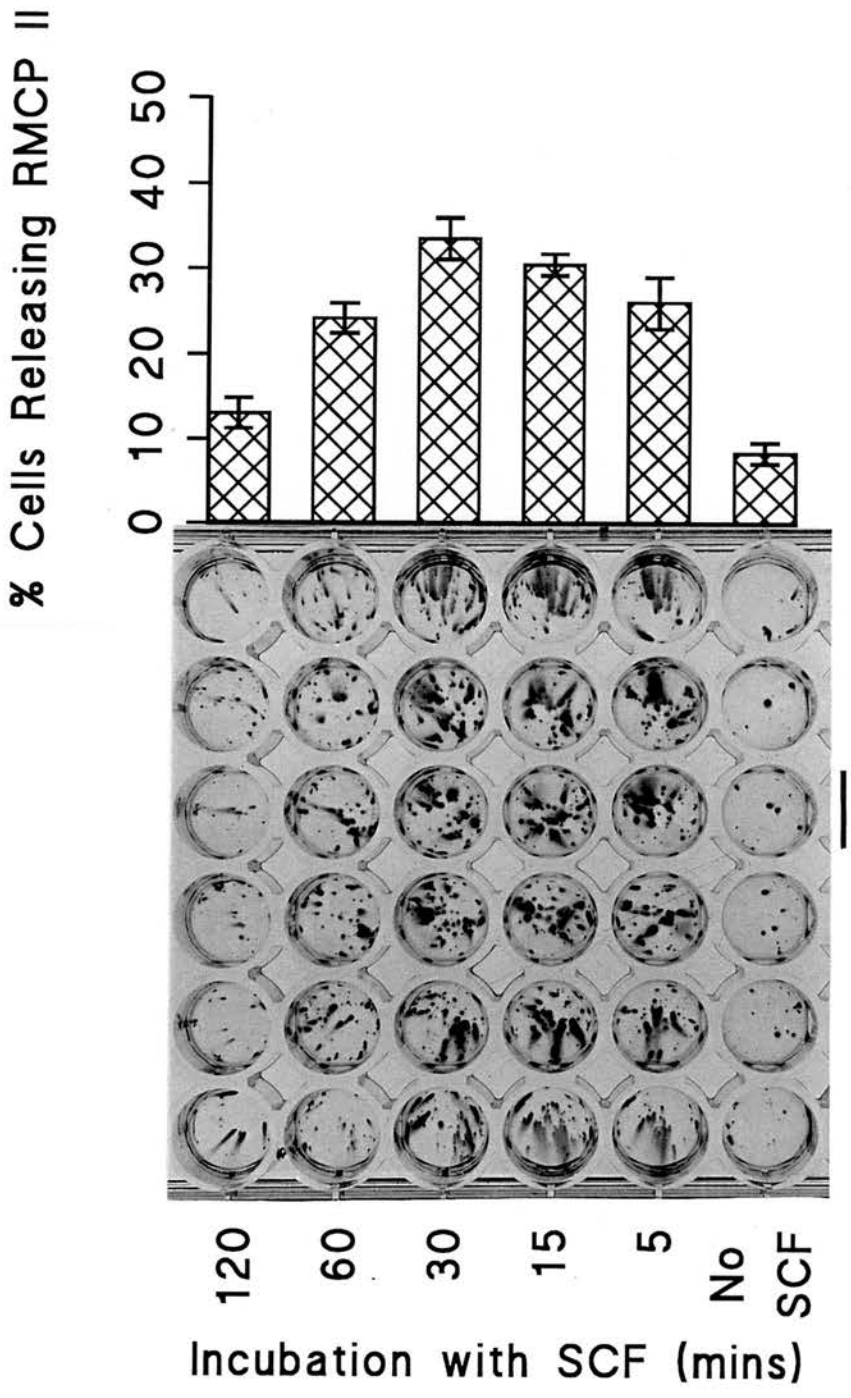

Figure 4.4 - Release of RMCP-II from anti-IgE challenged BMMCs (200 BMMCs per well, from a culture containing >99% mast cells) after incubation with SCF (50 ng/ml) for varying periods of time. The graphic illustrates the increased number of spots in wells after 5, 15, or 30 min preincubations with SCF compared to 60 or 120 min, or control wells (no SCF). The spot counts in each well were halved to yield the percentage of cells releasing RMCP-II. Bars represent the mean ± s.e.m. of the halved spot counts from 6 wells. Scale marker = 1cm.

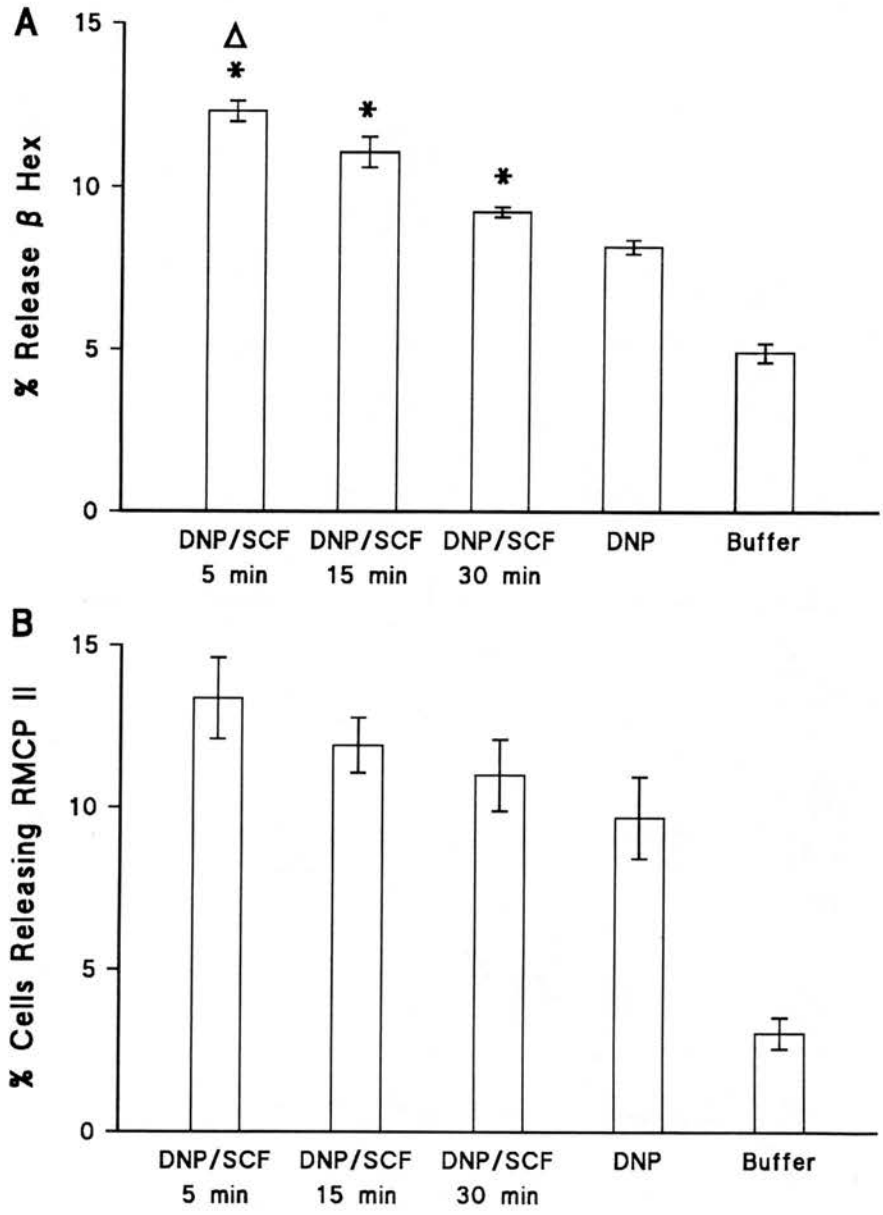

Figure 4.5 - The effect of SCF incubation time on the total percentage release of β-hexosaminidase from BMMC populations (**A**), and the proportion of BMMCs responding to IgE-dependent challenge (**B**). BMMCs from a culture containing >99% mast cells were sensitised with mouse IgE anti-DNP and preincubated with SCF (50 ng/ml) for 5, 15, or 30 min, or with buffer alone. After washing the cells to remove the SCF, BMMCs were challenged with DNP-BSA or TB^+ in a conventional mediator release assay (**A**), or in an ELISPOT assay (**B**).

A: Each bar represents the mean ± s.e.m. of triplicate release assay tubes, each containing 0.6 x10^6 BMMCs. *= significant difference from DNP alone, $p<0.05$; Δ= significant difference from a 30 min incubation with SCF, $p<0.05$.

B: The spot counts from each well (each containing 200 BMMCs) were halved to yield the percentage of BMMCs responding to challenge with DNP-BSA. Each bar represents the mean ± s.e.m. of the halved spot counts from 8 wells.

4.4 - The effect of SCF on anti-IgE-induced RMCP-II release from BMMC populations at various stages of culture

Aims

In chapter 3, the response of BMMCs to anti-IgE was shown to be influenced by the stage of culture from which the cells were derived (section 3.7 and Table 3.3). In some of the experiments summarised in Table 3.3, the effect of SCF on the proportion of BMMCs responding to anti-IgE was also investigated (those performed using cultures 2 and 3). These experiments were designed to determine if the effect of SCF was dependent on the maturity of BMMC cultures.

Methods

For each experiment in this series, a suspension of cells was removed from one of two different cultures at various stages of maturity. After three washes, the cells were counted, assessed for viability, and the percentage mast cells determined (as described in chapter 2, sections 2.1-2.10).. The details of the cultures are provided in Table 4.1.

Table 4.1 - Percentage BMMCs and viabilities for experiments performed throughout the growth of two cultures

Culture	Day	% BMMCs	% Viability
2	4	8	>99
	8	41	>99
	11	64	97
	15	85	96
	18	92	96
	21	98	93
3	9	36	98
	17	87	98
	21	95	96
	24	95	92
	28	99	77

For each experiment, the cell suspension was diluted to yield 400, 200 or 100 viable BMMCs per triplicate well in each of two separate 48 well plates. The cells were preincubated with 50 ng/ml SCF or buffer alone for 5 min, followed by challenge with anti-IgE or NGS as shown in the plate map below (Figure 4.6).

		1	2	3	4	5	6	7	8
Anti-IgE	A	400	200	100	400	200	100	a	e
	B	400	200	100	400	200	100	b	f
	C	400	200	100	400	200	100	c	g
NGS	D	400	200	100	400	200	100	d	h
	E	400	200	100	400	200	100	-	-
	F	400	200	100	400	200	100	⊕	⊕
		Buffer			50 ng/ml SCF			No cells	

Figure 4.6 - ELISPOT plate map. Each number indicates the approximate number of viable BMMCs per well. Columns 7 and 8 contained no cells but a,b = SCF/anti-IgE; c,d = SCF/NGS; e,f = buffer/anti-IgE; g,h = buffer/NGS. - = Tyrode's buffer; ⊕ = 100 ng/ml RMCP-II. Each experiment comprised two replicate plates.

The plates were developed and the spots counted as described previously (section 3.3). Apart from confirming the relationship between cell density and number of spots per well (see chapter 3, section 3.5), the serial dilution of cells from 400 to 100 BMMCs per well was not particularly useful, especially for statistical analysis. The spot counts in each well were therefore expressed as a percentage of the number of BMMCs in each well, and the overall percentage of BMMCs responding to each treatment was calculated by averaging the data from 18 corresponding wells (9 wells from each plate containing 400 (n=3), 200 (n=3), and 100 (n=3) cells per well - see figure 4.6). The data from each treatment group were compared by ANOVA and Student's t test, and the results are expressed as mean ± s.e.m.

Results

The proportions of BMMCs responding to each treatment throughout the course of two cultures are shown in Figure 4.7. The response of BMMCs to SCF fell into two categories. In four experiments performed using cultures containing 8, 36, 41, or 64% BMMCs, a highly significant ($p<0.001$) proportion of BMMCs responded to anti-IgE alone when compared to NGS controls, but addition of SCF had no significant effect (Figure 4.7). In contrast, SCF significantly increased ($p<0.001$) the proportion of BMMCs responding to anti-IgE in 4 out of 5 experiments performed using cultures containing 85, 87, 92, 95, or 95% mast cells. In addition, the spots in SCF treated wells appeared to be larger than those treated with anti-IgE alone, although this was not quantified. At no stage did SCF alter the response of cells treated with NGS, providing additional evidence that, in isolation, it had no detectable secretagogue activity in these BMMC populations (Figure 4.7).

In three experiments performed during this series, there was no significant effect of either anti-IgE or SCF (Day 21, culture 2; Days 21 and 28, culture 3). The lack of response of BMMCs in the experiments performed on days 21 of culture 2, and 28 of culture 3, is probably related to cell viability. In both cultures, the viability had started to decline at this stage (93% and 77% respectively). This was associated with a high background release of RMCP-II, suggesting that the cells had become "leaky" and unable to respond to specific stimuli. The reason for the failure of the BMMCs from day 21/culture 3 to respond to SCF is not known, but the most likely explanation is a technical error during the assay procedure (buffer preparation, pH, SCF dilution).

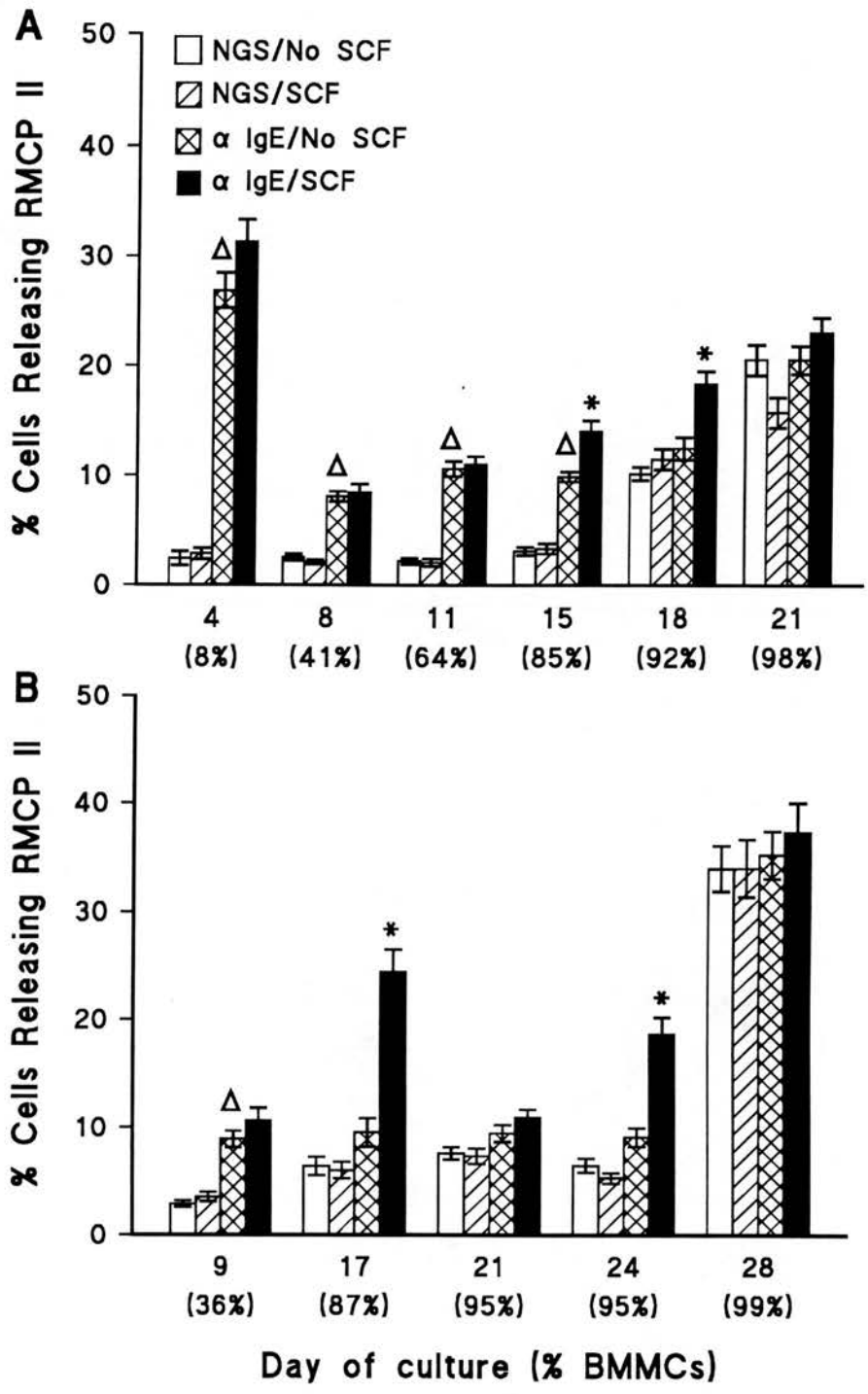

Figure 4.7 - The effect of SCF on IgE-dependent RMCP-II release from individual BMMCs derived from cultures at different stages of maturity. A: Culture 2. B: Culture 3. Cells were incubated in the presence (50 ng/ml for 5 min) or absence of SCF before challenge with goat anti-rat IgE or normal goat serum (NGS). Each bar represents the mean ± s.e.m. of the percentage of BMMCs responding to each treatment in 18 wells (9 from two separate ELISPOT plates). Δ = significant effect of anti-IgE vs. NGS, $p<0.001$. * = significant effect of SCF vs. anti-IgE, $p<0.001$.

4.5 - The effect of SCF on the release of RMCP-II from individual IgE-sensitised BMMCs compared directly with the percent mediator release by an entire population of BMMCs

Aims

The aim of these experiments was to determine the relationship between the increased proportion of BMMCs that responded to IgE-dependent stimulation after treatment with SCF and the increase in total mediator release by a BMMC population. In addition, the previous experiments had shown that the effect of SCF was limited to mature cultures, in which IgE binding is sub-optimal. To determine if SCF was merely compensating for insufficient IgE, these experiments were performed using BMMCs sensitised with IgE anti-DNP.

Methods

The responses of BMMCs to SCF and IgE-dependent stimulation in conventional mediator release assays were compared to those obtained in parallel ELISPOT assays using aliquots of the same cell populations. BMMCs from a culture containing 99% mast cells (100% viability) were removed on two consecutive days (for two separate experiments). The cells were washed and sensitised with mouse IgE anti-DNP as described previously, and divided into four treatment groups. Each group was diluted to yield 0.8×10^6 BMMCs per quadruplicate release assay tube, and 200 cells per ELISPOT well (9 wells per treatment group). After preincubation with 50 ng/ml SCF or buffer alone for 5 min, the cells were challenged with DNP-BSA or TB^+ as described previously. The pellets and supernatants from the release assay tubes were assayed for RMCP-II and β hexosaminidase as described previously, and the percentage of BMMCs responding was calculated from the spot counts in each ELISPOT well. Results from different treatment groups were compared by ANOVA and Student's t test, and are reported as mean ± s.e.m.

Results

The percentage release of RMCP-II and β-hexosaminidase from populations of BMMCs is compared to the proportion of responding BMMCs in Figure 4.8. The mean specific IgE-dependent release of RMCP-II or β-hexosaminidase (calculated by subtracting the % release in control tubes from the % release in DNP tubes) in the absence of SCF was 9 ± 0.5% and 12 ± 0.3% respectively ($p<0.01$ vs. results with buffer alone). After pretreatment with 50 ng/ml SCF, the response to antigen mediated stimulation increased significantly ($p<0.001$) to 26 ± 1% or 36 ± 3% for RMCP-II and β-hexosaminidase respectively. In the ELISPOT assays, a mean of 14 ± 1% individual IgE sensitized BMMCs released RMCP-II in response to DNP-BSA alone, and this increased significantly ($p<0.01$) to 21 ± 1% after pretreatment with SCF. Background release from cells treated with buffer alone was 3 ± 0.3%.

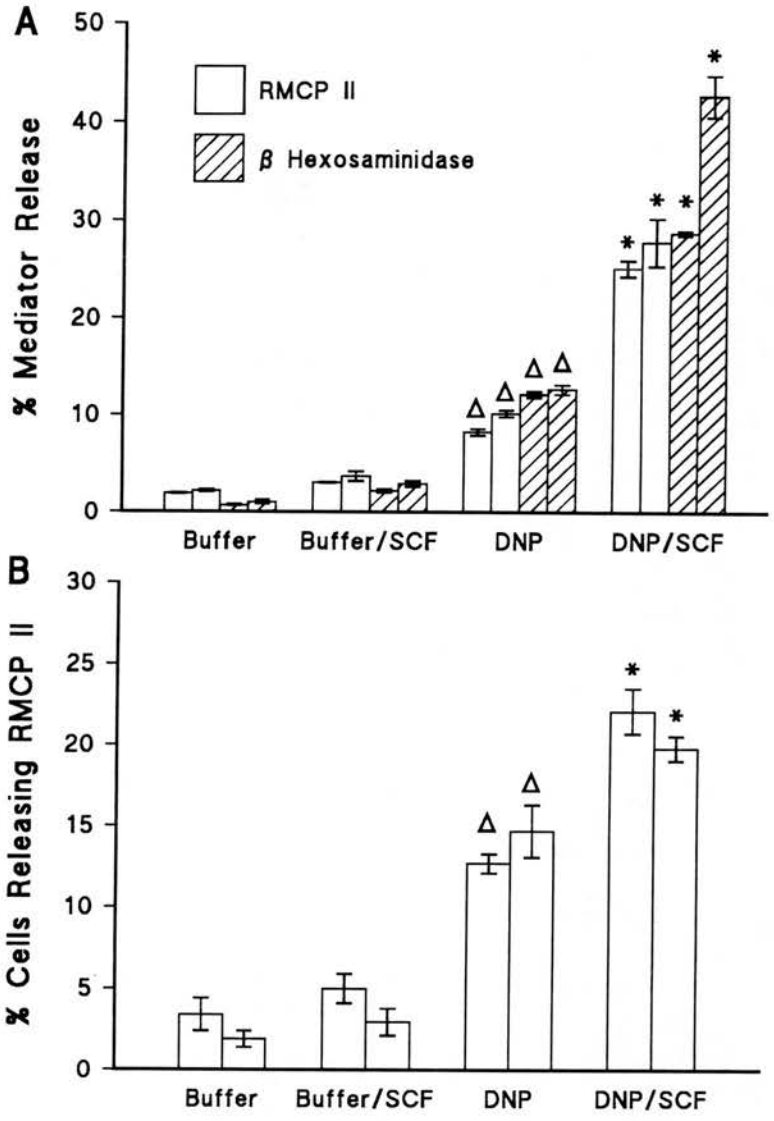

Figure 4.8 - **A**: Conventional mediator release assay showing percentage release of β hexosaminidase and RMCP II from entire populations of BMMCs (from a culture containing >99% mast cells) tested in two separate experiments. BMMCs were sensitised with mouse monoclonal IgE anti-DNP and then stimulated with DNP-BSA in the presence (50 ng/ml for 5 min before challenge) or absence of SCF. Each bar represents the mean ± s.e.m. from quadruplicate aliquots of 0.8 x10^6 BMMCs.
B: ELISPOT assays measuring the proportion of BMMCs that released RMCP-II, performed in parallel to the experiments in A using aliquots of the same cell populations. The spot counts in each well (200 BMMCs/well) were used to calculate the percentage of cells releasing RMCP-II. Each bar represents the mean ± s.e.m. of data from 9 wells in each ELISPOT assay. The increased mediator release in the conventional assay (A) is clearly associated with an increase in the number of cells responding to immunological stimulation as demonstrated in the ELISPOT assay (B).
Δ - significant difference from buffer or buffer/SCF ($p<0.01$).
* - significant difference from cells stimulated with DNP alone ($p<0.05$).

DISCUSSION

In contrast to mouse (Coleman *et al,* 1993) or rat (Nakajima *et al,* 1992; Koike *et al,* 1993; Taylor *et al,* 1996) peritoneal mast cells, or mouse (Wershil *et al,* 1992) or human (Columbo *et al,* 1992) skin mast cells, SCF did not directly induce significant mediator release from rat BMMCs, either in conventional release assays (Figures 4.1 and 4.8A) or in ELISPOT assays (Figures 4.2, 4.7 and 4.8B). However, pretreatment of mature BMMCs with SCF (50 ng/ml) for 5 min before challenge with anti-IgE resulted in a 1.5 - 2.5 fold increase in total mediator release (Figures 4.1, 4.5A and 4.8A). These results suggest that SCF can "prime" rat BMMCs for subsequent activation via the IgE receptor, but can not directly induce degranulation. Similar results have been described for other mucosal type mast cells including human lung mast cells (Bischoff and Dahinden, 1992) and human intestinal mast cells isolated from patients with inflammatory bowel disease and controls (Bischoff *et al,* 1996). In the latter study, IgE receptor stimulation or treatment with SCF alone induced only marginal mediator release. However, preincubation of the mast cells with 100 ng/ml SCF for 15 min before challenge with an antibody to the IgE receptor resulted in significant release of histamine and leukotrienes. Perhaps more interestingly, the SCF-enhanced mediator release was significantly greater in mast cells isolated from actively inflamed tissue compared to normal tissue. These results, and the experiments described in this chapter, suggest that SCF may play a role in the regulation of mast cells responses in the gut, acting as a modulator of gastro-intestinal immune responses.

The enhancement in IgE-dependent mediator release from rat BMMCs following preincubation with SCF was similar to that described when mouse BMMCs were cocultured with fibroblasts (Levi-Schaffer *et al,* 1987b). In the latter study, the release of histamine increased 2- to 3-fold after challenge with specific antigen, but only in cells that were adherent to the fibroblast monolayer. These results suggest that mast cells in close contact with fibroblasts, as occurs *in vivo*, are likely to be

"primed" for subsequent mediator release as suggested by the *in vitro* studies in this chapter.

One of the aims of this study was to determine whether SCF-dependent enhancement of mediator release reflected individual cells releasing more mediator, or increased numbers of cells responding to stimulation. The results of the ELISPOT assays clearly demonstrate, for the first time, that the proportion of mature BMMCs responding to IgE-dependent stimulation was significantly increased by pretreatment with SCF (Figures 4.2, 4.3, 4.4, 4.7 and 4.8B). In addition, preincubation with SCF typically resulted in a 1.5 - 2.5 fold increase in the proportion of responding cells, which is similar to that reported for increases in total mediator release from populations of BMMCs (MacDonald, 1994, and Figure 4.1). When the results of ELISPOT assays and conventional mediator release assays were directly compared (using the same populations of cells as in Figures 4.5 and 4.8), the increase in percent total mediator release was similar to the increase in the proportion of responding cells. Taken together, these results suggest that SCF upregulates secretion from mature BMMCs primarily by activating previously unresponsive cells. However, close analysis of Figure 4.8 shows that the percentage release of total mediators increases $\approx$ 3-fold whereas the proportion of responding cells increases $\approx$ 1.5-fold. Although this may reflect biological variation within the two assay systems, it does suggest that there was a concomitant increase in mediator release from individual cells. The latter conclusion was also suggested by an increase in spot size from BMMCs treated with SCF, but this effect was not quantified objectively. It is possible, therefore, that SCF upregulates secretion from mature BMMCs in two ways: firstly by "priming" previously unresponsive cells, allowing a subsequent response to IgE-mediated challenge, and secondly, by enhancing mediator release from individual cells.

The enhancement of IgE-dependent mediator release by SCF was previously found to be maximal after short pre-incubations (5 min) and was not evident after incubations over 3 hours (MacDonald, 1994, and see Figure 2 in Hill *et al,* 1996 at the back of this thesis). In the ELISPOT assays, the same effect was observed, although incubations of 5 - 30 min yielded similar results. This phenomenon has also been reported for human skin (Columbo *et al,* 1992) and lung (Bischoff and Dahinden, 1992) mast cells, and is most likely due to internalisation of c-kit receptor/SCF complexes following ligand binding (Yee *et al,* 1993). The significance of this finding is not known, and it is complicated by the potential role of membrane bound SCF in providing a constant stimulus for mast cells *in vivo*. However, it could be a control mechanism to prevent mast cells from being in a state of heightened sensitivity for prolonged periods following stimulation with soluble SCF.

The ELISPOT assay was used to investigate the effect of SCF on the secretory pattern of individual BMMCs at various stages during culture. Pretreatment of BMMCs with SCF enhanced IgE dependent mediator release from mature BMMCs (i.e. from cultures containing at least 85% mast cells), but did not upregulate secretion from cells derived from immature cultures containing less than 85% mast cells. The lack of an effect of SCF on IgE-dependent mediator release from immature populations of BMMCs might have reflected effects of "contaminating cells" in these preparations. Immature cultures contain other bone marrow derived cells (especially macrophages), which could potentially influence the effects of cytokines on mast cells. Alternatively, lower expression of the SCF receptor (c-*kit*) in developing cells, or differences between mature and immature BMMCs in the intracellular signal transduction mechanisms may have contributed to the apparent lack of SCF responsiveness in these populations. Whether the different effects of SCF on BMMC at various stages of growth/maturation *in vitro* reflect a similar phenomenon *in vivo* remains to be determined.

As discussed in chapter 3, the response of unsensitised BMMCs to anti-IgE decreased in mature cultures, probably due to sub-optimal IgE binding. This raised the possibility that SCF was merely compensating for a reduced signal through the FcεR1 receptor rather than specifically enhancing the secretory response. This could occur because activation of both the FcεR1 receptor (Kawakami *et al,* 1992; Sagi-Eisenberg, 1993; Benhamou *et al,* 1993; Fukamachi *et al,* 1994; Kinet, 1992) and the *c-kit* receptor (Welham and Schrader, 1992) leads to extensive tyrosine phosphorylation of multiple cytosolic proteins, and overlap between the two signaling pathways has already been demonstrated in mouse bone marrow-derived cultured mast cells (Tsai *et al,* 1993; Tsai *et al,* 1993)and rat peritoneal mast cells (Koike *et al,* 1993). To address the possibility that SCF was in some way compensating for sub-optimal binding of endogenous IgE, the BMMCs were sensitised with IgE anti-DNP and challenged with DNP-BSA. In these experiments, pre-treatment with SCF resulted in a similar augmentation of the secretory response as was observed when unsensitised cells were stimulated with SCF and anti-IgE (compare the enhancement of mediator release between sensitised and unsensitised cells in Figure 4.1, and the increased proportion of responding cells in Figure 4.8B with Figure 4.7). These results suggest that the effect of the cytokine was not dependent on the degree of IgE binding.

Is the effect of SCF on IgE-dependent mediator release from rat BMMCs and other mast cell types unique? For example, a number of cytokines and growth factors are known to modulate mediator release from basophils, including IL-3, IL-5, granulocyte/macrophage colony stimulating factor (GM-CSF) and nerve growth factor (Bischoff and Dahinden, 1992). In mouse peritoneal mast cells, SCF (20 - 100 ng/ml) enhanced the antigen-mediated release of serotonin after a 15 min preincubation, whereas IL-3 and IL-4 were without effect (Coleman *et al,* 1993). Likewise, in human lung mast cells, the cytokines IL-1, -2, -3, -4, -5, -6, -7, -8, and -9, along with G-CSF, M-CSF, GM-CSF, TNF-α, TGF-β, IFN-γ, and NGF did not

induce, or enhance, mediator release either alone or when preceding activation of the IgE receptor (Bischoff and Dahinden, 1992). Preincubation of human intestinal mast cells with IL-3 for 15 min before stimulation of the IgE receptor enhanced the release of histamine and leukotrienes, but the effect was less pronounced than with SCF (Bischoff *et al,* 1996). In contrast, IFN-γ inhibited IgE-dependent mediator release from rat (Holliday *et al,* 1994; Bissonnette *et al,* 1995) and mouse (Coleman *et al,* 1991) peritoneal mast cells. Hence, in terms of cytokine regulation of secretory function, SCF appears to have a unique and potent role in the modulation of mast cell responses.

In summary, the experiments in this chapter showed that the cytokine, SCF, enhanced mediator release from a population of mature, but not immature, BMMCs. This upregulation was shown to be due to activation of previously unresponsive cells and possibly augmentation of the secretory response in individual cells. The many similarities between rat BMMCs and rat MMCs suggest that SCF may also be involved in regulation of mast cell responses in the gut, acting as a unique modulator of gastrointestinal immune responses.

Chapter 5

ELECTROPHYSIOLOGICAL PROPERTIES OF RAT BONE MARROW-DERIVED MAST CELLS

INTRODUCTION

The previous chapters were concerned with characterisation of IgE-dependent mediator release from rat bone marrow-derived mast cells. In this chapter, the electrophysiological properties of rat BMMCs are described.

In chapter 1, the electrophysiological properties of various mast cell types were reviewed. These studies revealed marked differences in properties between mast cell phenotypes which are summarised in Tables 5.1 and 5.2.

Table 5.1 - Ionic conductances in resting mast cells. IR_K = inwardly rectifying K^+ current; OR_{Cl} = outwardly rectifying Cl^- current; RBL-2H3 = rat basophilic leukaemia cell; WCR = conventional whole-cell recording configuration; RT = room temperature.

Conductance	Mast Cell Type	Technique	References
IR_K current	RBL-2H3 cell	WCR at RT	Lindau and Fernandez, 1986
	Rat BMMC (grown in IL-3)	WCR at RT	Qian and McCloskey, 1993
	Mouse BMMC	WCR at RT	Kuno et al, 1995
OR_{Cl} current	Mouse BMMC	WCR at RT	Kuno et al, 1995
Volume-regulated Cl current	RBL-2H3 cell	Perforated-patch at RT	Nilius et al, 1994
None	Rat peritoneal mast cell	WCR at RT	Lindau and Fernandez, 1986 McCloskey and Qian, 1994

Table 5.2 - Ionic conductances in stimulated mast cells. I_{CRAC} = calcium release activated calcium current; OR_{Cl} = outwardly rectifying Cl^- current; OR_K = outwardly rectifying K^+ current; WCR = conventional whole-cell recording configuration; RT = room temperature; 48/80 = compound 48/80; Sub P = substance P.

Conductance	Mast Cell Type	Technique	References
Ca^{2+} selective channels	Rat peritoneal mast cell	WCR at RT, cell stimulated with 48/80, Sub P, IP_3, GTP-γ-S	Kuno et al, 1989 Mathews et al, 1989
I_{CRAC}	Rat peritoneal mast cell	WCR at RT, cell stimulated with IP_3, ionomycin	Hoth and Penner, 1993
	RBL-2H3 cell	Perforated-patch at 37°C, cell stimulated with antigen	Zhang and McCloskey, 1995
Cation-selective channels	Rat peritoneal mast cell	WCR at RT, cell stimulated with 48/80, IP_3, GTP-γ-S	Kuno et al, 1989 Mathews et al, 1989 Fasolato et al, 1993
OR_{Cl} channels	Rat peritoneal mast cell	WCR at RT, cell stimulated with 48/80, Sub P, c-AMP, GTP-γ-S	Mathews et al, 1989 Janiszewski et al, 1994 Dietrich and Lindau. 1994
	RBL-2H3 cell	Single channel study, patches stimulated via FcεR1	Romanin et al, 1991
OR_K channels	RBL-2H3 cells Rat BMMCs (grown in IL-3)	WCR at RT, cells stimulated with GTP-γ-S, ADP, ATP	Qian and McCloskey, 1993 McCloskey and Qian, 1994

Most of the above studies were performed using the conventional whole-cell recording configuration (Hamill *et al,* 1981) which causes dialysis of the intracellular milieu and loss of many cytoplasmic components including solutes, enzymes and messengers (Penner *et al,* 1987; Horn and Marty, 1988). This "washout" phenomenon can greatly influence the function of ion channels and can lead to the absence or rundown of whole-cell currents. Two methods have been used to overcome the problem of washout. The first is to add back various cytosolic components such as cyclic AMP, ATP or GTP as described in some of the above experiments. This method can also allow intracellular signalling mechanisms to be elucidated by selectively replacing or removing critical cytoplasmic factors (Penner *et al,* 1987). The second method (Lindau and Fernandez, 1986a), originally referred

to as "slow whole-cell recording", was developed to prevent washout in rat peritoneal mast cells so that degranulation could be observed concurrently with electrical recording. In this method, the cell-attached patch was partially permeabilised by including ATP in the pipette solution, thus allowing electrical access to the cell. Peritoneal mast cells contain purinergic receptors that bind ATP resulting in an increase in conductance. However, the access resistance in such recordings was 200 - 5000 MΩ which is 100 - 5000 fold higher than conventional whole-cell recordings. This methodology was improved by the use of the pore-forming polyene antibiotic nystatin (Cass *et al,* 1970; Horn and Marty, 1988). Inclusion of nystatin in the pipette solution perforated the cell-attached patch to a much greater degree than ATP (access resistances as low as 4 - 10 MΩ could be achieved) and the method did not rely on the presence of ATP receptors. The perforated-patch technique, as it is now known, was further developed by Rae et al. (1991) who used the structurally similar amphotericin B to permeabilise 13 different cellular preparations including various lens and corneal epithelia, guinea pig ventricle cells, human gastric smooth muscle cells, neuroblastoma and flounder enterocytes. The importance of this method was recently highlighted when the perforated-patch technique allowed the first demonstration of the IgE receptor-activated Ca^{2+} influx in RBL-2H3 cells (Zhang and McCloskey, 1995). In parallel experiments, the conductance was not observed in any cells using the conventional whole-cell recording technique, indicating that preservation of cytoplasmic components was critical for demonstration of the currents. In addition to the use of the conventional whole-cell recording technique, most investigators have studied mast cells at room temperature which can also influence the results of electrical recordings. For example, Zhang and McCloskey (1995) could only detect the IgE receptor-activated Ca^{2+} conductance if the cells were warmed to 37°C.

To date, the electrophysiological studies of mucosal type mast cells have concentrated on the RBL-2H3 cell. Although this cell line shares certain similarities with intestinal mucosal mast cells (Seldin *et al,* 1985), it possesses a number of important differences. First, it is neoplastic, which could influence many of its properties. Second, it is poorly granulated and contains low levels of RMCP-II (Seldin *et al,* 1985). And thirdly, it is substantially larger than rat mucosal mast cells (McCloskey and Qian, 1994). Hence, it can not be assumed that the RBL-2H3 cell is a functional analog of intestinal mucosal mast cells. To avoid this problem, McCloskey and Qian (1994) studied rat mast cells derived from bone marrow in the presence of rat recombinant IL-3. However, this culture system has not been extensively characterised in the rat, and it is not known for certain how the cells compare to mucosal mast cells in terms of functional or biochemical properties.

The purpose of this study was to characterise the whole-cell currents of rat BMMCs grown in the presence of a mixture of cytokines (including IL-3) derived from concanavalin A stimulated T-lymphocytes. These cells have not been studied electrophysiologically but they have been extensively characterized biochemically and immunologically and in all respects so far studied they are identical to intestinal mucosal mast cells (McMenamin *et al,* 1987; Broide *et al,* 1988; MacDonald *et al,* 1989; Befus *et al,* 1982). They may, therefore, represent a better model for electrophysiological studies of mucosal mast cells than RBL-2H3 cells (Lindau and Fernandez, 1986b) or mast cells grown solely in the presence of rat recombinant IL-3 (McCloskey and Qian, 1994).

Specific Aims of the Electrophysiological Studies

1. To characterise the basic electrophysiological properties of resting rat BMMCs (membrane potential, capacitance and whole-cell currents) to allow comparison with other studies of rat mast cells.

2. To determine if cytoplasmic disruption or bath temperature affected the whole-cell currents of rat BMMCs by comparing conventional whole-cell recordings with perforated-patch recordings at various temperatures.

3. A further aim was to determine if stem cell factor (SCF) influenced the electrophysiological properties of rat mast cells. As shown in chapter 4, SCF has a dramatic effect on IgE-mediated secretion from rat BMMCs after only 5 min incubations, yet in isolation it does not directly induce degranulation. As secretion is critically dependent on ion channel function, it was hypothesised that SCF might modulate or activate ion channels in rat BMMCs. However, as this series of experiments did not demonstrate electrophysiological effects, the data has been summarised in appendix 5.

EXPERIMENTAL METHODS

Cells and Solutions

The preparation of BMMCs for these experiments has been described in detail in chapter 2 (sections 2.1-2.10). Thirteen mature bone marrow cultures ranging in age from 13 - 37 days and each containing more than 85% mast cells (>95% viability) were used with consistent results. The mast cell Ringer, used to suspend BMMCs for electrophysiological recordings, was initially formulated to be as similar to Tyrode's buffer as possible. Hence, standard mast cell Ringer (section 2.22) was Tyrode's buffer/Ca^{2+}/Mg^{2+} (section 2.12) without the BSA or NaH_2PO_4 (these were omitted because they can inhibit pipette-membrane seals). However, in a number of preliminary experiments, the sealing rate with standard mast cell Ringers was still very low. Therefore, to improve sealing, the mast cell Ringers was modified to include 2 mM $CaCl_2$ and 5 mM $MgCl_2$ instead of 1 mM of each (section 2.22).

Preparation of cells for electrophysiological recordings

The BMMCs or peritoneal mast cells were removed from the culture medium (IMDM or RPMI) by gently mixing a 2 - 5ml aliquot of cell suspension with approximately 10 ml of mast cell Ringer in a 15 ml centrifuge tube. After centrifugation at 1100 r.p.m. (200 x g) for 5 min, the supernatant was removed and the cells were resuspended in 1.5 ml of mast cell Ringer and plated onto glass coverslips in petri dishes. The coverslips were maintained at 37°C in an incubator without extraneous CO_2 for up to 7 hours, and were transferred to the recording chamber when needed.

Electrophysiological techniques

The procedures for obtaining seals, recording membrane potentials, measuring cell capacitance and recording whole cell currents have been described in detail in chapter 2 (sections 2.24-2.33). Briefly, in this study, experiments were performed

with both the conventional whole-cell recording configuration and the amphotericin B perforated-patch technique (section 2.31), allowing the effects of cytoplasmic disruption to be determined. Whole-cell voltage-clamp recording (in both configurations) was performed with a patch-clamp amplifier (EPC-7, List) by applying voltage steps over a set voltage range from the holding potential of -40 mV (section 2.33). The evoked currents were filtered, and stored on video tape and a personal computer for later analysis (sections 2.34 and 2.36). In this chapter, the currents are shown as superimposed steps with accompanying current/voltage relationships, or as continuous pen recordings (see relevant sections).

Control of the bath temperature

The temperature of the recording chamber was controlled with a Peltier device (section 2.26). To determine the effect of temperature on the recordings, currents were measured at various bath temperatures. At 37°C, it was difficult to obtain pipette-membrane seals, and the stability of seals at this temperature was unreliable, often resulting in breakdown of the preparation. To overcome this problem, seals were formed at room temperature (16 - 20°C) and the temperature of the bath was increased in 5°C increments. Currents from individual cells were therefore recorded at room temperature, and 25°C, 30°C and 37°C if possible. For most of the statistical analysis, data acquired at the three temperatures has been grouped and the results are reported for the range 25 - 37°C.

Detection of spontaneous degranulation

The studies described here were concerned with the electrophysiological properties of resting BMMCs. In this chapter, "resting" is defined as cells not stimulated via the IgE receptor, by extracellular agonists or by intracellular messengers. In addition, the term refers to a cell not undergoing degranulation. Occasionally, during these studies, a mast cell degranulated spontaneously. This usually resulted in breakdown of the seal and a morphological transformation that was visible under the

microscope. The appearance of this process differed between the two cell types and was much more obvious in peritoneal cells than in BMMCs. This is illustrated in Figure 5.1 which shows the appearance of rat BMMCs and rat peritoneal mast cells in the recording chamber both in the resting state (A and C), and after a stimulus to induce degranulation (B and D). The results that follow were all obtained from mast cells in the absence of visible degranulation, and can therefore be interpreted as the electrophysiological properties of resting BMMCs.

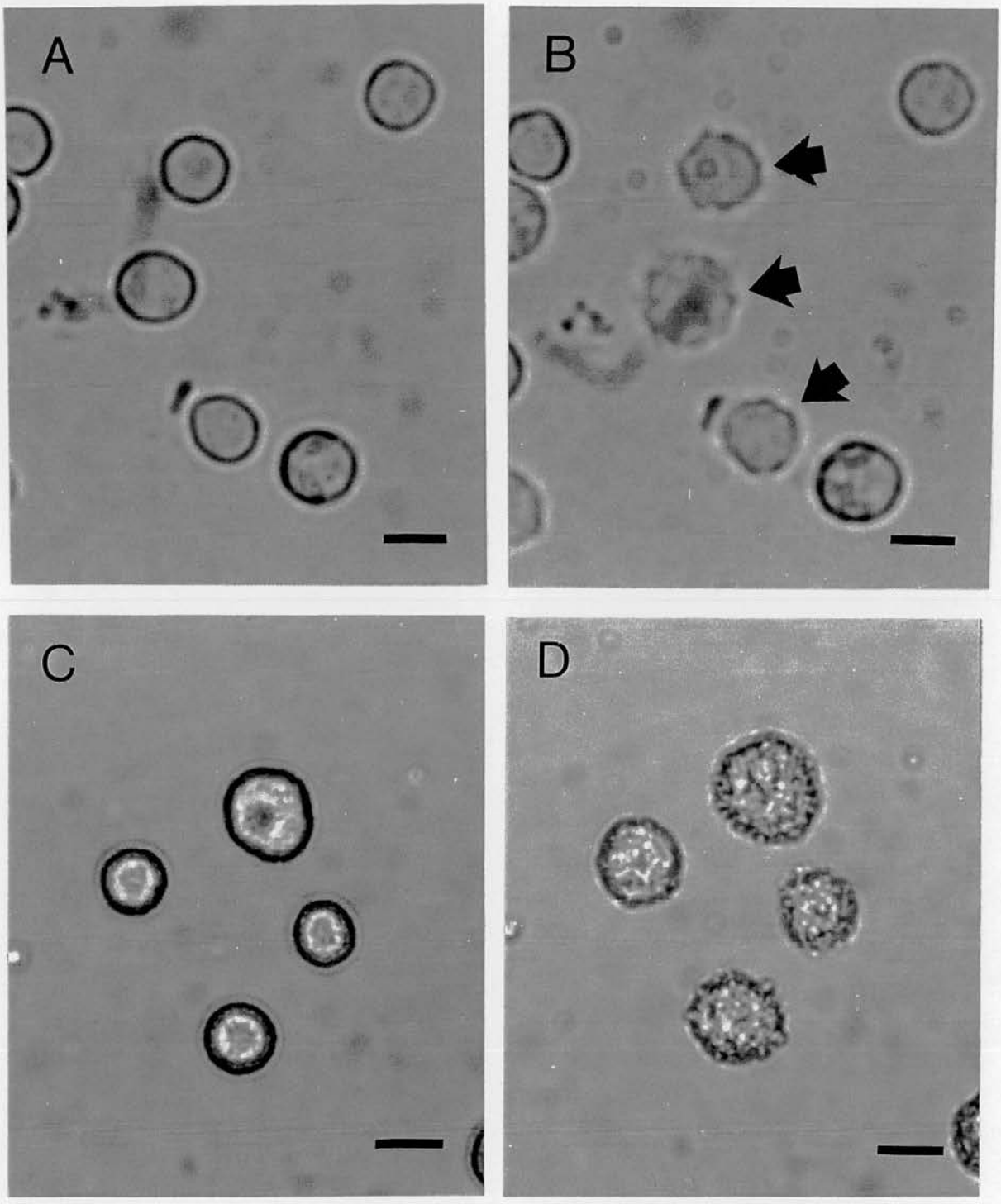

Figure 5.1 - Microscopic appearance of rat BMMCs (**A**) and rat peritoneal mast cells (**C**) in the electrophysiological recording chamber. The cells are adhered to glass cover slips and bathed in mast cell Ringer. The BMMCs had been previously sensitised with IgE anti-DNP. **B**: Appearance of the same BMMCs as in **A**, 15 min after addition of DNP-BSA. Degranulation has occurred in the 3 cells in which the cellular outline is angular and less distinct (arrows). **D**: Appearance of the same peritoneal mast cells as in **C**, 15 min after addition of 10 μg/ml compound 48/80. Degranulation is more obvious than in BMMCs because the cells are covered in a tight mass of refractile granules. Scale bars = 10 μm.

RESULTS

5.1 - Membrane Potential of Rat Bone Marrow-Derived Mast Cells (BMMCs)

The membrane potential was measured by switching the patch-clamp amplifier to the current clamp mode immediately after breaking in to the cell to establish the whole cell recording configuration (section 2.32). This measured the voltage required to keep the membrane current at zero which by definition is the resting membrane potential. The membrane potentials of 33 BMMCs measured with standard KCl pipette solution (section 2.2) at room temperature are shown in Table 5.3. The membrane potential in individual cells fluctuated as shown by the range of values. The distribution of the membrane potentials (taken as the mid-point of the observed range) is shown in Figure 5.2, with a mean and s.d. of -28.5 ± 16.5 mV.

5.2 - Whole-Cell Capacitance in Rat BMMCs

The capacitance of a cell is an important electrophysiological parameter because it is related to the surface area of the plasma membrane and can thus give an indication of cell size. It can also be used to monitor cellular processes such as secretion because incorporation of granule membranes into the plasma membrane results in an increase in cell surface area (Fernandez *et al,* 1984). In these experiments, cell capacitance was determined by measuring the transient current that arises during charging of the cell membrane in response to a voltage pulse. This capacitance transient can be cancelled using the cancellation circuitry of the patch-clamp amplifier, yielding the whole-cell capacitance (section 2.31). Appearance of capacitance transients was also used to monitor perforation of the membrane patch by amphotericin B as described in chapter 2. Capacitance measurements obtained throughout the course of these studies are summarised in Figure 5.3. The perforated-patch technique and the conventional whole cell recording configuration yielded similar values for cell capacitance, being 4.8 ± 1.6 pF (n=116) and 4.2 ± 1.6 pF (n=62) respectively (Figure 5.3).

Cell	M.P. Range (mV)	Median M.P. (mV)
1	-27.9 to -30	-29
2	-19 to -25	-22
3	-17 to -24	-20.5
4	-15 to -17	-16
5	-41 to -50	-45.5
6	-9 to -15	-12
7	-30 to -34	-32
8	-22 to -26	-24
9	-38 to -40	-39
10	-19 to -25	-22
11	-68 to -74	-71
12	-33 to -38	-35.5
13	-19 to -20	-19.5
14	-19 to -28	-23.5
15	-3 to -5	-4
16	-13 to -17	-15
17	-14 to -20	-17
18	-60 to -64	-62
19	-23 to -28	-25.5
20	-18 to -23	-20.5
21	-8 to -11	-9.5
22	-46 to -49	-47.5
23	-42 to -45	-43.5
24	-29 to -39	-34
25	-47 to -50	-48.5
26	-26 to -30	-28
27	-28 to -32	-30
28	-27 to -34	-30.5
29	-18 to -22	-20
30	4 to 5	4.5
31	-25 to -30	-27.5
32	-10 to -14	-12
33	-57 to -58	-57.5

Table 5.3 - Membrane potential of rat BMMCs. The membrane potential was measured by switching the patch-clamp amplifier to the current-clamp mode immediately after establishing the whole-cell recording configuration. Extracellular solution = standard mast cell Ringers, pipette solution = standard KCl solution.

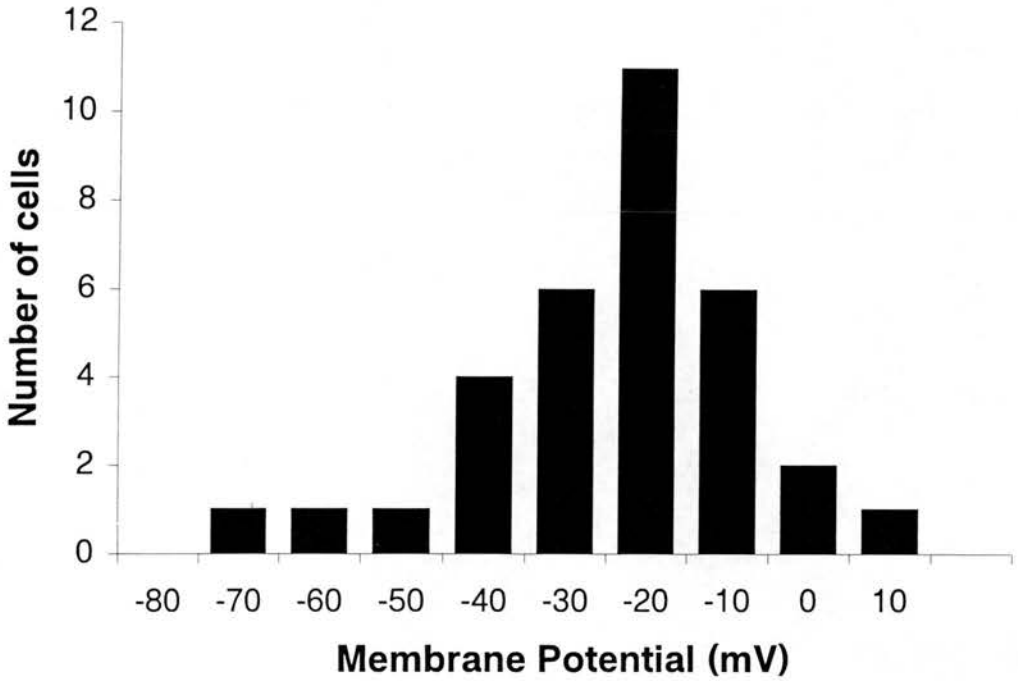

Figure 5.2 - Distribution of membrane potentials in rat BMMCs. The membrane potential was measured by switching the patch-clamp amplifier to the current-clamp mode immediately after establishing the whole-cell recording configuration. Extracellular solution = standard mast cell Ringers, pipette solution = standard KCl solution, bath temperature = RT

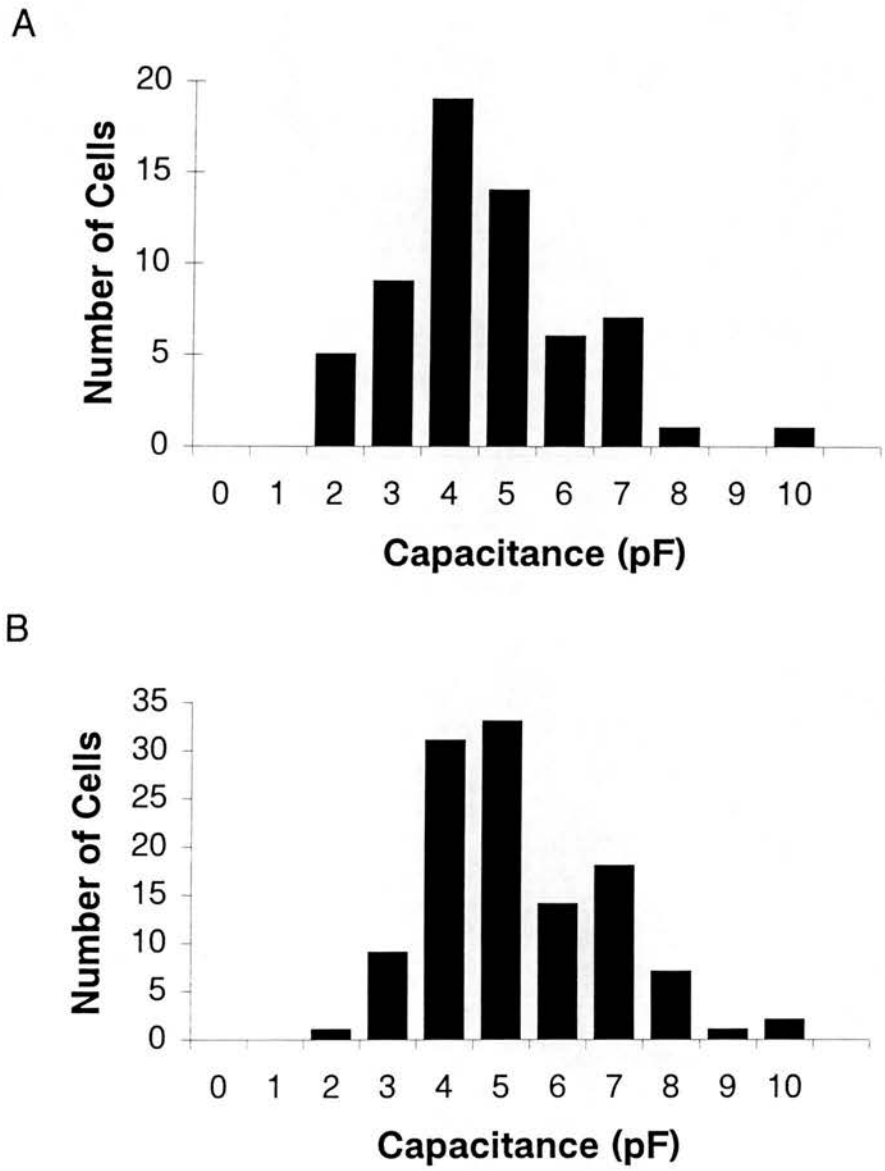

Figure 5.3 - Whole-cell capacitance in rat BMMCs measured in the conventional whole-cell recording configuration (**A**, n=62) or with the perforated-patch technique (**B**, n=116). The capacitance was measured by cancelling the transient that develops in response to a voltage pulse (see text for details). The extracellular solution was either standard or modified mast cell Ringer. The pipette solution was either standard (KCl) or modified (K-methane sulfonate).

5.3 - Characterisation of Whole-Cell Currents in Rat BMMCs

In this section, the results from experiments performed with the perforated patch technique at temperatures between 25 - 37°C are described first, because this group most closely approximates the normal physiological state of the cells. The results are then compared to those obtained at room temperature and/or with the conventional whole-cell configuration.

Two types of whole-cell current were observed in rat BMMCs using the perforated-patch technique at temperatures between 25- 37°C. In 51 out of 79 cells (65%), there was an inwardly rectifying (IR) current that was rapidly activated by hyperpolarizing potential steps (Figure 5.4). The I/V curves typically contained a region showing a small outward current just positive to the reversal potential as shown in Figure 5.4. The second type of current, seen in 52 out of 79 cells (66%), was an outwardly rectifying (OR) current that was activated by depolarizing potential steps (Figure 5.5). At potentials between -100 mV and +40 mV, the OR currents were instantaneous and sustained, but at more positive potentials the current exhibited a degree of time-dependent inactivation (Figure 5.6). In individual cells, the expression of the two currents was variable. 37 out of 79 cells (47%) exhibited the inwardly and outwardly rectifying currents concurrently (Figure 5.7). 15 cells (19%) showed only the outward current, and in 14 cells (18%) only the inward current was observed. In the remaining 13 cells (16%), no voltage-dependent currents were observed and the current-voltage relationship was ohmic and resembled a basal leak conductance (Figure 5.8). Both the IR and OR currents were observed in experiments performed with pipette solutions containing either KCl (n=69) or KCH_3SO_4 (n=13) suggesting that movement of Cl^- from the pipette into the cell was not responsible for induction of the currents.

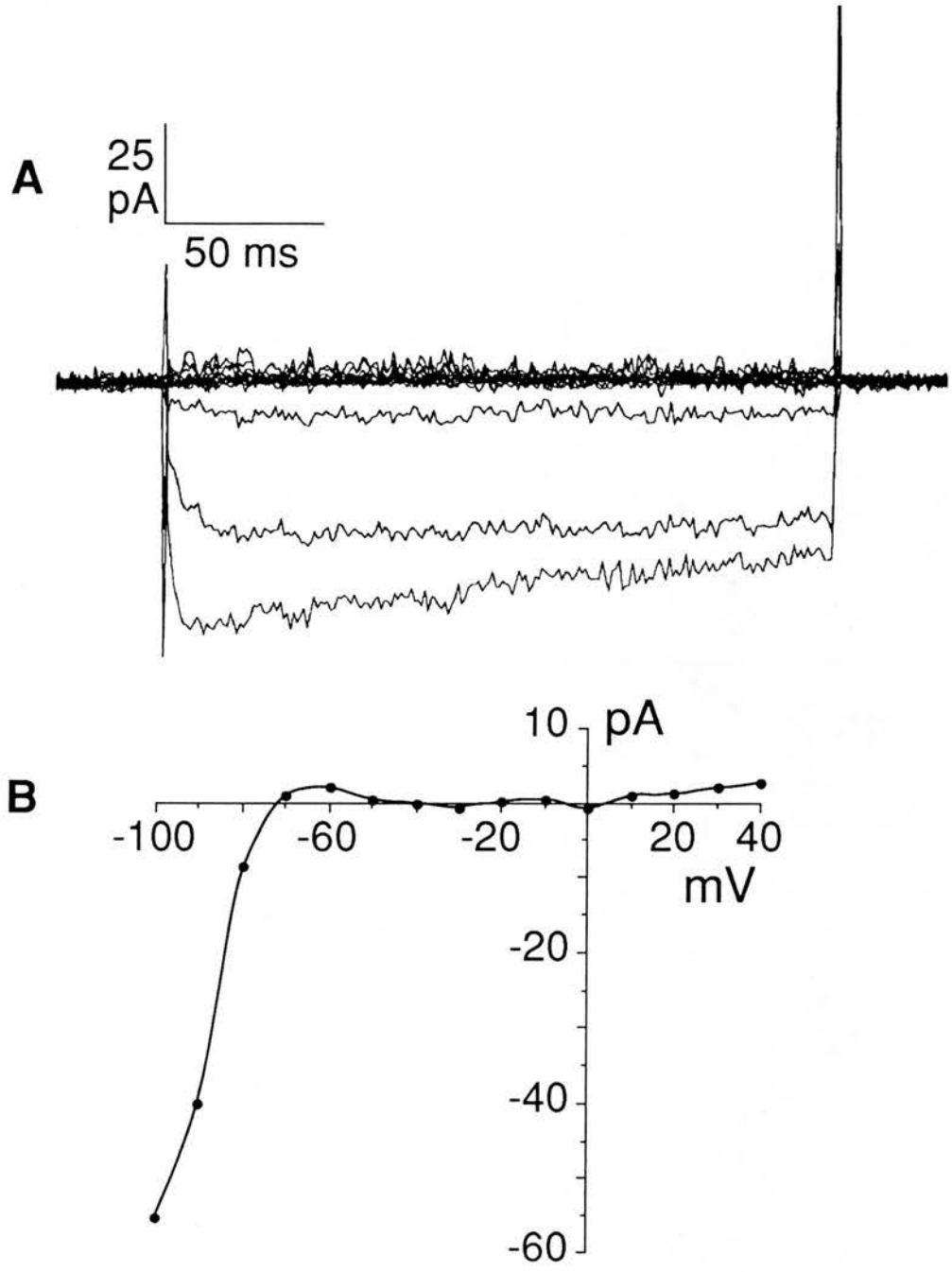

Figure 5.4 - **A**: Whole-cell membrane currents recorded from a rat BMMC using the amphotericin B perforated-patch technique. **B**: The accompanying leak subtracted current-voltage relationship. The cell was clamped at a holding potential of -40 mV and voltage pulses of 200 ms duration were applied from -100 mV to + 40 mV in 10 mV steps at 1 s intervals. The current shows strong inward rectification, reverses at about -70 mV, and exhibits slight time-dependent inactivation. A small outward current is also passed at potentials just positive to the reversal potential. This type of current/voltage relationship was seen in 14 out of 79 BMMCs (18%) at temperatures between 25 - 37°C. Recording solutions: modified mast cell Ringer, standard KCl pipette solution.

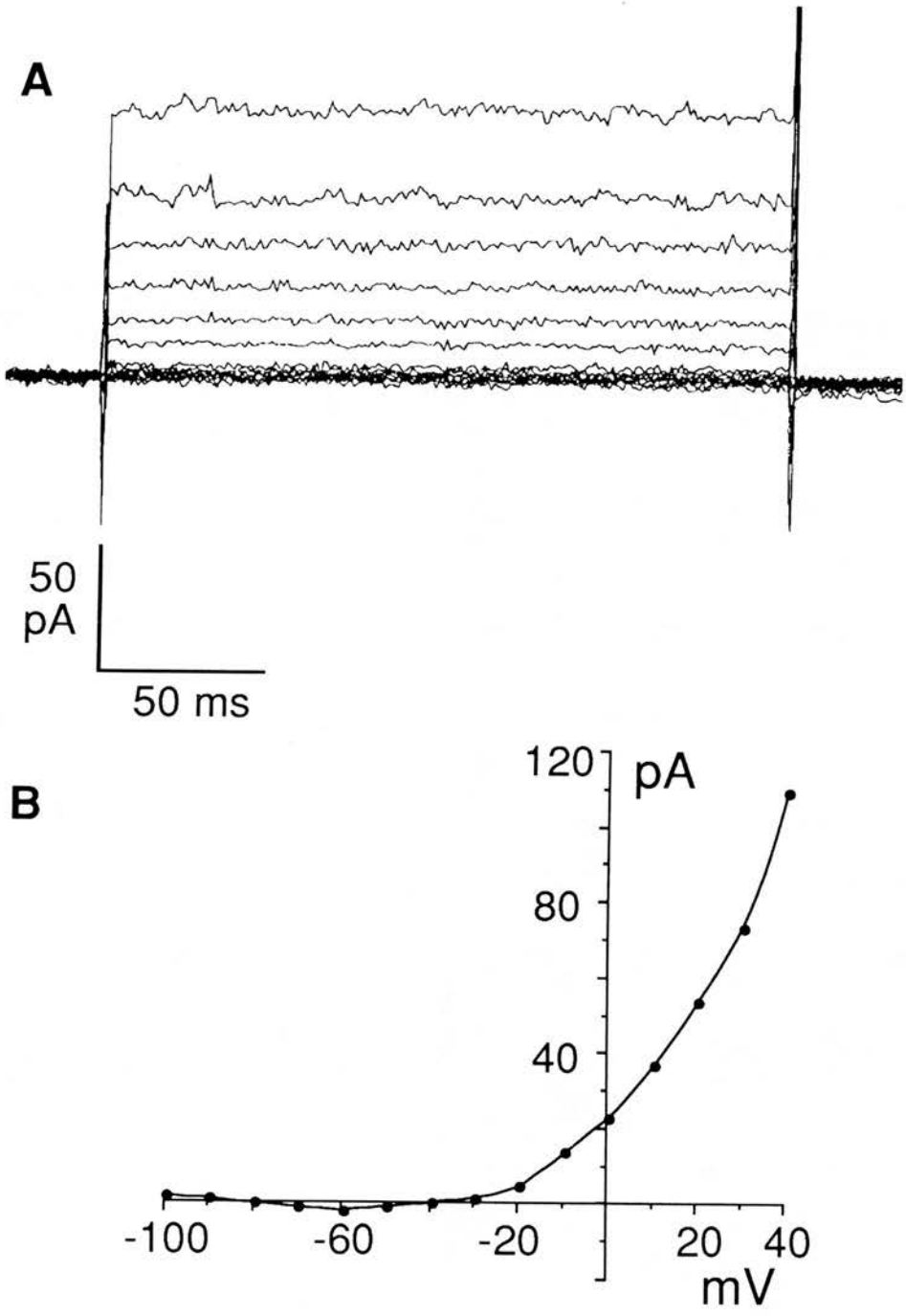

Figure 5.5 - **A**: Whole-cell membrane currents recorded from a rat BMMC using the amphotericin B perforated-patch technique. **B**: The accompanying leak subtracted current-voltage relationship. The cell was clamped at a holding potential of -40 mV and voltage pulses of 200 ms duration were applied from -100 mV to + 40 mV in 10 mV steps at 1 s intervals. The current show strong outward rectification, reverses at about -30 mV, activates instantaneously and shows no inactivation over the voltage range shown. This type of current/voltage relationship was seen in 15 out of 79 BMMCs (19%) at temperatures between 25 - 37°C. Recording solutions: modified mast cell Ringer, standard KCl pipette solution.

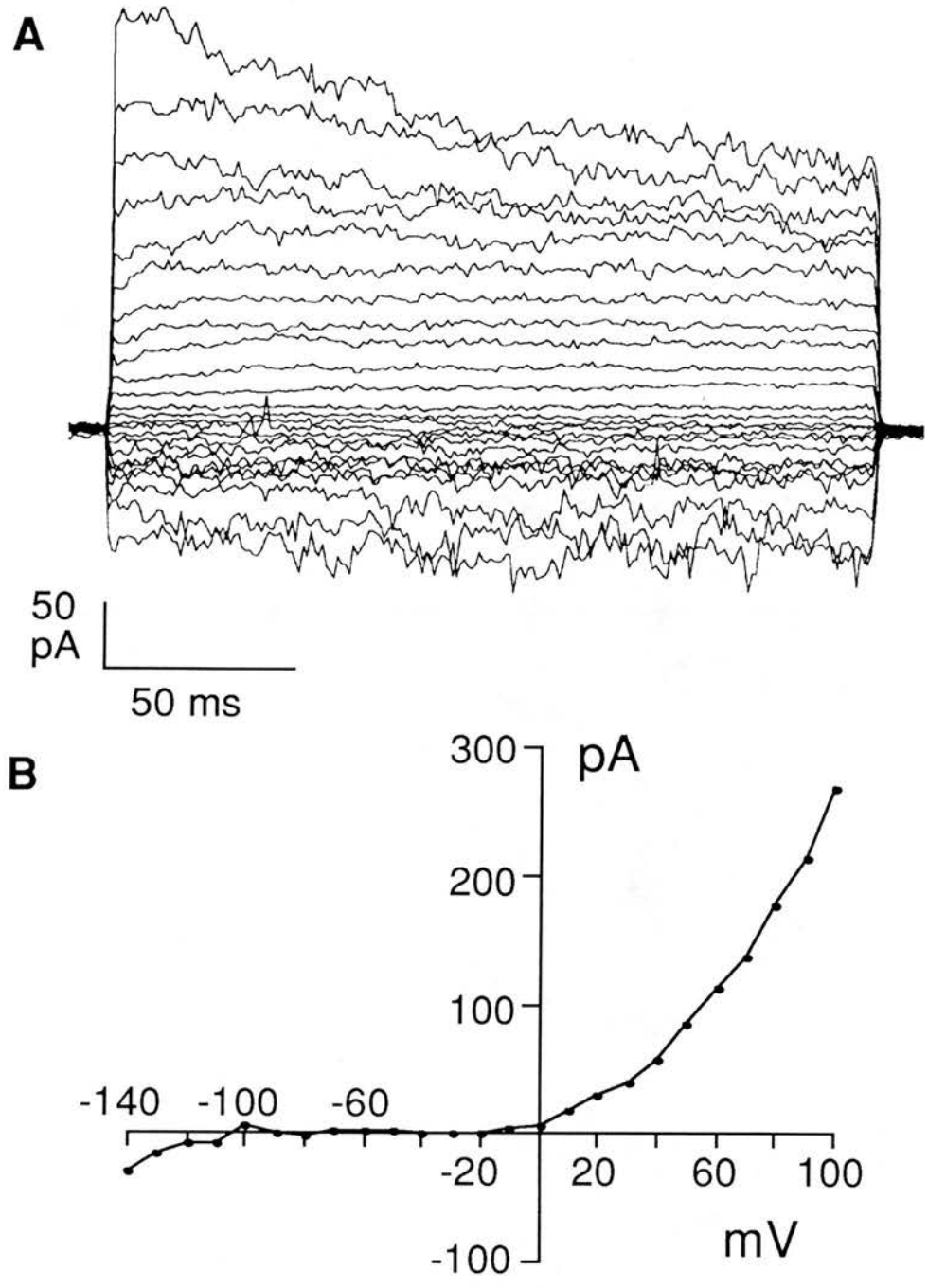

Figure 5.6 - **A**: Whole-cell membrane currents recorded from a rat BMMC over an extended voltage range. **B**: The accompanying leak subtracted current-voltage relationship. The cell was clamped at a holding potential of -40 mV and voltage pulses of 200 ms duration were applied from -140 mV to +100 mV in 10 mV steps at 1 s intervals. The current shows time-dependent inactivation at potentials over +40 mV. Recording solutions: modified mast cell Ringer, standard KCl pipette solution.

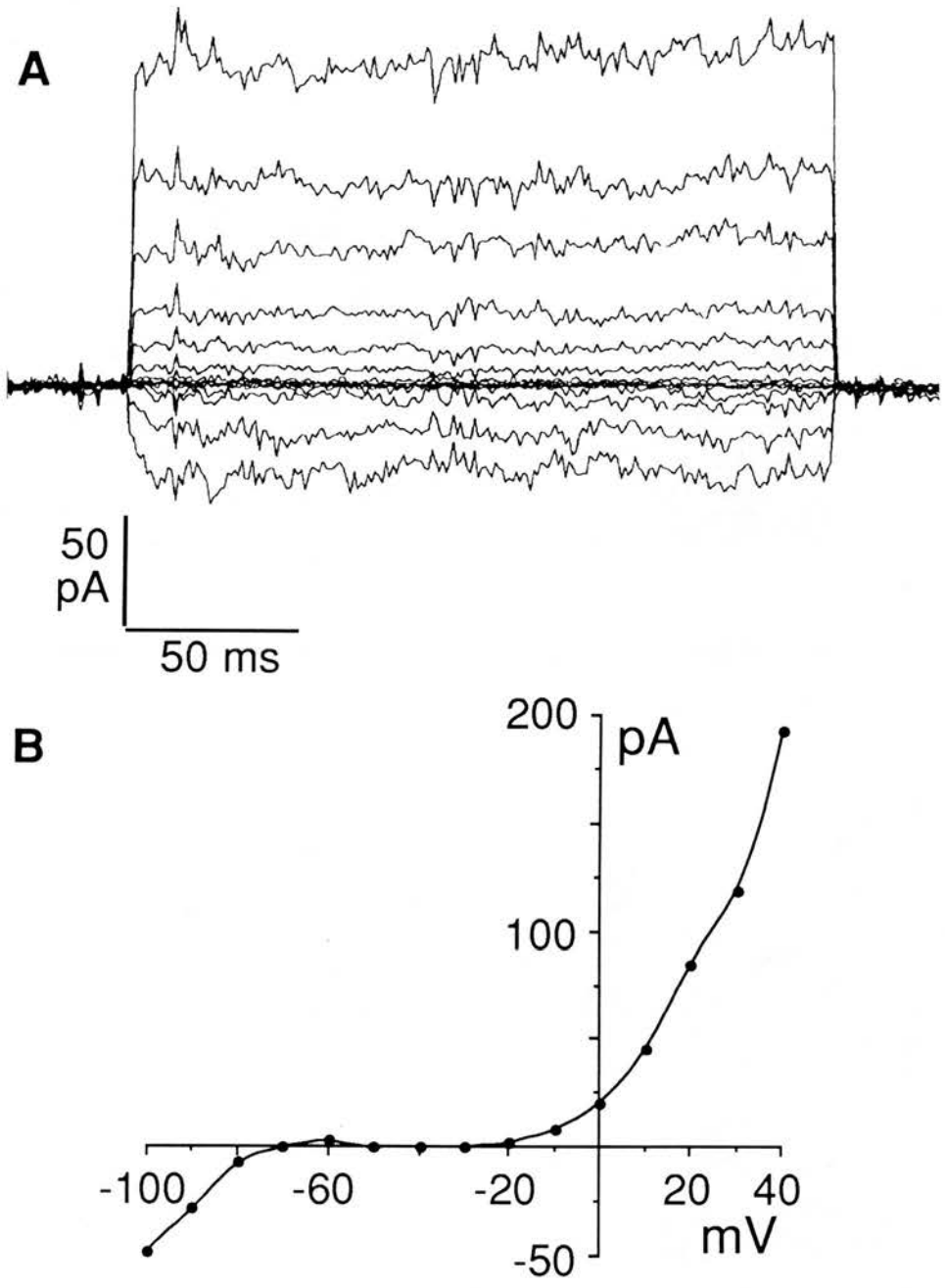

Figure 5.7 - **A**: Whole-cell membrane currents recorded from a rat BMMC using the amphotericin B perforated-patch technique. **B**: The accompanying leak subtracted current-voltage relationship. The cell was clamped at a holding potential of -40 mV and voltage pulses of 200 ms duration were applied from -100 mV to +40 mV in 10 mV steps at 1 s intervals. Both inwardly rectifying and outwardly rectifying currents are present with features similar to those described in Figures 5.4 and 5.5 respectively. This type of current/voltage relationship was seen in 37 out of 79 BMMCs (47%) at temperatures between 25 - 37°C. Recording solutions: modified mast cell Ringer, standard KCl pipette solution.

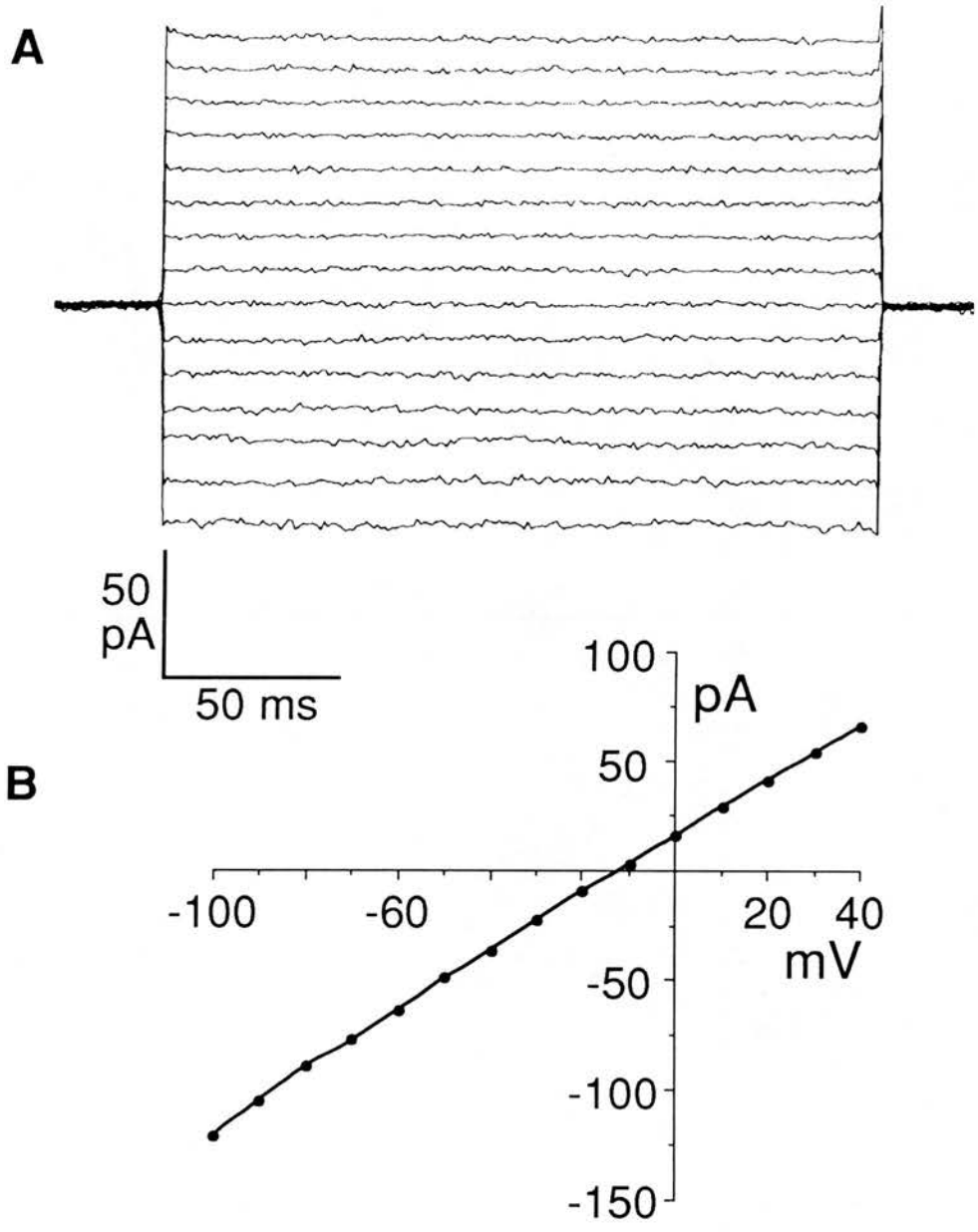

Figure 5.8 - **A**: Whole-cell membrane currents recorded from a rat BMMC using the amphotericin B perforated-patch technique. **B**: The accompanying current-voltage relationship. The cell was clamped at a holding potential of -40 mV and voltage pulses of 200 ms duration were applied from -100 mV to +40 mV in 10 mV steps at 1 s intervals. No voltage-dependent currents are present and the current/voltage relationship represents a basal leak conductance. In this experiment, the current traces are less noisy than in the preceding figures, suggesting a lack of ion channel activity. This type of current/voltage relationship was seen in 13 out of 79 BMMCs (16%) at temperatures between 25 - 37°C. Recording solutions: modified mast cell Ringer, standard KCl pipette solution.

The expression of IR and OR currents in the 79 BMMCs recorded at 25 - 37°C is summarised in Table 5.4.

Table 5.4 - The number and proportion of BMMCs showing inwardly rectifying (IR) or outwardly rectifying (OR) whole-cell currents with the perforated-patch technique at temperatures between 25 - 37°C (n=79).

IR only	IR and OR	OR only	No Currents
14 (18%)	37 (47%)	15 (19%)	13 (16%)

The voltage range over which the above currents were recorded varied as described in chapter 2 (section 2.33), and is shown in Appendix 4. To allow comparison between cells, slope conductances were only calculated from I/V curves obtained over the range -140 mV to -100 mV for inward currents and +80 mV to +100 mV for outward currents. The IR conductance in the range 25 - 37°C was 1.74 ± 1.1 nS (n = 41) and the OR conductance was 2.21 ± 1.4 nS (n = 31). Linear leak currents were subtracted from the I/V curves before calculating the above slope conductances (see chapter 2, section 2.36). The mean leak conductance in the range 25 - 37°C was 0.75 ± 0.62 nS (n=53).

5.4 - Ionic Selectivity of the Inwardly Rectifying Current

The inwardly rectifying currents observed in rat BMMCs were very similar in appearance to those described in RBL-2H3 cells (Lindau and Fernandez, 1986b; Qian and McCloskey, 1993), rat BMMCs grown in the presence of IL-3 (McCloskey and Qian, 1994), and cultured mouse BMMCs (Kuno *et al,* 1995), in which the currents were characterised as a potassium-selective inward rectifier. To determine the ionic selectivity of the IR current, current-voltage relationships were obtained from BMMCs in extracellular solutions containing different concentrations of K^+. In an initial series of 21 perforated-patch experiments, whole-cell currents were recorded from BMMCs suspended in both mast cell Ringer and 10 mM K^+ Ringer (section 2.22). In mast cell Ringer (2.7 mM K^+), 15 out of 21 cells (71%) showed the IR current but when the extracellular K^+ was increased to 10 mM, the current was present in all 21 cells (100%), suggesting that expression of the IR current in BMMCs was dependent on extracellular K^+ concentration. In a further series of experiments, the effect of increasing extracellular K^+ concentration on the conductance and reversal potential of the IR current was investigated. As the extracellular K^+ was increased from 2.7 mM to 165 mM (with a corresponding decrease in the Na^+ concentration), the reversal potential of the I/V curves shifted in a positive direction (Figure 5.9A). The linear relationship between reversal potential and log extracellular K^+ concentration with a least squares slope of 52 mV/decade indicates that the conductance is essentially potassium selective (Figure 5.9B). The slope conductance measured between -100 mV and -80 mV also increased with extracellular K^+ and was 1.48 ± 0.7 nS in 10 mM K^+(n=9), 4.27 ± 1.4 nS in 50 mM K^+ (n=9), 5.50 ± 2.3 nS in 90 mM K^+(n=5), 6.24 ± 2.8 nS in 137 mM K^+(n=7), and

5.8 ± 4.0 nS in 165 mM K^+(n=3). Increase in conductance with increasing extracellular K^+ concentration also indicates that the current is predominantly carried by K^+ ions. Taken together, these results indicate that the IR current in rat BMMCs is a K^+ selective inwardly rectifying current.

Increasing the extracellular K^+ concentration in the above experiments also increased the slope conductance and reversal potential of the linear range of the I/V curves (Figure 5.10). Although this effect was small in comparison to the effect on the rectifying part of the curve, it indicates that at least a proportion of the conductance in this region represents a basal K^+ conductance in addition to non-selective leak.

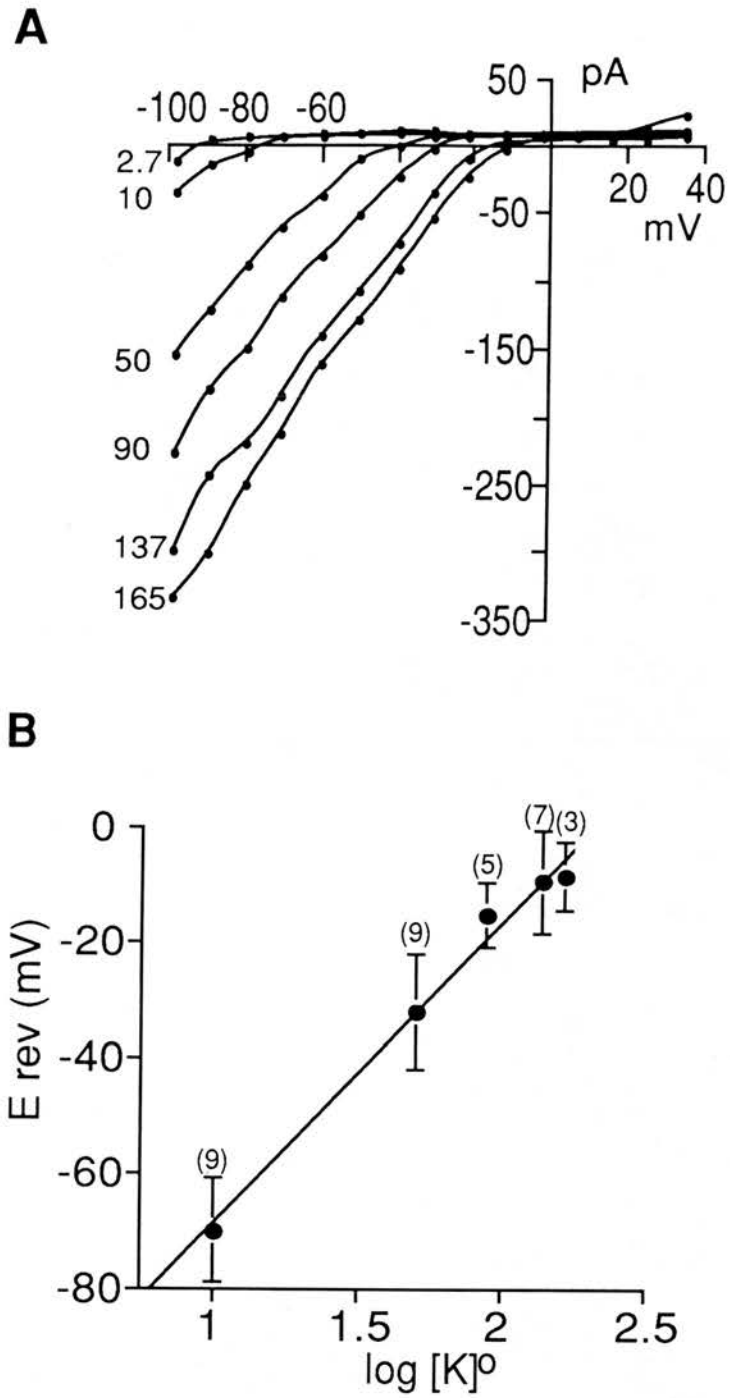

Figure 5.9 - Effect of extracellular K^+ concentration on inwardly rectifying currents.
A: Whole-cell I/V curves of a BMMC in six different concentrations of extracellular K^+. The cell was held at a holding potential of -40 mV and voltage pulses of 200 ms duration were applied from -100 mV to + 40 mV in 10 mV steps at 1 s intervals. There is a positive shift in reversal potential as the extracellular K^+ increases from 2.7 mM to 165 mM. The curves were leak subtracted. Pipette solution = standard KCl, bath temperature = 20°C.
B: Reversal potentials (E rev) plotted against $\log_{10}$ extracellular K^+ (mM). The line is a least-squares fit to the data. The slope of 52 mV/decade is close to that predicted for a K^+-selective membrane. The numbers above each data point represent the number of recordings made at each K^+ concentration.

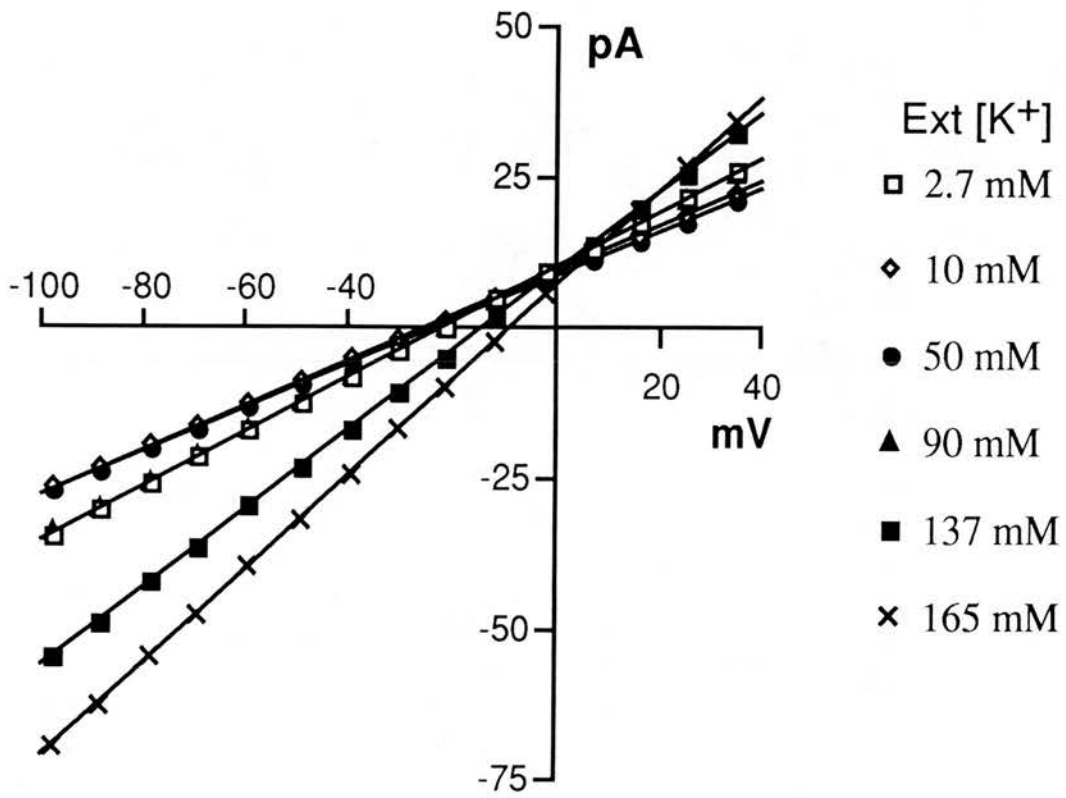

Figure 5.10 - Effect of extracellular K^+ concentration on the linear region of the I/V curves. The I/V curves in Figure 5.9 were leak subtracted before calculation of the conductance and reversal potential. The 4 data points in the linear region of the curves just positive to the reversal potential were used for leak subtraction. However, extrapolation from these points shows that the conductance and reversal potential of the "leak" current is also increased by the increase in extracellular K^+ concentration, suggesting a basal K^+ conductance in this region.

5.5 - Ionic Selectivity of the Outwardly Rectifying Current

The OR current was not affected by changes in extracellular K^+ concentration. However, when the extracellular Cl^- concentration was reduced to 51 mM by substituting Na acetate for NaCl, the OR conductance decreased by 82 ± 8.5 % (Figure 5.11), from a mean of 2.7 ± 2.1 nS to 0.51 ± 0.53 nS (n=5). In three cells bathed in extracellular solution containing 14 mM Cl^- the peak OR conductance was reduced to 0.24 nS in one cell and completely abolished in the other two cells.

As substitution of acetate could cause cytoplasmic acidification, which might influence the above results, the experiments were repeated using Na-isethionate as the impermeant anion. When Na-isethionate was substituted for NaCl to yield an extracellular solution containing 16.7 mM Cl^-, the OR conductance decreased from 3.39 ± 2.3 nS to 0.88 ± 1.2 nS (n=4), and this effect was reversible on washout of the bath. A typical experiment showing the effect of Na-isethionate substitution is shown in Figure 5.12. The figure shows continuous pen recordings made during the solution exchange, and demonstrates the reduction in both current amplitude and slope conductance as the extracellular Cl^- concentration is reduced to 16.7 mM.

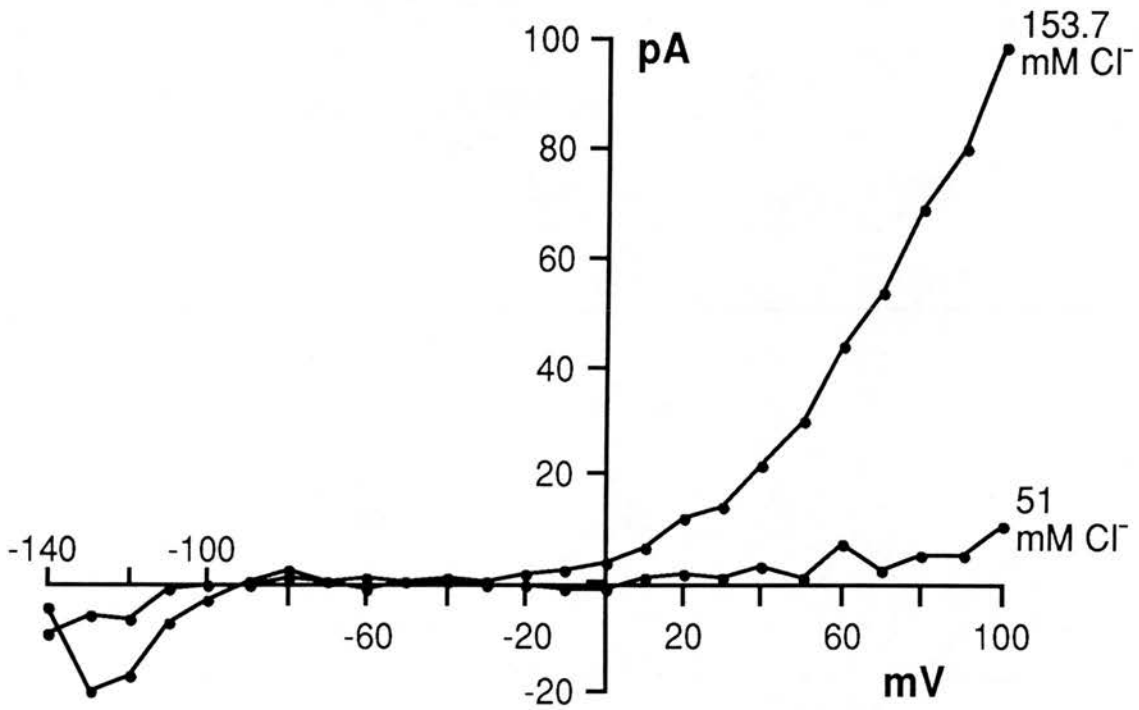

Figure 5.11 - Effect of extracellular Cl^- concentration on the outwardly rectifying current. The BMMC was held at a holding potential of -40 mV and voltage pulses of 200 ms duration were applied from -140 mV to +100 mV in 10 mV steps at 1 s intervals. When the extracellular Cl^- concentration was decreased from 153.7 mM to 51 mM by substituting Na-acetate for NaCl, the outwardly rectifying conductance was markedly decreased. The curves were leak subtracted. Pipette solution = standard KCl, bath temperature = 25°C.

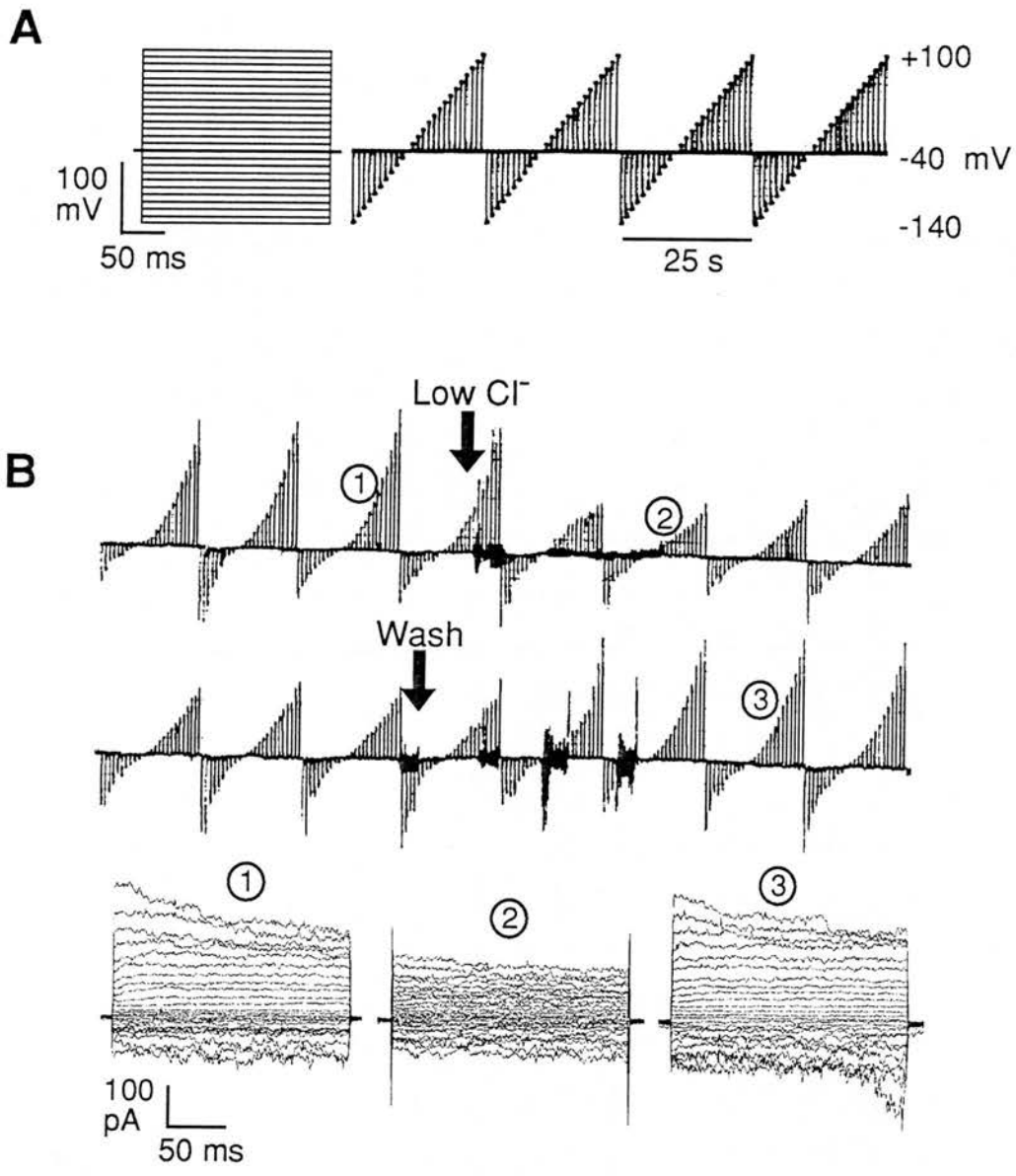

Figure 5.12 - Effect of extracellular Cl^- concentration on the outwardly rectifying current. **A**: The voltage step protocol. The BMMC was held at a holding potential of -40 mV and voltage pulses of 200 ms duration were applied from -140 mV to +100 mV in 10 mV steps at 1 s intervals. **B**: Typical continuous pen recording of the I/V relationship. Below the tracings are the original superimposed currents evoked by the 25 voltage steps labelled by each encircled number. At the first arrow, the mast cell Ringer (153.7 mM Cl^-) was exchanged for an extracellular solution containing Na-isethionate (16.7 mM Cl^-). The outwardly rectifying (OR) current, showing time-dependent inactivation at potentials above +60 mV, is markedly reduced between (1) and (2). At the second arrow, the bath was washed out with mast cell Ringer resulting in restoration of the current (3). Noise indicates the time taken for solution exchange. Pipette solution contained KCH_3SO_4. Bath temperature = 30°C.

5.6 - Reversal Potential of the Outwardly Rectifying Current

The above results suggested that the OR conductance was Cl^- selective. However, determination of the reversal potential of the Cl^- current from the I/V curves proved problematical for a number of reasons. First, the linear region, and reversal potential, of the I/V curves was influenced by the basal K^+ conductance and leak as described in the previous section. This region was not influenced by changes in extracellular Cl^- concentration as shown in the non-leak subtracted curves in Figure 5.13 (A and B), suggesting that the OR current was minimally active over this voltage range. To overcome this problem, the linear range of the I/V curve was used for leak subtraction, and the point at which the current became positive was used as an estimate of the reversal potential in different extracellular Cl^- concentrations (Figure 5.13, C and D). However, this approach would not yield the actual reversal potential of the OR current if the Cl^- conductance was a component of the linear range of the I/V curve. A second problem arises in perforated-patch experiments because the contents of the pipette solution are not the same as the cytosol, so the cytoplasmic Cl^- concentration is not known. Pipette Cl^- ions either diffuse into or out of the cell (depending on pipette Cl^- concentration) until a Donnan equilibrium is established (Horn and Marty, 1988). The time taken for Cl^- redistribution is not known for each cell, so the OR current could be measured under different cytoplasmic Cl^- concentrations which could actually vary during the solution exchange. This latter problem could be overcome by using the conventional whole-cell recording configuration, in which the cytosolic Cl^- concentration is known. Unfortunately, as described later in section 5.9, the OR current was dependent on the maintenance of cytoplasmic integrity and was rarely observed with this configuration. A potential solution to the problem is to determine the *shift* in reversal potential that occurs as the extracellular Cl^- concentration is changed. This allows comparison with the change in reversal potential predicted by the Nernst equation for a Cl^- selective membrane, which can be calculated independently of cytosolic Cl^- as shown below.

Expected Reversal Potential Change for a Chloride Selective Membrane

$$\text{Chloride Reversal Potential at 25°C, } E_{Rev} = \frac{RT}{F} \ln \frac{Cl_i}{Cl_o}$$

$$= 59.16 \log_{10} \frac{Cl_i}{Cl_o}$$

Expected shift in E_{rev} as extracellular Cl^- changes from X mM to Y mM

$$= 59.16 \log_{10} \frac{Cl_i}{Y} - 59.16 \log_{10} \frac{Cl_i}{X}$$

$$= 59.16 \log_{10} \left(\frac{Cl_i}{Y} \div \frac{Cl_i}{X}\right)$$

$$= 59.16 \log_{10} \frac{[X]}{[Y]}$$

As the extracellular Cl^- concentration changes from 153.7 mM to either 51 mM (Na-acetate) or 16.7 mM (Na-isethionate), the expected change in reversal potential predicted by this equation is 28 mV or 57 mV respectively. When the extracellular Cl^- concentration was reduced from 153.7 mM to 51 mM the reversal potential of the OR current shifted by +31 ± 21 mV (n=5), thus approximating the change predicted by the Nernst equation (Figure 5.11). However, changing the extracellular Cl^- from 153.7 mM to 16.7 mM resulted in a reversal potential shift of only +34 ± 19 mV (n=4). The departure from theory, and the large standard deviations, may reflect both the inherent problems described above, or, in addition, partial selectivity for anions.

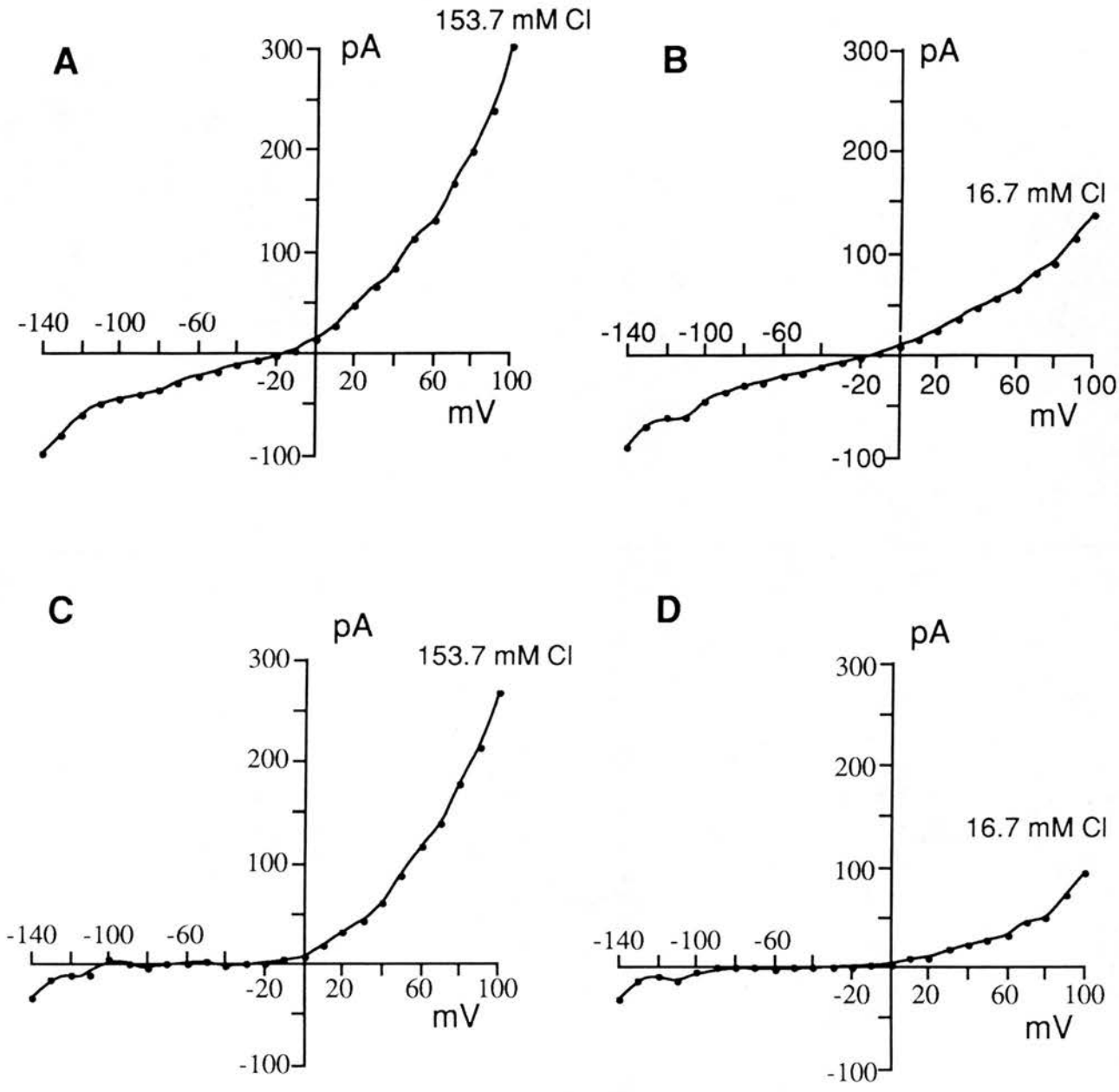

Figure 5.13 - Effect of extracellular Cl^- concentration on the reversal potential of the current/voltage relationship.

A and B: Non leak subtracted curves. Reducing the extracellular Cl^- from 153.7 mM to 16.7 mM decreases the current amplitude and slope conductance, but does not change the reversal potential, probably because this region of the curve is dominated by a basal leak conductance.

B and C: Leak subtracted curves derived from A and B. The data points at voltages ranging from -30 mV to -70 mV were used for leak subtraction. The estimated reversal potential shifts in a positive direction by approximately 15 mV, although the expected shift for a Cl^--selective membrane is 57 mV. The discrepancy could reflect changes in intracellular Cl^- concentration, partial anion selectivity, or a contribution by the K^+-selective current.

5.7 - Effect of Channel Blockers on the Outwardly Rectifying Current

In preliminary experiments, the outwardly rectifying current was not affected by the K^+ channel blockers 4-amino pyridine (100 μM) or tetraethylammonium (25 mM). However, the OR conductance was reversibly decreased by the chloride channel blocker 4,4'-diisothiocyano-2,2'-stilbenedisulfonate (DIDS). Addition of 20 μM DIDS to the extracellular solution reduced the outwardly rectifying conductance by 69 ± 23% from a mean of 2.8 ± 2.0 nS to 1.0 ± 1.3 nS (n=7). Figure 5.14 shows a pen recording from a typical experiment in which the OR current amplitude and slope conductance decreased after addition of 20 μM DIDS to the bath, but partially recovered after the blocker was washed out. Taken together with the effects of extracellular Cl^- concentration on the OR current, the above observations indicate that the outwardly rectifying currents in rat BMMCs are predominantly carried by Cl^- ions.

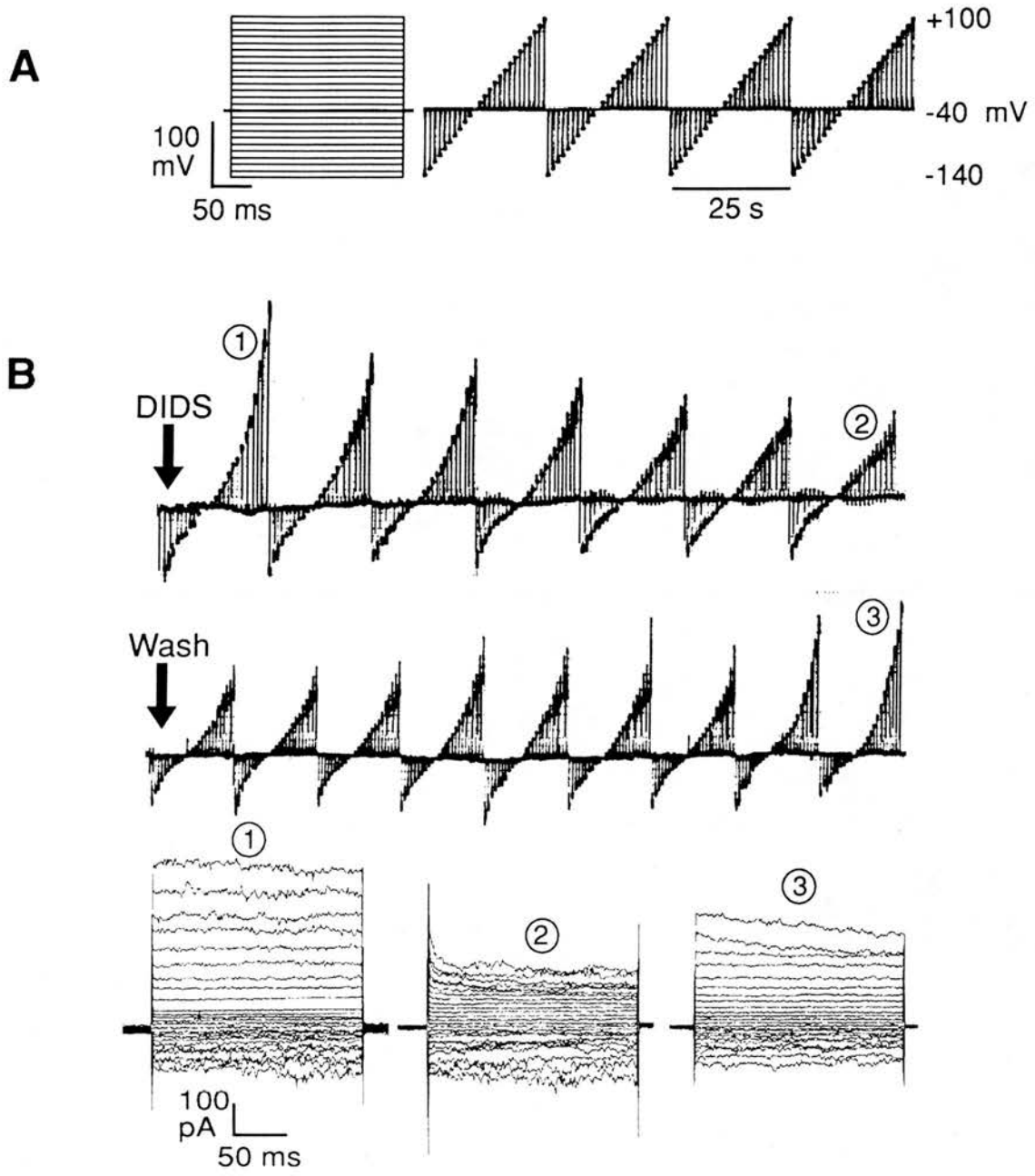

Figure 5.14 - Effect of the Cl^- channel blocker DIDS on whole-cell membrane currents in rat BMMCs. **A**: The voltage step protocol. The cell was held at a holding potential of -40 mV and voltage pulses of 200 ms duration were applied from -140 mV to +100 mV in 10 mV steps at 1 s intervals. **B**: Typical continuous pen recording of the current-voltage relationships. Below the trace are the original superimposed currents evoked by the 25 voltage steps labelled by each encircled number. At the first arrow, 20 μm DIDS was added to the bath resulting in gradual diminution of the OR current. At the second arrow, the DIDS was washed out of the bath resulting in recovery of the OR current. Extracellular solution = modified mast cell Ringer, pipette solution = standard KCl, bath temperature = 25°C.

5.8 - Effect of Temperature on the Expression of Whole-Cell Currents

The outwardly rectifying chloride conductance was not described in two previous studies of rat mucosal type mast cells (Lindau and Fernandez, 1986b; McCloskey and Qian, 1994). However, in contrast to the methods described above, these studies used conventional whole-cell recording techniques at room temperature. To determine if the OR_{Cl} current was influenced by bath temperature, the results of 117 perforated-patch recordings obtained at room temperature (16 - 20°C) were compared with the results obtained at temperatures between 25 - 37°C. At room temperature, 23% of BMMCs displayed both IR_K and OR_{Cl} currents concurrently, with a further 49% showing only IR_K currents. In marked contrast to the results obtained at 25 - 37°C, only 3% of BMMCs displayed exclusively outward currents. 25% of cells appeared quiescent, displaying neither inward nor outward currents. The difference between these results and those described earlier is primarily attributable to the decreased proportion of cells showing OR_{Cl} currents at room temperature compared to 25 - 37°C (26% as shown in Table 5.5 vs. 66% as shown in Table 5.4).

Table 5.5 - The number and proportion of BMMCs showing inwardly rectifying (IR) or outwardly rectifying (OR) whole-cell currents with the perforated-patch technique at room temperature (16 - 20°C) (n=117).

IR only	IR and OR	OR only	No Currents
57 (49%)	27 (23%)	3 (3%)	30 (25%)

This effect is illustrated in Figure 5.15, which shows the effect of warming on a population of 31 BMMCs that showed the OR_{Cl} conductance at 25 - 37°C. The shift in the distribution of conductances to the right indicates the activation of the OR_{Cl} current by the rise in temperature. In addition, the development of the OR_{Cl} current could be seen in individual cells by monitoring the I/V relationships as BMMCs were warmed (Figure 5.16). The temperature at which the OR_{Cl} current developed varied from cell to cell; in most BMMCs, the current developed at 25°C, but in some cells the current only appeared at 30 or 37°C. In cells that exhibited the OR_{Cl} current, the time from the start of warming to development of the peak conductance ranged from 132 to 696 s with a mean and s.d. of 309 ± 132 s (n=21). After activation, the OR_{Cl} current was typically stable for long periods, and in one cell it was monitored for 60 min without deterioration. Taken together, these results indicate that detection of the OR_{Cl} current is more likely if the temperature of the cells is increased towards physiological values.

The slope conductances of the IR_K and OR_{Cl} currents at room temperature were significantly lower than those recorded at 25 - 37°C ($p<0.005$). Although the expression of the IR_K current was not affected by temperature in the same way as the OR_{Cl} current, its conductance was 1.22 ± 0.7 nS (n=56) at room temperature compared to 1.74 ± 1.1 nS (n=41) at 25 - 37°C (Figure 5.17). A similar difference was found when cells showing the OR_{Cl} conductance at room temperature (1.25 ± 0.9 nS, n=20) were compared to those showing the conductance at 25 - 37°C (2.21 ± 1.4 nS, n=31, Figure 5.18). The median OR_{Cl} conductance increased with each temperature increment (25, 30 and 37°C) but the difference between the three temperatures did not reach statistical significance, probably due to small group sizes.

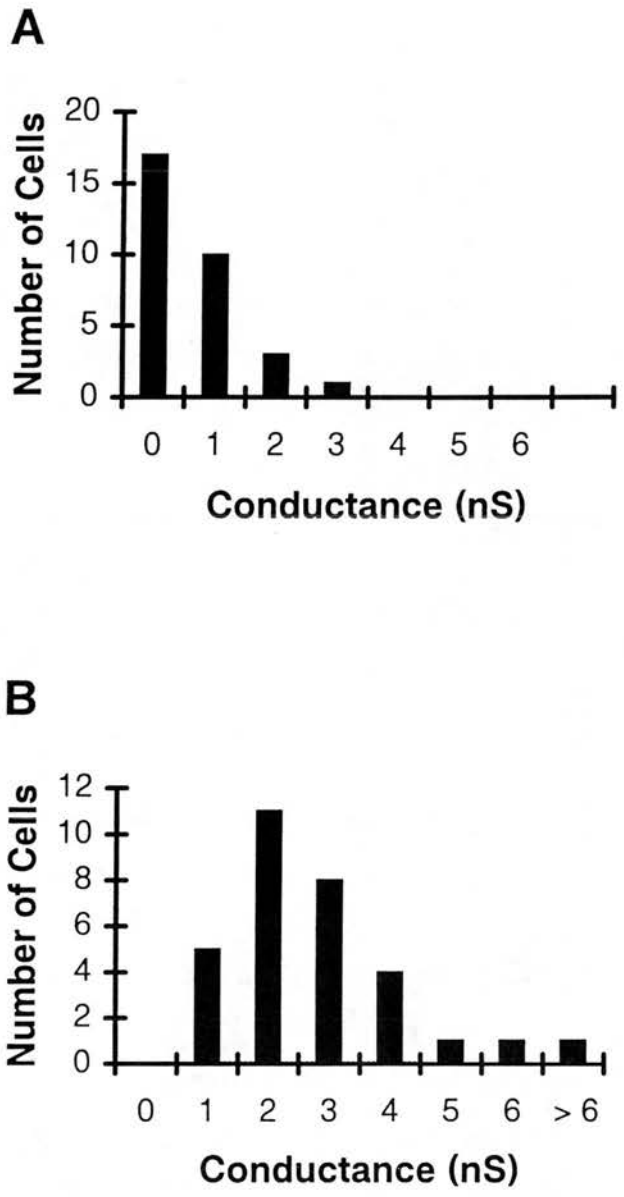

Figure 5.15 - Effect of increasing bath temperature on a population of 31 BMMCs that showed the OR_{Cl} current at 25 - 37°C. The distribution of OR_{Cl} conductances at room temperature (16 - 20°C) is shown in **A**, and at 25 - 37°C in **B**. The shift of the distribution to the right indicates activation of the current by the rise in temperature. Extracellular solution = modified mast cell Ringer, pipette solution = standard KCl solution.

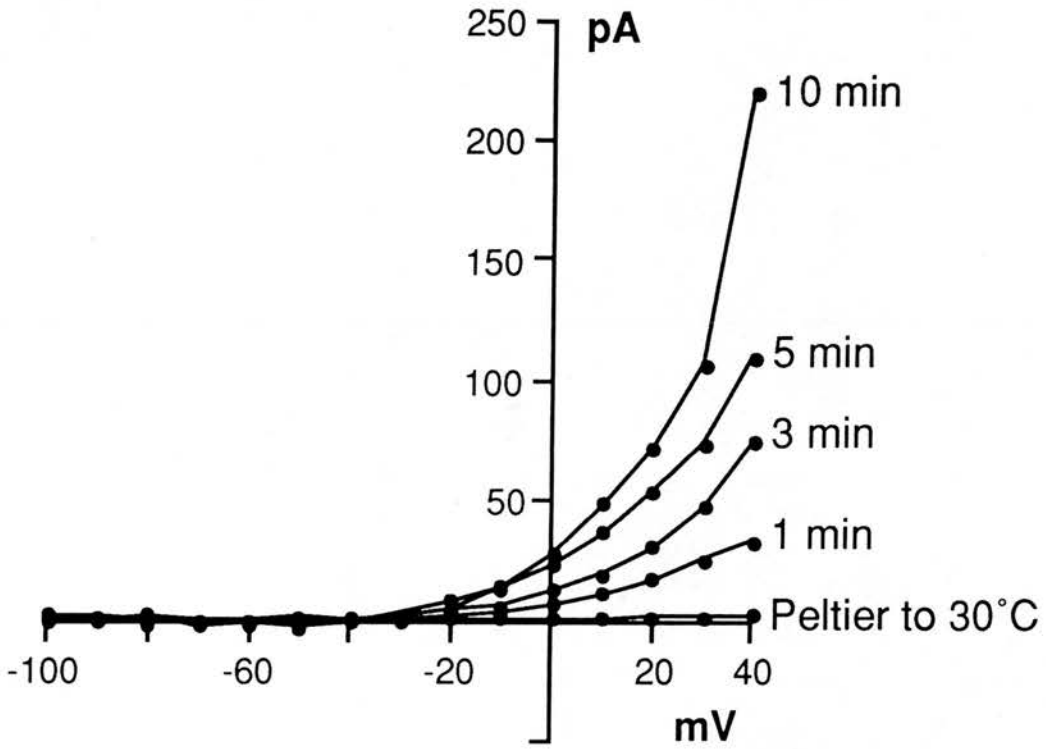

Figure 5.16 - Perforated-patch experiment showing activation of the OR_{Cl} current as the bath temperature was increased from room temperature to 30°C. The BMMC was clamped at a holding potential of -40 mV and voltage pulses of 200 ms duration were applied from -100 mV to +40 mV in 10 mV steps at 1 s intervals. I/V relationships are shown at intervals following activation of the Peltier device. Leak currents were subtracted. Extracellular solution = modified mast cell Ringer, pipette solution = standard KCl solution.

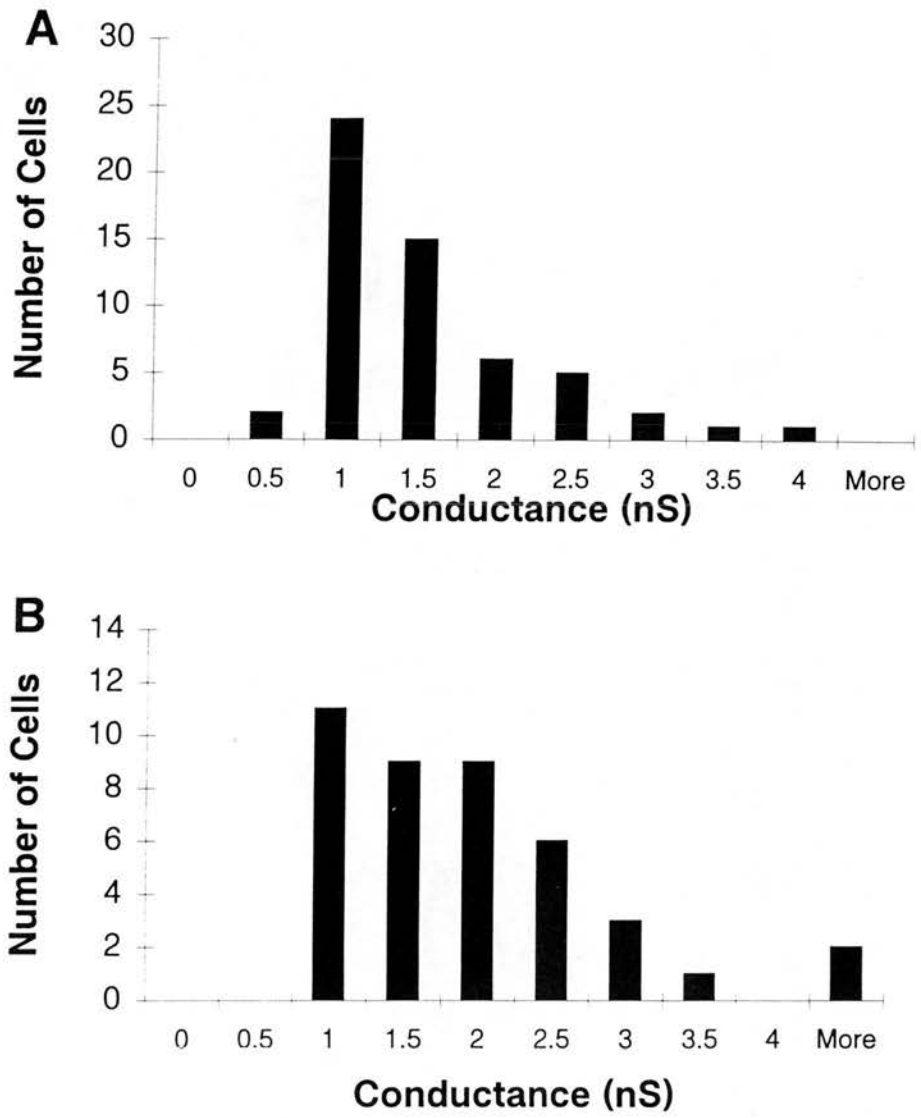

Figure 5.17 - Comparison of the IR_K current slope conductances at room temperature (**A**), and in the range 25 - 37°C (**B**). Slope conductances were calculated using a least squares fit to data points in the voltage range of the I/V curve running from -140 mV to -100mV. The IR conductance was significantly higher at temperatures between 25 - 37°C (1.74 ± 1.1 nS, n=41) than at room temperature (1.22 ± 0.7 nS, n=56, $p<0.005$). Only those cells showing the current were included in the analysis.

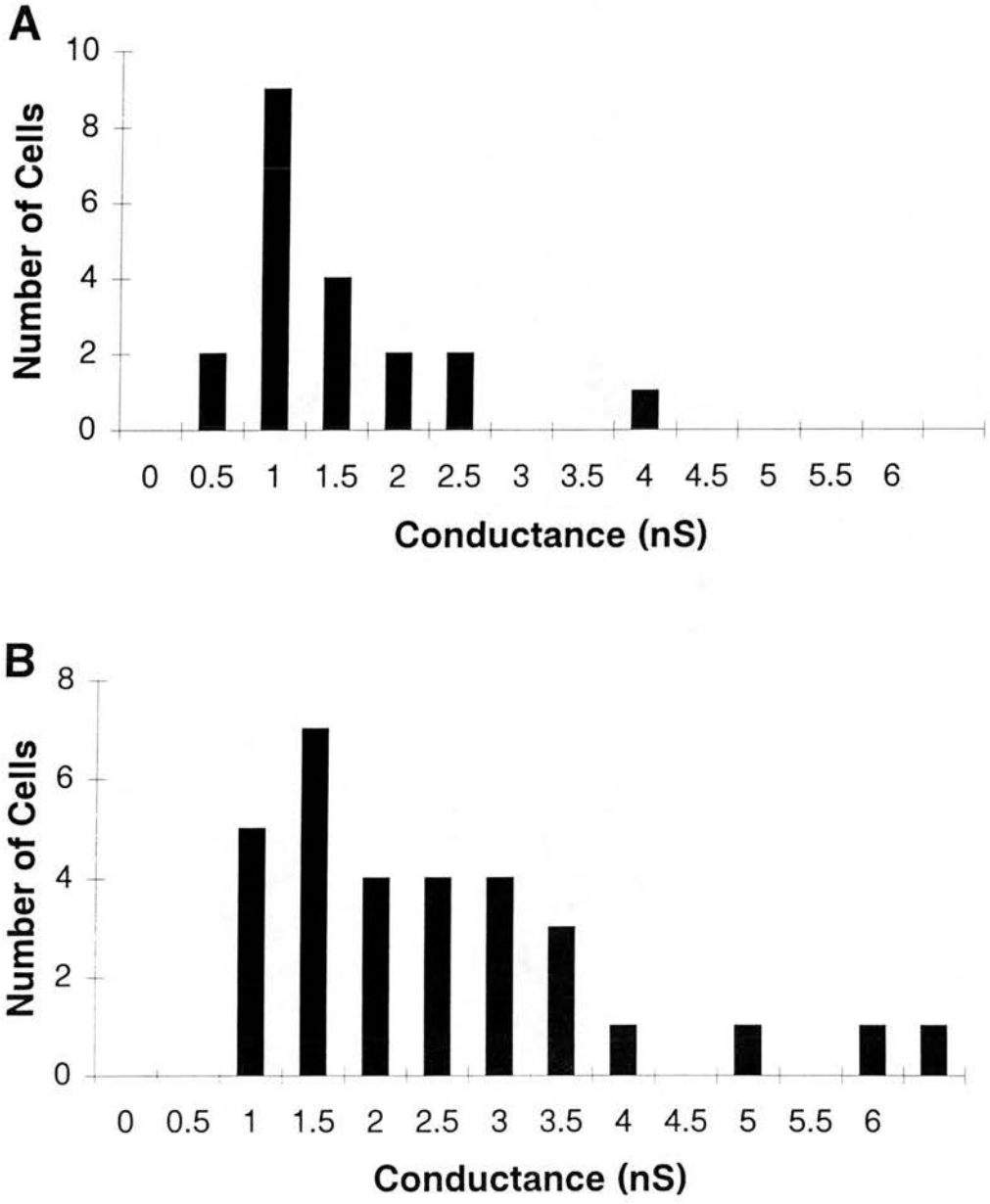

Figure 5.18 - Comparison of the OR_{Cl} current slope conductances at room temperature (**A**), and in the range 25 - 37°C (**B**). Slope conductances were calculated using a least squares fit to data points in the voltage range of the I/V curve running from +80 mV to +100mV. The OR conductance was significantly higher at temperatures between 25 - 37°C (2.21 ± 1.4 nS, n=31) than at room temperature (1.25 ± 0.9 nS, n=20, $p<0.005$). Only those cells showing the current were included in the analysis.

5.9 - Effect of Cytoplasmic Disruption on the Whole-Cell Currents

To determine if maintenance of cytoplasmic integrity was also important for demonstration of the OR_{Cl} current, a series of experiments was performed using the conventional whole-cell recording technique. In this method, the cytoplasm of the cell is dialysed with the pipette solution, thus removing enzymes or second messengers which could be critical to the function of ion channels. Current-voltage relationships showed that 41 out of 44 BMMCs at room temperature (93%) displayed the IR_K current (Figure 5.19), with a mean slope conductance of 0.83 ± 0.5 nS (n=22). The OR current was only present at room temperature in 3 out of 44 BMMCs (7%), with a mean slope conductance of 0.87 ± 0.6 nS. These 3 cells came from a series of experiments in which KCH_3SO_4 was used in the pipette solution (n=13). The OR current was also present in 3 out of 6 BMMCs (50%) when conventional whole-cell recordings were performed at room temperature using standard KCl pipette solution containing 0.3 mM GTP and 0.2 mM ATP (mean slope conductance = 1.43 ± 1.4 nS, Figure 5.20). These experiments suggest that the OR conductance may be dependent on one of these cytosolic factors.

Increasing the temperature of cells to 25°C in the whole-cell configuration often resulted in breakdown of the pipette-membrane seal. Hence, it was not possible to obtain a large series of recordings under these conditions. However, when 14 cells dialysed with KCH_3SO_4 pipette solution were successfully warmed to temperatures between 25 - 37°C, 3 BMMCs showed some OR current, but the conductance was much lower than that measured in perforated-patch recordings (0.69 ± 0.1 nS).

A summary of the effects of temperature and cytoplasmic disruption on the whole-cell currents in rat BMMCs is shown in Table 5.6. The results indicate that the activity of the OR_{Cl} current is dependent both on temperature and the maintenance of cytoplasmic integrity. In contrast, the IR_K current was active both at room temperature and with the conventional whole-cell recording configuration.

Interestingly, the proportion of BMMCs showing the IR_K current actually decreased with the perforated-patch technique at higher temperatures. Although the explanation for this phenomenon is not known, it may reflect differences between intracellular and extracellular K^+ concentrations with the two techniques (the proportion of cells showing the IR_K current with the perforated-patch technique was increased to 100% when the extracellular K^+ concentration was raised to 10 mM - see section 5.4).

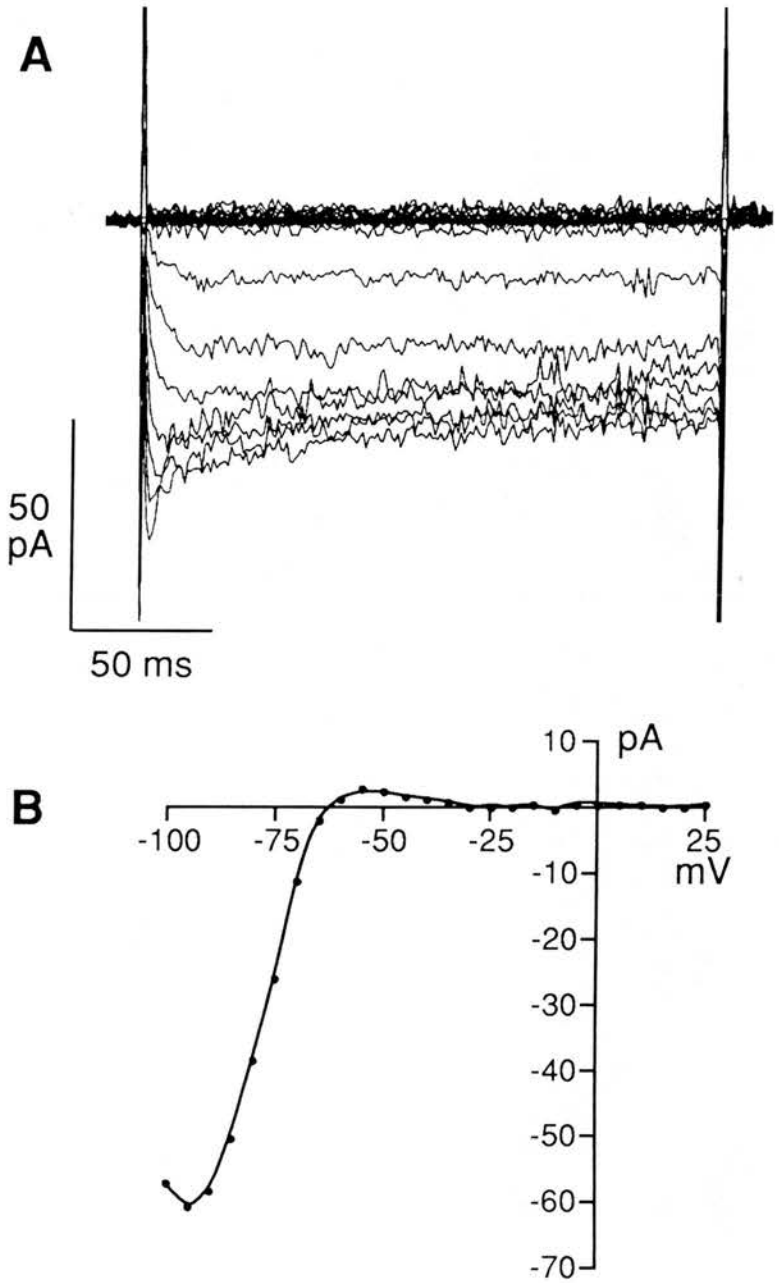

Figure 5.19 - **A**: Whole-cell membrane currents recorded from a rat BMMC using the conventional whole-cell recording configuration at room temperature. **B**: The accompanying leak subtracted current-voltage relationship. The cell was clamped at a holding potential of -40 mV and voltage pulses of 200 ms duration were applied from -100 mV to + 35 mV in 5 mV steps at 1 s intervals. The current shows strong inward rectification, reverses at -60 mV, and exhibits time-dependent inactivation at potentials more negative than -85 mV. A small outward current is also passed at potentials just positive to the reversal potential. Recording solutions: standard mast cell Ringer, standard KCl pipette solution.

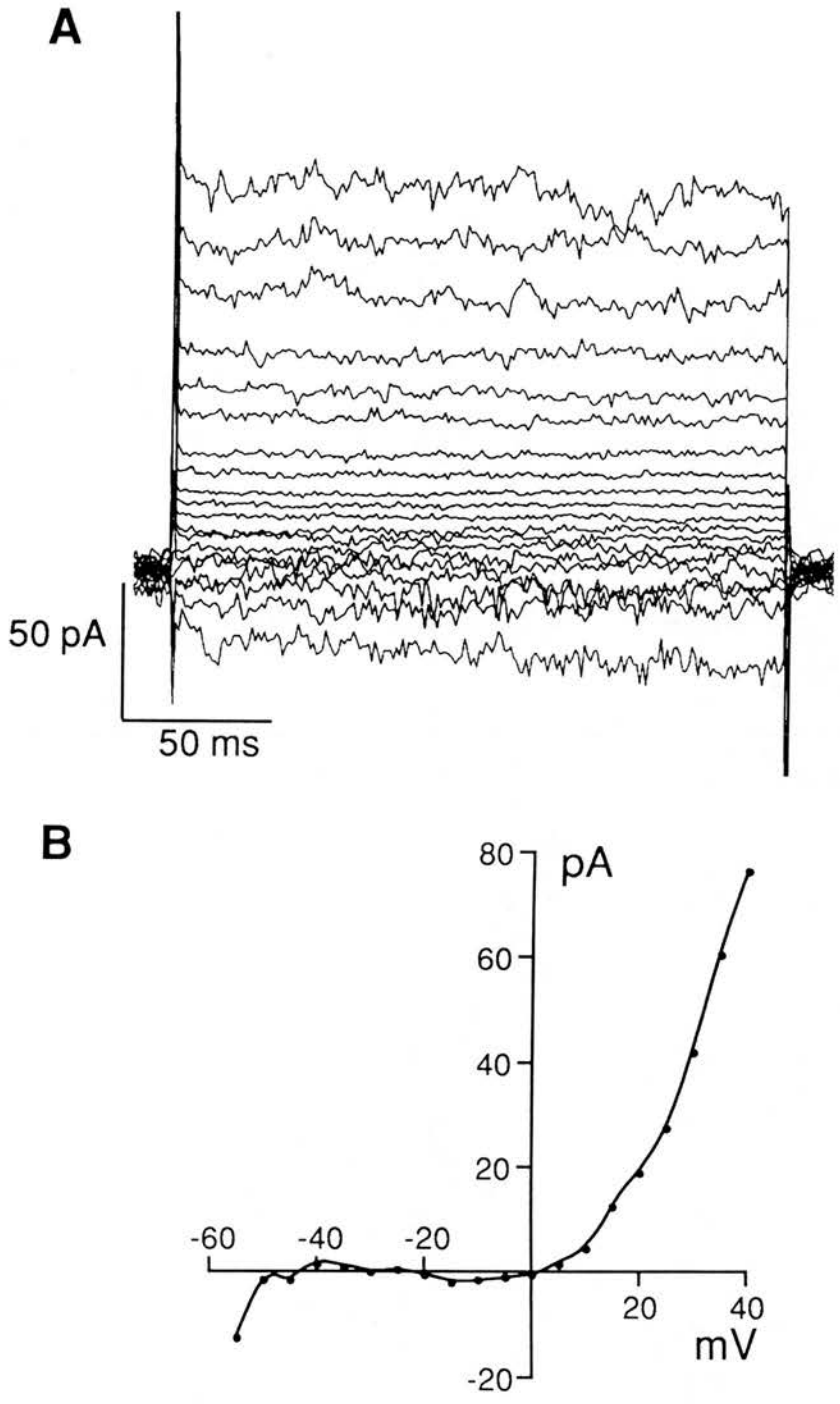

Figure 5.20 - **A**: Whole-cell membrane currents recorded from a rat BMMC using the conventional whole-cell recording configuration. The pipette solution contained KCl and 0.3 mM GTP/0.2 mM ATP. **B**: The accompanying leak subtracted current-voltage relationship. The cell was clamped at a holding potential of -40 mV and voltage pulses of 200 ms duration were applied from -55 mV to +40 mV in 5 mV steps at 1 s intervals. The current is very similar to the OR_{Cl} current seen with the perforated-patch technique, showing strong outward rectification, instantaneous activation and no inactivation over the voltage range shown. The current reverses at about 0 mV, as expected with almost symmetrical Cl^- concentrations. The bath contained standard mast cell Ringer at room temperature.

A

Parameter	Conventional WCR: Cytoplasm Disrupted		Perforated Patch Recording: Cytoplasm Preserved	
Temperature	16 - 20°C	25 - 37°C	16 - 20°C	25 - 37°C
% Cells showing IR_K	93%	86%	72%	65%
Number cells showing IR_K	41/44	12/14	84/117	51/79
Mean conductance ± s.d. (nS)	0.83 ± 0.5	1.04 ± 0.6	1.22 ± 0.7	1.74 ± 1.1

B

Parameter	Conventional WCR: Cytoplasm Disrupted		Perforated Patch Recording: Cytoplasm Preserved	
Temperature	16 - 20°C	25 - 37°C	16 - 20°C	25 - 37°C
% Cells showing OR_{Cl}	7%	21%	26%	66%
Number cells showing OR_{Cl}	3/44	3/14	30/117	52/79
Mean conductance ± s.d. (nS)	0.87 ± 0.6	0.69 ± 0.1	1.25 ± 0.9	2.21 ± 1.4

Table 5.6 - Effect of recording conditions on the IR_K (**A**) or OR_{Cl} (**B**) currents. Expression of the IR_K current is not dependent on temperature or the maintenance of cytoplasmic integrity, whereas the probability of observing the OR_{Cl} current increases as the conditions approach physiological. The whole-cell conductance (for both currents) increases significantly with the perforated-patch technique at the warmer temperatures ($p<0.005$).
WCR = Whole-cell recording. Conventional WCR was performed with pipette solutions containing either KCl or KCH_3SO_4, without added GTP or ATP (see section 2.22 and appendix 4 for details).

5.10 - Whole-cell currents in rat peritoneal mast cells

The outwardly rectifying chloride current in rat BMMCs was similar to that described in rat peritoneal mast cells (RPMCs) when c-AMP was included in the pipette solution or when the cells were stimulated with secretagogues (Matthews *et al,* 1989a; Dietrich and Lindau, 1994; Janiszewski *et al,* 1994). The aim of this section was to determine if an OR_{Cl} current could also be detected in resting RPMCs. Peritoneal mast cells were obtained and purified as described in chapter 2 (section 2.11), and were used either on the day of collection, or after 24 - 48 hours incubation in the presence or absence of 10 ng/ml SCF (see appendix 4 for details). The cells were prepared for electrophysiological recording as described previously (section 2.28), and the perforated-patch technique was used to obtain current-voltage relationships from cells at room temperature and in the range 25 - 37°C. Figure 5.21 shows the superimposed whole-cell currents from a RPMC warmed to 25°C with the accompanying leak-subtracted I/V curve. An outwardly rectifying current is present that closely resembles the OR_{Cl} current described in rat BMMCs. Figure 5.22 shows the development of the OR current in a RPMC as the cell was warmed to 25°C, and the abrupt decrease in current amplitude and slope conductance following addition of 20 μM DIDS to the bath. In five similar experiments, 20μM DIDS reduced the mean OR conductance in RPMCs by 53 ± 28% from 1.7 ± 0.96 nS to 0.75 ± 0.53 nS (n=5). A similar effect was observed when RPMCs showing the OR conductance in mast cell Ringer were bathed in an extracellular solution containing 16.7 mM Cl^- (Figure 5.23), again indicating that the conductance was Cl^- selective. As in rat BMMCs, the expression of the OR_{Cl} current was variable and dependent on recording conditions. 10 out of 40 RPMCs (25%) showed the OR current between 25 - 37°C in contrast to

9 out of 55 cells (16%) recorded at room temperature. The slope conductance also increased with temperature from 1.15 ± 0.36 nS (n=9) to 1.51 ± 0.86 nS (n=10) although the difference did not reach statistical significance, probably due to small group sizes. The OR_{Cl} was also more commonly observed in RPMCs that had been incubated for ≥ 24 hours with 10 ng/ml SCF. From 55 RPMCs recorded at room temperature, 12 cells had been incubated with SCF; the OR_{Cl} was present in 5 cells from this subgroup (42%) in contrast to 4 out of the remaining 43 cells (9%). The mean OR conductance was higher in the SCF treated group (1.3 ± 0.4 nS vs. 0.96 ± 0.23 nS) but the difference was not statistically significant.

In accordance with previous reports (Lindau and Fernandez, 1986b; McCloskey and Qian, 1994), a K^+ selective inwardly rectifying current was not observed in RPMCs under these experimental conditions (see Figure 5.21), and in 3 cells bathed in high K^+ Ringer (50 mM), there was no change in conductance in the range -140 mV to -100 mV.

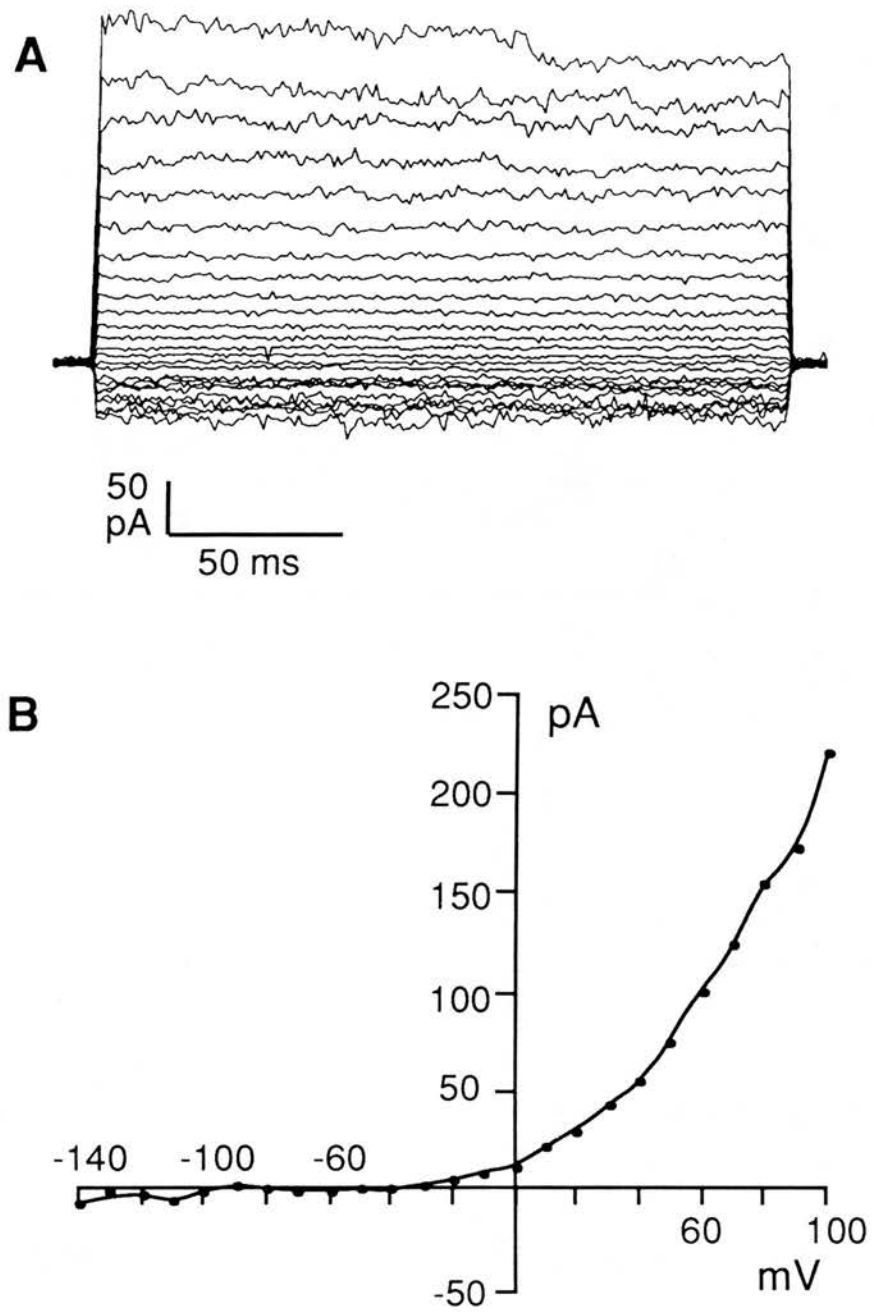

Figure 5.21 - **A**: Whole-cell membrane currents recorded from a rat peritoneal mast cell (RPMC) using the perforated-patch technique. **B**: The accompanying leak subtracted current-voltage relationship. The cell was clamped at a holding potential of -40 mV and voltage pulses of 200 ms duration were applied from -140 mV to +100 mV in 10 mV steps at 1 s intervals. The current is very similar to the OR_{Cl} current seen in rat BMMCs (see Figure 5.5), showing strong outward rectification, instantaneous activation, and time-dependent inactivation at potentials over 60 mV. The bath contained modified mast cell Ringer at 25°C.

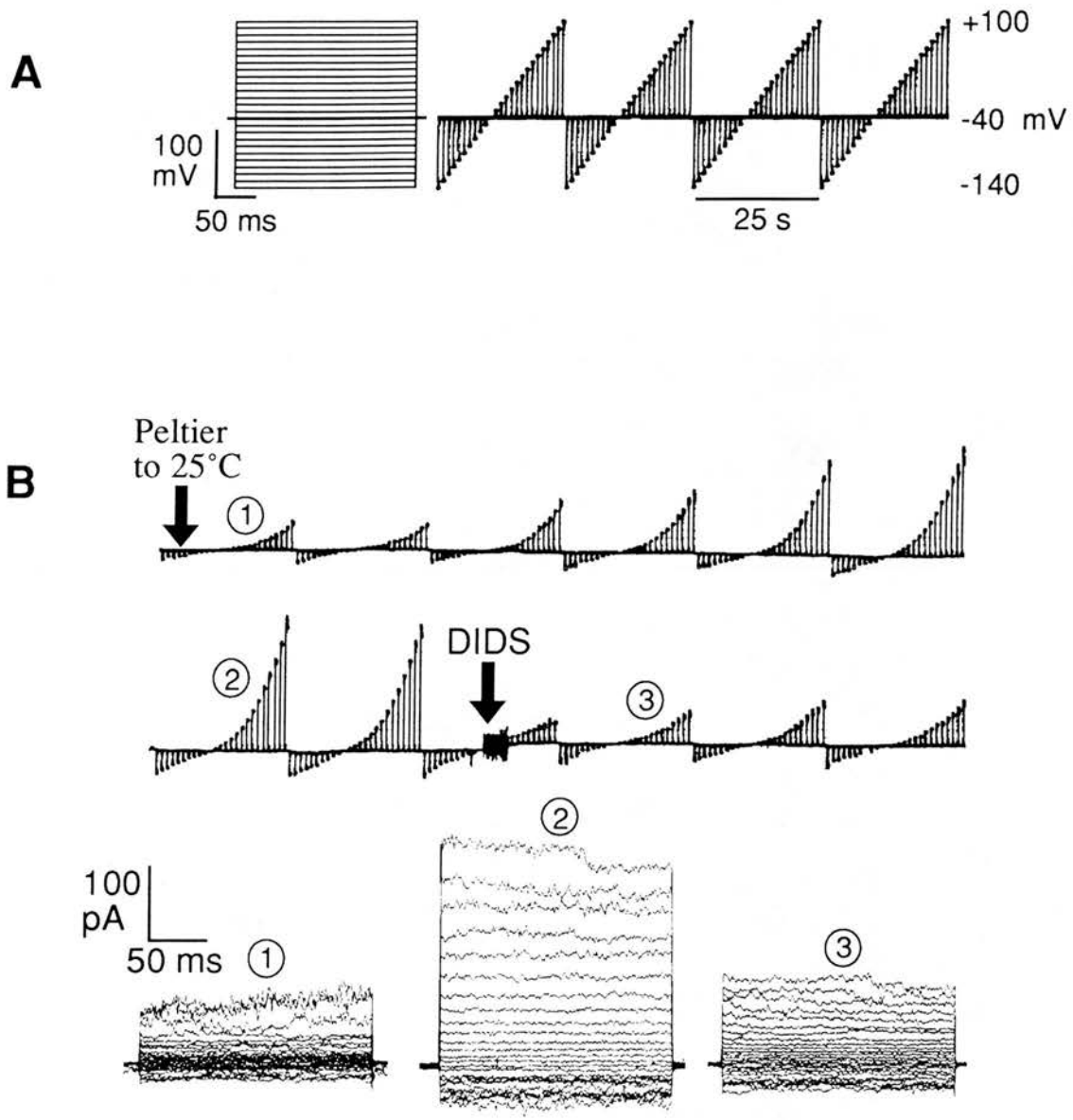

Figure 5.22 - Effect of temperature and DIDS on whole-cell membrane currents in rat peritoneal mast cells (RPMCs). **A**: The voltage step protocol. Cells were held at a holding potential of -40 mV and voltage pulses of 200 ms duration were applied from -140 mV to +100 mV in 10 mV steps at 1 s intervals. **B**: As the cell was warmed to 25°C (first arrow), an outwardly rectifying (OR) current developed between (1) and (2). The current exhibited slight time-dependent inactivation at potentials greater than +60 mV (2). At the second arrow, 20 μm DIDS was added to the bath resulting in a sudden diminution of the OR current (3). The bath contained modified mast cell Ringer and the pipette solution contained KCH_3SO_4.

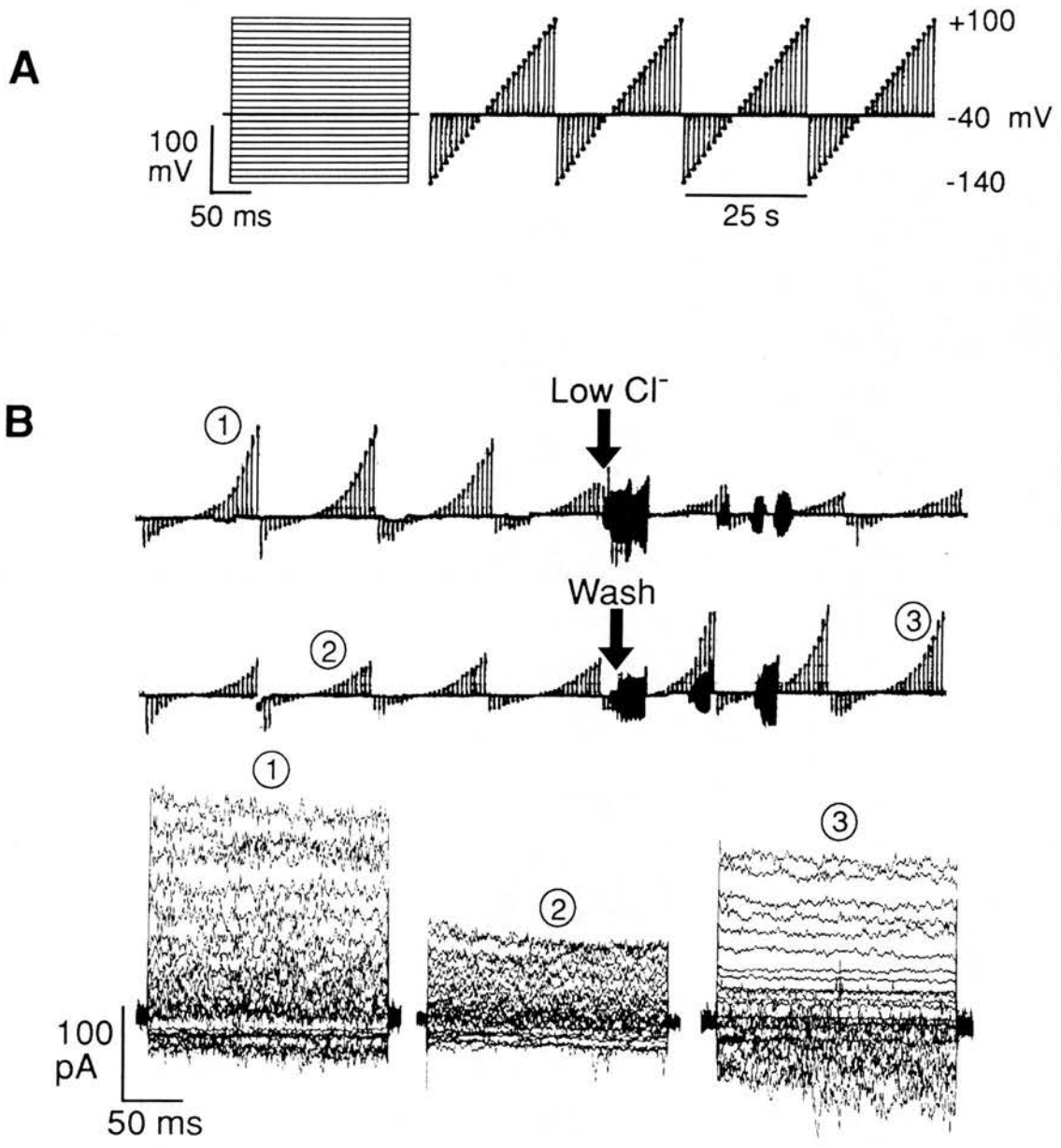

Figure 5.23 - Effect of extracellular Cl^- concentration on whole-cell membrane currents in rat peritoneal mast cells (RPMCs). **A**: The voltage step protocol. Cells were held at a holding potential of -40 mV and voltage pulses of 200 ms duration were applied from -140 mV to +100 mV in 10 mV steps at 1 s intervals. **B**: Whole cell currents in a RPMC after the mast cell Ringer (153.7 mM Cl^-) was exchanged for an extracellular solution containing Na-isethionate (16.7 mM Cl^-, first arrow). The OR current is markedly reduced between (1) and (2). At the second arrow, the bath was washed out with mast cell Ringer resulting in restoration of the current (3). Noise indicates the time taken for solution exchange. Pipette solution contained KCH_3SO_4.

5.11 - Effect of Osmolality on the Outwardly Rectifying Current

The OR_{Cl} conductance in rat BMMCs and RPMCs shares certain similarities with volume regulated Cl^- conductances in other cell types (Lewis *et al,* 1993; Nilius *et al,* 1994). In these cells, positive transmembrane osmotic pressure (intracellular osmolality > extracellular osmolality) induces the slow induction of a Cl^- conductance. Two possible sources of such an osmotic imbalance exist in perforated-patch recordings. First, a difference in Cl^- concentration between the pipette solution and cytoplasm can result in movement of Cl^- ions either into or out of the cell, accompanied by osmotically obliged water. Hence, with pipette solutions containing 137 mM KCl, as in many of the experiments described above, the pipette Cl^- concentration would be higher than that in the cytoplasm and Cl^- ions would diffuse into the cell, possibly resulting in cell swelling (Horn and Marty, 1988). However, when the KCl was replaced with KCH_3SO_4, the OR_{Cl} current was still observed in both rat BMMCs and RPMCs, suggesting that the current was not induced by movement of Cl^- and water from the pipette into the cell.

A second potential source of osmotic stress arises because cells subjected to perforated-patch recordings are very susceptible to small osmotic imbalances between the cytosol and bath (Axon guide, 1993). This occurs because the cell volume is not buffered by the large pipette volume as in conventional whole-cell recordings. Hence, a slight discrepancy in the osmolality of the cytoplasm (which is usually about 300 mOsm/Kg H_20) and the bath solution could result in movement of water into or out of the cell.

The osmolalities of the solutions used in these experiments are listed below (measured with an Advanced Wide-Range Osmometer 3WII, Advanced Instruments Inc., MA, USA):

KCl Pipette solution	243 mOsm/Kg H_2O
Amphotericin B pipette solution	265 mOsm/Kg H_2O
Mast Cell Ringer	291 mOsm/Kg H_2O
Low Cl^- Ringer (16.7 mM)	266 mOsm/Kg H_2O

The osmolalities of the above solutions provide some evidence that the OR_{Cl} currents in rat mast cells developed as a result of cell swelling. For example, the osmolality of the mast cell Ringer is slightly lower than that expected for the cytosol, so movement of water, if any, is likely to be into the cell. In contrast, the KCl pipette solution used for conventional whole-cell recordings has a lower osmolality than mast cell Ringer so water would tend to move out of the cell. Due to time constraints, a full evaluation of the effects of osmolality on the activity of the OR_{Cl} current was beyond the scope of these studies. However, in this section, a few preliminary experiments are described that address two questions. 1) Does a hypo-osmolar extracellular solution activate an outwardly rectifying Cl^- current in rat BMMCs and 2) is the current the same as that observed in perforated-patch experiments?

The first question was addressed by monitoring the current/voltage relationships of BMMCs with the conventional whole-cell recording technique as the mast cell Ringer was exchanged for mast cell Ringer diluted to 67% with distilled water. Under these conditions, water would tend to move into the cell resulting in swelling. In 4 out of 4 BMMCs at room temperature, an outwardly rectifying current was activated when the cell was bathed in 67% dilute Ringer, with a mean conductance of 1.8 ± 1.6 nS (Figure 5.24). Furthermore, the induced current could be inactivated either by returning the cell to an isosmotic environment (mast cell Ringer, Figure

5.24) or by replacing the 67% mast cell Ringer with a 67% low Cl^- Ringer (originally containing 16.7 mM Cl^-, Figure 5.25). The latter observation indicates that the induced current was predominantly carried by Cl^- ions.

The OR_{Cl} current recorded from a rat BMMC with the perforated-patch technique at 25°C was also susceptible to changes in extracellular osmolality. When the bath solution was replaced with mast cell Ringer containing 100 mM sucrose (real osmolality 401 mOsm/Kg H_2O), the current decreased in amplitude and the conductance decreased from 2.0 nS to 0.8 nS (Figure 5.26). Although these results represent preliminary observations, they suggest that the OR_{Cl} current in rat BMMCs may be activated by osmotic stress.

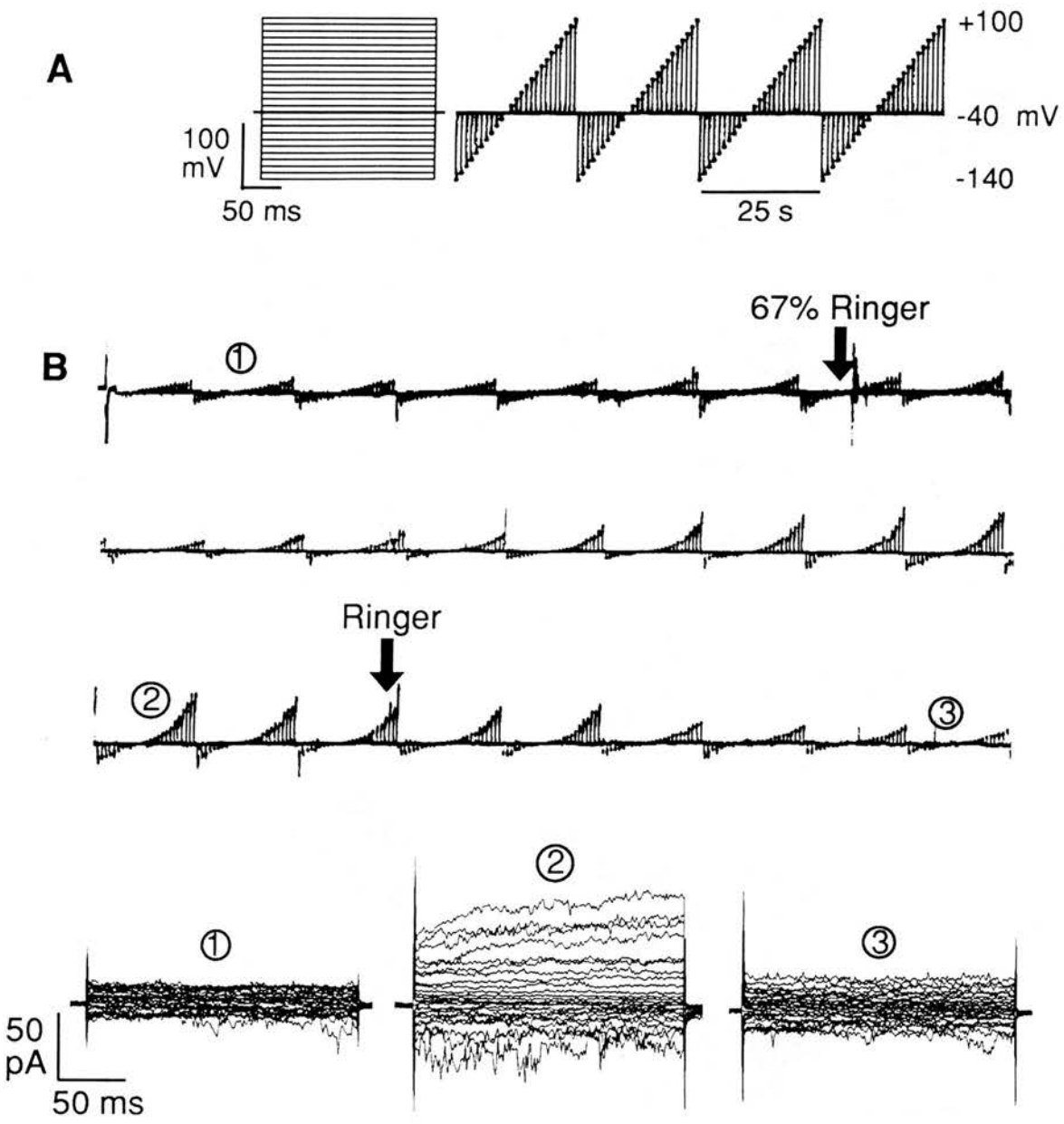

Figure 5.24 - Effect of osmolality on whole-cell membrane currents in rat BMMCs, measured with the conventional whole-cell recording configuration at room temperature. **A**: The voltage step protocol. Cells were held at a holding potential of -40 mV and voltage pulses of 200 ms duration were applied from -140 mV to +100 mV in 10 mV steps at 1 s intervals. **B**: Continuous pen recording of the whole-cell currents. At the first arrow, the extracellular solution was changed from mast cell Ringer to 67% mast cell Ringer, resulting in the development of an outwardly rectifying current (2). At the second arrow, the mast cell Ringer was replaced, causing a rapid inactivation of the current (3). The current tracing has been reduced in size for the purpose of the figure. The pipette solution contained KCH_3SO_4.

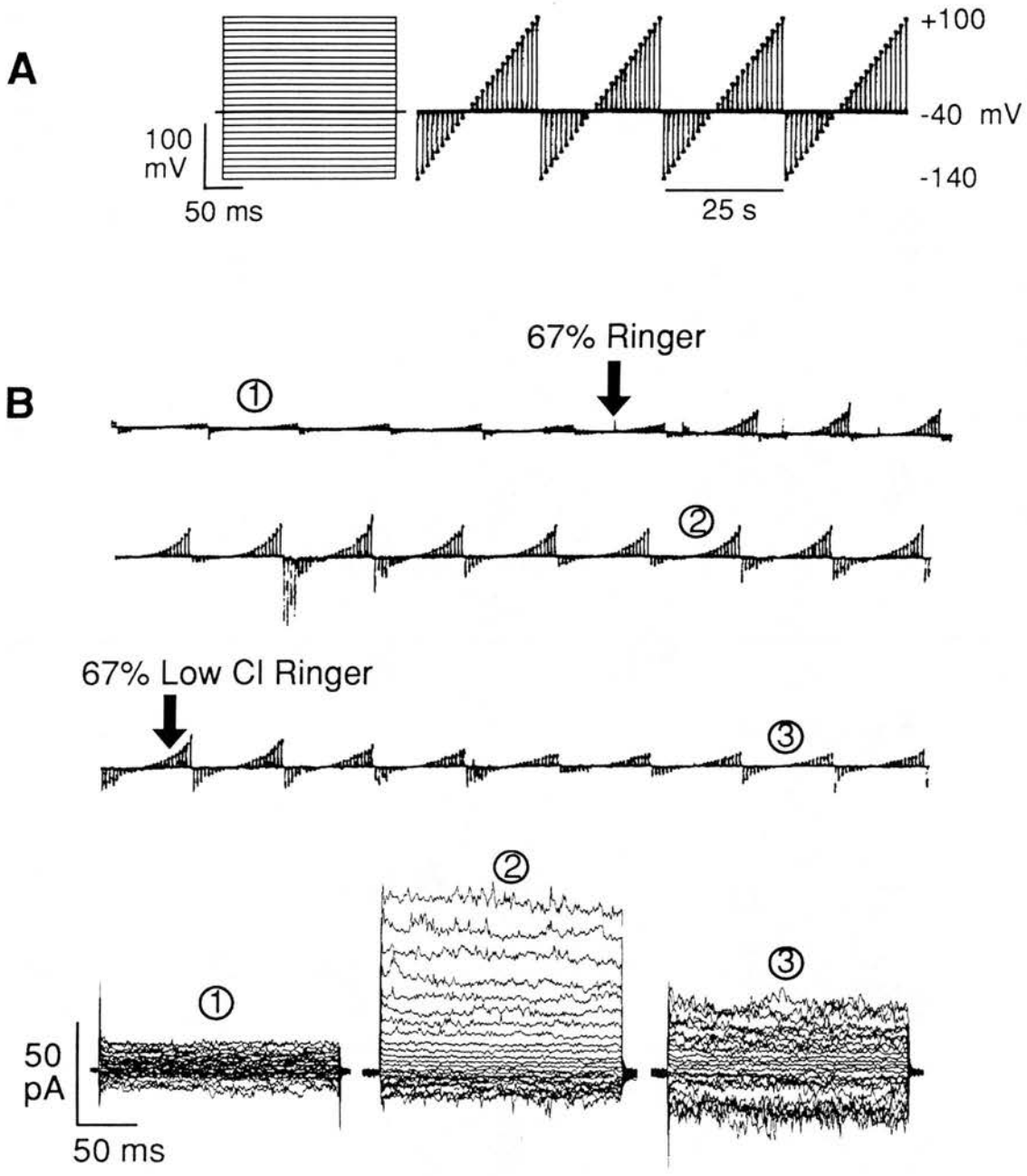

Figure 5.25 - Effect of osmolality on whole-cell membrane currents in rat BMMCs, measured with the conventional whole-cell recording configuration at room temperature. **A**: The voltage step protocol. Cells were held at a holding potential of -40 mV and voltage pulses of 200 ms duration were applied from -140 mV to +100 mV in 10 mV steps at 1 s intervals. **B**: Continuous pen recording of the whole-cell currents. At the first arrow, the extracellular solution was changed from mast cell Ringer to 67% mast cell Ringer, resulting in the development of an outwardly rectifying current (2). At the second arrow, the 67% Ringer was replaced with a 67% low Cl^- Ringer (originally containing 16.7 mM Cl^-), resulting in rapid inactivation of the current (3). The current tracing has been reduced in size for the purpose of the figure. The pipette solution contained KCH_3SO_4.

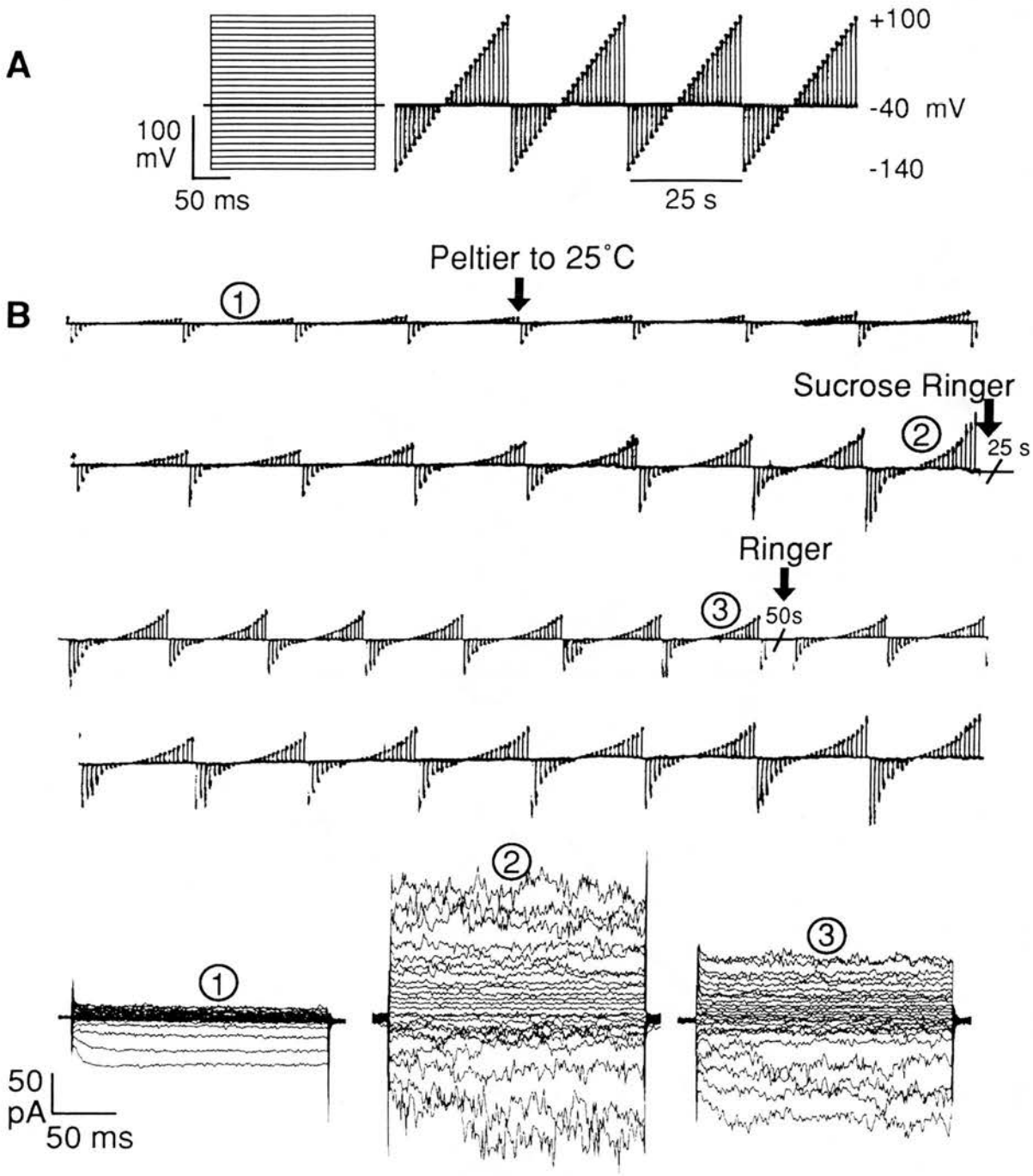

Figure 5.26 - Effect of osmolality on whole-cell membrane currents in a rat BMMC, measured with the perforated-patch technique. **A**: The voltage step protocol. Cells were held at a holding potential of -40 mV and voltage pulses of 200 ms duration were applied from -140 mV to +100 mV in 10 mV steps at 1 s intervals. **B**: Continuous pen recording of the whole-cell currents. At the first arrow, the bath was warmed to 25°C, resulting in development of an outwardly rectifying current between (1) and (2). At the second arrow, during a 25 s break in the tracing, the mast cell Ringer was replaced with mast cell Ringer containing 100 mM sucrose. The OR current amplitude and slope conductance were gradually reduced (3). At the third arrow, during a 50 s break in the tracing, the mast cell Ringer was replaced, resulting in gradual recovery of the current. The current tracing has been reduced in size for the purpose of the figure. The pipette solution contained KCH_3SO_4.

DISCUSSION

Membrane Potentials in rat BMMCs

In previous studies of RBL-2H3 cells, the resting membrane potential was about -90 mV and was set by the inwardly rectifying K^+ current at the K^+ reversal potential (Lindau and Fernandez, 1986b). In this study, the membrane potential of rat BMMCs, which also possessed an IR_K current, ranged from -62 mV to +4.5 mV with a mean and s.d. of -28.5 ± 16.5 mV. These values are very similar to those reported for mouse BMMCs (Kuno *et al,* 1995), but appear low compared to RBL-2H3 cells. A possible explanation for these apparently low values is that a non-specific leakage conductance (E_{rev} = 0 mV) at the pipette-membrane seal could partially depolarize the cell. This would be more likely in conditions of low extracellular K^+ when the IR conductance is small (Lindau and Fernandez, 1986b). However, in an intact cell, the true resting membrane potential would be determined by the K^+ reversal potential. The lack of a detectable IR_K in RPMCs explains why the resting potential of these cells is close to 0 mV (Lindau and Fernandez, 1986b), but whether this accurately reflects the situation *in vivo* remains to be determined.

Heterogeneity of ion channel expression in rat mast cells

In the mouse BMMC system, the presence or absence of IR_K and OR_{Cl} currents in individual mast cells was interpreted as heterogeneity of ion channel expression i.e. some cells had IR_K channels, others had OR_{Cl} channels, some cells had both channels and others had none (Kuno *et al,* 1995). This interpretation was based on the observation that mouse BMMCs have the potential to differentiate into different mast cell phenotypes depending on the microenvironments in which they reside (Nakano *et al,* 1985). Hence, individual mast cells within the mouse BMMC population could have different functional characteristics as reflected by the variation in ion channel expression. However, rat BMMCs appear to be committed mucosal mast cells and, unlike mouse BMMCs, do not differentiate to the connective tissue phenotype when

exposed to fibroblasts or stem cell factor (MacDonald *et al,* 1996). Therefore, although variation was found in the presence of the two currents in rat BMMC populations, it is unlikely to be due to phenotypic heterogeneity of ion-channel expression. It is more likely that a normal rat BMMC possesses the ion-channels for both the IR_K and OR_{Cl} currents, and that the heterogeneous distribution of current patterns within the population results from extrinsic factors (i.e. experimental conditions) rather than intrinsic factors (i.e. restricted expression of ion channels). This is highlighted in Table 5.6 which shows the variation in expression of the OR_{Cl} conductance in BMMCs under different conditions. Likewise, the inwardly rectifying current was not seen in some cells in mast cell Ringer, but when the extracellular K^+ concentration was raised, it was present in all cells tested. In both cases, the lack of a detectable current did not reflect the lack of the appropriate ion channel. However, although the OR_{Cl} current was demonstrated in both BMMCs and RPMCs, the IR_K current was only detectable in BMMCs. This may reflect true heterogeneity between the cell phenotypes as rat BMMCs and RPMCs have distinct biochemical and functional characteristics. However, the possibility still remains that the lack of the IR_K current may be an artifact of the isolation procedure, similar to that affecting IgE responses in freshly isolated RPMCs (Taylor *et al,* 1996). RPMCs undergo apoptosis on removal from the abdominal cavity, unless stimulated with the appropriate growth factors (Galli *et al,* 1994; Horigome *et al,* 1994), and the apparent influence of the cytokine SCF on the expression of the OR_{Cl} current lends support to this hypothesis.

Activity of the OR_{Cl} Current in rat BMMCs

In contrast to previous studies (Lindau and Fernandez, 1986b; McCloskey and Qian, 1994; Qian and McCloskey, 1993), this study showed that rat BMMCs possessed an outwardly rectifying chloride conductance (OR_{Cl}) in addition to the previously described K^+ selective inwardly rectifying (IR_K) current. This apparent discrepancy, which has important physiological significance, can be explained by three different

hypotheses. First, the results may reflect variations in mucosal mast cell phenotypes. The BMMCs in this study were grown in lymph node conditioned medium which contains T-cell-derived cytokines in addition to concanavalin A. These additional factors could be necessary for expression of the outwardly rectifying chloride channel which was not observed in either RBL-2H3 cells or mast cells grown in the presence of IL-3 alone. However, this explanation seems unlikely because the OR_{Cl} current was also present in RPMCs (an example of the connective tissue phenotype) and these cells were not exposed to the above factors.

A second possibility for the above discrepancy is the apparent dependency of the OR_{Cl} conductance on temperature and the maintenance of cytoplasmic integrity. With the conventional whole-cell recording technique at room temperature (as used in previous studies) only 3/44 BMMCs showed an OR_{Cl} current. However, when the integrity of the cell's cytoplasm was preserved using the perforated patch-technique, the OR_{Cl} current was readily demonstrable both in BMMCs and RPMCs. In addition, increasing the bath temperature towards physiological values increased the proportion of cells that possessed the OR_{Cl} current, although the conductances were lower with the conventional whole-cell technique. These findings suggest that the OR_{Cl} current may be dependent on an essential intracellular component that is leached out of the cell during conventional voltage-clamp recordings. The increased expression of the OR_{Cl} current when ATP and GTP were included in the pipette solution in conventional whole-cell recordings lends support to this hypothesis. The OR_{Cl} conductance observed in these experiments is also similar to that induced in RPMCs when c-AMP is included in the pipette solution (Penner *et al,* 1988; Dietrich and Lindau, 1994). For example, the time course for development of the OR_{Cl} current in RPMCs following "break-in" is similar to that following warming of BMMCs or RPMCs; the shape of the I/V curve is similar in both cases; and both currents are blocked by 20μM DIDS. In previous studies of RPMCs (Penner *et al,* 1988), it was concluded that *in vivo* a rise in intracellular c-AMP following

stimulation of the cells with secretagogues or antigen was responsible for activation of the OR_{Cl} current. In this study, neither secretagogues nor exogenous second messengers were required to elicit the current. This suggests that if c-AMP is the "missing" cytosolic factor in conventional whole cell recordings, then only basal levels of the messenger are required to support the OR_{Cl} conductance.

The third possibility for the discrepancy in results is the influence of osmolality on the OR_{Cl} current. In this study, an OR_{Cl} current was activated in BMMCs by placing the cell in a hyposmotic environment, and inactivated by returning the cell to isosmotic or hyperosmotic solutions. This effect could also explain the results of the perforated-patch recordings in which small osmotic imbalances between cytosol and bath could lead to activation of volume regulated Cl^- channels. The significance of these findings is discussed below.

In summary, it seems likely that the OR_{Cl} current in rat BMMCs is dependent on temperature, a cytoplasmic component and/or differences in transmembrane osmolality.

Physiological relevance of the OR_{Cl} current in rat mast cells

Based on previous studies and the data presented above, two theories have emerged to account for the function of the OR_{Cl} current in rat mast cells: the Cl^- potential clamp hypothesis, and the volume regulation hypothesis. The first hypothesis originated in studies of RPMCs (Matthews *et al,* 1989a; Penner *et al,* 1988). In these studies, it was suggested that activation of the OR_{Cl} current by agonists would shift the membrane potential of the cell to the Cl^- reversal potential, assumed to be about -30 to -40 mV. The membrane potential would then be "clamped" at a sufficiently negative value to support Ca^{2+} influx during degranulation. Support for this hypothesis is provided by studies of RBL-2H3 cells using potential sensitive indicators such as *bis*-oxonal (Mohr and Fewtrell, 1987b; Mohr and Fewtrell, 1987a;

Labrecque *et al,* 1989), and the lipophilic [^{3}H] tetraphenylphosphonium cation (Kanner and Metzger, 1983; Sagi-Eisenberg and Pecht, 1983). Following stimulation of the IgE receptor with antigen, RBL-2H3 cells were depolarised within 2 - 3 minutes (Kanner and Metzger, 1983; Sagi-Eisenberg and Pecht, 1983; Mohr and Fewtrell, 1987a). However, over the subsequent 5 minutes there was a partial repolarization towards the resting membrane potential (Mohr and Fewtrell, 1987a; Labrecque *et al,* 1989). This repolarization could be mediated by the FcεR1 receptor-activated Cl^- current in RBL-2H3 cells (Romanin *et al,* 1991) in a similar way to that proposed for RPMCs. Further evidence for the Cl^- potential clamp hypothesis is provided by the observations that persistent depolarization (Mohr and Fewtrell, 1987b) and Cl^- channel blockade (Romanin *et al,* 1991) in RBL-2H3 cells inhibited Ca^{2+} influx and exocytosis. In addition, studies of rat peritoneal mast cells showed that Cl^- uptake was required for optimum histamine release (Glenert *et al,* 1993). The I/V curves obtained from rat BMMCs indicate that the OR_{Cl} current was activated when the cell was depolarized to potentials more positive than -30mV. If this occurred during degranulation of BMMCs, then the OR_{Cl} current would tend to repolarize the cell as described above.

Despite the evidence for the role of the OR_{Cl} current in voltage control of the cell during degranulation, some problems persist with this interpretation. The activation of the current in RPMCs by agonists such as compound 48/80 or substance P is slower than the kinetics of secretion in these cells. Also, the Cl^- channel in RPMCs can be effectively blocked by DIDS at concentrations that do not inhibit exocytosis, except at the lowest concentrations of secretagogue (Dietrich and Lindau, 1994). These observations suggest that the Cl^- current is not essential for stimulation of exocytosis, but may enhance secretion following sub-optimal stimulation with secretagogues. There is also evidence that the repolarization of RBL-2H3 cells that occurs during degranulation is mediated by an efflux of K^+ ions from the cell (Labrecque *et al,* 1989; Labrecque *et al,* 1991). The outwardly rectifying K^+ current

described by Qian and McCloskey (1993) offers a potential mechanism for this pathway.

The above discussion centres on the role of the OR_{Cl} current during degranulation. In previous studies, the current was activated by agonists and second messengers known to initiate secretion. However, the results of this study indicate that the OR_{Cl} current can be active in both rat BMMCs and RPMCs without stimulation with intracellular or extracellular agonists, and not undergoing degranulation. This detachment from the process of exocytosis suggests that the current may have an alternative, or additional, role to that proposed above. If the current was constitutively active in normal resting cells it would contribute to the resting membrane potential of the cell, as suggested in mouse BMMCs (Kuno *et al,* 1995). The results using the perforated-patch technique at temperatures > 25°C initially appear to support a constitutively active OR_{Cl} current. However, this technique could result in the activation of volume-regulated Cl^- currents as described earlier. Hence, a second hypothesis for the function of OR_{Cl} currents in rat BMMCs is a role in volume regulation.

The OR_{Cl} conductance in rat mast cells shares similar properties to volume regulated Cl^- conductances in a number of other cell types including RBL-2H3 cells (Nilius *et al,* 1994), fibroblasts (Nilius *et al,* 1994), T lymphocytes (Lewis *et al,* 1993), osteoblasts (Gosling *et al,* 1995), neutrophils (Stoddard *et al,* 1993), hepatocytes (Meng and Weinman, 1995), and aortic endothelial cells (Nilius *et al,* 1994). The Cl^- conductances in these cells are thought to be involved in regulatory volume decrease if the cells encounter a hyposmotic environment (Stoddard *et al,* 1993), and although they have broadly similar properties, including outward rectification, there is a degree of variation between cell types. For example, in mouse fibroblasts, the volume-regulatory OR_{Cl} channel passes a large inward current at negative voltages (Nilius *et al,* 1994). In contrast, there was virtually no activation of current at

negative voltages in RBL-2H3 cells (Ra *et al,* 1989). The latter observation is in agreement with the findings reported here for the OR_{Cl} current in rat BMMCs. The possibility of volume regulated Cl^- channels in RPMCs was raised by Dietrich and Lindau (1994), but this was based on the similarity of the current to Cl^- currents in lymphocytes (Lewis *et al,* 1993) and no experimental evidence was provided. Other investigators concluded that the c-AMP activated Cl^- current in RPMCs was not dependent on changes in cell volume and did not, therefore, play a role in volume control (Matthews *et al,* 1989a). The results of this study showing the effects of changes in transmembrane osmotic pressure on the OR_{Cl} current provide the first direct evidence for the presence of volume regulatory Cl^- channels in rat BMMCs.

In summary, rat BMMCs possessed an outwardly rectifying Cl^- conductance in addition to the previously described K^+-selective inwardly rectifying current. The current was dependent on temperature and the maintenance of cytoplasmic integrity, and could be activated by a reduction in extracellular osmolality. A similar current was observed in RPMCs in the absence of external agonists or intracellularly applied second messengers. The true physiological role of chloride channels in mast cells awaits further clarification. However, based on these studies, and those previously reported, two hypotheses remain for the type of Cl^- channels that are present in mast cells. First, two types of Cl^- channel may be present in mast cells: a volume regulatory channel and an agonist-activated channel; and second, a single type of Cl^- channel may be present in mast cells, but it can be activated in a variety of ways, including by agonists, second messengers and changes in osmolality. The significance of these hypotheses, and the importance of future work in this area, is discussed in chapter 6.

Chapter 6

GENERAL DISCUSSION

The involvement of mast cells in the pathogenesis of allergic diseases has prompted extensive investigations into their origin, biochemistry and function (reviewed in Chapter 1). The realisation that rodents and humans possess at least two phenotypes of mast cell has generated widespread interest in the possibility of differing roles for these cells *in vivo*. Further characterisation of mucosal and connective tissue-type mast cells *in vitro* has demonstrated that, at least in rodents, the cells have distinct functional properties, including the response to cytokines, secretagogues and anti-allergic drugs.

The participation of the mucosal mast cell (MMC) phenotype in the inflammatory response against intestinal helminths is demonstrated by the prominence of these cells in parasite-infested mucosal tissue, and the finding that MMCs are functionally active during expulsion of experimental nematode infestations in laboratory rodents and sheep (reviewed in Miller, 1993b). These observations, suggestive of a direct protective role for MMCs in the intestinal tract, have prompted studies to further characterise the properties of these cells in the rat both *in vivo* (Moqbel *et al,* 1986; MacDonald, 1994; Scudamore *et al,* 1995a) and *in vitro* (Befus *et al,* 1982; Pearce *et al,* 1982).

The development of techniques to culture rat bone marrow-derived mast cells (BMMCs), which are morphologically, biochemically and functionally identical to rat intestinal MMCs (Haig *et al,* 1982), has provided an opportunity for more widespread study of the mucosal mast cell phenotype (MacDonald *et al,* 1989; MacDonald, 1994; MacDonald *et al,* 1996). Studies of the IgE-dependent release of the MMC- and BMMC-specific granule chymase, rat mast cell protease-II (RMCP-

II), from BMMCs are particularly relevant because this protease may be directly involved in the process of worm expulsion (Miller *et al,* 1983; Woodbury *et al,* 1984), through its capacity to promote epithelial permeability (Scudamore *et al,* 1995b).

In this study, the release of RMCP-II from individual BMMCs was detected using a novel ELISPOT assay (Chapter 3). Within a population of BMMCs, only 6 - 24% of the cells responded to IgE-dependent stimulation, even after sensitisation with exogenous IgE. This novel finding may represent a key regulatory mechanism, with the IgE receptor providing a trigger for degranulation, but a number of other factors determining the final response of individual mast cells. The experiments described in Chapter 4 identified the cytokine, stem cell factor (SCF), as one of these factors. SCF enhanced total IgE-dependent mediator release from populations of mature BMMCs, and, in a similar percentage increase, the proportion of cells that responded to stimulation. These results suggested that SCF augmented mediator release from rat BMMCs by primarily activating previously unresponsive cells. Interestingly, this effect was not observed in BMMCs derived from immature cultures. Therefore, when taken with the pre-existing data describing the effects of SCF on mucosal mast cell development (reviewed in Chapter 1), these results allow a model to be proposed for the role of SCF in the modulation of gastro-intestinal immune responses *in vivo*.

<u>A simplified scheme outlining the potential role of SCF in gastrointestinal mast cell responses (based on collective data from a variety of species)</u>

1) Infection with intestinal helminths leads to cytokine production (IL-3, IL-4, IL-9, IL10) by activated T_{H2}-type cells (Mosmann *et al,* 1991). These cytokines, and probably SCF (Newlands *et al,* 1995), signal the differentiation of mucosal mast cells from bone marrow-derived progenitors (Haig *et al,* 1988; Schmitt *et al,* 1987; Moeller *et al,* 1989; Thompson-Snipes *et al,* 1991; Haig *et al,* 1994).

2) The committed mast cell precursors circulate through the bloodstream (Kitamura *et al,* 1979; Rodewald *et al,* 1996) and "home" to the gastro-intestinal tract, possibly using SCF/*c-kit* interactions (Adachi *et al,* 1992; Kinashi and Springer, 1994) and/or surface integrins (Smith and Weis, 1996) as adhesion molecules.

3) The committed precursors complete their proliferation and differentiation into mature mucosal mast cells under the continued influence of T-cell-derived cytokines and SCF (either membrane bound or soluble forms).

4) Production of IL-4 by T_{H2} cells (Mosmann *et al,* 1991) and mast cells (Plaut *et al,* 1989) induces immunoglobulin class switching of B cells from IgM to IgE (Devries *et al,* 1993). The parasite-specific IgE binds to high-affinity IgE receptors on the surface of intestinal mucosal mast cells (similar to the binding to BMMCs of lymph node conditioned medium-derived IgE - Chapter 3).

5) On reaching maturity, the mucosal mast cells are "primed" by membrane bound or soluble SCF (and possibly other factors), increasing the probability that they will degranulate in response to aggregation of the surface IgE receptors by specific antigen (Chapter 4). An interesting possibility is that the expression of SCF on the surface of fibroblasts, or the levels of soluble SCF in the local tissue microenvironment, could also be under the control of cytokines, although this awaits further study. However, this would provide a mechanism for controlling the "releasability" of the intestinal mast cell population, with an upregulation of SCF expression leading to activation of previously quiescent cells, and enhanced mediator release following IgE-dependent stimulation (Chapter 4).

Although the above scheme is speculative and based mainly on data from *in vitro* studies from a variety of species, it provides a framework for understanding the possible roles of SCF *in vivo*. In addition, the mechanisms described may also be involved in the pathogenesis of allergic reponses. Hence, an exciting possibility for future studies is the development of ELISPOT assays to detect proteases from other mast cells types in other species. For example, detection of tryptase release from

individual human mast cells could be used as an *in vitro* model of allergic reactions. The advantage of this method over conventional mediator release assays is that statistically quantifiable results can be obtained with as few as 5000 mast cells per assay. Hence, a tryptase ELISPOT assay could be used to investigate the function of mast cells derived from clinical material such as broncho-alveolar lavage fluid or skin biopsies. The latter approach would also be extremely valuable in species of veterinary importance in which it is difficult to obtain large numbers of purified mast cells. For example, future studies are planned to develop an ELISPOT assay to detect the release of tryptase from canine mast cells. Such an assay would be useful for investigating mast cell responses in canine atopic dermatitis, including the response to various secretagogues, cytokines and anti-allergic drugs.

The release of mediators from mast cells also depends on the activation of ionic conductances (reviewed in Chapter 1). A critical (and probably the most important) signal for degranulation is the rise in intracellular Ca^{2+} following activation of the Ca^{2+} influx pathways (Penner *et al,* 1988; Zhang and McCloskey, 1995). Although not investigated in this study, these pathways have been demonstrated in rat peritoneal mast cells (Matthews *et al,* 1989b), RBL-2H3 cells (Zhang and McCloskey, 1995) and human basophils (MacGlashan and Botana, 1993) using a combination of patch-clamp and Fura-2 fluorescence techniques. Similar studies in the future might identify these pathways in rat BMMCs.

The electrophysiological properties of resting rat BMMCs were described in Chapter 5. As described in previous studies of RBL-2H3 cells (Lindau and Fernandez, 1986b) and IL-3-derived BMMCs (McCloskey and Qian, 1994), rat BMMCs possessed an inwardly rectifying (IR) K^+ current that is probably involved in setting the resting membrane potential. However, in contrast to the latter studies, rat BMMCs possessed an outwardly rectifying (OR) Cl^- current. The dependency of the current on temperature and the maintenance of cytoplasmic integrity suggested that

an intracellular messenger might be required for its activity. In addition, the effects of changes in extracellular osmolality suggested that the OR_{Cl} current in rat BMMCs was involved in volume regulation, as described for the similar outwardly rectifying Cl^- currents in RBL-2H3 cells and a number of other cell types (Nilius *et al,* 1994). Hence, one model for the proposed function of the current *in vivo* is shown below.

A scheme outlining the proposed role of the OR_{Cl} current in volume regulation

1) Conditions of extracellular hypotonicity would lead to an influx of water into the mast cell, resulting in cell swelling. Such conditions might arise following mast cell activation in the tissues, resulting in sites of inflammation or oedema.

2) Cell swelling leads to activation of the OR_{Cl} current (Chapter 5). If the resting membrane potential of the cell was more negative than the chloride reversal potential, Cl^- ions would move out of the cell carrying an inward current until the cell was depolarised to the Cl^- reversal potential. In some cells, this depolarisation activates voltage-dependent K^+ channels leading to a concurrent efflux of K^+ ions (Stoddard *et al,* 1993), although such currents were not observed in rat BMMCs.

3) The movement of Cl^- ions out of the cell along with osmotically obliged water reduces the cell volume to its original size (regulatory volume decrease), resulting in inactivation of the OR_{Cl} current.

Despite the evidence for the effect of osmolality on the OR_{Cl} current in rat BMMCs, a number of problems persist with the above interpretation. First, in rat BMMCs (Chapter 5) and RBL-2H3 cells (Nilius *et al,* 1994), the OR_{Cl} current does not appear to pass appreciable amounts of inward current at potential more negative than the Cl^- reversal potential. However, passage of only small currents may be sufficient to initiate regulatory volume decrease. Second, the activation of concurrent K^+ conductance pathways has not been demonstrated in rat mast cells. And third, an OR_{Cl} current with similar properties has been described in rat peritoneal mast cells following stimulation with compound 48/80, substance P, or intracellularly applied

messengers such as c-AMP or GTP-γ-S (Matthews *et al,* 1989a; Dietrich and Lindau, 1994; Janiszewski *et al,* 1994). A completely different function was proposed for the latter current as described below.

A scheme outlining the proposed role of the OR_{Cl} current in voltage control during degranulation

1) Stimulation of the cell with antigen or external ligands generates G-proteins, IP_3 and c-AMP (Gomperts, 1983; Sagi-Eisenberg, 1993; Penner *et al,* 1988).

2) The Ca^{2+} influx pathways are activated resulting in a rise in intracellular Ca^{2+} (Matthews *et al,* 1989b; Zhang and McCloskey, 1995), the onset of degranulation (Crews *et al,* 1981), and depolarization of the membrane potential to beyond the Cl^- reversal potential (Kanner and Metzger, 1983; Mohr and Fewtrell, 1987a).

3) Persistent depolarization would decrease Ca^{2+} entry and inhibit exocytosis (Mohr and Fewtrell, 1987b). However, the generation of c-AMP and GTP-γ-S also activates the OR_{Cl} current (Matthews *et al,* 1989a). At potentials more positive than the Cl^- reversal potential, Cl^- ions move into the cell carrying an outward current. This shifts the membrane potential towards the Cl^- reversal potential, thus maintaining the hyperpolarization-driven Ca^{2+} influx.

Although some of the data in the above scheme was obtained from RBL-2H3 cells, there is no direct evidence, as yet, that the above mechanisms operate in rat BMMCs. Furthermore, in this study, the OR_{Cl} current was observed in both resting peritoneal mast cells and BMMCs which were not stimulated with extracellular ligands or intracellular messengers (Chapter 5). Hence, key questions remain concerning the role of OR_{Cl} currents in different mast cell types. Is there more than one type of Cl^- channel present in mast cells, each with a different function, or one type with multiple functions? Can the channels be activated in a variety of ways, including by messengers or changes in osmolality? Are the channels important in voltage control during degranulation? Due to time constraints, these questions could not be

addressed fully in this study. However, future studies are planned to determine more precisely the nature and function of Cl^- channels in rat mast cells. These studies would involve a direct comparison of Cl^- currents in both rat peritoneal mast cells and BMMCs and would include: activation of the currents by secretagogues and intracellular messengers such as c-AMP, ATP, GTP-γ-S and Ca^{2+}; effects of changing osmolality on the OR_{Cl} current in both cell types; analysis of the Cl^- channel permeability to other anions such as SCN^-, NO_3^-, I^-, Br^-, SO_4^{2-}, and glucuronate$^-$; analysis of Cl^- channel pharmacology by testing various blockers such as DIDS, NPPB, dideoxyforskolin, tamoxifen, verapamil, and quinine; determination of the single channel conductance by noise analysis; and analysis of the effect of extracellular Cl^- concentration on secretion. Comparative studies such as these could determine the true role of Cl^- channels in mast cells. This is a critical question because a proven role for the OR_{Cl} current in the process of degranulation may provide a basis for the future development of Cl^- channel blockers as anti-allergic drugs.

In conclusion, this study has contributed to our understanding of the function of rat BMMCs, and suggested factors that may be involved in the immunological and electrophysiological regulation of intestinal mucosal mast cell function *in vivo*. It is hoped that these findings can be extended in future studies of other mast cell types to further define the regulation of these cells in physiological and pathological processes. Such studies might lead to novel pharmacological approaches to control mast cell degranulation in allergic reactions.

APPENDIX 1

Preparation of Solutions, Buffers and Substrates

Phosphate-buffered saline (PBS)
8 g NaCl
0.2 g KCl
1.15 g Na_2HPO_4
0.2 g KH_2PO_4

Dissolve in 1 litre de-ionised, distilled water and adjust pH to 7.2 - 7.3.

Serumless IMDM
Add the following reagents to a 500ml bottle of IMDM

500 units penicillin
500 µg streptomycin
50 µl 2-mercaptoethanol
714 µl sterile 35% stock solution of BSA (Sigma)
0.5 ml sterile stock solution of human transferrin (Sigma) - 25 mg/ml
50 µl sterile palmitic acid (Sigma) - 10 mg/ml in 100% ethanol)
50 µl sterile oleic acid (Sigma) - 10 mg/ml in 50% ethanol in sterile distilled water
5 µl sterile linoleic acid (Sigma) - 10 mg/ml in sterile PBS

β-hexosaminidase buffers
A: Substrate buffer - 0.15 M disodium citrate buffer, pH 4.5
7.9 g citric acid
75 ml 1 N NaOH

Dissolve citric acid and make up to 250 ml with de-ionised, distilled water. Adjust pH to 4.5 with 1 M HCl

B: Stop buffer - 0.2 M glycine-NaOH buffer, pH 10.7
1. 1.88 g glycine + 1.45 g NaCl, dissolved in 125 ml de-ionised, distilled water.
2. 0.4 g NaOH, dissolved in 50 ml de-ionised, distilled water.

To 6.6 ml of (1), add approximately 5.8 ml of (2) until pH reaches 10.7. Keep at 4°C prior to use.

RMCP-II ELISA coating buffer
1.59 g Na_2CO_3
2.93 g $NaHCO_3$

Dissolve in de-ionised, distilled water and make up to 1 litre. Adjust pH to 9.6 (if necessary). Use for dissolving primary antibody and coating plate.

RMCP-II ELISPOT buffer and substrate

A: To Prepare Stock AMP solution (2-amino-2-methyl-1-propanol) :-

1. For 500ml dissolve 35.15mg $MgCl_2$ and 50µl Triton-X-405 in a small volume of distilled water.
2. Add 47.9ml AMP (Sigma) and mix well.
3. Add distilled water to 90% (450ml). Adjust pH to 10.25 with concentrated HCl.
4. Leave overnight at room temperature and readjust pH. Make up volume with de-ionised, distilled water and store at 4°C.

B: To Prepare Gel Substrate :-

5. Prepare a 3% w/v solution of agarose (Type 1, Sigma) in distilled water and dissolve by boiling.
6. Make up BCIP (5-bromo-4-chloro-3-indoyl phosphate, Sigma) in stock AMP solution. Weigh out 12.5mg BCIP and dissolve in 200µl dimethylformamide (wear gloves and perform in fume cupboard).
7. Add 12.5 ml stock AMP. Warm solution to 40°C . Keep agarose melted by holding at 60°C.
8. Add 3 ml agarose to substrate solution to give final dilution of ≈ 0.6% w/v.

COSHH warning - see risk assessments for AMP, dimethylformamide and BCIP.

APPENDIX 2

The Effect of Iscove's Modified Dulbecco's Medium on the Survivability of Rat Peritoneal Mast Cells

Introduction

The purification of rat peritoneal mast cells using Percoll density step gradients was a simple and reliable method for isolating virtually pure populations of mast cells (see chapter 2, section 2.11). For the studies described in chapter 5, purified peritoneal mast cells were used on the day of collection, as well as after 1 - 2 days in culture in the presence or absence of stem cell factor (SCF). However, all initial attempts to maintain peritoneal mast cells in culture (either with or without SCF) ended in failure. Typically, after 24 - 48 hours, the entire population of cells had a "ghost-like" appearence with no distinct cellular outlines, and this was interpreted as cell death. This appendix describes a series of experiments that were performed to investigate this problem. The results indicate that the cytotoxicity was caused by the use of Iscove's Modified Dulbeccos Medium (IMDM) to wash and culture the cells.

Experiment 1 - Effect of SCF concentration on peritoneal mast cell survival

Peritoneal mast cells were purified as described in chapter 2 and resuspended in 10 ml of IMDM/20%HS/PS (standard medium for culturing rat BMMCs). The cells were washed twice and resuspended in 12 ml of the above medium. 1 ml aliquots of the cell suspension containing 1.5 x 10^4 mast cells were added to each well of a 12 well tissue culture plate (Costar, Cambridge, MA, USA), and incubated for 24 hours with 400, 200, 100, 50, 25, 12.5, 6.25, 3.125, 1.56, 0.8, 0.4 or 0 ng/ml SCF.
Results - After 24 hours, all the cells in all wells appeared to be dead.

Experiment 2 - Effect of cell density on the survival of rat peritoneal mast cells

Percoll purified peritoneal mast cells were added to cell culture wells in triplicate at densities of $5x10^5$, $5x10^4$, $5x10^3$ or $5x10^2$ cells/ml in IMDM/20%HS/PS, and incubated for 48 hours with 100, 10 or 0 ng/ml SCF.
Results - Most of the cells were dead after 24 hours incubation, and all the cells were dead after 48 hours.

Experiment 3 - Comparison of Percoll from two different sources

To investigate the effect of different batches of Percoll, peritoneal cells from the same rat were purified with either a batch of Percoll previously used successfully at the Moredun Research Institute, UK, or with a batch used for these studies. 1 ml aliquots of cell suspensions from both purifications containing 1.8 x 10^4 mast cells were added to wells and incubated for 48 hours with 200, 100, 50, 25, 12.5 or 0 ng/ml SCF.
Results - All cells from both groups were dead after 48 hours.

Experiment 4 - Use of a different Percoll purification method

To determine if the cells were being damaged during centrifugation in the Percoll gradient, an alternative protocol was tried which prevents the cells from pelleting on the base of the tube. Peritoneal lavage cells were layered on top of 10 ml of isotonic Percoll and centrifuged at 35,000 g for 20 mins. The mast cells, which accumilated

in the lower 1/3 of the gradient, were washed and resuspended in IMDM/20%HS/PS. They were then incubated for 48 hours with 200, 100, 50 or 0 ng/ml SCF.
Result - All cells were dead after 48 hours.

Experiment 5 - Comparison of rats from two different sources, and two different culture media

Peritoneal mast cells were purified from two different rats. One rat was obtained from Bantam and Kingman, Hull, UK and the other was obtained from the Moredun Research Institute, Edinburgh, UK. Cells from both groups were resuspended in either IMDM/20%HS/PS or RPMI/10%FCS at 1 x 10^5 cells/ml in the presence or absence of 100 ng/ml SCF.

Results - After 24 hours, the cells in all groups showed good viability when assessed subjectively. However, after 48 hours, the cells suspended in RPMI/10%FCS were clearly healthier than those in IMDM. After 36 hours, the cells in IMDM were all dead, whereas those in RPMI still appeared viable.

Experiment 6 - Effect of washing and resuspending cells in IMDM on the survival of rat peritoneal mast cells

Percoll purified peritoneal mast cells were either washed three times in IMDM/20%HS/PS or Hanks balanced salt solution containing 2%FCS, P/S and 10 units/ml heparin (HBSS). Cells were resuspended in RPMI/10%FCS and quadruplicate aliquots (250 μl) of cell suspensions containing 6.5 x 10^5 mast cells/ml were then incubated for 24 hours in the presence or absence of 100 ng/ml SCF.

Results - All the cells washed in IMDM were dead after 24 hours. All the cells washed in HBSS appeared viable, in both SCF and non-SCF treated groups.

Experiment 7 - To determine the effect of washing cells in various media on the survivability of peritoneal mast cells

Percoll purified peritoneal mast cells were divided into 7 groups and washed three times in one of the following solutions, as described in chapter 2, section 2.3.

1. HBSS + 2% FCS + P/S + Heparin
2. HBSS + 20% HS + P/S
3. HBSS + 10% FCS + P/S
4. IMDM + 20% HS + P/S
5. IMDM + 10% FCS + P/S
6. RPMI + 20% HS + P/S
7. RPMI + 10% FCS + P/S

The cells from each group were then resuspended in RPMI/10%FCS/PS and 200μl aliquots containing 1.6 x 10^5 viable cells/ml were added to tissue culture wells in triplicate and incubated for 48 hours in the presence of 100 ng/ml SCF. After 48 hours, the viable cells in each well were counted in a hemocytometer (chapter 2, section 2.4).

Results - When assessed subjectively, all the cells in groups 4 and 5 appeared to be dead, whereas cells in all the other groups appeared to be viable. The cell counts in all wells after 48 hours are compared to the starting cell count in Figure A2.1. The results indicate that the peritoneal mast cells had died following washing in IMDM, but had proliferated in all the other wells, regardless of the washing medium or serum.

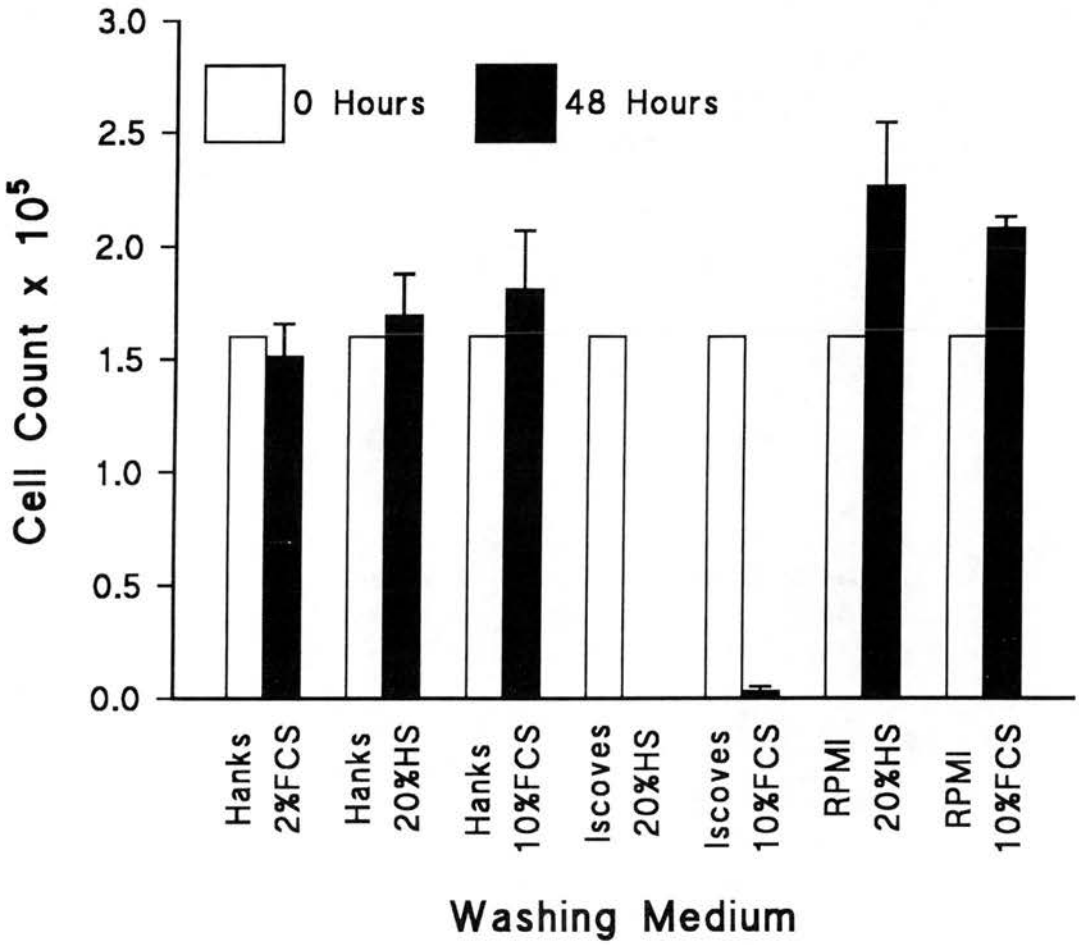

Figure A2.1 - Viable cell counts of Percoll purified peritoneal mast cells after washing in various media. Peritoneal mast cells were purified in a two stage density step Percoll gradient and washed three times in one of the stated media. The cells were then resuspended in RPMI/10%FCS/PS, and 200 µl aliquots containing 1.6 x 10^5 viable mast cells/ml were cultured for 48 hours in the presence of 100 ng/ml SCF. The bars at 48 hours represent the mean ± s.e.m. of viable cell counts from triplicate wells.

Experiment 8 - To determine the survivability of peritoneal mast cells in various media

Percoll purified peritoneal mast cells were washed twice in HBSS/2%FCS/PS/Heparin and then resuspended in 1 ml of one of the following media.

1. HBSS + 20%HS + P/S
2. HBSS + 10%FCS + P/S
3. IMDM + 20%HS + P/S
4. IMDM + 10% FCS + P/S
5. RPMI + 20% HS + P/S
6. RPMI + 10% FCS + P/S

Duplicate aliquots (250µl) containing 0.6 x 10^5 mast cells/ml from each group were added to tissue culture wells and incubated for 24 hours in the presence or absence of 100 ng/ml SCF. The viable cells in each well were then counted in a hemocytometer.

Results - The cell counts from each group are compared to the starting cell count in Figure A2.2. The results provide further evidence for the cytopathic effect of IMDM on peritoneal mast cells. However, the effect was not as marked as seen following washing of the cells in IMDM. In this experiment, the cells also appeared to die off in the RPMI/20% HS but the cause of this was not established.

Experiment 9 - To determine the effect of the Ca^{2+} concentration of the washing medium on the survivability of peritoneal mast cells

One obvious difference between the three solutions used in the previous experiments was the Ca^{2+} concentration (1.5 mM in IMDM, 0.4 mM in RPMI, 0 mM in HBSS). To ensure that reduced Ca^{2+} concentration was not having a "protective" effect during centrifugation and resuspension, percoll purified peritoneal mast cells were washed three times in HBSS, HBSS + 1.5 mM Ca^{2+}, or IMDM + 8 mM EDTA. The cells were then resuspended in RPMI/10%FCS/PS and quadruplicate aliquots were incubated for 24 hours without SCF.

Results - The cell counts at 24 hours are compared to the starting cell counts in Figure A2.3. The results indicate that the presence of 1.5 mM Ca^{2+} during washing did not have a detrimental effect on the survivability of peritoneal cells, and confirm once again the cytopathic effect of IMDM.

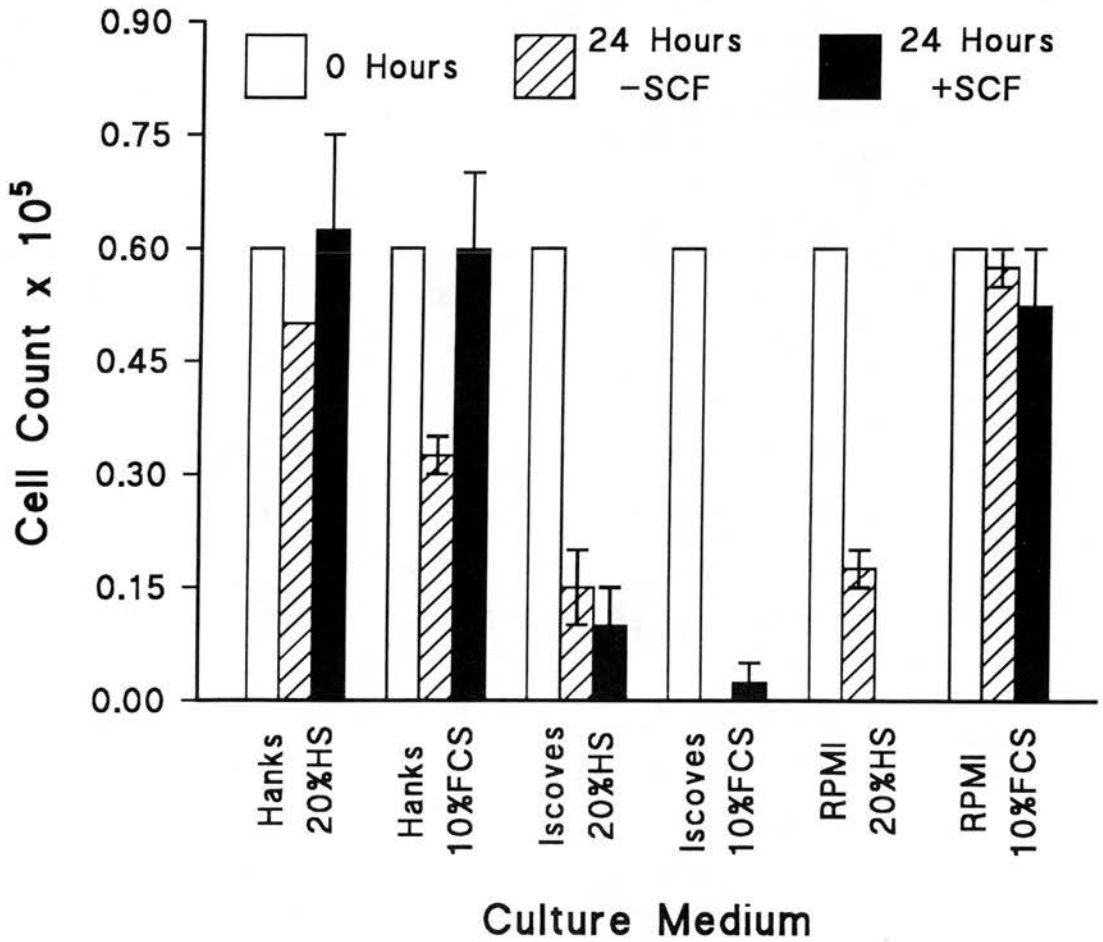

Figure A2.2 - Viable cell counts of Percoll purified peritoneal mast cells after culture in various media. After washing in HBSS/2%FCS/PS, cells were resuspended in one of the stated media and cultured for 24 hours in the presence or absence of 100 ng/ml SCF. Each bar represents the mean ± range of viable cell counts from duplicate wells, each containing 0.6 x 10^5 cells.

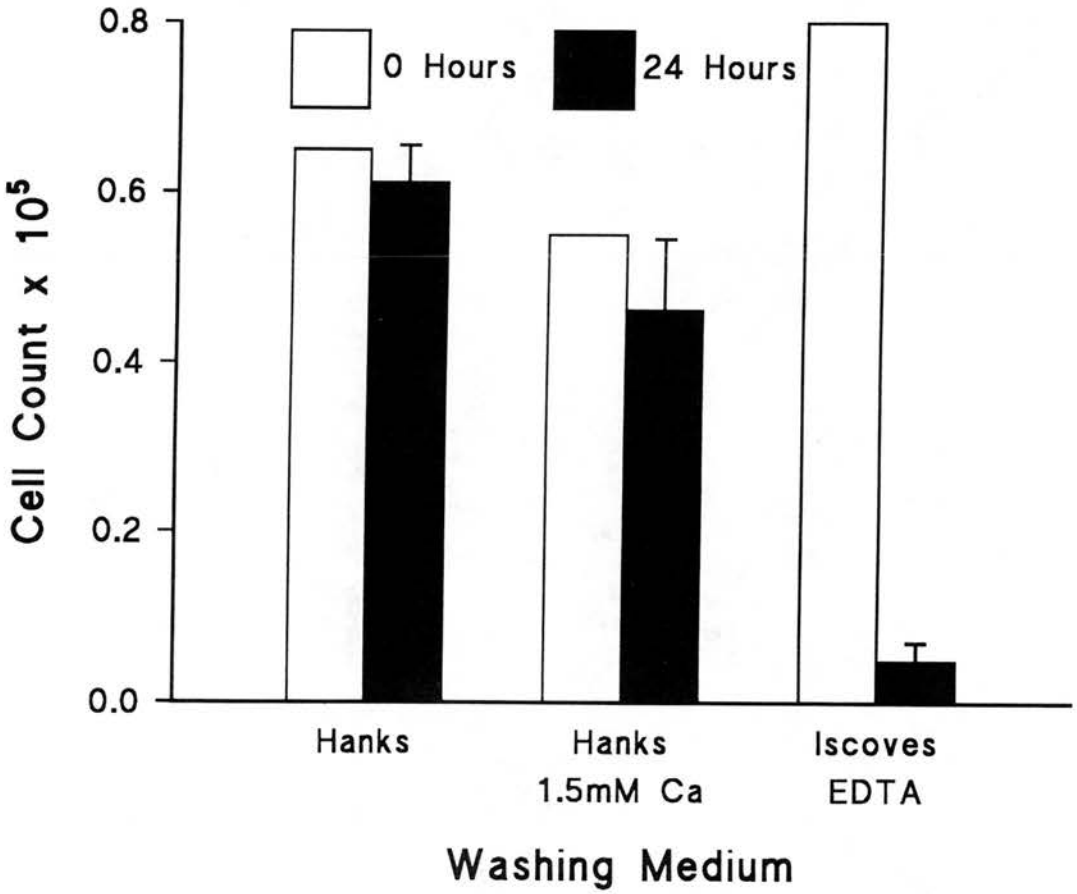

Figure A2.3 - Viable cell counts of peritoneal mast cells after washing in media with different Ca^{2+} concentrations. After Percoll purification, cells were washed and resuspended in one of the three media, and cultured for 24 hours in the absence of SCF. The bars at 24 hours represent the mean ± s.e.m. of cell counts from quadruplicate wells. In this experiment, the starting cell counts in the three groups were not identical and were $0.65x10^5$/ml, $0.55x10^5$/ml and $0.8x10^5$/ml respectively.

Discussion

This series of experiments demonstrated that washing or culturing Percoll purified rat peritoneal mast cells in IMDM resulted in cell death within 48 hours. As a result, IMDM was not used for washing or culturing peritoneal mast cells, and the protocol used was that shown in chapter 2, section 2.11 i.e. after Percoll purification, cells were washed in HBSS and then resuspended in RPMI/10%FCS.

The cause of the cytopathic effect remains unknown. It is clearly not due to the absence of a critical factor in IMDM because the cells were not damaged by washing or culturing in HBSS. Equally unlikely is the presence of external influences such as Mycoplasma infection, because the same medium was being used to successfully grow rat bone marrow-derived mast cells. It therefore seems likely that a component of the IMDM was having a specific cytopathic effect on peritoneal mast cells, even after short exposures such as during washing. Both IMDM and RPMI contain over 40 components including inorganic salts, amino acids, vitamins, glucose and buffers. The concentration of every component differs between the two media, and some components are present in one and not the other. It was therefore totally beyond the scope of these studies to attempt to elucidate the factor that was causing the cytopathic effect. However, these experiments did uncover an unusual phenomenon, and the results may be of benefit to future investigators.

APPENDIX 3

Spot counts from ELISPOT assays

Key: Unless stated otherwise, numbers in plate maps = the approximate number of BMMCs per well.
Numbers in results = the number of spots per well.
- = negative control wells with no cells
⊕ = positive control wells (50 ng/ml RMCP-II)
anti-IgE = goat anti-rat IgE at 1/250
NGS = normal goat serum at 1/250
DNP-BSA = dinitrophenyl-bovine serum albumin at 1μg/ml (1/1000).
Buffer = Tyrode's buffer with 1 mM Ca^{2+}/1 mM Mg^{2+}

Chapter 3, Section 3.3

Plate Map: No. of BMMCs per well

	1	2	3	4	5	6	7	8
DNP-BSA	134	134	134	134	134	134	134	-
	134	134	134	134	134	134	134	-
	134	134	134	134	134	134	134	-
	134	134	134	134	134	134	134	-
	134	134	134	134	134	134	134	-
Buffer	134	134	134	134	134	134	134	⊕

Results: No. of spots per well

9	19	15	18	15	19	14	0
17	21	24	19	21	19	20	0
21	20	23	18	24	14	24	0
15	17	30	26	16	21	13	0
29	12	20	16	9	10	14	0
4	1	2	4	2	1	1	⊕

Chapter 3, Section 3.5

Culture containing 38% BMMCs

48 well plate map

Anti-IgE	150	75	38	19	9	5	2	⊕
	150	75	38	19	9	5	2	⊕
	150	75	38	19	9	5	2	-
NGS	150	75	38	19	9	5	2	-
	150	75	38	19	9	5	2	-
	150	75	38	19	9	5	2	-

Results

28	12	3	2	2	0	0	⊕
30	24	16	1	5	0	2	⊕
40	20	9	3	1	0	0	0
3	2	0	0	0	0	0	0
2	0	0	0	0	0	0	0
0	0	0	0	0	0	0	0

24 well plate map

Anti-IgE	150	75	38	19	9	⊕
	150	75	38	19	9	⊕
NGS	150	75	38	19	9	-
	150	75	38	19	9	-

Results

28	12	9	7	0	⊕
28	17	3	4	2	⊕
1	0	0	0	0	0
2	0	0	0	0	0

Culture containing 53% BMMCs

Plate map

Anti-IgE	210	105	52	26	13	7	3	⊕
	210	105	52	26	13	7	3	⊕
NGS	210	105	52	26	13	7	3	-
	210	105	52	26	13	7	3	-

Results

42	20	6	9	4	0	3	⊕
28	13	15	6	2	2	1	⊕
2	4	0	0	0	0	0	0
2	3	0	3	1	0	0	1

Culture containing 95% BMMCs

Plate map - 2 replicate plates

DNP-BSA	380	190	95	48	24	12	6	-
	380	190	95	48	24	12	6	-
	380	190	95	48	24	12	6	-
	380	190	95	48	24	12	6	-
Buffer	380	190	95	48	24	12	6	-
	380	190	95	48	24	12	6	⊕

Results - Plate 1

64	37	22	15	2	1	1	0
57	34	25	5	5	0	0	1
51	37	26	9	8	6	1	0
69	45	23	12	17	1	0	0
9	9	2	1	0	3	0	0
21	8	1	1	0	1	0	⊕

Results - Plate 2

56	21	9	7	2	0	2	0
49	29	18	8	8	2	1	0
56	30	15	9	3	1	0	0
67	38	13	10	7	5	2	0
16	8	4	1	7	0	2	2
18	2	5	3	2	0	0	⊕

Culture containing 97% BMMCs

Plate map - 2 replicate plates

DNP-BSA	390	195	98	49	25	12	6	-
	390	195	98	49	25	12	6	-
	390	195	98	49	25	12	6	-
	390	195	98	49	25	12	6	-
Buffer	390	195	98	49	25	12	6	-
	390	195	98	49	25	12	6	⊕

Results - Plate 1

48	23	13	6	2	1	0	0
69	37	14	7	9	4	2	0
59	69	21	5	5	2	2	0
74	35	13	11	4	2	1	0
15	15	5	3	1	2	0	1
11	7	1	1	0	0	0	⊕

Results - Plate 2

56	24	4	3	2	3	0	0
82	40	31	6	10	3	0	0
64	43	15	12	6	1	3	0
95	34	25	15	5	3	2	0
29	15	9	2	0	2	0	0
41	10	3	2	0	2	0	⊕

Chapter 3, section 3.6

Plate map - 5 replicate plates

DNP-BSA	100	100	100	100	100	100	100	-
	100	100	100	100	100	100	100	-
	100	100	100	100	100	100	100	-
	100	100	100	100	100	100	100	-
Buffer	100	100	100	100	100	100	100	-
	100	100	100	100	100	100	100	⊕

Results

Plate 1

7	12	16	11	10	16	5	0
5	13	20	11	15	5	26	0
8	15	11	16	17	23	12	0
9	13	9	21	18	18	17	0
2	2	3	2	1	3	2	0
3	1	1	1	2	6	0	⊕

Plate 2

17	6	13	13	6	9	11	0
11	5	21	12	18	12	16	0
11	11	14	7	19	20	15	0
17	12	13	8	11	16	13	0
0	1	1	5	1	4	2	0
1	1	1	4	2	1	5	⊕

Plate 3

9	15	14	7	13	8	11	0
8	12	13	9	23	8	14	0
11	14	11	17	17	8	14	0
8	22	14	12	22	22	12	0
1	3	4	2	1	2	3	0
2	1	0	3	1	1	1	⊕

Plate 4

18	11	13	10	12	13	12	0
10	18	26	14	25	13	10	0
7	17	16	16	24	33	17	0
9	16	12	20	20	16	25	1
3	3	2	5	1	1	1	0
3	1	1	2	1	0	0	⊕

Plate 5

14	16	12	11	9	9	10	0
15	12	17	19	25	11	16	0
14	14	17	17	27	20	14	0
12	16	18	20	11	27	11	0
4	3	2	4	2	0	0	0
0	2	1	3	2	2	3	⊕

Chapter 3, Section 3.7

Culture containing 66% BMMCs

Plate map

Anti-IgE	264	132	66	33	17	8	4	⊕
	264	132	66	33	17	8	4	⊕
NGS	264	132	66	33	17	8	4	-
	264	132	66	33	17	8	4	-

Results

38	14	6	5	4	4	0	⊕
42	22	8	10	5	3	1	⊕
3	0	1	3	0	2	2	1
2	4	2	2	0	0	0	0

Culture containing 89% BMMCs

Plate map

	356	178	89	356	178	89	-	-
Anti-IgE	356	178	89	356	178	89	-	-
	356	178	89	356	178	89	-	-
	356	178	89	356	178	89	-	-
NGS	356	178	89	356	178	89	-	⊕
	356	178	89	356	178	89	-	⊕
	No SCF			SCF			No cells	

Results

6	1	1	10	4	2	0	0
20	5	4	8	6	3	0	0
4	5	4	13	6	2	0	0
11	2	3	1	3	3	0	0
4	0	1	3	2	0	0	⊕
2	3	1	4	1	0	0	⊕

Chapter 4, Section 4.2

Culture containing 96% BMMCs

Plate map

	384	192	96	384	192	96	-	-
Anti-IgE	384	192	96	384	192	96	-	-
	384	192	96	384	192	96	-	-
	384	192	96	384	192	96	-	-
NGS	384	192	96	384	192	96	-	⊕
	384	192	96	384	192	96	-	⊕
	Buffer			SCF			No cells	

Results

10	7	7	16	8	5	0	0
8	7	1	26	18	10	0	0
14	7	0	27	18	8	0	1
9	1	4	3	9	0	2	0
1	5	4	2	3	4	1	⊕
1	1	3	5	1	1	1	⊕

Culture containing >99% BMMCs

N.B. Plate map - 100 BMMCs per well

Numbers in wells = SCF concentration (ng/ml)

Anti-IgE	400	400	50	50	6.25	6.2	anti-IgE	
	400	400	50	50	6.25	6.2	anti-IgE	
	200	200	25	25	3.1	3.1	NGS	
	200	200	25	25	3.1	3.1	SCF	
	100	100	12.5	12.5	1.5	1.5	-	-
	100	100	12.5	12.5	1.5	1.5	⊕	⊕

Results: No. spots per well

32	31	36	22	36	18	4	3
30	38	44	37	37	21	6	3
26	29	39	38	25	21	6	3
35	38	39	28	26	18	7	8
30	26	27	34	17	17	0	0
24	26	25	28	19	6	⊕	⊕

Chapter 4, Section 4.3

1st Experiment

N.B. Plate map - 200 BMMCs per well

Numbers in wells = Incubation time (min) with 50 ng/ml SCF

Anti-IgE	120	60	30	15	5	0	NGS	
	120	60	30	15	5	0	NGS	
	120	60	30	15	5	0	anti-IgE	
	120	60	30	15	5	0	anti-IgE	
	120	60	30	15	5	0	-	-
	120	60	30	15	5	0	⊕	⊕

Results: No. spots per well

22	44	60	53	38	12	5	3
44	47	52	57	62	13	14	6
24	56	76	66	65	12	6	9
23	51	76	69	55	16	23	3
20	58	81	64	63	21	0	0
24	35	58	57	30	17	⊕	⊕

2nd Experiment

N.B. Plate map - 200 BMMCs per well

Numbers in wells = Incubation time (min) with 50 ng/ml SCF, Buf = cells treated with buffer alone

DNP-BSA	30	15	5	0	Buf	30	30	-
	30	15	5	0	Buf	15	15	-
	30	15	5	0	Buf	5	5	-
	30	15	5	0	Buf	0	0	-
	30	15	5	0	Buf	Buf	Buf	-
	30	15	5	0	Buf	⊕	⊕	-

Results: No. spots per well

24	20	18	17	2	15	24	0
29	23	26	33	5	18	28	1
24	19	34	14	8	20	19	1
30	26	33	10	10	25	15	1
13	32	29	19	6	7	3	1
17	25	35	22	8	⊕	⊕	0

Chapter 4, Section 4.4

Plate map - 2 replicate plates for each assay

Key: a,b = SCF/anti-IgE; c,d = SCF/NGS; e,f = buffer/anti-IgE; g,h = buffer/NGS

Anti-IgE	400	200	100	400	200	100	a	e
	400	200	100	400	200	100	b	f
	400	200	100	400	200	100	c	g
NGS	400	200	100	400	200	100	d	h
	400	200	100	400	200	100	-	-
	400	200	100	400	200	100	⊕	⊕
	Buffer			50 ng/ml SCF			No cells	

Culture 2 - Day 4 (8% BMMCs)

Results - Plate 1

95	49	16	87	56	22	0	3
141	73	23	85	45	46	0	1
107	68	42	147	74	30	1	0
9	4	5	19	8	6	0	0
8	3	1	7	7	6	1	1
3	5	2	3	0	3	⊕	⊕

Results - Plate 2

103	41	21	86	66	29	1	3
104	56	24	107	78	39	0	1
79	66	23	119	89	37	1	1
17	2	12	21	10	4	0	0
13	1	1	9	2	0	0	1
9	0	0	2	2	2	⊕	⊕

Culture 2 - Day 8 (41% BMMCs)

Results - Plate 1

30	19	11	35	20	10	2	1
39	17	6	24	18	7	0	0
37	11	6	24	24	8	0	0
18	3	3	12	4	3	0	0
7	8	5	10	3	2	0	0
8	4	1	2	5	2	⊕	⊕

Results - Plate 2

39	14	7	29	19	14	0	0
20	24	8	27	14	12	0	0
31	13	9	32	20	7	0	0
9	3	5	7	6	3	0	0
5	5	3	7	1	4	1	0
8	3	1	2	3	2	⊕	⊕

Culture 2 - Day 11 (64% BMMCs)

Results - Plate 1

38	21	6	58	22	14	0	0
52	22	16	41	26	15	0	0
39	28	6	29	21	-	0	3
6	8	3	8	8	4	0	0
8	6	3	3	4	1	0	0
0	1	2	4	1	0	⊕	⊕

Results - Plate 2

49	17	15	33	20	5	0	0
43	25	7	46	21	12	0	0
52	18	7	44	21	14	0	0
6	10	2	6	7	4	1	0
8	4	3	7	7	0	0	0
7	3	1	6	7	2	⊕	⊕

Culture 2 - Day 15 (85% BMMCs)

Results - Plate 1

45	17	5	49	16	20	0	0
42	21	11	54	31	17	3	0
39	20	8	38	36	8	1	0
11	8	3	8	7	4	0	0
10	7	8	16	11	0	1	0
12	5	1	10	5	1	⊕	⊕

Results - Plate 2

48	19	11	44	27	15	0	0
28	18	9	56	39	21	0	0
44	23	13	43	28	13	0	0
13	4	5	18	6	9	0	0
8	3	3	15	8	2	0	0
8	4	4	14	3	3	⊕	⊕

Culture 2 - Day 18 (92% BMMCs)

Results - Plate 1

46	15	4	65	47	18	1	0
71	32	19	66	51	26	4	0
57	25	18	56	32	27	2	1
33	34	11	49	21	15	0	0
32	22	13	44	34	16	0	1
33	14	10	38	13	10	⊕	⊕

Results - Plate 2

43	29	14	59	36	16	1	0
36	20	10	57	31	24	1	0
35	18	18	50	33	17	0	0
26	20	13	37	22	11	0	0
37	18	13	34	39	4	0	0
38	16	11	31	36	15	⊕	⊕

Culture 2 - Day 21 (98% BMMCs)

Results - Plate 1

76	46	19	60	49	25	3	0
77	51	24	82	59	29	3	1
51	59	27	77	56	34	3	4
76	61	27	73	30	15	5	0
73	59	26	74	46	14	5	0
57	45	20	57	53	25	⊕3	⊕

Results - Plate 2

76	27	11	88	46	15	2	0
76	48	28	98	60	18	3	0
58	43	20	80	35	21	0	3
58	59	15	77	44	24	0	5
74	43	19	55	41	21	3	3
41	35	17	44	46	18	⊕	⊕

Culture 3 - Day 9 (36% BMMCs)

Results - Plate 1

25	30	10	22	16	15	1	0
45	11	14	38	33	11	3	1
18	21	13	45	32	10	0	0
9	2	2	23	12	2	2	0
5	6	2	5	6	6	2	3
9	3	6	6	3	6	⊕	⊕

Results - Plate 2

41	18	7	33	11	6	1	0
32	14	4	44	46	5	2	0
21	21	9	34	27	9	0	0
13	6	5	12	13	5	0	0
12	6	4	10	5	3	2	2
14	6	3	5	6	4	⊕	⊕

Culture 3 - Day 17 (87% BMMCs)

Results - Plate 1

32	19	5	57	45	38	1	3
42	20	23	80	46	32	0	2
44	20	5	95	85	30	2	2
17	11	7	20	22	3	4	0
17	17	5	27	13	5	3	3
23	12	6	10	7	2	⊕	⊕

Results - Plate 2

16	17	6	46	31	19	2	1
19	25	24	75	44	26	1	0
29	15	5	72	56	36	1	0
16	12	7	30	20	7	0	0
6	17	5	29	10	13	0	0
5	9	6	5	6	9	⊕	⊕

Culture 3 - Day 21 (95% BMMCs)

Results - Plate 1

29	13	8	43	22	7	1	0
47	17	9	43	33	8	0	0
45	16	14	45	28	7	1	0
37	15	7	48	22	9	0	0
20	21	8	28	24	5	0	0
27	18	13	20	4	3	⊕	⊕

Results - Plate 2

39	15	14	36	27	11	1	0
29	23	3	36	16	16	0	1
27	18	17	45	24	12	0	0
32	15	11	27	25	7	0	0
26	9	8	29	13	6	0	0
13	10	7	21	12	9	⊕	⊕

Culture 3 - Day 24 (94% BMMCs)

Results - Plate 1

20	15	4	39	38	22	0	1
38	19	16	61	42	27	0	1
18	22	14	65	41	31	0	0
28	12	11	24	9	8	0	0
22	22	10	24	11	5	0	0
17	18	2	20	8	6	⊕	⊕

Results - Plate 2

43	15	6	31	26	19	0	0
20	28	12	54	35	23	0	0
21	24	10	54	43	27	1	0
14	16	10	21	6	9	0	0
20	8	7	13	10	10	0	0
16	10	4	13	7	3	⊕	⊕

Culture 3 - Day 28 (99% BMMCs)

Results - Plate 1

108	77	57	100	65	39	0	0
126	75	48	107	89	65	0	0
106	62	46	124	83	42	1	0
124	77	43	106	64	48	1	3
105	93	36	112	53	45	2	1
117	72	41	87	73	39	⊕	⊕

Results - Plate 2

81	56	42	114	54	33	0	0
106	66	35	125	69	61	1	0
114	71	43	121	87	37	0	0
109	61	47	119	81	53	0	0
102	84	46	120	51	59	1	1
75	49	23	76	51	27	⊕	⊕

Chapter 4, Section 4.5

Plate map for 2 separate experiments

Key: a,b =DNP-BSA; c,d =Buffer; e,f = SCF/DNP-BSA; g,h = SCF/Buffer

DNP-BSA	200	200	200	200	200	200	a	b
	200	200	200	200	200	200	c	d
	200	200	200	200	200	200	e	f
Buffer	200	200	200	200	200	200	g	h
	200	200	200	200	200	200	-	-
	200	200	200	200	200	200	⊕	⊕
	50 ng/ml SCF			Buffer			No cells	

Results - Experiment 1

Culture containing 99% BMMCs

52	50	38	31	25	28	5	12
48	48	65	36	32	29	9	0
46	57	39	31	27	34	6	12
22	20	21	9	18	11	0	0
10	18	12	12	24	8	4	3
10	14	8	6	5	13	⊕	⊕

Results - Experiment 2

Culture containing 99% BMMCs

29	42	40	27	16	21	-	-
44	39	38	24	41	22	-	-
38	43	43	39	31	43	-	-
3	5	15	2	3	9	-	-
1	7	11	2	7	6	-	-
5	3	1	4	1	0	⊕	⊕

N.B. Spot counts in negative control wells in experiment 2 were disregarded because cells were added to the wells in error.

Appendix 4 - Summary of Whole-Cell Conductances

Key to Abbreviations - Cul = Culture Number, R_{el} = Pipette Resistance (MΩ), R_{sl} = Seal Resistance (GΩ)
Rs = Access Resistance (MΩ), Cm = Cell Capacitance (pF), G(IR) = Inwardly Rectifying Conductance (nS)
G(OR) = Outwardly Rectifying Conductance (nS), G_{leak} = Leak Conductance (nS)
R_{cell} = Cell Resistance (Reciprocal of G_{leak}, GΩ), °C = Temperature at which Conductance Calculated
0 = Current not observed

BONE MARROW DERIVED MAST CELLS (BMMCs)

Amphotericin B Perforated-Patch Experiments

1. Voltage Pulse Protocol -80mV to +50mV, 10mV steps, KCl Pipette Solution

								< ----Room Temp----- >				< --------25-37°C--------- >				°C
Cell	Filename	Cul	Age	Rel	Rsl	Rs	Cm	$G_{(IR)}$	$G_{(OR)}$	G_{leak}	R_{cell}	$G_{(IR)}$	$G_{(OR)}$	G_{leak}	R_{cell}	
1	ampb1aa	14	23	0.5				2.73	0	0.24	4.17					
2	ampb1aj	14	24	0.8		13	5.9	2.54	0	0.19	5.26					
3	ampb3ab	14	24	0.5		33	9.9	1.39	0.43	0.4	2.5					
4	ampb5ab	17	13					5.99	1.98	1.28	0.78					
5	ampb6ab	17	14			30	4.3	6.05	0	2.17	0.46	10.39	0	2.07	0.48	37
6	ampb6ad	17	14					2.46	1.99	3.07	0.33					
7	ampb8aa	17	26		0.5	33	4	7.18	1.13	1.83	0.55					
8	ampb8ab	17	26		2	20	5.5	5.67	0	0.54	1.85					
9	ampb9aa	17	27		1	25	3.5	2.07	0	0.39	2.56	2.48	0	0.8	1.25	37
10	ampb9af	17	27		1			2.98	0	1.94	0.52					
11	ampb10aa	17	34		1	12	4.9	10.3	10.5	1.2	0.83					
12	ampb11aa	19	14		1	20	5	1.87	3.95	3.35	0.3					
13	ampb11ac	19	14		1	33	6.3	3.11	0	0.75	1.33					
14	ampb12aa	19	15	1	2	33	3.2	2.1	1.07	0.41	2.43					

								< ----Room Temp----- >				< --------25-37°C--------- >				°C
Cell	Filename	Cul	Age	R_{el}	R_{sl}	R_s	C_m	$G_{(IR)}$	$G_{(OR)}$	G_{leak}	R_{cell}	$G_{(IR)}$	$G_{(OR)}$	G_{leak}	R_{cell}	
15	ampb13aa	19	16	1	5	25	3.8	2.02	7.43	0.37	2.7	2.45	12.83	3.35	0.3	37
16	ampb13af	19	16	0.5	2	13	6.7	2.31	0	0.21	4.76	0	8.4	0.6	1.67	37
17	ampb13am	19	16	0.6	1	25	6	5.67	0	0.29	3.45					
18	ampb14aa	19	17	1	2	45	6.1	4.95	0	1.2	0.83	4.94	0	0.8	1.25	37
19	ampb15aa	19	17	0.6	1	25	5.6					0	2.12	0.45	2.22	37
20	ampb16aa	19	17	0.6	1	25	6	8.97	2.75	2.06	0.49					
21	ampb17aa	19	17	0.6	2	25	5.3	0.71	0	0.12	8.3					
22	ampb18aa	19	18	0.6	1	33	5.1	8.64	0	1.57	0.64					
23	ampb19aa	19	18	0.6	1	50	4.5	4.98	0	1.65	0.61					
24	ampb20aa	19	18	1	1	25	3.2					0	5.86	0.78	1.28	37
2. Voltage Pulse Protocol -100mV to + 40mV, 10mV steps, KCl Pipette Solution																
25	amp1ab	19	25	2	2	20	3.5	0	0	0.23	4.35	0	0.64	0.56	1.79	37
26	ampb22aa	19	28		1	25	3.6	0	0	1.39	0.72					
27	ampb22ab	19	30	2	1	28	4.9	0	0	2.18	0.46					
28	ampb23aa	19	30	2	2	14	4.3	0	0	0.14	7.14	0	0	0.41	2.44	30
29	ampb24aa	19	30	2	5	33	2.9	0	0	0.25	4	0	0	0.34	2.94	25
30	ampb25aa	19	30	2	1	25	3.5	0	0	0.35	2.86	0	0	0.29	3.45	37
31	ampb26aa	19	30	2	2	30	2.4	0	0	0.62	1.61	0	1.67	1.49	0.67	30
32	ampb26aa*	19	32	2	10	14	4.5	0	0	0.19	5.26	0	2.81	0.57	1.75	30
33	ampb28aa	19	35	3	2	18	6.1	0	0	0.52	1.92	0	1.08	0.33	3.03	30
34	ampb29aa	19	35	2	5	20	3.8	0	0	0.1	10			0.35	2.86	37
35	ampb30aa	19	36	2	10	20	4	2.13	0	0.13	7.69	0.56	1.67	0.31	3.23	30
36	ampb31aa	19	36	2	1	25	3.1	0	0	0.34	2.94	0	0	0.43	2.33	30
37	ampb32aa	19	37	2	2	20	5	0	0	0.04	25	0	0	0.09	11.1	25
38	ampb33aa	19	37	2.5	2	33	4.8	0	0	0.11	9.09	0	1.41	0.51	1.96	30
39	ampb34aa	21	14	1	5	25	4.1	1.07	0	1.2	0.83	0	1.16	1.41	0.71	25
40	ampb35aa	21	14	1.5	2	33	4	0	1.91	0.05	20					

								< ----Room Temp----- >				< --------25-37°C--------- >				°C
Cell	Filename	Cul	Age	Rel	Rsl	Rs	Cm	$G_{(IR)}$	$G_{(OR)}$	G_{leak}	R_{cell}	$G_{(IR)}$	$G_{(OR)}$	G_{leak}	R_{cell}	
41	ampb36aa	21	16		5	25	3.7					0.82	0	0.21	4.76	30
42	ampb34aa*	22	17	1.5	2	20	6.1	0	0	0.2	5					
43	ampb35aa*	22	17		5	16	5.1	0	0	0.21	4.76	0		1.99	0.5	25
44	ampb36aa*	22	18		1	20	8.6	0	0	1.19	0.84					
45	ampb36ab	22	18			11	7	0	0							
46	ampb37aa	22	18		5	20	5.1	0	0							
47	ampb38aa	22	19	2.5	2	22	4.2	0	0	0.32	3.13	0	0.38	0.57	1.75	30
48	ampb38al	22	19	2.5	5	15	5	0	0	0.61	1.64	0	0	0.66	1.52	25
49	ampb39ab	22	19	2.5	5	25	3.7	0	0	0.3	3.33					
50	ampb40aa	22	24	2.5	2	33	3									
51	ampb41aa	22	24	2.5	10	20	4.9	1.43	0	0.55	1.82					
52	ampb43aa	22	25	2.5	5	25	4.7	1.43	0	0.55	1.82					
53	amp43aa	22	25	2.5	5	16	5.5	0	0	0.19	5.26	0	1.49	0.79	1.27	30
54	ampb44aa	22	26	2.5	5	25	5.5	0.69	0	0.84	1.19	0	0	1	1	25
55	ampb45aa	22	26	2.5	5	16	3	0	0	0.41	2.44	0	0	0.32	3.13	37
56	ampb46aa	22	27	2.5	5	16	8	0	0	0.11	9.09	0	0.45	0.24	4.17	37
57	ampb47aa	22	27	2.5	5	20	6.1	0	0	0.22	4.55	0		0.18	5.56	30
3. Voltage Pulse Protocol -140mV to +40mV, 10mV steps, KCl Pipette Solution																
58	ampb49ad	23	21	2.5	5	20	6.7	0.53	0	0.27	3.7		2.45	0.62	1.61	25
59	ampb50aa	23	21	2.5	2	20	4.6	0.99	0	0.65	1.54		0			
60	ampb51ab	23	25	2.5	2	20	3.4	1.99	0	0.7	1.43	1.35	0	0.69	1.45	30
61	ampb53aa	23	26	2.5	2	8	5.8	0.95	0	1.09	0.92					
62	ampb54aa	23	26	2.5	5	25	4.5	3.56	0	0.71	1.41	2.21	0	1.17	0.85	25
63	ampb54ad	23	26	2.5	5	25	4.9	0.6	0	0.14	7.14	0.94	0.92	0.33	3.03	30
64	ampb55aa	23	26	2.5	5	14	7.5	2.02	0	0.15	6.67	1.51	0.57	0.43	2.33	30
65	ampb56aa	23	26	2.5	5	20	5	2.38	0	0.51	1.96	6.6	1.92	0.76	1.32	25

4. Voltage Pulse Protocol -140mV to +100mV, 10mV steps, KCl Pipette Solution

							< ----Room Temp----- >				< --------25-37°C--------- >				°C
Cell	Filename	Cul	Age	Rel	Rsl	Rs	Cm	$G_{(IR)}$	$G_{(OR)}$	G_{leak}	R_{cell}	$G_{(IR)}$	$G_{(OR)}$	G_{leak}	R_{cell}	
66	ampb57aa	23	27	2.5	10	20	5.4		0	0.85	1.18			1.31	0.76	25
67	ampb58aa	23	28	2.5	1	22	6.5	2.63	0	1.41	0.71					
68	ampb59aa	23	28	2.5	5	16	6.8	1.38	0	0.08	12.5	2.4	2.61	0.36	2.78	25
69	ampb60aa	23	28	2.5	5	18	3.8	0.9	0.35	0.06	16.7	4.2	2.82	0.28	3.57	25
70	ampb61aa	23	28	2.5	5	20	6.1	0.65	0.62	0.18	5.56	0.65	0.74	0.31	3.26	25
71	ampb62aa	23	28	2.5	5	22	7.2	1.08	0	0.15	6.67	1.47	1.08	0.34	2.94	25
72	ampb63aa	23	29	2.5	5	20	6.3	1.37	0	0.28	3.57	1.64	1.6	0.56	1.79	25
73	ampb64aa	24	24	2.5	5	28	2	0.72	1.12	0.61	1.64					
74	ampb65aa	24	27	2.5	5	22	4.7	0.55	0.38	0.1	10	1.25	1.52	0.25	4	25
75	ampb65ag	24	27	2.5	5	25	4.7	2.53	0	0.22	4.55		0			
76	ampb66aa	24	27	3	5	25	4.3	0	0.91	0.62	1.61					
77	ampb67aa	24	27	2.5	5	25	3.3	0.98	0	0.43	2.33					
78	ampb67ac	24	28	2.5	2	25	2.7	3.02	3.98	1.53	0.65					
79	ampb68aa	24	32	2	5	22	4.3	0.68	0	0.19	5.26	0.96	0	0.51	1.96	30
80	ampb69ab	24	32	2	5	25	3.2	0.59	0	0.4	2.5	1.33	1.43	0.73	1.37	25
81	ampb70aa	24	33	2	10	28	4.8	0.62	0	0.29	3.45					
82	ampb71aa	24	33	2.5	10	25	4.3	1.21	0	0.3	3.33	0.76	0	0.55	1.82	30
83	ampb72aa	25	20	2.5	10	20	3.7	0.76	0.77	0.2	5	0.88	2.6	0.38	2.63	25
84	ampb74aa	25	21	5	5	33	3.1	0	0	1.42	0.7					
85	ampb75aa	25	24		10	31	3.7	1.63	0	0.36	2.78	1.35	1.04	0.32	3.13	25
86	ampb76aa	25	24		5	25	3.5	1.61	1.39	0.16	6.25	1.05	6.37	0.81	1.23	25
87	ampb77aa	25	24		5	25	4.7	1.04	0	0.87	1.15	2.86	0.71	0.95	1.05	30
88	ampb78aa	25	24		5	25	3.3	0.52	0.89	0.58	1.72	2.6	1.23	0.73	1.37	25
89	ampb79aa	25	25	2.5	10	20	4.3	0.55	0	0.22	4.55	2.85	0.94	0.38	2.63	25
90	ampb80aa	25	25		1	22	3.4	1.41	1.88	1.44	0.69	1.8	2.23	1.78	0.56	25
91	ampb82aa	25	26		5	25	2.9	1.16	2.32	0.91	1.1	1.65	1.07	1.21	0.83	25
92	ampb83aa	25	27	2.5	5	25	4.6	1.37	0.75	1.47	0.68	0	1.05	2.56	0.39	25

Cell	Filename	Cul	Age	Rel	Rsl	Rs	Cm	<----Room Temp-----> $G_{(IR)}$	$G_{(OR)}$	G_{leak}	R_{cell}	<--------25-37°C---------> $G_{(IR)}$	$G_{(OR)}$	G_{leak}	R_{cell}	°C
93	ampb84aa	25	27		5	25	6.7	1.16	1.5	0.78	1.28					
94	ampb85aa	25	27		5	25	6.1	0.92	0	0.47	2.13	1.61	1.6	0.78	1.28	30
95	ampb85ac	25	27		2.5	22	2.8	1.16	1.1	0.32	3.13	1.24	2.02	0.4	2.5	25
96	ampscf1aa	26	22		2	22	4.1	1.01	0			1.89	0			30
97	ampscf2aa	26	23		5	28	2.6	2.08	0							
98	ampscf2ab	26	23		10	25	3.3	0.66	0			0	0			37
99	scf3aa	26	24		5	22	3.2	0.79	0			1.74	2.49			30
100	scf4aa	26	24		2	25			2.36							
101	scf5aa	26	24		10	25	6.8	0.36	0.56			3.26	3.19			37
102	scf6aa	26	25		2	25	7.3	1.52	0			1.11	3.21			30
103	scf7aa	26	25		2	20	9.7	2.08	1.82							
104	bmc1aa	29	17		5	31	3.1	1.37	0			0.59	2.27			30
105	bmc2aa	29	23		5	33	7.5	0.29	0.94			2.28	3.06			30
106	bmc3aa	29	23		5	33	5.6	0.65	0			0.83	3.61			30
107	bmc4aa	29	29		5	33	7.4	0.7	0			2.38	0			30
108	bmc5aa	29	29		10	25	6.4	0.56	0			0.68	5.8			30
109	bmc6aa	29	29		10	20	6.2	2.01	0			1.67	2.94			25
Voltage Pulse Protocol -140mV to +100mV, 10mV steps, KCH_3SO_4 Pipette Solution																
110	kso4 1aa	30	25		2	100	4.7	0	0			0	0			37
111	kso4 2aa	30	28			100	3.6	0	0			0	0			25
112	kso4 3aa	30	28			16	2.7	0	0							
113	kso4 5aa	30	29		5	43	4.5	1.31	0			0.77	1.78			30
114	kso4 6aa	30	30		2	50	3.4	1.53	0							
115	kso4 7aa	30	31		10	25	4.5		0				5.38			37
116	kso4 8aa	30	31		5	22	4.3	1.22	0.76			0.9	0.96			30
117	kso4 9aa	30	31		10	23	3.6	1.06	0			2.1	0.56			30
118	kso4 10aa	30	31		2	22	4	0.74	0			1.94	1.09			30

Cell	Filename	Cul	Age	Rel	Rsl	Rs	Cm	< ----Room Temp----- > $G_{(IR)}$	$G_{(OR)}$	G_{leak}	R_{cell}	< --------25-37°C--------- > $G_{(IR)}$	$G_{(OR)}$	G_{leak}	R_{cell}	°C
119	kso4 11aa	30	32		10	25	6.1	1.89	0.71			2.11	4.82			30
120	kso4 12aa	30	32		5	20	4.1	0.62	0			0.91	0			30
121	kso4 13aa	30	32		5	40	8	0.82	0			1.16	0			37

Conventional Whole-Cell Recordings - BMMCs

1. Voltage Pulse Protocol -100mV to +40mV, 5mV steps, KCl Pipette Solution

1	bmmc12ab	4	15	2.5	4	2.15	0	0.15	
2	bmmc13aa	4	15	2.5	1.8				
3	bmmc13ac	4	15	3	6.3	2.57	0	0.28	
4	bmmc14ab	4	19	5	10	5.3	0	0.27	
5	bmmc14ad	4	19	5	3.1		0		
6	bmmc15ab	4	20	5	5	2.51	0	0.15	
7	bmmc16ab	4	23	3	2.5	1.59	0	0.22	
8	bmmc17aa	4	26	3	1.5	1.08	0	0.18	
9	bmmc18ab	4	27	5	2	0	0	0.17	
10	bmmc19aa	4	29	5	2.5				
11	bmmc19ac	4	29	5	6	0.62	0	0.3	
12	bmmc19ae	4	29	5	3.8	2.35	0	0.18	
13	bmmc20ab	4	30	4	4.4	0.93	0	0.12	
14	bmmc21ab	4	33	5	3.8	1.22	0	0.23	
15	bmmc21ad	4	33	5	3.8	1.44	0	0.14	
16	bmmc22ab	4	34	5	5	2.58	0	0.27	
17	bmmc22ad	4	34	5	5	3.77	0	0.18	
18	bmmc22af	4	34	5	3.8	2.67	0	0.11	
19	bmmc22ah	4	34	5	3.3	0.74	0	0.29	
20	bmmc22ai	4	34	5	2.3				

								< ----Room Temp----- >				< --------25-37°C--------- >				°C
Cell	Filename	Cul	Age	Rel	Rsl	Rs	Cm	$G_{(IR)}$	$G_{(OR)}$	G_{leak}	R_{cell}	$G_{(IR)}$	$G_{(OR)}$	G_{leak}	R_{cell}	
21	bmmc23ab	5	9	5			5	0.59	0	0.17						
22	bmmc23ad	5	9	5			5	0	0	0.3						
23	bmmc23af	5	9	5			3.1	0.92	0	0.14						
24																
25	**KCl Pipette Solution with 0.3mM GTP and 0.2mM ATP**															
26	bmmc24aa	5	19	5			3.1	2.24	3.03	0.66						
27	bmmc24ac	5	19	5			6	0	0	0.16						
28	bmmc24ad	5	19	5			6.6	2.47	0.45	0.28						
29	bmmc24ae	5	19	5			4.4									
30	bmmc25ab	5	19	5			6.6	3.36	0	0.12						
31	bmmc25ad	5	19	5			7.5	4.03	0.81	0.36						
2. Voltage Pulse Protocol		**-140mV to +100mV, 10 mV steps, KCl Pipette Solution**														
32	bmmc41aa	25	28		10	30	3	0.77	0	0.21			0	0.69		25
33	bmmc42aa	25	28		5	13	3.3	0.63	0	0.15		0.39	0	0.13		25
34	bmmc43aa	25	28		5	10	2.7	0	0			0	0			25
35	bmmc44aa	25	28		10	4.2	4.1	0.76	0	0.22						
36	bmmc45aa	25	30		10	9	2.1	0	0	0.37						
37	bmmc46aa	25	31		10	7	2.3	2.4	0	0.58						
38	bmmc47aa	25	31		10	8	3.2	0.63	0	0.08						
39	bmmc48aa	25	31		5	6	3.2	1.33	0	0.36		1.43	0.83	0.57		25
40	bmmc49aa	25	31		5	10	6.4	1.63	0	0.18						
41	bmmc50aa	25	31		10	7.1	4.7	0.43	0	0.07		0.41	0	0.09		25
42	bmmc51aa	25	33		5	13	4	0.52	0	0.09						

Voltage Pulse Protocol -140mV to +100mV, 10 mV steps, KCH_3SO_4 Pipette Solution

								< ----Room Temp----- >				< --------25-37°C--------- >				°C
Cell	Filename	Cul	Age	Rel	Rsl	Rs	Cm	$G_{(IR)}$	$G_{(OR)}$	G_{leak}	R_{cell}	$G_{(IR)}$	$G_{(OR)}$	G_{leak}	R_{cell}	
43	kso4 14aa	30	35		10	10	6	0.42	0			1.31	0			37
44	kso4 15aa	30	36		10	20	3.7	0.58	0			0.79	0			37
45	kso4 16aa	30	36		10	12	5.3	0.43	0			0.53	0.68			25
46	kso4 17aa	30	36		2	10	6.1	1.35	1.59							
47	kso4 18aa	30	36		10	11	5.9	0.62	0			1.22	0			25
48	kso4 19aa	30	36		5	7	6.6	1.22	0			1.44	0			30
49	kso4 20aa	30	36		10	9	4.5	0.51	0			1.89	0			30
50	kso4 21aa	30	37		10	6	6.1	1.67	0			1.87	0			30
51	kso4 22aa	30	37		10	13	5.6	0.41	0							
52	kso4 23aa	30	37		2	8	2	0.67	0.37							
53	kso4 24aa	30	37		10	8	3.5	0.37	0			0.25	0			30
54	kso4 25aa	30	37		10	8	3.8	0.42	0							
55	kso4 26aa	30	37		10	10	5	0.58	0.65			0.89	0.55			30

PERITONEAL MAST CELLS

Amphotericin B Perforated-Patch Experiments

Key to Abbreviations - Day = Age of Cells i.e. Day 0 is the day of collection
SCF? = Whether cultured in 10ng/ml SCF (Y means Yes)

1. Voltage Pulse Protocol -100mV to +40mV, 10mV steps, KCl Pipette Solution

							Room Temp		25-37°C		
Cell	Filename	Day	SCF?	R_{sl}	R_s	C_m	$G_{(IR)}$	$G_{(OR)}$	$G_{(IR)}$	$G_{(OR)}$	°C
1	ampct1aa	0		5	14	5.7	0	0	0	0	25
2	ampct2aa	0		2	22	4	0	0			
3	ampct3aa	1		1	25	5	0	0	0	0	37
4	ampct4aa	1		1	16	5.4	0	0	0	0	30
5	ampct5aa	2		2	20	5.5	0	0			
6	ampct6aa	0		5	20	8	0	0			
7	ampct6ac	0		5	20	4.6	0	0	0	0	30
8	ampct7ac	0		1	16	6.5	0	0.99	0	2.1	30
9	ampct8aa	0		2	20	5.4	0	0	0	0	37
10	ampct9aa	0		2	14	4.9	0	0	0	0	30
11	ampct10aa	1		5	20	4.3	0	0	0	0	30
12	ampct11aa	2		1	20	4.1	0	0	0	0	25
13	ampct12aa	2		2	16	4.6	0	0	0	0	30

2. Voltage Pulse Protocol -140mV to +100 mV, 10 mV steps, KCl Pipette Solution

							Room Temp		25-37°C		
Cell	Filename	Day	SCF?	R_{sl}	R_s	C_m	$G_{(IR)}$	$G_{(OR)}$	$G_{(IR)}$	$G_{(OR)}$	°C
14	ctmc15aa	1	Y	5	16	5.9	0.92	0	2	0	30
15	ctmc16aa	2	Y	1	16	5.1	0	0	0	0	37
16	ctmc17aa	2	Y	2	17	4.8	0.86	0.77			
17	ctmc20aa	1	Y		25	5.3	0	1.42			
18	ctmc21aa	1	Y	1	22	5.5	0	1.65			
19	ctmc22aa	1	Y	1	25	7.4	0	0.99			
20	ctmc23aa	1	Y	5	20	8.1	0	1.67			
21	ctmc24ac	0		1	22	5.5	0	1.1			
22	ctmc25aa	0		10	25	6.5	0	0			
23	ctmc26aa	0		10	25	4.3	0	0	0	1	37
24	ctmc27aa	0		1	20	9.3	0	0	0	0	25
25	ctmc29aa	0		2	18	6.8	0	0	0	0	37
26	ctmc30aa	0		2	25	5.5	0.81	0	0	0	37
27	ctmc31aa	0		1	20	7.7	0	0	0	0	25
28	ctmc32aa	0		1	25	5.5	0	0	0	0	30
29	ctmc34aa	0		5	20	6.4	0	0	1.46	1.06	37
30	ctmc35aa	0		1	25	3.6	0	0	0	0	30
31	ctmc36aa	0		5	15	6.3	0	0	0	0	30
32	ctmc37aa	0		10	25	4.2	0.72	0	0	0	25
33	ctmc38aa	0		5	22	5	0	0	0	0.81	30
34	ctmc39aa	0		5	20	6.5	0	1.12			
35	ctmc40aa	0		2	33	5.5	0	0			
36	ctmc41aa	0		2		5.8	0	0	1.38	0.41	30
37	ctmc42aa	0		10	25	3	0	0	0	1.09	25
38	ctmc43aa	0		10	25	4	0	0.63	0	1.36	25
39	ctmc44aa	1	Y	10	17	5.5	0	0	0	3.38	25

Voltage Pulse Protocol -140mV to +100mV, 10mV steps, KCH_3SO_4 Pipette Solution

				Room Temp					25-37°C		
Cell	Filename	Day	SCF?	R_{sl}	R_s	C_m	$G_{(IR)}$	$G_{(OR)}$	$G_{(IR)}$	$G_{(OR)}$	°C
40	mc16aa	0		5	33	3.7	0.73	0	0.47	0	25
41	mc17aa	0		10	25	5.1	0	0	3.9	0	30
42	mc18aa	0		5	25	4.6	0	0	2.2	0	30
43	mc19aa	0		2	25	3.7	0	0	0	2.2	30
44	mc20aa	1	Y	5	33	6.5	0	0	0	0	25
45	mc21aa	0		5	26	9.3	0	0	0	0	25
46	mc22aa	0		10	25	4.7	0	0	0	0	37
47	mc23aa	1	Y	5	25	5.7	0	0	2.6	0	30
48	mc24aa	1	Y	5	25	4.9	0	0	0	0	30
49	mc25aa	1	Y	10	25	4.8	0	0	0.7	0	
50	mc26aa	0		5	25	8.7	0	0			
51	mc26ab	0		10	25	4.8	0	0	0	0	30
52	mc28aa	1		5	25	6.5	0	0	0	1.7	25
53	mc29aa	1		2	25	5.6	0	0			
54	mc30aa	1		2	25	6.5	0	0	0	0	25
55	mc31aa	0		10	25	4.8	0.43	0			

Conventional Whole-Cell Recordings - Peritoneal Mast Cells

Voltage Pulse Protocol -140mV to +100 mV, KCH_3SO_4 Pipette Solution

1	mc2aa	0		10	12	5.1	0.4	2.1			
2	mc3aa	0		1	6	4.8	0	0	0	0	25
3	mc4aa	0		10	18	5.6	0	0			
4	mc5aa	0			17	4.5	0	0			
5	mc6aa	1		10	13	6.6	0.8	0			
6	mc6ad	1		10	14	4.6	0	0			
7	mc8aa	1		10	14	5.9	0	0			

				Room Temp					25-37°C		
Cell	Filename	Day	SCF?	R_{sl}	R_s	C_m	$G_{(IR)}$	$G_{(OR)}$	$G_{(IR)}$	$G_{(OR)}$	°C
8	mc9aa	1		2	15	5.2	0	0			
9	mc10aa	1		10	14	5.5	0	0			
10	mc11aa	1		5	18	5.2	0	0			
11	mc12aa	1	Y	10	11	6	0.7	0	2.1	0	25
12	mc13aa	1	Y	10	9	6.9	0.3	1.2			
13	mc14aa	1	Y	5	20	4.7					
14	mc15aa	1	Y	10	16	4.2	0	0	0	0	25

APPENDIX 5

EFFECTS OF STEM CELL FACTOR ON THE WHOLE-CELL CURRENTS OF RAT BMMCS

INTRODUCTION

The effects of SCF on IgE-dependent mediator release from rat BMMCs were described in chapter 4. These results demonstrated that SCF was not, in itself, a secretagogue for BMMCs, but it significantly enhanced mediator release in response to anti-IgE or specific antigen. The mode of action of this "priming" effect is currently not known. However, in other mast cell types, activation of the *c-kit* receptor induces the tyrosine phosphorylation of multiple cytosolic proteins (Welham and Schrader, 1992), and overlap between the IgE and SCF signalling pathways has been demonstrated in mouse BMMCs (Tsai *et al*, 1993) and rat peritoneal mast cells (Koike *et al*, 1993). Hence, one hypothesis for the priming effect of SCF is that it modulates the function of ion channels by phosphorylation, thus activating whole-cell currents. Other ligands that induce whole-cell currents in mast cells without causing degranulation include ADP and ATP, which induce an outwardly rectifying K^+ current in RBL-2H3 cells (Qian and McCloskey, 1993), and picomolar doses of substance P, which activate an outwardly rectifying Cl^- current in rat peritoneal mast cells (Janiszewski *et al*, 1994). Both these studies suggested that activation of the currents might enhance the subsequent response to secretagogues, presumably by enhancing Ca^{2+} influx. The purpose of this study was to determine if SCF activated whole-cell currents in rat BMMCs.

EXPERIMENTAL METHODS AND RESULTS

A5.1 - Efficacy of SCF in the electrophysiological recording chamber

Preliminary experiments were performed to determine if SCF enhanced mediator release from rat BMMCs under conditions used for electrophysiological studies (i.e. with electrophysiological solutions in the patch-clamp recording chamber). A suspension of BMMCs from a culture containing 99% mast cells was sensitised with mouse IgE (see chapter 2, section 2.15) and resuspended in modified mast cell

Ringer (instead of the usual Tyrode's buffer). Aliquots of 1 x 10^5 cells were added to four separate baths (similar to the recording bath described in section 2.26) in each of two electrophysiological recording chambers, and stimulated at either room temperature or 37°C as shown below.

Experimental Design

Chamber 1 - Room Temp

Bath 1 Ringer	Bath 2 Ringer/SCF
Bath 3 DNP	Bath 4 DNP/SCF

Chamber 2 - 37°C

Bath 5 Ringer	Bath 6 Ringer/SCF
Bath 7 DNP	Bath 8 DNP/SCF

The cells were incubated with 50 ng/ml SCF (or Ringers alone) for 5 min before challenge with DNP-BSA (or Ringers) for a further 30 min. The cells were then removed from the baths, pelleted by centrifugation, and the pellets and supernatants assayed for β-hexosaminidase as described previously (chapter 2, sections 2.17 and 2.19).

Figure A5.1 shows that SCF enhanced the percent release of β-hexosaminidase from BMMCs challenged with DNP-BSA at 37°C, but not at room temperature. This result (one of four similar experiments) confirms the previous observations described in chapter 4, but indicates that mediator release, and its upregulation by SCF, is temperature dependent. There is a high background release in this experiment because it was not possible to remove all the BMMCs from the bath, thus artifactually lowering the concentration of β-hexosaminidase in the cell pellet.

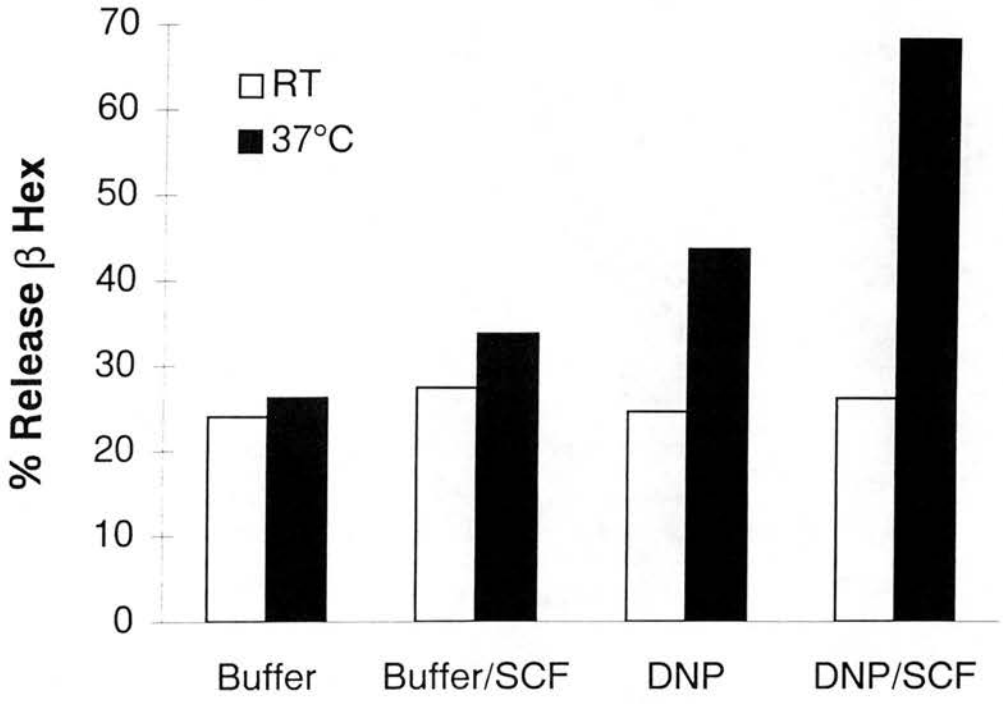

Figure A5.1 - One of four similar experiments showing the effect of SCF on IgE-dependent β-hexosaminidase release from rat BMMCs. The cells were sensitised with mouse IgE, and aliquots of 1 x 10^5 BMMCs (suspended in 1 ml of mast cell Ringer) were placed in electrophysiological recording baths. After incubation with 50 ng/ml SCF (or Ringer alone) for 5 min, the cells were challenged with DNP-BSA (or Ringer alone) either at room temperature or 37°C. Release of β-hexosaminidase was enhanced only at 37°C.

A5.2 - Effect of SCF on the whole-cell currents of rat BMMCs

For these experiments, whole-cell currents were recorded with the perforated-patch technique as described in chapter 2, section 2.31. This was considered important because signal transduction through the *c-kit* receptor probably requires a full complement of cytosolic messengers and enzymes. After recording the whole-cell currents for a control period (usually 2 - 5 min), SCF was added to the bath with a pipette to a final concentration of 50 - 100 ng/ml. The currents were then recorded continuously on a pen recorder and observed for the subsequent 10 - 30 min.

Recordings were obtained from 29 BMMCs before and after the addition of SCF. 7 were obtained at room temperature, 4 at 25°C, 10 at 30°C and 8 at 37°C. SCF did not activate or change the amplitude of whole-cell currents in rat BMMCs at any of the indicated temperatures. The presence or absence of the outwardly rectifying Cl^- (OR_{Cl}) current was dependent on temperature as described in chapter 5, but its amplitude was not increased by SCF (Figure A5.2). In addition, there was no observable effect on the IR_K current (Figure A5.2).

DISCUSSION

These experiments demonstrated that SCF had no observable effect on the whole-cell currents of rat BMMCs. It is unlikely that the negative results reflected experimental conditions because SCF enhanced IgE-dependent β-hexosaminidase release from rat BMMCs under the same conditions as those used for patch-clamping (Figure A5.1). In addition, the perforated-patch technique was used, thus ensuring that essential intracellular messengers and enzymes were preserved. It is possible that SCF activates conductances that are too small to be detected with the solutions and conditions used in these experiments. For example, Ca^{2+} imaging techniques would be required to monitor the influx of Ca^{2+} through I_{CRAC} or non-specific cation pathways. However, the results indicate that SCF does not activate, or modulate, the activity of the IR_K or OR_{Cl} currents in rat BMMCs.

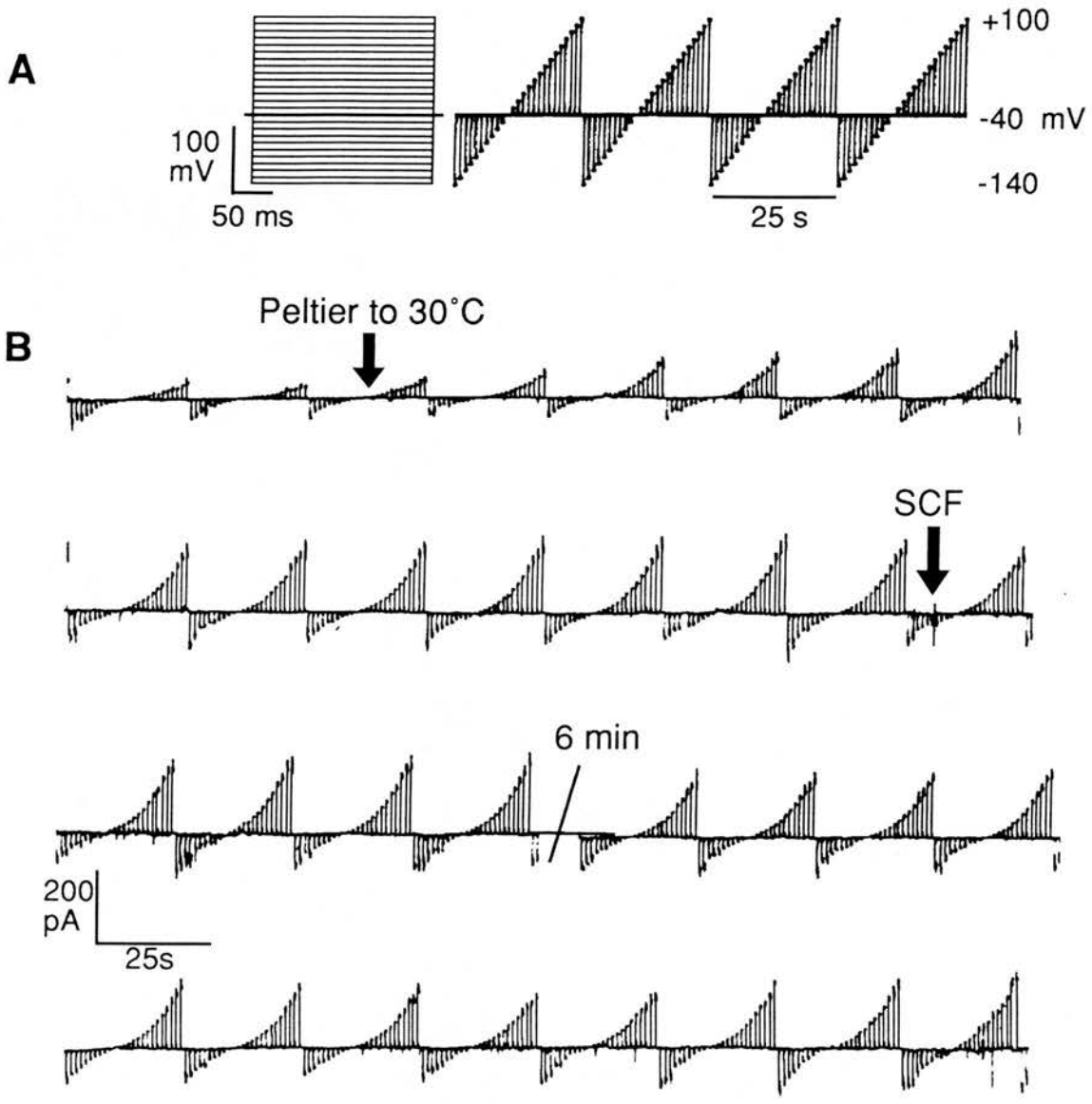

Figure A5.2 - Typical experiment showing the effect of SCF on the whole-cell currents of rat BMMCs. **A**: The voltage pulse protocol. The cell was clamped at a holding potential of -40 mV and voltage pulses of 200 ms duration were applied every second from -140 mV to +100 mV in 10 mV steps. **B**: Continuous pen recording showing the whole cell currents. At the first arrow, the bath was warmed to 30°C, resulting in activation of the OR_{Cl} current. At the second arrow, 50 ng/ml SCF was added to the bath. There was no observable effect on the amplitude of the inward or outward currents over the subsequent 10 min period (a 6 min section of the tracing was removed to produce the figure). Extracellular solution = modified mast cell Ringer, pipette solution contained KCl. Similar results were obtained in 29 experiments.

BIBLIOGRAPHY

Advanced Methods in Electrophysiology. *The Axon Guide for Electrophysiology and Biophysics Laboratory Techniques.* (Sherman-Gold R, editor), Axon Instruments, Inc. Foster City, 1993: pp. 114-118.

Abe, T., Ochiai, H., Minamishima, Y., & Nawa, Y. (1988) Induction of intestinal mastocytosis in nude mice by repeated injection of interleukin 3. *International Archives Of Allergy And Applied Immunology,* **86,** 356-358.

Abe, T. & Nawa, Y. (1988) Worm expulsion and mucosal mast cell response induced by repetitive IL-3 administration in *Strongyloides ratti*-infected nude mice. *Immunology,* **63,** 181-185.

Adachi, S., Ebi, Y., Nishikawa, S.I., Hayashi, S.I., Yamazaki, M., Kasugai, T., Yamamura, T., Nomura, S., & Kitamura, Y. (1992) Necessity of extracellular domain of w (c-kit) receptors for attachment of murine cultured mast cells to fibroblasts. *Blood,* **79,** 650-656.

Agis, H., Willheim, M., Sperr, W.R., Wilfing, A., Kromer, E., Kabrna, E., Spanblochl, E., Strobl, H., Geissler, K., Spittler, A., Boltznitulescu, G., Majdic, O., Lechner, K., & Valent, P. (1993) Monocytes do not make mast cells when cultured in the presence of SCF: characterization of the circulating mast cell progenitor as a c-kit$^+$, CD34$^+$, Ly$^-$, CD14$^-$, CD17$^-$, colony-forming cell. *Journal Of Immunology,* **151,** 4221-4227.

Alber G, Metzger H. (1993) The high-affinity IgE receptor. *Immunopharmacology of mast cells and basophils.* (Foreman JC, editor), Academic Press, London: pp. 43-51.

Alberts B, Bray D, Lewis J, et al.(1994) Protein function. *Molecular biology of the cell.* (Robertson M, Adams R, editors), Garland Publishing, Inc. London: pp. 195-222.

Aloe, L. & Levi-Montalcini, R. (1977) Mast cells increase in tissues of neonatal rats injected with nerve growth factor. *Brain Research,* **133,** 358-366.

Anderson, D.M., Lyman, S.D., Baird, A., Wignall, J.M., Eisenman, J., Rauch, C., March, C.J., Boswell, H.S., Gimpel, S.D., Cosman, D., & Williams, D.E. (1990) Molecular-cloning of mast-cell growth-factor, a hematopoietin that is active in both membrane-bound and soluble forms. *Cell,* **63,** 235-243.

Aridor, M., Rajmilevich, G., Beaven, M.A., & Sagi-Eisenberg, R. (1993) Activation of exocytosis by the heterotrimeric G-protein G_{i3}. *Science,* **262,** 1569-1572.

Arizono, N., Kasugai, T., Yamada, M., Okada, M., Morimoto, M., Tei, H., Newlands, G.F.J., Miller, H.R.P., & Kitamura, Y. (1993) Infection of *Nippostrongylus brasiliensis* induces development of mucosal type but not connective tissue type mast cells in genetically mast cell-deficient Ws/Ws rats. *Blood,* **81,** 2572-2578.

Ashman, R.I., Jarboe, D.L., Conrad, D.H., & Huff, T.F. (1991) The mast cell committed progenitor. In vitro generation of committed progenitors from bone marrow. *Journal Of Immunology,* **146,** 211-216.

Baird, B., Shopes, R.J., Oi, V.T., Erickson, J., Kane, P., & Holowka, D. (1989) Interaction of IgE with its high affinity receptor. *International Archives Of Allergy And Applied Immunology,* **88,** 23-28.

Barane, D. & Razin, E. (1991) Protein kinase C regulates proliferation of mast cells and the expression of the mRNA of *fos* and *jun* proto-oncogenes during activation by IgE-Ag or calcium ionophore A23187. *Blood,* **78,** 2534-2364.

Barrett, K.E., Ali, H., & Pearce, F.L. (1985) Studies on histamine secretion from enzymically dispersed cutaneous mast cells of the rat. *Journal Of Investigative Dermatology,* **84,** 22-26.

Barrett, K.E. & Pearce, F.L. (1983) A comparison of histamine secretion from isolated peritoneal mast cells of the mouse and rat. *International Archives Of Allergy And Applied Immunology,* **72,** 234-238.

Barrett KE, Pearce FL. (1993) Mast cell heterogeneity. *Immunopharmacology of mast cells and basophils.* (Foreman JC, editor), Academic Press, London: pp. 29-38.

Barrowman, M.M., Cockroft, S., & Gomperts, B.D. (1986) Two roles for guanine nucleotides in stimulus-secretion sequence of neutrophils. *Nature,* **319,** 504-507.

Barsumian, E.L., Isersky, C., Petrino, M.G., & Siraganian, R.P. (1981) IgE-induced histamine release from rat basophilic leukemia cell lines: isolation of releasing and nonreleasing clones. *European Journal Of Immunology,* **11,** 317-323.

Beaven, M.A. & Metzger, H. (1993) Signal transduction by Fc receptors - the FcεRI case. *Immunology Today,* **14,** 222-226.

Befus, A.D., Pearce, F.L., Gauldie, J., Horsewood, P., & Bienenstock, J. (1982) Mucosal mast cells 1. Isolation and functional characteristics of rat intestinal mast cells. *Journal Of Immunology,* **128,** 2475-2480.

Befus, A.D. & Bienenstock, J. (1979) Immunologically mediated intestinal mastocytosis in *Nippostrongylus brasiliensis* infected rats. *Immunology,* **38,** 95-101.

Benhamou, M., Gutkind, K.C., Robbins, K.C., & Siraganian, R.P. (1990) Tyrosine phosphorylation coupled to IgE receptor-mediated signal transduction and histamine release. *Proceedings Of The National Academy Of Sciences Of The United States Of America,* **87,** 5327-5330.

Benhamou, M., Stephan, V., Robbins, K.C., & Siraganian, R.P. (1992) High-affinity IgE receptor-mediated stimulation of rat basophilic leukemia (RBL-2H3) cells induces early and late protein tyrosine phosphorylations. *Journal Of Biological Chemistry,* **267,** 7310-7314.

Benhamou, M., Ryba, N.J.P., Kihara, H., Nishikata, H., & Siraganian, R.P. (1993) Protein-tyrosine kinase $p72^{syk}$ in high-affinity IgE receptor signaling: identification as a component of pp72 and association with the receptor γ-chain after receptor aggregation. *Journal Of Biological Chemistry,* **268,** 23318-23324.

Benyon, R.C., Robinson, C., & Church, M.K. (1989) Differential release of histamine and eiconasoids from human skin mast cells activated by IgE-dependent and non-immunological stimuli. *British Journal Of Pharmacology,* **97,** 898-904.

Berridge, M.J. & Irvine, R.F. (1984) Inositol trisphosphate, a novel second messenger in cellular signal transduction. *Nature,* **312,** 315-321.

Bischoff, S.C., Schwengberg, S., Wordelmann, K., Weimann, A., Raab, R., & Manns, M.P. (1996) Effect of *c-kit* ligand, stem cell factor, on mediator release by human intestinal mast cells isolated from patients with inflammatory bowel disease and controls. *Gut,* **38,** 104-114.

Bischoff, S.C. & Dahinden, C.A. (1992) C-kit ligand: a unique potentiator of mediator release by human lung mast cells. *Journal Of Experimental Medicine,* **175,** 237-244.

Bissonnette, E.Y., Chin, B., & Befus, A.D. (1995) Interferons differentially regulate histamine and TNF-α in rat intestinal mucosal mast cells. *Immunology,* **86,** 12-17.

Blank, U., Ra, C., Miller, L., Metzger, H., & Kinet, J. (1989) Complete structure and expression in transfected cells of high affinity IgE receptor. *Nature,* **337,** 187-189.

Blumejensen, P., Claessonwelsh, L., Siegbahn, A., Zsebo, K.M., Westermark, B., & Heldin, C.H. (1991) Activation of the human c-kit product by ligand-induced dimerization mediates circular actin reorganization and chemotaxis. *Embo Journal,* **10,** 4121-4128.

Bormann, J., Hamill, O.P., & Sakmann,B. (1987) Mechanism of anion permeation through channels gated by glycine and γ-amino butyric acid in mouse cultured spinal neurones. *Journal of Physiology*, **385**, 243-286

Broide, D.H., Wasserman, S.I., Alvaro-Garcia, J., Zvaifer, N.J., & Firestein, G.S. (1989) Transforming growth factor-β1 selectively inhibits IL-3-dependent mast cell proliferation without affecting mast cell function or differentiation. *Journal Of Immunology,* **143,** 1591-1597.

Broide, D.H., Metcalfe, D.D., & Wasserman, S.I. (1988) Functional and biochemical characterization of rat bone marrow-derived mast cells. *Journal Of Immunology,* **141,** 4298-4305.

Brostoff J, Hall T. (1993) Hypersensitivity - Type I. *Immunology.* (Roitt, I, Brostoff J, Male DK, editors), Mosby, London: pp. 19.1-19.22.

Burd, P.R., Rogers, H.W., Gordon, J.R., Martin, C.A., Jayaraman, S., Wilson, S.D., Dvorak, A.M., Galli, S.J., & Dorf, M.E. (1989) Interleukin-3-dependent and interleukin-3-independent mast cells stimulated with IgE and antigen express multiple cytokines. *Journal Of Experimental Medicine,* **170,** 245-257.

Burnet, F.M. (1977) The probable relationship of some or all mast cells to the T-cell system. *Cellular Immunology,* **30,** 358-360.

Cass, A., Finkelstein, A., & Krespi, V. (1970) The ion permeability induced in thin lipid membranes by the polyene antibiotics nystatin and amphotericin B. *Journal Of General Physiology,* **56,** 100-124.

Chabot, B., Stephenson, D.A., Chapman, V.M., Besmer, P., & Bernstein, A. (1988) The proto-oncogene *c-kit* encoding a transmembrane tyrosine kinase receptor maps to the mouse W locus. *Nature,* **335,** 88-89.

Chaikin, E., Hakeem, I., & Razin, E. (1994) Enhancement of Interleukin-3-dependent mast cell proliferation by suppression of *c-jun* expression. *Journal Of Biological Chemistry,* **269,** 8498-8503.

Chen, Z., Irani, A.A., Bradford, T.R., Craig, S.S., Newlands, G.F.J., Miller, H.R.P., Huff, T., Simmons, W.H., & Schwartz, L.B. (1993) Localization of rat tryptase to a subset of the connective tissue type of mast cell. *Journal Of Histochemistry & Cytochemistry,* **41,** 961-969.

Chi, E. & Lagunoff, D. (1975) Abnormal mast cell granules in the beige (Chediak-Higashi) mouse. *Journal Of Histochemistry & Cytochemistry,* **23,** 117-122.

Chiu, H.F. & Burrall, B.A. (1990) Effect of interleukin-3 on the differentiation and histamine content of cultured bone marrow mast cells. *Agents And Actions,* **31,** 197-203.

Chock, S.P. & Schmauderchock, E.A. (1992) The secretory granule and the mechanism of stimulus-secretion coupling. *Current Topics In Cellular Regulation,* **32,** 183-208.

Choi, O.H., Kim, J., & Kinet, J. (1996) Calcium mobilization via sphingosine kinase in signaling by the FcεRI antigen receptor. *Nature,* **380,** 634-636.

Clegg, L.S., Church, M.K., & Holgate, S.T. (1985) Histamine secretion from human skin slices induced by anti-IgE and artificial secretagogues and effects of sodium chromoglycate and salbutamol. *Clinical Allergy,* **15,** 321-328.

Coleman, J.W., Buckley, M.G., Holliday, M.R., & Morris, A.G. (1991) Interferon-γ inhibits serotonin release from mouse peritoneal mast cells. *European Journal Of Immunology,* **21,** 2559-2564.

Coleman, J.W., Holliday, M.R., Kimber, I., Zsebo, K.M., & Galli, S.J. (1993) Regulation of mouse peritoneal mast cell secretory function by stem cell factor, IL-3 or IL-4. *Journal Of Immunology,* **150,** 556-562.

Columbo, M., Horowitz, E.M., Botana, L.M., MacGlashan, D.W., Bochner, B.S., Gillis, S., Zsebo, K.M., Galli, S.J., & Lichtenstein, L.M. (1992) The human recombinant c-kit receptor ligand, rhSCF, induces mediator release from human cutaneous mast cells and enhances IgE-dependent mediator release from both skin mast cells and peripheral blood basophils. *Journal Of Immunology,* **149,** 599-608.

Combs, J.W., Lagunoff, D., & Bendith, E.P. (1963) Differentiation and proliferation of embryonic mast cells of the rat. *Journal Of Cell Biology,* **25,** 577-583.

Connelly, P.A., Farrell, C.A., Merenda, J.M., Conklyn, M.J., & Showell, H.J. (1991) Tyrosine phosphorylation is an early signalling event common to Fc receptor crosslinking in human neutrophils and rat basophilic leukemia cells (RBL-2H3). *Biochemical And Biophysical Research Communications,* **177,** 192-201.

Conrad, D.H., Bazin, H., Sehon, A.H., & Froese, A. (1975) Binding parameters of the interaction between rat IgE and rat mast cell receptors. *Journal Of Immunology,* **114,** 1688-1691.

Copeland, N.G., Gilbert, D.J., Cho, B.C., Donovan, P.J., Jenkins, N.A., Cosman, D., Anderson, D., Lyman, S.D., & Williams, D.E. (1990) Mast cell growth factor maps near the steel locus on mouse chromosome 10 and is deleted in a number of steel alleles. *Cell,* **63,** 175-183.

Costa, J.J., Demetri, G.D., Harrist, T.J., Dvorak, A.M., Hayes, D.F., Merica, E.A., Menchaca, D.M., Gringeri, A.J., Schwartz, L.B., & Galli, S.J. (1996) Recombinant human stem cell factor (kit-ligand) promotes human mast cell and melanocyte hyperplasia and functional activation in vivo. *Journal Of Experimental Medicine,* **183,** 2681-2686.

Crews, F.T., Morita, Y., McGivney, A., Hirata, F., Siraganian, R.P., & Axelrod, J. (1981) IgE-mediated histamine release in rat basophilic leukemia cells: receptor activation, phospholipid methylation, Ca^{2+} flux, and release of arachidonic acid. *Archives Of Biochemistry And Biophysics,* **212,** 561-571.

Crowle, P.K. & Phillips, D.E. (1983) Characteristics of mast cells in Chediak-Higashi mice: light and electron microscopic studies of connective tissue and mucosal mast cells. *Experimental Cell Biology,* **51,** 130-139.

Czerkinsky, C.C., Nilsson, L.A., Nygren, H., Ouchterlony, O., & Tarkowski, A. (1983) A solid-phase enzyme-linked immunospot (ELISPOT) assay for enumeration of specific antibody-secreting cells. *Journal Of Immunological Methods,* **65,** 109-121.

Dastych, J. & Metcalfe, D.D. (1994) Stem cell factor induces mast cell adhesion to fibronectin. *Journal Of Immunology,* **152,** 213-219.

Dayton, E.T., Pharr, P., Ogawa, M., Serafin, W.E., Austen, K.F., Levi-Schaffer, F., & Stevens, R.L. (1988) 3T3 fibroblasts induce cloned interleukin 3-dependent mouse mast cells to resemble connective tissue mast cells in granular constituency. *Proceedings Of The National Academy Of Sciences Of The United States Of America,* **85,** 569-572.

Dekker, L.V. & Parker, P.J. (1994) Protein kinase C - a question of specificity. *Trends in Biochemical Sciences,* **19,** 73-77.

Devries, J.E., Punnonen, J., Cocks, B.G., Malefyt, R.D., & Aversa, G. (1993) Regulation of the human IgE response by IL-4 and IL-13. *Research In Immunology,* **144,** 597-601.

Dietrich, J. & Lindau, M. (1994) Chloride channels in mast cells: block by DIDS and role in exocytosis. *Journal Of General Physiology,* **104,** 1099-1111.

Donaldson, L.E., Schmitt, E., Huntley, J.F., Newlands, G.F.J., & Grencis, R.K. (1996) A critical role for stem cell factor and *c-kit* in host protective immunity to an intestinal helminth. *International Immunology,* **8,** 559-567.

Dvorak, A.M., Saito, H., Estrella, P., Kissell, S., Arai, N., & Ishizaka, T. (1989) Ultrastructure of eosinophils and basophils stimulated to develop in human cord blood mononuclear cell cultures containing recombinant human interleukin-5 or interleukin-3. *Laboratory Investigation,* **61,** 116-132.

Dvorak, A.M., Dvorak, H.F., & Galli, S.J. (1983) Ultrastructural criteria for identification of mast cells and basophils in humans, guinea pigs and mice. *American Review Of Respiratory Disease,* **128,** 549-552.

Echtenacher, B., Mannel, D.N., & Hultner, L. (1996) Critical protective role of mast cells in a model of acute septic peritonitis. *Nature,* **381,** 75-77.

Edwardson, J.M. & Marciniak, S.J. (1995) Molecular Mechanisms in Exocytosis. *J. Membrane. Biol.* **146,** 113-122.

Eiseman, E. & Bolen, J.B. (1992) Engagement of the high-affinity IgE receptor activates *src* protein-related tyrosine kinases. *Nature,* **355,** 78-80.

Eliakim, R., Gilead, L., Ligumsky, M., Oxon, E., Rachmilewitz, D., & Razin, E. (1986) Possible presence of E-mast cells in the human colon. *Proceedings Of The National Academy Of Sciences Of The United States Of America,* **83,** 461-464.

Else, K.J., Finkelman, F.D., Maliszewski, C.R., & Grencis, R.K. (1994) Cytokine-mediated regulation of chronic intestinal helminth infection. *Journal Of Experimental Medicine,* **179,** 347-351.

Emadikhiav, B., Mousli, M., Bronner, C., & Landry, Y. (1995) Human and rat cutaneous mast cells: involvement of a G-protein in the response to peptidergic stimuli. *European Journal Of Pharmacology,* **272,** 97-102.

Enerback, L. (1966a) Mast cells in gastrointestinal mucosa. 3. Reactivity towards compound 48/80. *Acta Pathologica et Microbiologica Scandinavica,* **66,** 313-322.

Enerback, L. (1966b) Mast cells in gastrointestinal mucosa. 2. Dye-binding and metachromatic properties. *Acta Pathologica et Microbiologica Scandinavica,* **66,** 303-312.

Enerback, L. (1966c) Mast cells in rat gastrointestinal mucosa. 1. Effects of fixation. *Acta Pathologica et Microbiologica Scandinavica,* **66,** 289-302.

Enerback, L. (1974) Ultrastructure of mucosal mast cells in normal and compound 48/80 treated rats. *Cell And Tissue Research,* **150,** 95-101.

Enerback, L. (1987) Mucosal mast cells in the rat and in man. *International Archives Of Allergy And Applied Immunology,* **82,** 249-255.

Fasolato, C., Hoth, M., Matthews, G., & Penner, R. (1993) Ca^{2+} and Mn^{2+} influx through receptor-mediated activation of nonspecific cation channels in mast cells. *Proceedings Of The National Academy Of Sciences Of The United States Of America,* **90,** 3068-3072.

Fasolato, C., Hoth, M., & Penner, R. (1993) A GTP-dependent step in the activation mechanism of capacitative calcium influx. *Journal Of Biological Chemistry,* **268,** 20737-20740.

Fasolato, C., Innocenti, B., & Pozzan, T. (1994) Receptor-activated Ca^{2+} influx - how many mechanisms for how many channels. *Trends In Pharmacological Sciences,* **15,** 77-83.

Feltelius, N., Gudmundsson, S., Wennersten, L., Sjoberg, O., Hallgren, R., & Klareskog, L. (1991) Enumeration of IgA producing cells by the enzyme linked immunospot (ELISPOT) technique to evaluate sulfasalazine effects in inflammatory arthritides. *Annals Of The Rheumatic Diseases,* **50,** 369-371.

Fernandez, J.M., Neher, E., & Gomperts, B.D. (1984) Capacitance measurements reveal stepwise fusion events in degranulating mast cells. *Nature,* **312,** 453-455.

Finotto, S., Dolovich, J., Denburg, J.A., Jordana, M., & Marshall, J.S. (1994) Functional heterogeneity of mast cells isolated from different microenvironments within nasal polyp tissue. *Clinical And Experimental Immunology,* **95,** 343-350.

Flanagan, J.G., Chan, D.C., & Leder, P. (1991) Transmembrane form of the *kit* ligand growth factor is determined by alternative splicing and is missing in the Sl^d mutant. *Cell,* **64,** 1025-1035.

Flanagan, J.G. & Leder, P. (1990) The kit ligand: a cell surface molecule altered in steel mutant fibroblasts. *Cell,* **63,** 185-194.

Flint, K.C., Leung, K.B.P., Pearce, F.L., Hudspith, B.N., Brostoff, J., & Johnson, N.M. (1985) Human mast cells recovered by bronchoalveolar lavage: their morphology, histamine release and the effects of sodium cromoglycate. *Clinical Science,* **68,** 427-432.

Foreman JC. (1993) Introduction to mast cells and basophils. *Immunopharmacology of mast cells and basophils.* (Foreman JC, editor), Academic Press LTD. London: pp. 1-4.

Foreman, J.C., Hallet, M.B., & Mongar, J.L. (1977) The relationship between histamine secretion and $^{45}Ca^{2+}$ uptake by mast cells. *Journal of Physiology,* **271,** 193-214.

Foreman, J.C. & Mongar, J.L. (1972) The role of the alkaline earth ions in anaphylatic histamine secretion. *Journal of Physiology,* **224,** 753-769.

Foreman, J.C., Mongar, J.L., & Gomperts, B.D. (1973) Calcium ionophores and movement of calcium ions following the physiological stimulus to a secretory process. *Nature,* **245,** 249-251.

Friis, U.G., Johansen, T., Hayes, N.A., & Foreman, J.C. (1994) IgE-receptor activated chloride uptake in relation to histamine secretion from rat mast cells. *British Journal Of Pharmacology,* **111,** 1179-1183.

Fujihashi, K., Mcghee, J.R., Beagley, K.W., Mcpherson, D.T., Mcpherson, S.A., Huang, C.M., & Kiyono, H. (1993) Cytokine-specific ELISPOT assay: single cell analysis of IL-2, IL-4 and IL-6 producing cells. *Journal Of Immunological Methods,* **160,** 181-189.

Fukamachi, H., Kawakami, Y., Takei, M., Ishizaka, T., Ishizaka, K., & Kawakami, T. (1992) Association of protein tyrosine kinase with phospholipase C-γ-1 in bone marrow-derived mouse mast cells. *Proceedings Of The National Academy Of Sciences Of The United States Of America,* **89,** 9524-9528.

Fukamachi, H., Yamada, N., Miura, T., Kato, T., Ishikawa, M., Gulbins, E., Altman, A., Kawakami, Y., & Kawakami, T. (1994) Identification of a protein, spy75, with repetitive helix-turn-helix motifs and an SH3 domain as a major substrate for protein tyrosine kinase(s) activated by FcεRI cross-linking. *Journal Of Immunology,* **152,** 642-652.

Fukamachi, H., Takei, M., & Kawakami, T. (1993) Activation of multiple protein kinases including a MAP kinase upon FcεRI cross-linking. *International Archives Of Allergy And Immunology,* **102,** 15-25.

Furitsu, T., Saito, H., Dvorak, A.M., Schwartz, L.B., Irani, A.M.A., Burdick, J.F., Ishizaka, K., & Ishizaka, T. (1989) Development of human mast cells in vitro. *Proceedings Of The National Academy Of Sciences Of The United States Of America,* **86,** 10039-10043.

Galli, S.J. (1990) Biology of disease: new insights into the riddle of the mast cells - microenvironmental regulation of mast cell development and phenotypic heterogeneity. *Laboratory Investigation,* **62,** 5-33.

Galli, S.J., Iemura, A., Garlick, D.S., Gamba-Vitalo, C., Zsebo, K.M., & Andrews, R.G. (1993) Reversible expansion of primate mast cell populations *in vivo* by stem cell factor. *Journal Of Clinical Investigation,* **91,** 148-152.

Galli, S.J. & Kitamura, Y. (1987) Genetically mast cell-deficient W/W^v and Sl/Sl^d mice: their value for the analysis of the roles of mast cells in biologic responses *in vivo*. *American Journal Of Pathology,* **127,** 191-198.

Galli, S.J., Zsebo, K.M., & Geissler, E.N. (1994) The kit-ligand, stem cell factor. *Advances In Immunology,* **55,** 1-96.

Gat-Yablonski, G. & Sagi-Eisenberg, R. (1990) Evaluation of the role of inositol trisphosphate in IgE-dependent exocytosis. *Biochemical Journal,* **270,** 685-689.

Geissler, E.N., Ryan, M.A., & Houseman, D.E. (1988) The dominant white spotting (W) locus of the mouse encodes the *c-kit* proto-oncogene. *Cell,* **55,** 185-192.

Gericke, M., Dar, O., Droogmans, G., Pecht, I., & Nilius, B. (1995) Immunological stimulation of single rat basophilic leukemia RBL-2H3 cells co-activates Ca^{2+} entry and K^{+} channels. *Cell Calcium,* **17,** 71-83.

Gibson, S., Mackeller, A., Newlands, G.F.J., & Miller, H.R.P. (1987) Phenotypic expression of mast cell granule proteinases: distribution of mast cell proteinase-I and proteinase-II in the rat digestive system. *Immunology,* **62,** 621-627.

Gibson, S. & Miller, H.R.P. (1986) Mast cell subsets in the rat distinguished immunohistochemically by their content of serine proteinases. *Immunology,* **58,** 101-104.

Gilead, L., Liuni, N., Eliakim, R., Ligumsky, M., Fich, A., Oxon, E., Rachmilewitz, D., & Razin, E. (1987) Human gastric mucosal mast cells are chondroitin sulphate E-containing cells. *Immunology,* **62,** 23-28.

Girault, J. (1994) Protein kinases and phosphatases. *Neurotransmissions (published by Research Biochemicals International),* **10,** 1-6.

Glenert, U., Johansen, T., Hayes, N.A., & Foreman, J.C. (1993) The role of chloride ions in histamine secretion from rat mast cells. *Journal Of Physiology-London,* **459,** 184

Gomperts, B.D. (1983) Involvement of guanine nucleotide binding protein in the gating of Ca^{2+} by receptors. *Nature,* **306,** 64-66.

Gordon, J.R., Burd, P.R., & Galli, S.J. (1990) Mast cells as a source of multifunctional cytokines. *Immunology Today,* **11,** 458-464.

Gosling, M., Smith, J.W., & Poyner, D.R. (1995) Characterization of a volume-sensitive chloride current in rat osteoblast-like (ROS 17/2.8) cells. *J. Physiol,* **485,** 671-682.

Grencis, R.K., Else, K.J., Huntley, J.F., & Nishikawa, S.I. (1993) The in vivo role of stem cell factor (c-kit ligand) on mastocytosis and host protective immunity to the intestinal nematode *Trichinella spiralis* in mice. *Parasite Immunology,* **15,** 55-59.

Gurish, M.F., Pear, W.S., Stevens, R.L., Scott, M.L., Sokol, K., Ghildyal, N., Webster, M.J., Xuzhen, H., Austen, K.F., Baltimore, D., & Friend, D. (1995) Tissue-regulated differentiation and maturation of a *v-abl*-immortalized mast cell-committed progenitor. *Immunity,* **3,** 175-186.

Guy-Grand, D., Griscelli, C., & Vassali, P. (1978) The mouse gut T lymphocyte. Nature, origin and traffic in mice in normal and graft versus host conditions. *Journal Of Experimental Medicine,* **148,** 1661-1667.

Habara, Y. & Kanno, T. (1996) Perimetric $[Ca^{2+}]_i$ rise and exocytosis detected by ultraviolet laser scanning confocal microscopy in rat peritoneal mast cells. *Experimental Physiology,* **81,** 319-328.

Haig, D.M., Mckee, T.A., Jarrett, E.E.E., Woodbury, R., & Miller, H.R.P. (1982) Generation of mucosal mast cells is stimulated in vitro by factors derived from T-cells of helminth-infected rats. *Nature,* **300,** 188-190.

Haig, D.M., McMenamin, C., Gunneberg, C., Woodbury, R., & Jarrett, E.E.E. (1983) Stimulation of mucosal mast cell growth in normal and nude rat bone marrow cultures. *Proceedings Of The National Academy Of Sciences Of The United States Of America Biological Sciences,* **80,** 4499-4503.

Haig, D.M., McMenamin, C., Redmond, J., Brown, D., Young, I.G., Cohen, S.D.R., & Hapel, A.J. (1988) Rat IL-3 stimulates the growth of rat mucosal mast cells in culture. *Immunology,* **65,** 205-211.

Haig, D.M., Huntley, J.F., MacKellar, A., Newlands, G.F.J., Inglis, L., Sangha, R., Cohen, D., Hapel, A., Galli, S.J., & Miller, H.R.P. (1994) Effects of stem cell factor (kit-ligand) and interleukin-3 on the growth and serine proteinase expression of rat bone marrow-derived or serosal mast cells. *Blood,* **83,** 72-83.

Hamill, O.P., Marty, A., Neher, E., Sakmann, B., & Sigworth, F.J. (1981) Improved patch-clamp techniques for high-resolution current recording from cells and cell-free membrane patches. *Pflugers Archiv-European Journal Of Physiology,* **391,** 85-100.

Harvima RJ, Schwartz LB. (1993) Mast cell derived mediators. *Immunopharmacology of mast cells and basophils.* (Foreman JC, editor), Academic Press, London: pp. 115-138.

Hasthorpe, S. (1980) A hemopoietic cell line dependent upon a factor in pokeweed mitogen-stimulated spleen cell conditioned medium. *Journal Of Cellular Physiology,* **105,** 379-384.

He, D., Esquenazi-Behar, S., Soter, N.A., & Lim, H.W. (1990) Mast cell heterogeneity: functional comparison of purified mouse cutaneous and peritoneal mast cells. *Journal Of Investigative Dermatology,* **95,** 178-185.

Heavey, D.J., Ernst, P.B., Stevens, R.L., Befus, A.D., Bienenstock, J., & Austen, K.F. (1988) Generation of leukotriene C_4, leukotriene B_4 and prostaglandin D_2 by immunologically activated rat intestinal mucosa mast cells. *Journal Of Immunology,* **140,** 1953-1957.

Hide, I., Bennett, J.P., Pizzey, A., Boonen, G., Barsagi, D., Gomperts, B.D., & Tatham, P.E.R. (1993) Degranulation of individual mast cells in response to Ca^{2+} and guanine nucleotides: an all-or-none event. *Journal Of Cell Biology,* **123,** 585-593.

Hill, P.B., MacDonald, A.J., Thornton, E.M., Newlands, G.F.J., Galli, S.J., & Miller, H.R.P. (1996) Stem cell factor enhances immunoglobulin E-dependent mediator release from cultured rat bone marrow-derived mast cells: activation of previously unresponsive cells demonstrated by a novel ELISPOT assay. *Immunology,* **87,** 326-333.

Hirasawa, N., Scharenberg, A., Yamamura, H., Beaven, M.A., & Kinet, J.P. (1995) A requirement for Syk in the activation of the microtubule-associated protein kinase/ phospholipase-A2 pathway by FcεRI is not shared by a G protein-coupled receptor. *Journal Of Biological Chemistry,* **270,** 10960-10967.

Hirasawa, N., Santini, F., & Beaven, M.A. (1995) Activation of the mitogen-activated protein kinase cytosolic phospholipase A_2 pathway in a rat mast cell line: indications of different pathways for release of arachidonic acid and secretory granules. *Journal Of Immunology,* **154,** 5391-5402.

Holliday, M.R., Banks, E.M.S., Dearman, R.J., Kimber, I., & Coleman, J.W. (1994) Interactions of IFN-gamma with IL-3 and IL-4 in the regulation of serotonin and arachidonate release from mouse peritoneal mast cells. *Immunology,* **82,** 70-74.

Horigome, K., Bullock, E.D., & Johnson, E.M. (1994) Effects of nerve growth factor on rat peritoneal mast cells: survival promotion and immediate early gene induction. *Journal Of Biological Chemistry,* **269,** 2695-2702.

Horn, R. & Marty, A. (1988) Muscarinic activation of ionic currents measured by a new whole-cell recording method. *Journal Of General Physiology,* **92,** 145-159.

Horner, A.A. (1971) Macromolecular heparin from rat skin. *Journal Of Biological Chemistry,* **246,** 231-239.

Hoth, M. & Penner, R. (1992) Depletion of intracellular calcium stores activates a calcium current in mast cells. *Nature,* **355,** 353-356.

Hoth, M. & Penner, R. (1993) Calcium release-activated calcium current in rat mast cells. *Journal Of Physiology-London,* **465,** 359-386.

Huang, E., Nocka, K., Beier, D.R., Chu, T.Y., Buck, J., Lahm, H.W., Wellner, D., Leder, P., & Besmer, P. (1990) The hematopoietic growth factor KL is encoded by the Sl-locus and is the ligand of the c-kit receptor, the gene product of the W-locus. *Cell,* **63,** 225-233.

Hulett, M.D., McKenzie, I.F.C., & Hogarth, P.M. (1993) Chimeric Fc receptors identify immunoglobulin-binding regions in human FcγRII and FcεRI. *European Journal Of Immunology,* **23,** 640-645.

Hultner, L., Moeller, J., Schmitt, E., Jager, G., Reisbach, G., Ring, J., & Dormer, P. (1989) Thiol-sensitive mast cell lines derived from mouse bone marrow respond to a mast cell growth-enhancing activity different from both IL-3 and IL-4. *Journal Of Immunology,* **142,** 3440-3446.

Hultner, L., Druez, C., Moeller, J., Uyttenhouse, C., Schmitt, E., Rude, E., Dormer, P., & Van Snick, J. (1990) Mast cell growth enhancing activity (MEA) is structurally related and functionally identical to novel T cell growth factor P40/TCGFIII (interleukin 9). *European Journal Of Immunology,* **20,** 1413-1416.

Huntley, J.F., Gibson, S., Brown, D., Smith, W.D., Jackson, F., & Miller, H.R.P. (1987) Systemic release of a mast cell proteinase following nematode infections in sheep. *Parasite Immunology,* **9,** 603-614.

Huntley, J.F., George, A.M., Newlands, F.J., Irvine, J., & Miller, H.R.P. (1990a) Mapping of the rat mast cell granule proteinases RMCP-I and RMCP-II by enzyme linked immunosorbent assay and paired immunofluorescence. *APMIS,* **98,** 933-944.

Huntley, J.F., Gooden, C., Newlands, G.F.J., MacKellar, A., Lammas, D.A., Wakelin, D., Tuohy, M., Woodbury, R.G., & Miller, H.R.P. (1990b) Distribution of intestinal mast cell proteinase in blood and tissues of normal and *Trichinella*-infected mice. *Parasite Immunology,* **12,** 85-95.

Huppi, K., Mock, B.A., Hilgers, J., Kochan, J., & Kinet, J. (1988) Receptors for Fcε and Fcγ are linked on mouse chromosome 1. *Journal Of Immunology,* **141,** 2807-2810.

Huppi, K., Siwarski, D., Mock, B.A., & Kinet, J. (1989) Gene mapping of the three subunits of the high affinity FcR for IgE to mouse chromosomes 1 and 19. *Journal Of Immunology,* **143,** 3787-3791.

Iemura, A., Tsai, M., Ando, A., Wershil, B.K., & Galli, S.J. (1994) The *c-kit* ligand, stem cell factor, promotes mast cell survival by suppressing apoptosis. *American Journal Of Pathology,* **144,** 321-328.

Ihle, J.N., Keller, J., Oroszlan, S., Henderson, L.E., Copeland, T.D., Fitch, F., Prystowsky, M.B., Goldwasser, E., Schrader, J.W., Paraszynski, E., Dy, M., & Lebel, B. (1983) Biological properties of homogeneous interleukin 3. 1. Demonstration of WEHI-3 growth factor activity, mast cell growth factor activity, P-cell-stimulating factor activity, colony stimulating factor activity and histamine producing cell-stimulating factor activity. *Journal Of Immunology,* **131,** 282-287.

Innocenti, B., Pozzan, T., & Fasolato, C. (1996) Intracellular ADP modulates the Ca^{2+} release-activated Ca^{2+} current in a temperature-dependent and Ca^{2+}-dependent way. *Journal Of Biological Chemistry,* **271,** 8582-8587.

Irani, A.A., Schecter, N.M., Craig, S.S., Deblois, G., & Schwartz, L.B. (1986) Two types of human mast cells that have distinct neutral protease compositions. *Proceedings Of The National Academy Of Sciences Of The United States Of America,* **83,** 4464-4468.

Irani, A.M., Craig, S.S., Deblois, G., Elson, C.O., Schecter, N.M., & Schwartz, L.B. (1987) Deficiency of the tryptase-positive, chymase-negative mast cell type in gastrointestinal mucosa of patients with defective T lymphocyte function. *Journal Of Immunology,* **138,** 4381-4386.

Irani, A.M.A., Nilsson, G., Miettinen, U., Craig, S.S., Ashman, L.K., Ishizaka, T., Zsebo, K.M., & Schwartz, L.B. (1992) Recombinant human stem cell factor stimulates differentiation of mast cells from dispersed human fetal liver cells. *Blood,* **80,** 3009-3021.

Isersky, C., Taurog, J.D., Poy, G., & Metzger, H. (1978) Triggering of cultured neoplastic mast cells by antibodies to the receptor for IgE. *Journal Of Immunology,* **121,** 549-558.

Ishimoto, T., Akiba, S., Sato, T., & Fujii, T. (1994) Contribution of phospholipases A_2 and D to arachidonic acid liberation and prostaglandin D_2 formation with increase in intracellular Ca^{2+} concentration in rat peritoneal mast cells. *European Journal Of Biochemistry,* **219,** 401-406.

Ishizaka, T., Foreman, J.C., Sterk, A.R., & Ishizaka, K. (1979) Induction of calcium flux across the rat mast cell membrane by bridging IgE receptors. *Proceedings Of The National Academy Of Sciences Of The United States Of America,* **76,** 5858-5862.

Ishizaka, T., Mitsui, H., Yanagida, M., Miura, T., & Dvorak, A.M. (1993) Development of human mast cells from their progenitors. *Current Opinion In Immunology,* **5,** 937-943.

Ishizaka, T., Hirata, F., & Ishizaka, K. (1980) Stimulation of phospholipid methylation, Ca^{2+} influx and histamine release by bridging of IgE receptors on rat mast cells. *Proceedings Of The National Academy Of Sciences Of The United States Of America,* **77,** 1903-1906.

Ishizaka, T. & Ishizaka, K. (1978) Triggering of histamine release from rat mast cells by divalent antibodies against IgE receptors. *Journal Of Immunology,* **120,** 800-805.

Jaffar, Z.H. & Pearce, F.L. (1993) Some characteristics of the ATP-induced histamine release from and permeabilization of rat mast cells. *Agents And Actions,* **40,** 18-27.

Janiszewski, J., Bienenstock, J., & Blennerhassett, M. (1994) Picomolar doses of substance P trigger electrical responses in mast cells without degranulation. *American Journal Of Physiology,* **267,** C138-C145.

Jouvin, M.H.E., Adamczewski, M., Numerof, R., Letourneur, O., Valle, A., & Kinet, J.P. (1994) Differential control of the tyrosine kinases Lyn and Syk by the two signaling chains of the high affinity immunoglobulin E receptor. *Journal Of Biological Chemistry,* **269,** 5918-5925.

Kanakura, Y., Thompson, H., Nakano, T., Yamamura, T.I., Asai, H., Kitamura, Y., Metcalfe, D.D., & Galli, S.J. (1988) Multiple bidirectional alterations of phenotype and changes in proliferative potential during the in vitro and in vivo passage of clonal mast cell populations derived from mouse peritoneal mast cells. *Blood,* **72,** 877-885.

Kanner, B.I. & Metzger, H. (1983) Crosslinking of the receptors for immunoglobulin E depolarizes the plasma membrane of rat basophilic leukemia cells. *Proceedings Of The National Academy Of Sciences Of The United States Of America,* **80,** 5744-5748.

Kaplan, A.P., Reddigari, S., Baeza, M., & Kuna, P. (1991) Histamine releasing factors and cytokine-dependent activation of basophils and mast cells. *Advances In Immunology,* **50,** 237-260.

Kasugai, T., Tei, H., Okada, M., Hirota, S., Morimoto, M., Yamada, M., Nakama, A., Arizono, N., & Kitamura, Y. (1995) Infection with *Nippostrongylus brasiliensis* induces invasion of mast cell precursors from peripheral blood to small intestine. *Blood,* **85,** 1334-1340.

Katanuma, N., Kominami, E., Kobayashi, K., Banno, Y., Suzuki, K., Chichibu, K., Hamaguchi, Y., & Katsunuma, T. (1975) Studies on new intracellular proteases in various organs of the rat. 1. Purification and comparison of their properties. *European Journal Of Biochemistry,* **52,** 37-50.

Katz, H.R., Stevens, R.L., & Austen, K.F. (1985) Heterogeneity of mammalian mast cells differentiated in vivo and in vitro. *Journal Of Allergy And Clinical Immunology,* **76,** 250-259.

Kawakami, T., Inagaki, N., Takei, M., Fukamachi, H., Coggeshall, K.M., Ishizaka, K., & Ishizaka, T. (1992) Tyrosine phosphorylation is required for mast cell activation by FcεRI cross-linking. *Journal Of Immunology,* **148,** 3513-3519.

Kawanashi, H. (1986) Role of IgE as a mast cell development co-factor in the differentiation of murine gut-associated mast cells in vitro. *European Journal Of Immunology,* **16,** 689-692.

Kemeny DM. A practical guide to ELISA. Oxford: Pergamon Press; 1991.

Kinashi, T. & Springer, T.A. (1994) Steel factor and c-kit regulate cell matrix adhesion. *Blood,* **83,** 1033-1038.

Kinet, J., Metzger, H., Hakimi, J., & Kochan, J. (1987) A cDNA presumptively coding for the α subunit of the receptor with high affinity for immunoglobulin E. *Biochemistry,* **26,** 4605-4610.

Kinet, J., Blank, U., Ra, C., Metzger, H., & Kochan, J. (1988) Isolation and characterization of cDNAs coding for the β subunit of the high-affinity receptor for immunoglobulin E. *Proceedings Of The National Academy Of Sciences Of The United States Of America,* **85,** 6483-6487.

Kinet, J. (1990) The high affinity receptor for IgE. *Current Opinion In Immunology,* **2,** 499-505.

Kinet, J.P. (1992) The γ-ζ dimers of Fc receptors as connectors to signal transduction. *European Journal Of Immunology,* **4,** 43-48.

Kirshenbaum, A.S., Goff, J.P., Dreskin, S.C., Irani, A.M., Schwartz, L.B., & Metcalfe, D.D. (1989) IL-3 dependent growth of basophil-like cells and mastlike cells from human bone marrow. *Journal Of Immunology,* **142,** 2424-2429.

Kirshenbaum, A.S., Kessler, S.W., Goff, J.P., & Metcalfe, D.D. (1991) Demonstration of the origin of human mast cells from $CD34^+$ bone marrow progenitor cells. *Journal Of Immunology,* **146,** 1410-1415.

Kirshenbaum, A.S., Goff, J.P., Kessler, S.W., Mican, J.M., Zsebo, K.M., & Metcalfe, D.D. (1992) Effect of IL-3 and stem cell factor on the appearance of human basophils and mast cells from $CD34^+$ pluripotent progenitor cells. *Journal Of Immunology,* **148,** 772-777.

Kitamura, Y., Shimada, M., Hatanaka, K., & Miyano, Y. (1977) Development of mast cells from grafted bone marrow cells in irradiated mice. *Nature,* **268,** 442-443.

Kitamura, Y., Hatanaka, K., Murakami, M., & Shibata, H. (1979) Presence of mast cell precursors in peripheral blood of mice demonstrated by parabiosis. *Blood,* **53,** 1085-1088.

Kitamura, Y., Yokoyama, M., Matsuda, H., Ohno, T., & Mori, K.J. (1981) Spleen colony-forming cell as common precursor for tissue mast cells and granulocytes. *Nature,* **291,** 159-160.

Kitamura Y, Kasugai T, Nomura S, et al.(1993) Development of mast cells and basophils. *Immunopharmacology of mast cells and basophils.* (Foreman JC, editor), Academic Press, London: pp. 5-27.

Kitamura, Y. & Go, S. (1979) Decreased production of mast cells in Sl/Sl^{d} anemic mice. *Blood,* **53,** 492-497.

Kitamura, Y., Go, S., & Hatanaka, K. (1978) Decrease of mast cells in W/W^{v} mice and their increase by bone marrow transplantation. *Blood,* **52,** 447-452.

Kitamura, Y., Matsuda, H., & Hatanaka, K. (1979) Clonal nature of mast cell clusters in W/W^{v} mice after bone marrow transplantation. *Nature,* **281,** 154-155.

Knoop, F.C. & Thomas, D.D. (1984) Effect of cholera enterotoxin on calcium uptake and cyclic AMP accumilation in rat basophilic leukemia cells. *International Journal Of Biochemistry,* **16,** 275-280.

Kobayashi, T., Nakano, T., Nakahata, T., Asai, H., Yagi, Y., Tsuji, K., Komiyama, A., Akabane, T., Kojima, S., & Kitamura, Y. (1986) Formation of mast cell colonies in methylcellulose by mouse peritoneal cells and differentiation of these cloned cells in both the skin and the gastric mucosa of W/W^{v} mice: evidence that a common precursor can give rise to both connective tissue type and mucosal mast cells. *Journal Of Immunology,* **136,** 1378-1384.

Koffer, A., Tatham, P.E.R., & Gomperts, B.D. (1990) Changes in the state of actin during the exocytotic reaction of permeabilized rat mast cells. *Journal Of Cell Biology,* **111,** 919-927.

Koike, T., Hirai, K., Morita, Y., & Nozawa, Y. (1993) Stem cell factor-induced signal transduction in rat mast cells: activation of phospholipase D but not phosphoinositide-specific phospholipase C in c-kit receptor stimulation. *Journal Of Immunology,* **151,** 359-366.

Kulczycki, A. & Metzger, H. (1974) The interaction of IgE with rat basophilic leukemia cells: II Quantitative aspects of the binding reaction. *Journal Of Experimental Medicine,* **140,** 1676-1695.

Kuno, M., Shibata, T., Kawawaki, J., & Kyogoku, I. (1995) A heterogeneous electrophysiological profile of bone marrow-derived mast cells. *Journal Of Membrane Biology,* **143,** 115-122.

Kuno, M., Okada, T., & Shibata, T. (1989) A patch-clamp study: secretagogue-induced currents in rat peritoneal mast cells. *American Journal Of Physiology,* **256,** C560 C568.

Kusche, M., Lindahl, U., Enerback, L., & Roden, L. (1988) Identification of oversulfated galactosaminoglycans in intestinal mucosal mast cells of rats infected with the nematode *Nippostrongylus brasiliensis*. *Biochemical Journal,* **253,** 885-894.

Kuster, H., Thompson, H., & Kinet, J. (1990) Characterization and expression of the gene for the human Fc receptor γ subunit. Definition of a new gene family. *Journal Of Biological Chemistry,* **265,** 6448-6452.

Labrecque, G.F., Holowka, D., & Baird, B. (1989) Antigen-triggered membrane potential changes in IgE sensitized rat basophilic leukemia cells: evidence for a repolarizing response that is important in the stimulation of cellular degranulation. *The Journal of Immunology,* **142,** 236-243.

Labrecque, G.F., Holowka, D., & Baird, B. (1991) Characterization of increased K^+ permeability associated with the stimulation of receptors for immunoglobulin E on rat basophilic leukemia cells. *Journal Of Biological Chemistry,* **266,** 14912-14917.

Lantz, C.S. & Huff, T.F. (1995a) Differential responsiveness of purified mouse c-kit^+ mast cells and their progenitors to IL-3 and stem cell factor. *Journal Of Immunology,* **155,** 4024-4029.

Lantz, C.S. & Huff, T.F. (1995b) Murine kit^+ $lineage^-$ bone marrow progenitors express Fc-γ RII but do not express FcεRI until mast cell granule formation. *Journal Of Immunology,* **154,** 355-362.

Lavens, S.E., Peachell, P.T., & Warner, J.A. (1992) Role of tyrosine kinases in IgE-mediated signal transduction in human lung mast cells and basophils. *American Journal Of Respiratory Cell And Molecular Biology,* **7,** 637-644.

Lawrence, I.D., Warner, J.A., Cohan, V.L., Hubbard, W.C., Kagey-Sobotka, A., & Lichtenstein, L.M. (1987) Purification and characterization of human skin mast cells: evidence for human mast cell heterogeneity. *Journal Of Immunology,* **139,** 3062-3069.

LeConiat, M., Kinet, J., & Berger, R. (1990) The human genes for the α and γ subunits of the mast cell receptor for immunoglobulin E are located on human chromosome band 1q23. *Immunogenetics,* **32,** 183-186.

Lee, T.D.G., Shanahan, F., Miller, H.R.P., Bienenstock, J., & Befus, A.D. (1985a) Intestinal mucosal mast cells: isolation from rat lamina propria and purification using unit gravity velocity sedimentation. *Immunology,* **55,** 721-728.

Lee, T.D.G., Sterk, A., Ishizaka, T., Bienenstock, J., & Befus, A.D. (1985b) Number and affinity of receptors for IgE on enriched populations of isolated rat intestinal mast cells. *Immunology,* **55,** 363-366.

Leung, K.B.P., Barrett, K.E., & Pearce, F.L. (1984) Differential effects of anti-allergic compounds on peritoneal mast cells of the rat, mouse and hamster. *Agents And Actions,* **14,** 461-467.

Levi-Schaffer, F., Austen, K.F., Gravallese, P.M., & Stevens, R.L. (1986) Coculture of interleukin-3-dependent mouse mast cells with fibroblasts results in a phenotypic change of the mast cells. *Proceedings Of The National Academy Of Sciences Of The United States Of America,* **83,** 6485-6488.

Levi-Schaffer, F., Austen, K.F., Caulfield, J.P., Hein, A., Gravallese, P.M., & Stevens, R.L. (1987a) Co-culture of human lung-derived mast cells with mouse 3T3 fibroblasts: morphology and IgE-mediated release of histamine, prostaglandin D_2, and leukotrienes. *Journal Of Immunology,* **139,** 494-500.

Levi-Schaffer, F., Dayton, E.T., Austen, K.F., Hein, A., Caulfield, J.P., Gravallese, P.M., Liu, F.T., & Stevens, R.L. (1987b) Mouse bone marrow-derived mast cells cocultured with fibroblasts: morphology and stimulation-induced release of histamine, leukotriene B_4, leukotriene C_4, and prostaglandin D_2. *Journal Of Immunology,* **139,** 3431-3441.

Lewis, R.A., Soter, N.A., Diamond, P.T., Austen, K.F., Oates, J.A., & Roberts, L.J. (1982) Prostaglandin D_2 generation after activation of rat and human mast cells with anti-IgE. *Journal Of Immunology,* **129,** 1627-1631.

Lewis, R.S., Ross, P.E., & Cahalan, M.D. (1993) Chloride channels activated by osmotic stress in T lymphocytes. *Journal of General Physiology,* **101,** 801-826.

Li, W., Deanin, G.G., Margolis, B., Schlessinger, J., & Oliver, J. (1992a) FcεRI-mediated tyrosine phosphorylation of multiple proteins, including phospholipase C-γ 1 and the receptor $\beta\gamma_2$ complex, in RBL-2H3 rat basophilic leukemia cells. *Molecular And Cellular Biology,* **12,** 3176-3182.

Li, W., Hu, P., Skolnik, E.Y., Ullrich, A., & Schlessinger, J. (1992b) The SH2 and SH3 domain-containing Nck protein is oncogenic and a common target for phosphorylation by different surface receptors. *Molecular And Cellular Biology,* **12,** 5824-5833.

Lin, S.Q., Cicala, C., Scharenberg, A.M., & Kinet, J.P. (1996) The FcεRI-β subunit functions as an amplifier of FcεRI-γ-mediated cell activation signals. *Cell,* **85,** 985-995.

Lindau, M. & Fernandez, J.M. (1986a) IgE-mediated degranulation of mast cells does not require opening of ion channels. *Nature,* **319,** 150-153.

Lindau, M. & Fernandez, J.M. (1986b) A patch-clamp study of histamine-secreting cells. *Journal Of General Physiology,* **88,** 349-368.

Lindau, M. & Neher, E. (1988) Patch-clamp techniques for time-resolved capacitance measurements in single cells. *Pflugers Archiv-European Journal Of Physiology,* **411,** 137-146.

Liu, W.L., Bosman, L., Boulos, P.B., Lau, H.Y., & Pearce, F.L. (1990) Mast cells from human colonic mucosa and submucosa/muscle: a comparison with human lung mast cells. *Agents And Actions,* **30,** 70-73.

Lowman, M.A., Benyon, R.C., & Church, M.K. (1988) Human skin mast cells: effects of salbutamol and sodium chromoglycate on histamine release induced by anti-IgE and substance P. *Skin Pharmacology,* **1,** 63

Ludowyke, R.I., Peleg, I., Beaven, M.A., & Adelstein, R.S. (1989) Antigen-induced secretion of histamine and the phosphorylation of myosin by protein kinase C in rat basophilic leukemia cells. *Journal Of Biological Chemistry,* **264,** 12492-12501.

MacDonald, A.J., Haig, D.M., Bazin, H., McGuigan, A.C., Moqbel, R., & Miller, H.R.P. (1989) IgE-mediated release of rat mast cell protease-II, β-hexosaminidase and leukotriene-C_4 from cultured bone marrow-derived rat mast cells. *Immunology,* **67,** 414-418.

MacDonald AJ. PhD Thesis, University of London - Studies on mediator release by cultured rat bone marrow derived mast cells: potential relevance to helminth-induced intestinal inflammation. 1994.

MacDonald, A.J., Thornton, E.M., Newlands, G.F.J., Galli, S.J., Moqbel, R., & Miller, H.R.P. (1996) Rat bone marrow-derived mast cells co-cultured with 3T3 fibroblasts in the absence of T-cell derived cytokines require stem cell factor for their survival and maintain their mucosal mast cell-like phenotype. *Immunology,* **88,** 375-383.

MacGlashan, D. & Botana, L.M. (1993) Biphasic Ca^{2+} responses in human basophils: evidence that the initial transient elevation associated with the mobilization of intracellular calcium is an insufficient signal for degranulation. *Journal Of Immunology,* **150,** 980-991.

MacGlashan, D. & Guo, C.P. (1991) Oscillations in free cytosolic calcium during IgE-mediated stimulation distinguish human basophils from human mast cells. *Journal Of Immunology,* **147,** 2259-2269.

MacGlashan, D.W. (1995) Graded changes in the response of individual human basophils to stimulation: distributional behavior of events temporally coincident with degranulation. *Journal Of Leukocyte Biology,* **58,** 177-188.

Madden, K.B., Urban, J.F., Ziltener, H.J., Schrader, J.W., Finkelman, F.D., & Katona, I.M. (1991) Antibodies to IL-3 and IL-4 suppress helminth-induced intestinal mastocytosis. *Journal Of Immunology,* **147,** 1387-1391.

Malaviya, R., Ikeda, T., Ross, E., & Abraham, S.N. (1996) Mast cell modulation of neutrophil influx and bacterial clearance at sites of infection through TNF-α. *Nature,* **381,** 77-80.

Mao, S., Varin-Blank, N., Edidin, M., & Metzger, H. (1991) Immobilization and internalization of mutated IgE receptors in transfected cells. *Journal Of Immunology,* **146,** 958-966.

Margolis, B., Hu, P., Katzav, S., Li, W., Oliver, J.M., Ullrich, A., Weiss, A., & Schlessinger, J. (1992) Tyrosine phosphorylation of *vav* proto-oncogene product containing SH2 domain and transcription factor motifs. *Nature,* **356,** 71-74.

Martin, R.J., Thorn, P., Gration, K.A.F., & Harrow, I.D. (1992) Voltage-activated currents in somatic muscle of the nematode parasite *Ascaris suum. Journal of Experimental Biology,* **173,** 75-90.

Matsuda, H., Coughlin, M.D., Bienenstock, J., & Denburg, J.A. (1988a) Nerve growth factor promotes human hematopoietic colony growth and differentiation. *Proceedings Of The National Academy Of Sciences Of The United States Of America,* **85,** 6508-6512.

Matsuda, H., Switzer, J., Coughlin, M.D., Bienenstock, J., & Denburg, J.A. (1988b) Human basophilic cell differentiation promoted by 2.5S nerve growth factor. *International Archives Of Allergy And Applied Immunology,* **86,** 453-457.

Matsuda, H., Kannan, Y., Ushio, H., Kiso, Y., Kanemoto, T., Suzuki, H., & Kitamura, Y. (1991) Nerve growth factor induces development of connective tissue type mast cells *in vitro* from murine bone marrow cells. *Journal Of Experimental Medicine,* **174,** 7-14.

Matsuda, H. & Kitamura, Y. (1981) Migration of stromal cells supporting mast cell differentiation into open wound produced in the skin of mice. *Experimental Hematology,* **9,** 38-43.

Matthews, G., Neher, E., & Penner, R. (1989a) Chloride conductance activated by external agonists and internal messengers in rat peritoneal mast cells. *Journal Of Physiology-London,* **418,** 131-144.

Matthews, G., Neher, E., & Penner, R. (1989b) Second messenger-activated calcium influx in rat peritoneal mast cells. *Journal Of Physiology-London,* **418,** 105-130.

Mayrhofer, G. & Fisher, R. (1979) Mast cells in severely T-cell depleted rats and the response to infestation with *Nippostrongylus brasiliensis*. *Immunology,* **37,** 145-155.

McCloskey, M.A. (1988) Cholera toxin potentiates IgE-coupled inositol phospholipid hydrolysis and mediator secretion by RBL-2H3 cells. *Proceedings Of The National Academy Of Sciences Of The United States Of America,* **85,** 7260-7264.

McCloskey, M.A. & Qian, Y.X. (1994) Selective expression of potassium channels during mast cell differentiation. *Journal Of Biological Chemistry,* **269,** 14813-14819.

McMenamin, C., Haig, D.M., Gibson, S., Newlands, G.F.J., & Miller, H.R.P. (1987) Phenotypic analysis of mast cell granule proteinases in normal rat bone marrow cultures. *Immunology,* **60,** 147-149.

Meininger, C.J., Yano, H., Rottapel, R., Bernstein, A., Zsebo, K.M., & Zetter, B.R. (1992) The c-kit receptor ligand functions as a mast cell chemoattractant. *Blood,* **79,** 958-963.

Mekori, Y.A., Oh, C.K., & Metcalfe, D.D. (1993) IL-3-dependent murine mast cells undergo apoptosis on removal of IL-3: prevention of apoptosis by c-kit ligand. *Journal Of Immunology,* **151,** 3775-3784.

Mendoza, G.R. & Metzger, H. (1976) Distribution and valency of receptor for IgE on rodent mast cells and related tumour cells. *Nature,* **264,** 548-550.

Meng, X.J. & Weinman, S.A. (1995) Cyclic-AMP and volume-activated chloride conductance in rat hepatocytes. *Hepatology,* **22,** SS805

Metcalfe, D.D., Soter, N.A., Wasserman, S.I., & Austen, K.F. (1980) Identification of sulfated mucopolysaccharides including heparin in the lesional skin of a patient with mastocytosis. *Journal Of Investigative Dermatology,* **74,** 210-215.

Michels, W.A. (1963) The mast cells. *Annals Of The New York Academy Of Sciences,* **103,** 235-372.

Millard, P.J., Gross, D., Webb, W.W., & Fewtrell, C. (1988) Imaging asynchronous changes in intracellular Ca^{2+} in individual stimulated tumor mast cells. *Proceedings Of The National Academy Of Sciences Of The United States Of America,* **85,** 1854-1858.

Millard, P.J., Ryan, T.A., Webb, W.W., & Fewtrell, C. (1989) Immunoglobulin E receptor cross-linking induces oscillations in intracellular free ionized calcium in individual tumor mast cells. *Journal Of Biological Chemistry,* **264,** 19730-19739.

Miller, H.R.P. (1971) Immune reactions in mucous membranes III. The discharge of intestinal mast cells during helminth expulsion in the rat. *Laboratory Investigation,* **24,** 348-354.

Miller, H.R.P., Woodbury, R.G., Huntley, J.F., & Newlands, G. (1983) Systemic release of mucosal mast cell protease in primed rats challenged with *Nippostrongylus brasiliensis*. *Immunology,* **49,** 471-479.

Miller, H.R.P. (1993a) Immunopathology of gastrointestinal nematode infestation and expulsion. *Current Opinion In Gastroenterology,* **9,** 986-993.

Miller HRP. (1993b) Mast cells in the gastrointestinal tract. *Immunopharmacology of mast cells and basophils.* (Foreman JC, editor), Academic Press, London: pp. 197-215.

Miller, H.R.P. & Jarrett, W.F.H. (1971) Immune reactions in mucous membranes. 1. Intestinal mast cell response during helminth expulsion in the rat. *Immunology,* **20,** 277-288.

Mitsui, H., Furitsu, T., Dvorak, A.M., Irani, A.M.A., Schwartz, L.B., Inagaki, N., Takei, M., Ishizaka, K., Zsebo, K.M., Gillis, S., & Ishizaka, T. (1993) Development of human mast cells from umbilical cord blood cells by recombinant human and murine c-kit ligand. *Proceedings Of The National Academy Of Sciences Of The United States Of America,* **90,** 735-739.

Moeller, J., Hultner, L., Schmitt, E., & Dormer, P. (1989) Partial purification of a mast cell growth-enhancing activity and its separation from IL-3 and IL-4. *Journal Of Immunology,* **142,** 3447-3451.

Mohr, F.C. & Fewtrell, C. (1987a) IgE receptor-mediated depolarization of rat basophilic leukemia cells measured with the fluorescent probe bis-oxonol. *Journal Of Immunology,* **138,** 1564-1570.

Mohr, F.C. & Fewtrell, C. (1987b) Depolarization of rat basophilic leukemia cells inhibits calcium uptake and exocytosis. *Journal Of Cell Biology,* **104,** 783-792.

Monck, J.R., Oberhauser, A.F., Alverez de Toledo, G., & Fernandez, J.M. (1991) Is swelling of the secretory granule matrix the force that dilates the exocytic fusion pore? *Biophysical Journal,* **59,** 39-47.

Moqbel, R., King, S., J., MacDonald, A.J., Miller, H.R.P., Cromwell, O., Shaw, R.J., & Kay, A.B. (1986) Enteral and systemic release of leukotrienes during anaphylaxis of *Nippostrongylus brasiliensis*-primed rats. *Journal Of Immunology,* **137,** 296-301.

Mosmann, T.R., Schumacher, J.H., Street, N.F., Budd, R.C., O'Garra, A., Fong, T.A.T., Bond, M.W., Moore, K.W., Sher, A., & Fiorentino, D.F. (1991) Diversity of cytokine synthesis and function of mouse $CD4^+$ T cells. *Immunological Reviews,* **123,** 209-229.

Nabel, G., Galli, S.J., Dvorak, A.M., Dvorak, H.F., & Cantor, H. (1981) Inducer T lymphocytes synthesize a factor that stimulates proliferation of cloned mast cells. *Nature,* **291,** 332-334.

Nafziger, J., Arock, M., Guillosson, J.J., & Wietzerbin, J. (1990) Specific high-affinity receptors for interferon γ on mouse bone marrow-derived mast cells: inhibitory effect of interferon γ on mast cell precursors. *European Journal Of Immunology,* **20,** 113-117.

Nagao, K., Yokoro, K., & Aaronson, S.A. (1981) Continuous lines of basophil-mast cells derived from normal mouse bone marrow. *Science,* **212,** 333-335.

Nakahata, T., Spicer, S., Cantry, J.R., & Ogawa, M. (1982) Clonal assay of mouse mast cell colonies in methylcellulose culture. *Blood,* **127,** 788-794.

Nakahata, T. & Ogawa, M. (1982) Identification in culture of a class of hemopoietic colony-forming units with extensive capability to self renew and generate multipotential hemopoietic colonies. *Proceedings Of The National Academy Of Sciences Of The United States Of America,* **79,** 3843-3847.

Nakajima, K., Hirai, K., Yamaguchi, M., Takaishi, T., Ohta, K., Morita, Y., & Ito, K. (1992) Stem cell factor has histamine releasing activity in rat connective tissue-type mast cells. *Biochemical And Biophysical Research Communications,* **183,** 1076-1083.

Nakano, T., Sonoda, T., Hayashi, C., Yamatodani, A., Kanayama, Y., Yamamura, T., Asai, H., Yonezawa, T., Kitamura, Y., & Galli, S.J. (1985) Fate of bone marrow-derived cultured mast cells after intracutaneous, intraperitoneal, and intravenous transfer into genetically mast-cell deficient W/W^v mice: evidence that cultured mast cells can give rise to both connective tissue type and mucosal mast cells. *Journal Of Experimental Medicine,* **162,** 1025-1043.

Narashimhan, V., Holowka, D., Fewtrell, C., & Baird, B. (1988) Cholera toxin increases the rate of antigen-stimulated calcium influx in rat basophilic leukemia cells. *Journal Of Biological Chemistry,* **263,** 19626-19632.

Nawa, Y. & Miller, H.R.P. (1979) Adoptive transfer of the intestinal mast cell response in rats infected with *Nippostrongylus brasiliensis*. *Cellular Immunology,* **42,** 225-239.

Neher, E. (1988) The influence of intracellular calcium concentration on degranulation of dialyzed mast cells from rat peritoneum. *Journal Of Physiology-London,* **395,** 193-214.

Neher, E. & Almers, W. (1986) Fast calcium transients in rat peritoneal mast cells are not sufficient to trigger exocytosis. *EMBO Journal,* **5,** 51-53.

Newlands, G.F.J., Lammas, D.A., Huntley, J.F., MacKellar, A., Wakelin, D., & Miller, H.R.P. (1991) Heterogeneity of murine bone marrow-derived mast cells: analysis of their proteinase content. *Immunology,* **72,** 434-439.

Newlands, G.F.J., Miller, H.R.P., MacKellar, A., & Galli, S.J. (1995) Stem cell factor contributes to intestinal mucosal mast cell hyperplasia in rats infected with *Nippostrongylus brasiliensis* or *Trichinella spiralis*, but anti-stem cell factor treatment decreases parasite egg production during *N brasiliensis* infection. *Blood,* **86,** 1968-1976.

Nick, S., Metzger, B., Muller, S., & Falke, D. (1987) Virus-specific IgM and IgG antibody production by B-cells during herpes-simplex virus type-2 induced immunosuppression as analyzed by an immunospot assay. *J. Gen. Virol.* **68,** 1951-1959.

Nielsen, E.H. (1990) A filamentous network surrounding secretory granules from mast cells. *Journal Of Cell Science,* **96,** 43-46.

Nielsen, E.H., Braun, K., & Johansen, T. (1989) Reorganization of the subplasmalemmal cytoskeleton in association with exocytosis in rat mast cells. *Histology And Histopathology,* **4,** 473-477.

Nilius, B., Sehrer, J., Viana, F., Degreef, C., Raeymaekers, L., Eggermont, J., & Droogmans, G. (1994) Volume-activated Cl currents in different mammalian non-excitable cell types. *Pflugers Archiv-European Journal Of Physiology,* **428,** 364-371.

Nilsson, G., Blom, T., Harvima, I., Kuschegullberg, M., Nilsson, K., & Hellman, L. (1996) Stem cell factor-dependent human cord blood derived mast cells express α-tryptase and β-tryptase, heparin and chondroitin sulfate. *Immunology,* **88,** 308-314.

Nissim, A. & Eshhar, Z. (1992) The human mast cell receptor binding site maps to the third constant domain of immunoglobulin E. *Molecular Immunology,* **29,** 1065-1072.

Nissim, A., Jouvin, M., & Eshhar, Z. (1991) Mapping of the high affinity Fcε receptor binding-site to the third constant domain of IgE. *EMBO Journal,* **10,** 101-107.

Niwa, Y., Kasugai, T., Ohno, K., Morimoto, M., Yamazaki, M., Dohmae, K., Nishimune, Y., Kondo, K., & Kitamura, Y. (1991) Anemia and mast cell depletion in mutant rats that are homozygous at "white spotting (Ws)" locus. *Blood,* **78,** 1936-1941.

Nocka, K., Buck, J., Levi, E., & Besmer, P. (1990a) Candidate ligand for the c-kit transmembrane kinase receptor: KL, a fibroblast derived growth factor stimulates mast cells and erythroid progenitors. *EMBO Journal,* **9,** 3287-3294.

Nocka, K., Tan, J.C., Chiu, E., Chu, T.Y., Ray, P., Traktman, P., & Besmer, P. (1990b) Molecular bases of dominant negative and loss of function mutations at the murine c-kit / white spotting locus: W^{37}, W^{v}, W^{41} and W. *EMBO Journal,* **9,** 1805-1813.

Norman, J.C., Price, L.S., Ridley, A.J., Hall, A., & Koffer, A. (1994) Actin filament organization in activated mast cells is regulated by heterotrimeric and small GTP-binding proteins. *Journal Of Cell Biology,* **126,** 1005-1015.

Ody, C., Kindler, V., & Vassali, P. (1990) Interleukin 3 perfusion in W/W^{v} mice allows the development of macroscopic spleen colonies and restores cutaneous mast cell number. *Journal Of Experimental Medicine,* **172,** 403-406.

Oliver, J.M., Debra, L.B., Wilson, B.S., Mclaughlin, J.L., & Geahlen, R.L. (1994) Inhibition of mast cell FcεRI-mediated signalling and effector function by the Syk-selective inhibitor, piceatannol. *Journal Of Biological Chemistry,* **269,** 29697-29703.

Ortega, E., Schweitzerstenner, R., & Pecht, I. (1988) Possible orientational constraints determine secretory signals induced by aggregation of IgE receptors on mast cells. *EMBO Journal,* **7,** 4101-4109.

Ozawa, K., Szallasi, Z., Kazanietz, M.G., Blumberg, P.M., Mischak, H., Mushinski, J.F., & Beaven, M.A. (1993a) Ca^{2+}-dependent and Ca^{2+}-independent isozymes of protein kinase C mediate exocytosis in antigen stimulated rat basophilic RBL-2H3 cells - reconstitution of secretory responses with Ca^{2+} and purified isozymes in washed permeabilized cells. *Journal Of Biological Chemistry,* **268,** 1749-1756.

Ozawa, K., Yamada, K., Kazanietz, M.G., Blumberg, P.M., & Beaven, M.A. (1993b) Different isozymes of protein kinase C mediate feedback inhibition of phospholipase C and stimulatory signals for exocytosis in rat RBL-2H3 cells. *Journal Of Biological Chemistry,* **268,** 2280-2283.

Paolini, R., Jouvin, M.H., & Kinet, J.P. (1991) Phosphorylation and dephosphorylation of the high-affinity receptor for immunoglobulin E immediately after receptor engagement and disengagement. *Nature,* **353,** 855-858.

Paolini, R., Numerof, R., & Kinet, J.P. (1992) Phosphorylation/dephosphorylation of high-affinity IgE receptors: a mechanism for coupling/uncoupling a large signaling complex. *Proceedings Of The National Academy Of Sciences Of The United States Of America,* **89,** 10733-10737.

Parekh, A.B. & Penner, R. (1995) Depletion-activated calcium current is inhibited by protein kinase in RBL-2H3 cells. *Proceedings Of The National Academy Of Sciences Of The United States Of America,* **92,** 7907-7911.

Park, D.J., Min, H.K., & Rhee, S.G. (1991) IgE-induced tyrosine phosphorylation of phospholipase C-γ-1 in rat basophilic leukemia cells. *Journal Of Biological Chemistry,* **266,** 24237-24240.

Paterson, N.A.M., Wasserman, S.I., Said, J.W., & Austen, K.F. (1976) Release of chemical mediators from partially purified human lung mast cells. *Journal Of Immunology,* **117,** 1356-1362.

Pearce, F.L., Befus, A.D., Gauldie, J., & Bienenstock, J. (1982) Mucosal mast cells 2. Effects of anti-allergic compounds on histamine secretion by isolated intestinal mast cells. *Journal Of Immunology,* **128,** 2481-2486.

Penner, R., Matthews, G., & Neher, E. (1988) Regulation of calcium influx by second messengers in rat mast cells. *Nature,* **334,** 499-504.

Penner, R. & Neher, E. (1988) The role of calcium in stimulus-secretion coupling in excitable and non-excitable cells. *Journal of Experimental Biology,* **139,** 329-345.

Penner, R., Pusch, M., & Neher, E. (1987) Washout phenomena in dialyzed mast cells allow discrimination of different steps in stimulus-secretion coupling. *Bioscience Reports,* **7,** 313-321.

Plaut, M., Pierce, J.H., Watson, C.J., Hanleyhyde, J., Nordan, R.P., & Paul, W.E. (1989) Mast cell lines produce lymphokines in response to cross-linkage of FcεRI or to calcium ionophores. *Nature,* **339,** 64-67.

Qian, Y.X. & McCloskey, M.A. (1993) Activation of mast cell K^+ channels through multiple G protein-linked receptors. *Proceedings Of The National Academy Of Sciences Of The United States Of America,* **90,** 7844-7848.

Qiu, F., Ray, P., Brown, K., Barker, P.E., Jhanwar, S., Ruddle, F.H., & Besmer, P. (1988) Primary structure of *c-kit*: relationship with the CSF-1/PDGF receptor kinase family -oncogenic activation of *v-kit* involves deletion of extracellular domain and C-terminus. *EMBO Journal,* **7,** 1003-1011.

Ra, C., Jouvin, M.H.E., & Kinet, J.P. (1989) Complete structure of the mouse mast cell receptor for IgE (FcεRI) and surface expression of chimeric receptors (rat-mouse-human) on transfected cells. *Journal Of Biological Chemistry,* **264,** 15323-15327.

Rae, J., Cooper, K., Gates, P., & Watsky, M. (1991) Low access resistance perforated patch recordings using amphotericin B. *Journal of Neuroscience Methods,* **37,** 15-26.

Randriamampita, C. & Tsien, R.Y. (1993) Emptying of intracellular Ca^{2+} stores releases a novel small messenger that stimulates Ca^{2+} influx. *Nature,* **364,** 809-814.

Razin, E., Stevens, R.L., Akiyama, F., Schmid, K., & Austen, K.F. (1982) Culture from bone marrow of a subclass of mast cells possessing a distinct chondroitin sulfate proteoglycan with glycosaminoglycans rich in N-acetylgalactosamine-4,6-disulfate. *Journal Of Biological Chemistry,* **257,** 7229-7236.

Razin, E., Menciahuerta, J.M., Stevens, R.L., Lewis, R.A., Liu, F.T., Corey, E.J., & Austen, K.F. (1983) IgE-mediated release of leukotriene C_4, chondroitin sulfate E proteoglycan, β-hexosaminidase, and histamine from cultured bone marrow-derived mouse mast cells. *Journal Of Experimental Medicine,* **157,** 189-201.

Razin, E., Ihle, J.N., Seldin, D., Menciahuerta, J.M., Katz, H.R., Leblanc, P.A., Hein, A., Caulfield, J.P., Austen, K.F., & Stevens, R.L. (1984) Interleukin-3: a differentiation and growth factor for the mouse mast cell that contains chondroitin sulfate E proteoglycan. *Journal Of Immunology,* **132,** 1479-1486.

Razin, E., Cordon-Cardo, C., & Good, R.A. (1981) Growth of a pure population of mouse mast cells *in vitro* with conditioned medium derived from concanavalin A-stimulated splenocytes. *Proceedings Of The National Academy Of Sciences Of The United States Of America,* **78,** 2559-2561.

Rees, P.H., Hillier, K., & Church, M.K. (1988) The secretory characteristics of mast cells isolated from the human large intestinal mucosa and muscle. *Immunology,* **65,** 437-442.

Rennick, D., Hunte, B., Holland, G., & Thompson-Snipes, L. (1995) Cofactors are essential for stem cell factor-dependent growth and maturation of mast cell progenitors: comparative effects of interleukin-3 (IL-3), IL-4, IL-10, and fibroblasts. *Blood,* **85,** 57-65.

Reynolds, D.S., Stevens, R.L., Lane, W.S., Carr, M.H., Austen, K.F., & Serafin, W.E. (1990) Different mouse mast cell populations express various combinations of at least 6 distinct mast cell serine proteases. *Proceedings Of The National Academy Of Sciences Of The United States Of America,* **87,** 3230-3234.

Rhee, S.G., Shu, P.G., Ryu, S.H., & Lee, S.Y. (1989) Studies of inositol phospholipid-specific phospholipase C. *Science,* **244,** 546-550.

Riley, J.F. & West, G.B. (1953) The presence of histamine in tissue mast cells. *Journal of Physiology,* **120,** 528-537.

Riske, F., Hakimi, J., Mallamaci, M., Griffin, M., Pilson, B., Tobkes, N., Lin, P., Danho, W., Kochan, J., & Chizzonite, R. (1991) High-affinity human IgE receptor (FCεRI): analysis of functional domains of the α-subunit with monoclonal antibodies. *Journal Of Biological Chemistry,* **266,** 11245-11251.

Rodewald, H.R., Dessing, M., Dvorak, A.M., & Galli, S.J. (1996) Identification of a committed precursor for the mast cell lineage. *Science,* **271,** 818-822.

Rohlich, P. (1975) Membrane-associated actin filaments in the cortical cytoplasm of the rat mast cell. *Experimental Cell Research,* **93,** 293-298.

Roitt I, Brostoff J, Male D., *Immunology*, London, Mosby; 1993.

Romanin, C., Reinsprecht, M., Pecht, I., & Schindler, H. (1991) Immunologically activated chloride channels involved in degranulation of rat mucosal mast cells. *EMBO Journal,* **10,** 3603-3608.

Ru, X.M., Onoue, H., Nakayama, H., Ebi, Y., Fujita, J., Kasugai, T., & Kitamura, Y. (1990) Regulation of mast cell differentiation studied using the diffusion chamber technique. *Experimental Hematology,* **18,** 238-242.

Ruitenberg, E.J. & Elgersma, A. (1976) Absence of intestinal mast cell response in congenitally athymic mice during *Trichinella spiralis* infection. *Nature,* **264,** 258-260.

Sagi-Eisenberg R. (1993) Signal Transmission Pathways in Mast Cell Exocytosis. *Immunopharmacology of Mast Cells and Basophils.* (Foreman JC, editor), Academic Press, London: pp. 71-88.

Sagi-Eisenberg, R. & Pecht, I. (1983) Membrane potential changes during IgE-mediated histamine release from rat basophilic leukemia cells. *Journal Of Membrane Biology,* **75,** 97-104.

Saito, H., Ebisawa, M., Tachimoto, H., Shichijo, M., Fukagawa, K., Matsumoto, K., Iikura, Y., Awaji, T., Tsujimoto, G., Yanagida, M., Uzumaki, H., Takahashi, G., Tsuji, K., & Nakahata, T. (1996) Selective growth of human mast cells induced by steel factor, IL- 6, and prostaglandin E_2 from cord blood mononuclear cells. *Journal Of Immunology,* **157,** 343-350.

Schiller, S. & Dorfman, A. (1959) The isolation of heparin from mast cells of the normal rat. *Biochimica Et Biophysica Acta,* **31,** 278-280.

Schlessinger, J., Webb, W.W., Elson, E.L., & Metzger, H. (1976) Lateral motion and valence of Fc receptors on rat peritoneal mast cells. *Nature,* **264,** 550-552.

Schmitt, E., Fassbender, B., Beyreuther, K., Spaeth, E., Schwarzkopf, R., & Rude, E. (1987) Characterization of a T cell-derived lymphokine that acts synergistically with IL-3 on the growth of murine mast cells and is identical with IL-4. *Immunobiology,* **174,** 406-419.

Schneider, H., Cohendayag, A., & Pecht, I. (1992) Tyrosine phosphorylation of phospholipase C-γ-1 couples the Fcε receptor mediated signal to mast cell secretion. *International Immunology,* **4,** 447-453.

Schrader, J.W., Lewis, S.J., Clark-Lewis, I., & Culvenor, J.G. (1981) The persistent (P) cell: histamine content, regulation by a T cell-derived factor, origin from a bone marrow precursor and relationship to mast cells. *Proceedings Of The National Academy Of Sciences Of The United States Of America,* **78,** 323-327.

Schulman, E.S., MacGlashan, D.W., Peters, S.P., Schleimer, R.P., Newball, H.H., & Lichtenstein, L.M. (1982) Human lung mast cells: purification and characterization. *Journal Of Immunology,* **129,** 2662-2667.

Schwartz, L.B., Riedel, C., Caulfield, J.P., Wasserman, S.I., & Austen, K.F. (1981) Cell association of complexes of chymases, heparin proteoglycan, and protein after degranulation by rat mast cells. *Journal Of Immunology,* **126,** 2071-2078.

Schwartz, L.B., Irani, A.A., Roller, K., Castells, M.C., & Schecter, N.M. (1987) Quantitation of histamine, tryptase and chymase in dispersed human T and TC mast cells. *Journal Of Immunology,* **138,** 2611-2615.

Schwartz, L.B. (1994) Mast cells: function and contents. *Current Opinion In Immunology,* **6,** 91-97.

Scudamore, C.L., Pennington, A.M., Thornton, E., McMillan, L., Newlands, G.F.J., & Miller, H.R.P. (1995a) Basal secretion and anaphylactic release of rat mast cell protease-II (RMCP-II) from ex-vivo perfused rat jejunum: translocation of RMCP-II into the gut lumen and its relation to mucosal histology. *Gut,* **37,** 235-241.

Scudamore, C.L., Thornton, E.M., McMillan, L., Newlands, G.F., & Miller, H.R.P. (1995b) Release of the mucosal mast cell granule chymase, rat mast cell protease-II, during anaphylaxis is associated with the rapid development of paracellular permeability to macromolecules in rat jejunum. *Journal Of Experimental Medicine,*

Seder, R.A., Paul, W.E., Dvorak, A.M., Sharkis, S.J., Kagey-Sobotka, A., Niv, Y., Finkelman, F.D., Barieri, S.A., Galli, S.J., & Plaut, M. (1991) Mouse splenic and bone marrow populations that express high affinity ε receptor and produce interleukin 4 are highly enriched in basophils. *Proceedings Of The National Academy Of Sciences Of The United States Of America,* **88,** 2836-2839.

Sedgwick, J.D. & Czerkinsky, C. (1992) Detection of cell-surface molecules, secreted products of single cells and cellular proliferation by enzyme-immunoassay. *Journal Of Immunological Methods,* **150,** 159-175.

Sedgwick, J.D. & Holt, P.G. (1983) A solid-phase immunoenzymatic technique for the enumeration of specific antibody-secreting cells. *Journal Of Immunological Methods,* **57,** 301-309.

Seldin, D.C., Adelman, S., Austen, K.F., Stevens, R.L., Hein, A., Caulfield, J.P., & Woodbury, R.G. (1985) Homology of the rat basophilic leukemia cell and the rat mucosal mast cell. *Proceedings Of The National Academy Of Sciences Of The United States Of America,* **82,** 3871-3875.

Seldin, D.C., Austen, K.F., & Stevens, R.L. (1985) Purification and characterisation of protease-resistant secretory granule proteoglycans containing chondroitin sulfate di-B and heparin-like glycosaminoglycans from rat basophilic leukemia cells. *Journal Of Biological Chemistry,* **260,** 11131-11139.

Shalit, M., Pickholz, D., & Levishaffer, F. (1993) Mast cells retain their responsiveness upon continuous and repetitive exposure to antigen. *Immunology,* **79,** 319-324.

Shanahan, F., Denburg, J.A., Fox, J., Bienenstock, J., & Befus, D. (1985) Mast cell heterogeneity: effects of neuroenteric peptides on histamine release. *Journal Of Immunology,* **135,** 1331-1337.

Shiue, L., Zoller, M.J., & Brugge, J.S. (1995) Syk is activated by phosphotyrosine-containing peptides representing the tyrosine-based activation motifs of the high-affinity receptor for IgE. *Journal Of Biological Chemistry,* **270,** 10498-10502.

Sillaber, C., Strobl, H., Bevec, D., Ashman, L.K., Butterfield, J.H., Lechner, K., Maurer, D., Bettelheim, P., & Valent, P. (1991) IL-4 regulates c-kit proto-oncogene product expression in human mast and myeloid progenitor cells. *Journal Of Immunology,* **147,** 4224-4228.

Smith, C.A. & Renwick, D.M. (1986) Characterisation of a murine lymphokine distinct from interleukin 2 and interleukin 3 (IL-3) possessing a T-cell growth factor activity and a mast cell growth factor activity that synergizes with IL-3. *Proceedings Of The National Academy Of Sciences Of The United States Of America,* **83,** 1857-1861.

Smith, T.J. & Weis, J.H. (1996) Mucosal T-cells and mast cells share common adhesion receptors. *Immunology Today,* **17,** 60-63.

Sonoda, T., Ohno, T., & Kitamura, Y. (1982) Concentration of mast cell precursors in bone marrow, spleen and blood of mice determined by limiting dilution analysis. *Journal Of Cellular Physiology,* **112,** 136-140.

Spat, A., Bradford, P.G., McKinney, J.S., Rubin, R.P., & Putney, J.W. (1986) A saturable receptor for ^{32}P-inositol-1,4,5-trisphosphate in hepatocytes and neutrophils. *Nature,* **319,** 514-516.

Spat, A., Fabiato, A., & Rubin, R.P. (1986) Binding of inositol trisphosphate by a liver microsomal fraction. *Biochemical Journal,* **233,** 929-932.

Sterk, A.R. & Ishizaka, T. (1982) Binding properties of IgE receptors on normal mouse mast cells. *Journal Of Immunology,* **128,** 838-843.

Stevens, R.L., Lee, T.D.G., Seldin, D.C., Austen, K.F., Befus, A.D., & Bienenstock, J. (1986) Intestinal mucosal mast cells from rats infected with *Nippostrongylus brasiliensis* contain protease-resistant chondroitin sulfate di-B proteoglycans. *Journal Of Immunology,* **137,** 291-295.

Stevens, R.L., Fox, C.C., Lichenstein, L.M., & Austen, K.F. (1988) Identification of chondroitin sulfate E proteoglycans and heparin proteoglycans in the secretory granules of human lung mast cells. *Proceedings Of The National Academy Of Sciences Of The United States Of America,* **85,** 2284-2287.

Stoddard, J.S., Steinbach, J.H., & Simchowitz, L. (1993) Whole-cell Cl currents in human neutrophils induced by cell swelling. *American Journal Of Physiology,* **265,** C156-C165.

Streb, H., Irvine, R.F., Berridge, M.J., & Schulz, I. (1983) Release of Ca^{2+} from a non-mitochondrial intracellular store in pancreatic acinar cells by inositol 1,4,5-trisphosphate. *Nature,* **306,** 67-69.

Stump, R.F., Pfeiffer, J.R., Schneebeck, M.C., Seagrave, J.C., & Oliver, J.M. (1989) Mapping gold-labelled receptors on cell surfaces by back scattered electron imaging and digital image analysis: Studies of the IgE receptor on mast cells. *American Journal of Anatomy,* **185,** 128-141.

Swieter, M., Chan, B.M.C., Rimmer, C., McNeill, K., Froese, A., & Befus, D. (1989) Isolation and characterization of IgE receptors from rat intestinal mucosal mast cells. *European Journal Of Immunology,* **19,** 1879-1885.

Swieter, M., Midura, R.J., Nishikata, H., Oliver, C., Berenstein, E.H., Mergenhagen, S.E., Hascall, V.C., & Siraganian, R.P. (1993) Mouse 3T3 fibroblasts induce rat basophilic leukemia (RBL-2H3) cells to acquire responsiveness to compound 48/80. *Journal Of Immunology,* **150,** 617-624.

Taguchi, T., Mcghee, J.R., Coffman, R.L., Beagley, K.W., Eldridge, J.H., Takatsu, K., & Kiyono, H. (1990) Detection of individual mouse splenic T-cells producing IFN-γ and IL-5 using the enzyme-linked immunospot (ELISPOT) assay. *Journal Of Immunological Methods,* **128,** 65-73.

Tainsh, K.R. & Pearce, F.L. (1992) Mast cell heterogeneity: evidence that mast cells isolated from various connective tissue locations in the rat display markedly graded phenotypes. *International Archives Of Allergy And Immunology,* **98,** 26-34.

Takagi, M., Nakahata, T., Kubo, T., Shiohara, M., Koike, K., Miyajima, A., Arai, K.I., Nishikawa, S.I., Zsebo, K.M., & Komiyama, A. (1992) Stimulation of mouse connective tissue-type mast cells by hematopoietic stem cell factor, a ligand for the c-kit receptor. *Journal Of Immunology,* **148,** 3446-3453.

Takagi, M., Koike, K., & Nakahata, T. (1990) Antiproliferative effect of IFN-γ on proliferation of mouse connective tissue-type mast cells. *Journal Of Immunology,* **145,** 1880-1884.

Tamir, I., Schweitzerstenner, R., & Pecht, I. (1996) Immobilization of the type-1 receptor for IgE initiates signal transduction in mast cells. *Biochemistry,* **35,** 6872-6883.

Tan, J.C., Nocka, K., Ray, P., Traktman, P., & Besmer, P. (1990) The dominant W^{42} spotting phenotype results from a missense mutation in the *c-kit* receptor kinase. *Science,* **247,** 209-212.

Tarkowski, A., Czerkinsky, C., Nilsson, L.A., Nygren, H., & Ouchterlony, O. (1984) Solid-phase enzyme-linked immunospot (ELISPOT) assay for enumeration of IgG rheumatoid factor secreting cells. *Journal Of Immunological Methods,* **72,** 451-459.

Tatham, P.E.R., Duchen, M.R., & Millar, J. (1991) Monitoring exocytosis from single mast cells by fast voltammetry. *Pflugers Archiv-European Journal Of Physiology,* **419,** 409-414.

Taylor, A.M., Galli, S.J., & Coleman, J.W. (1996) Stem cell factor, the kit ligand, induces direct degranulation of rat peritoneal mast cells in vitro and in vivo: dependence of the in vitro effect on period of culture and comparisons of stem cell factor with other mast cell-activating agents. *Immunology,* **86,** 427-433.

Tei, H., Kasugai, T., Tsujimura, T., Adachi, S., Furitsu, T., Tohya, K., Kimura, M., Zsebo, K.M., Newlands, G.F.J., Miller, H.R.P., Kanakura, Y., & Kitamura, Y. (1994) Characterization of cultured mast cells derived from Ws/Ws mast cell-deficient rats with a small deletion at tyrosine kinase domain of c-kit. *Blood,* **83,** 916-925.

Tertian, G., Yung, Y.P., Guy-Grand, D., & Moore, M.A.S. (1981) Long term in vitro culture of murine mast cells. 1. Description of a growth factor-dependent culture technique. *Journal Of Immunology,* **127,** 788-794.

Thomas, P. & Przybilla, B. (1992) Activity of human IgE-secreting cells in atopic eczema (AE) patients - evaluation in a modified ELISPOT assay. *Journal Of Allergy And Clinical Immunology,* **89,** 337

Thompson, H.L., Schulman, E.S., & Metcalfe, D.D. (1988) Identification of chondroitin sulfate E in human lung mast cells. *Journal Of Immunology,* **140,** 2708-2713.

Thompson-Snipes, L.A., Dhar, V., Bond, M.W., Mosmann, T.R., Moore, K.W., & Rennick, D.M. (1991) Interleukin-10: a novel stimulatory factor for mast cells and their progenitors. *Journal Of Experimental Medicine,* **173,** 507-510.

Tsai, M., Shih, L.S., Newlands, G.F.J., Takeishi, T., Langley, K.E., Zsebo, K.M., Miller, H.R.P., Geissler, E.N., & Galli, S.J. (1991a) The rat c-kit ligand, stem cell factor, induces the development of connective tissue type and mucosal mast cells in vivo: analysis by anatomical distribution, histochemistry, and protease phenotype. *Journal Of Experimental Medicine,* **174,** 125-131.

Tsai, M., Takeishi, T., Thompson, H., Langley, K.E., Zsebo, K.M., Metcalfe, D.D., Geissler, E.N., & Galli, S.J. (1991b) Induction of mast cell proliferation, maturation, and heparin synthesis by the rat *c-kit* ligand, stem cell factor. *Proceedings Of The National Academy Of Sciences Of The United States Of America,* **88,** 6382-6386.

Tsai, M., Chen, R.H., Tam, S.Y., Blenis, J., & Galli, S.J. (1993) Activation of MAP kinases, $pp90^{rsk}$ and pp70-S6 kinases in mouse mast cells by signaling through the c-kit receptor tyrosine kinase or FcεRI: rapamycin inhibits activation of pp70-S6 kinase and proliferation in mouse mast cells. *European Journal Of Immunology,* **23,** 3286-3291.

Tsai, M., Tam, S.Y., & Galli, S.J. (1993) Distinct patterns of early response gene-expression and proliferation in mouse mast cells stimulated by stem cell factor, interleukin-3, or IgE and antigen. *European Journal Of Immunology,* **23,** 867-872.

Tsuji, K., Nakahata, T., Takagi, M., Kobayashi, T., Ishiguro, A., Kikuchi, T., Naganuma, K., Koike, K., Miyajima, A., Arai, K., & Akabane, T. (1990) Effects of interleukin-3 and interleukin-4 on the development of connective tissue-type mast cells: interleukin-3 supports their survival and interleukin-4 triggers and supports their proliferation synergistically with interleukin-3. *Blood,* **75,** 421-427.

Tsujimura, T., Hirota, S., Nomura, S., Niwa, Y., Yamazaki, M., Tono, T., Morii, E., Kim, H.M., Kondo, K., Nishimune, Y., & Kitamura, Y. (1991) Characterization of Ws mutant allele of rats: a 12 base deletion in tyrosine kinase domain of *c-kit* gene. *Blood,* **78,** 1942-1946.

Tuohy, M., Lammas, D.A., Wakelin, D., Huntley, J.F., Newlands, G.F.J., & Miller, H.R.P. (1990) Functional correlations between mucosal mast cell activity and immunity to *Trichinella spiralis* in high and low responder mice. *Parasite Immunology,* **12,** 675-685.

Valent, P., Schmidt, G., Besmer, J., Mayer, P., Zenke, G., Liel, E., Hinterberger, W., Lechner, K., Mauer, D., & Bettelheim, P. (1989) Interleukin-3 is a differentiation factor for human basophils. *Blood,* **73,** 1763-1769.

Valent, P., Besemer, J., Sillaber, C., Butterfield, J.H., Eher, R., Majdic, O., Kishi, K., Klepetko, W., Eckersberger, F., Lechner, K., & Bettelheim, P. (1990a) Failure to detect IL-3-binding sites on human mast cells. *Journal Of Immunology,* **145,** 3432-3437.

Valent, P., Majdic, O., Maurer, D., Bodger, M., Muhm, M., & Bettelheim, P. (1990b) Further characterization of surface-membrane structures expressed on human basophils and mast cells. *International Archives Of Allergy And Applied Immunology,* **91,** 198-203.

Valent, P., Spanblochl, E., Sperr, W.R., Sillaber, C., Zsebo, K.M., Agis, H., Strobl, H., Geissler, K., Bettelheim, P., & Lechner, K. (1992) Induction of differentiation of human mast cells from bone marrow and peripheral blood mononuclear cells by recombinant human stem cell factor / kit ligand in long term culture. *Blood,* **80,** 2237-2245.

Varin-Blank, N. & Metzger, H. (1990) Surface expression of mutated subunits of the high affinity mast cell receptor for IgE. *Journal Of Biological Chemistry,* **265,** 15685-15694.

Walsh, L.J. (1995) Ultraviolet-B irradiation of skin induces mast cell degranulation and release of tumor necrosis factor-α. *Immunology And Cell Biology,* **73,** 226-233.

Weetall, M., Shopes, B., Holowka, D., & Baird, B. (1990) Mapping the site of interaction between murine IgE and its high affinity receptor with chimeric Ig. *Journal Of Immunology,* **145,** 3849-3854.

Welham, M.J. & Schrader, J.W. (1992) Steel factor-induced tyrosine phosphorylation in murine mast cells: common elements with IL-3-induced signal transduction pathways. *Journal Of Immunology,* **149,** 2772-2783.

Wershil, B.K., Tsai, M., Geissler, E.N., Zsebo, K.M., & Galli, S.J. (1992) The rat c-kit ligand, stem cell factor, induces c-kit receptor-dependent mouse mast cell activation in vivo: evidence that signaling through the c-kit receptor can induce expression of cellular function. *Journal Of Experimental Medicine,* **175,** 245-255.

White, J.R., Ishizaka, T., Ishizaka, K., & Shaafi, R.I. (1984) Direct demonstration of increased intracellular concentration of free calcium as measured by quin-2 in stimulated rat peritoneal mast cells. *Proceedings Of The National Academy Of Sciences Of The United States Of America-Biological Sciences,* **81,** 3978-3982.

White, J.R. & Pearce, F.L. (1982) Characteristics of histamine secretion from rat peritoneal mast cells sensitized to the nematode *Nippostrongylus brasiliensis*. *Immunology,* **46,** 353-359.

Williams, D.E., Eisenman, J., Baird, A., Rauch, C., Vanness, K., March, C.J., Park, L.S., Martin, U., Mochizuki, D.Y., Boswell, H.S., Burgess, G.S., Cosman, D., & Lyman, S.D. (1990) Identification of a ligand for the c-kit protooncogene. *Cell,* **63,** 167-174.

Wilson, B.S., Deanin, G.G., Standefer, J.C., Vanderjagt, D., & Oliver, J.M. (1989) Depletion of guanine nucleotides with mycophenolic acid suppresses IgE receptor-mediated degranulation in rat basophilic leukemia cells. *Journal Of Immunology,* **143,** 259-265.

Wolf, P.E., Edidin, M., & Dragsten, P.R. (1980) Effect of bleaching light on measurements of lateral diffusion in cell membranes by fluorescence photobleaching recovery method. *Proceedings Of The National Academy Of Scienccs Of The United States Of America,* **77,** 2043-2045.

Woodbury, R.G., Everitt, M., Sanada, Y., Katanuma, N., Lagunoff, D., & Neurath, H. (1978a) An intracellular serine protease from rat skeletal muscle is the chymotrypsin-like enzyme of mast cells. *Proceedings Of The National Academy Of Sciences Of The United States Of America,* **75,** 5311-5313.

Woodbury, R.G., Katanuma, N., Kobayashi, K., Titani, K., & Neurath, H. (1978b) Structure of a group-specific protease from rat small intestine. *Biochemistry,* **17,** 811-819.

Woodbury, R.G., Miller, H.R.P., Huntley, J.F., Newlands, G.F.J., Palliser, A.C., & Wakelin, D. (1984) Mucosal mast cells are functionally active during spontaneous expulsion of intestinal nematode infections in rat. *Nature,* **312,** 450-452.

Woodbury, R.G., Gruzenski, G.M., & Lagunoff, D. (1978) Immunofluorescent localisation of a serine protease in rat small intestine. *Proceedings Of The National Academy Of Sciences Of The United States Of America,* **75,** 2785-2789.

Woodbury, R.G. & Neurath, H. (1980) Structure, specificity and localisation of serine proteases of connective tissue. *FEBS Letters,* **114,** 189-196.

Xu, X., Kitamura, K., Lau, K.S., Muallem, S., & Miller, R.T. (1995) Differential regulation of Ca^{2+} release-activated Ca^{2+} influx by heterotrimeric G-proteins. *Journal Of Biological Chemistry,* **270,** 29169-29175.

Yanagida, M., Fukamachi, H., Ohgami, K., Kuwaki, T., Ishii, H., Uzumaki, H., Amano, K., Tokiwa, T., Mitsui, H., Saito, H., Iikura, Y., Ishizaka, T., & Nakahata, T. (1995) Effects of T-helper 2-type cytokines, interleukin-3 (IL-3), IL-4, IL- 5, and IL-6 on the survival of cultured human mast cells. *Blood,* **86,** 3705-3714.

Yarden, Y., Kwang, W.J., Yang-Feng, T., Coussens, L., Munemitsu, S., Dull, T.J., Chen, E., Schlessinger, J., Francke, U., & Ulrich, A. (1987) Human proto-oncogene c-kit: a new cell surface receptor tyrosine kinase for an unidentified ligand. *EMBO Journal,* **6,** 3341-3351.

Yee, N.S., Langen, H., & Besmer, P. (1993) Mechanism of kit-ligand, phorbol ester, and calcium-induced down-regulation of c-kit receptors in mast cells. *Journal Of Biological Chemistry,* **268,** 14189-14201.

Yoshida, N., Everitt, M., Neurath, H., Woodbury, R.G., & Powers, J.C. (1980) Substrate specificity of two chymotrypsin-like proteases from rat mast cells. Studies with peptide 4-nitroanilides and comparison with cathepsin G. *Biochemistry,* **19,** 5799-5804.

Yu, K.T., Lyall, R., Jariwala, N., Zilberstein, A., & Haimovich, J. (1991) Antigen- and ionophore-induced signal transduction in rat basophilic leukemia cells involves protein tyrosine phosphorylation. *Journal Of Biological Chemistry,* **266,** 22564-22568.

Yurt, R.W., Leid, R.W., Austen, K.F., & Silbert, J.E. (1977) Native heparin from rat peritoneal mast cells. *Journal Of Biological Chemistry,* **252,** 518-521.

Zhang, J., Berenstein, E.H., Evans, R.L., & Siraganian, R.P. (1996) Transfection of Syk protein tyrosine kinase reconstitutes high-affinity IgE receptor-mediated degranulation in a Syk-negative variant of rat basophilic leukemia RBL-2H3 cells. *Journal Of Experimental Medicine,* **184,** 71-79.

Zhang, L. & McCloskey, M.A. (1995) Immunoglobulin E receptor-activated calcium conductance in rat mast cells. *Journal of Physiology,* **483,** 59-66.

Zhu, X., Jiang, M.S., Peyton, M., Boulay, G., Hurst, R., Stefani, E., & Birnbaumer, L. (1996) Trp, a novel mammalian gene family essential for agonist-activated capacitative Ca^{2+} entry. *Cell,* **85,** 661-671.

Zimmerberg, J., Curran, M., Cohen, F.S., & Brodwick, M. (1987) Simultaneous electrical and optical measurements show that membrane fusion precedes secretory granule swelling during exocytosis of beige mouse mast cells. *Proceedings Of The National Academy Of Sciences Of The United States Of America,* **84,** 1585-1589.

Zsebo, K.M., Williams, D.A., Geissler, E.N., Broudy, V.C., Martin, F.H., Atkins, H.L., Hsu, R.Y., Birkett, N.C., Okino, K.H., Murdock, D.C., Jacobsen, F.W., Langley, K.E., Smith, K.A., Takeishi, T., Cattanach, B.M., Galli, S.J., & Suggs, S.V. (1990a) Stem cell factor is encoded at the Sl-locus of the mouse and is the ligand for the c-kit tyrosine kinase receptor. *Cell,* **63,** 213-224.

Zsebo, K.M., Wypych, J., Mcniece, I.K., Lu, H.S., Smith, K.A., Karkare, S.B., Sachdev, R.K., Yuschenkoff, V.N., Birkett, N.C., Williams, L.R., Satyagal, V.N., Tung, W.F., Bosselman, R.A., Mendiaz, E.A., & Langley, K.E. (1990b) Identification, purification, and biological characterization of hematopoietic stem cell factor from buffalo rat liver conditioned medium. *Cell,* **63,** 195-201.

Zucker-Franklin, D., Grusky, G., Hirayama, N., & Schnipper, E. (1981) The presence of mast cell precursors in rat peripheral blood. *Blood,* **58,** 544-551.

Zweifach, A. & Lewis, R.S. (1993) Mitogen-regulated Ca^{2+} current of T lymphocytes is activated by depletion of intracellular Ca^{2+} stores. *Proceedings Of The National Academy Of Sciences Of The United States Of America,* **90,** 6295-6299.

Publications Arising From This Thesis

Abstracts presented at meetings

1. Hill, P.B., Thornton, E., Newlands, G.F.J., Galli, S.J. and Miller, H.R.P. (1994) The effect of recombinant rat stem cell factor on the IgE-mediated secretion of rat mast cell protease-II by individual bone marrow-derived mast cells (BMMC): quantification by a novel ELISPOT assay. *Immunology*, **83** (supplement 1), 81.

2. Hill, P.B., Martin, R.J. and Miller, H.R.P. (1996) Effects of temperature and cytoplasmic disruption on whole-cell membrane currents of rat bone marrow-derived mast cells. *Journal of Physiology*, **491P**, 90.

3. Hill, P.B., Martin, R.J. and Miller, H.R.P. (1996) A comparison of whole-cell currents in isolated mucosal and connective tissue rat mast cells. *Journal of Physiology*, **495P**, 84.

Publications

4. Hill, P.B., MacDonald, A.J., Thornton, E.M., Newlands, G.F.J., Galli, S.J. and Miller, H.R.P. (1996) Stem cell factor enhances immunoglobulin E-dependent mediator release from cultured rat bone marrow-derived mast cells: activation of previously unresponsive cells demonstrated by a novel ELISPOT assay. *Immunology*, **87**, 326-333.

5. Hill, P.B., Martin, R.J. and Miller, H.R.P. (1996) Characterization of whole-cell currents in mucosal and connective tissue rat mast cells using amphotericin B perforated patches and temperature control. *Pflugers Archiv - European Journal of Physiology*, **432**, 986-994.

6. Hill, P.B. and Thornton, E. (1997) Detection of mediator release from rat bone marrow-derived mast cells using a novel ELISPOT assay. *Advances in Veterinary Dermatology - Volume 3*, (in press).

A comparison of whole-cell currents in isolated mucosal and connective tissue rat mast cells

P.B. Hill, R.J. Martin and H.R.P. Miller

Departments of Preclinical Veterinary Sciences and Veterinary Clinical Studies, R(D)SVS, University of Edinburgh, Edinburgh EH9 1QH

Subpopulations of mast cells with distinct biochemical and functional characteristics have been identified in rodents and man. Based on their anatomical locations, these cells are designated mucosal mast cells or connective tissue mast cells and differ in terms of protease content, proteoglycan content, and response to secretagogues. Previous studies have shown that this heterogeneity also extends to their electrophysiological properties: mucosal-type mast cells possessed only a K^+-selective inwardly rectifying current (McCloskey & Qian, 1994), whereas connective tissue mast cells did not appear to have whole-cell currents unless stimulated with secretagogues or second messengers (Matthews *et al.* 1989). We recorded whole-cell currents in fifty-six rat bone marrow-derived mast cells (mucosal phenotype) and fifty-four rat peritoneal mast cells (connective tissue phenotype) using the amphotericin B perforated patch technique. Voltage steps were applied from −140 to +100 mV from a holding potential of −40 mV. The pipette solution contained (mM): 137 KCH_3SO_4 or KCl, 2·7 NaCl, 1 $CaCl_2$, 3 $MgCl_2$ and 10 Hepes; pH 7·3. The extracellular solution contained (mM): 137 NaCl, 2·7 KCl, 2 $CaCl_2$, 5 $MgCl_2$, 10 Hepes and 5·6 glucose; pH 7·3. Bath temperature was varied between room temperature (16–20 °C) and 37 °C with a Peltier device.

As previously reported, only the mucosal-type mast cells exhibited an inwardly rectifying K^+ current. However, in contrast to previous studies, we found that an outwardly rectifying chloride current could be demonstrated in both cell types. Important features of the current were: (1) activation at potentials more positive than −30 mV; (2) reduction in current amplitude and chloride conductance when the extracellular Cl^- concentration was reduced to 16·7 mM by substituting Na^+-isethionate for NaCl; (3) reversible blockade by the chloride channel blocker DIDS (20 μM); (4) dependence on temperature – the current could be elicited in a significant proportion of cells by increasing the bath temperature to > 25 °C; (5) dependence on a cytoplasmic component – the current was rarely observed when currents were recorded using the conventional whole-cell voltage clamp technique; (6) the current was more commonly observed and was greater in magnitude when peritoneal mast cells were incubated overnight in the presence of 10 ng ml^{-1} stem cell factor, an important survival factor for connective tissue mast cells; (7) the current could also be activated by a 33% decrease in extracellular osmolality.

The results show that an outwardly rectifying chloride conductance can be observed in both mucosal and connective tissue-type mast cells without stimulating the cells with secretagogues or intracellular second messengers. This current could help to maintain a negative membrane potential when mast cells degranulate, and may play a role in volume regulation.

Supported by the Wellcome Trust.

REFERENCES

McCloskey, M.A. & Qian, Y.X. (1994). *J. Biol. Chem.* **269**, 14813–14819.

Matthews, G., Neher, E. & Penner, R. (1989). *J. Physiol.* **418**, 131–144.

Effects of temperature and cytoplasmic disruption on whole-cell membrane currents of rat bone marrow-derived mast cells

P.B. Hill, R.J. Martin and H.R.P. Miller

Departments of Preclinical Veterinary Sciences and Veterinary Clinical Studies, R(D)SVS, University of Edinburgh, Edinburgh EH9 1QH

In recent studies, rat mucosal type mast cells were shown to possess only a K^+-selective inwardly rectifying current (IR_K) with conventional whole-cell patch clamp techniques at room temperature (Lindau & Fernandez, 1986; McCloskey & Qian, 1994). To determine if these results were influenced by recording conditions, we compared whole-cell membrane currents obtained from rat bone marrow-derived mast cells (BMMCs) at various temperatures using the amphotericin B perforated-patch and conventional whole-cell voltage clamp techniques. Voltage steps were applied from −100 to +40 mV from a holding potential of −40 mV. Pipette solutions contained (mM): 137 KCl, 2·7 NaCl, 1 $CaCl_2$, 3 $MgCl_2$ and 10 Hepes, pH 7·3 (perforated patch) and 137 KCl, 2·7 NaCl, 0·1 $CaCl_2$, 1 $MgCl_2$, 10 Hepes and 1 EGTA, pH 7·3 (conventional whole-cell). The extracellular solution contained (mM): 137 NaCl, 2·7 KCl, 2 $CaCl_2$, 5 $MgCl_2$, 10 Hepes and 5·6 glucose, pH 7·3. Bath temperature was varied between room temperature (16–20 °C) and 37 °C with a Peltier device.

The IR_K current was present in rat BMMCs at all temperatures with both recording techniques. In contrast, an outwardly rectifying (OR) current at potentials more positive than −30 mV was only observed with the perforated patch method or if the bath temperature was increased to > 25 °C (Table 1). Lowering the extracellular Cl^- concentration to 50 mM reduced the conductance of the OR current from 2·7 ± 2·1 to 0·51 ± 0·53 nS (mean ± S.D., $n = 5$) and shifted its reversal potential by +31 ± 21 mV (mean ± S.D., $n = 5$). The chloride channel blocker DIDS decreased the OR current conductance from 2·7 ± 2·2 to 1·1 ± 1·5 nS (mean ± S.D., $n = 5$), also indicating that the OR current was carried by Cl^- ions.

Table 1. Percentage of BMMCs showing the OR current under various experimental conditions

	16–20 °C	25–37 °C
Cytoplasm disrupted: conventional WCR	0% ($n = 30$)	40% ($n = 5$)
Cytoplasm preserved: perforated patch	26% ($n = 91$)	68% ($n = 59$)

WCR, whole-cell recording.

The results indicate that detection of certain whole-cell currents depends upon experimental methodology. The effect of temperature and cytoplasmic disruption suggests that the OR_{Cl} current is dependent on a cytoplasmic messenger but it does not require stimulation of the cell with secretagogues for its activation. Activation of the current by depolarization suggests that it may contribute to the repolarization of the membrane potential that occurs following stimulation of mast cells with antigen, thus allowing sustained Ca^{2+} entry essential for exocytosis.

Supported by the Wellcome Trust.

REFERENCES

Lindau, M. & Fernandez, J.M. (1986). *J. Gen. Physiol.* **88**, 349–368.

McCloskey, M.A. & Qian, Y.X. (1994). *J. Biol. Chem.* **269**, 14813–14819.

Pflügers Arch – Eur J Physiol (1996) 432:986–994

ORIGINAL ARTICLE

P. B. Hill · R. J. Martin · H. R. P. Miller

Characterization of whole-cell currents in mucosal and connective tissue rat mast cells using amphotericin-B-perforated patches and temperature control

Received: 10 May 1996 / Received after revision: 4 July 1996 / Accepted: 8 July 1996

Abstract Rat mucosal type mast cells are thought to possess only a K^+-selective inwardly rectifying (IR_K) current in the resting state. We used rat-bone-marrow-derived mast cells (BMMCs) as a model of mucosal mast cells and recorded whole-cell membrane currents from cells perforated with amphotericin B. Under these conditions, both inwardly rectifying (IR) and outwardly rectifying (OR) currents were observed. The reversal potential and conductance of the IR current depended on the extracellular K^+ concentration, indicating that the channel was K^+ selective. The OR current was not affected by changes in extracellular K^+ concentration, but lowering extracellular Cl^- concentration reduced the conductance and shifted the reversal potential in a positive direction. The OR current was not affected by K^+ channel blockers, but was reversibly blocked by the chloride channel blocker 4,4'-diisothiocyanato-2,2'-stilbenedisulphonate (DIDS), again indicating a Cl^- conductance. The IR_K current was also detected in the majority of cells using the conventional whole-cell recording configuration at room temperature. In contrast, the OR_{Cl} current was only observed in 7% of recordings made at room temperature with the conventional whole-cell voltage-clamp mode, but was detected in 66% of cells if the bath temperature was increased and the integrity of the cell's cytoplasm was preserved by using the perforated-patch technique. Under similar conditions, the OR_{Cl} current was also present in rat peritoneal mast cells, a connective tissue phenotype previously thought to have no whole-cell currents in the resting state. The role of this current and factors affecting its activation are discussed.

P. B. Hill (✉) · R. J. Martin
Department of Preclinical Veterinary Sciences,
Royal (Dick) School of Veterinary Studies,
The University of Edinburgh,
Summerhall, Edinburgh, EH9 1QH, Scotland

H. R. P. Miller
Department of Veterinary Clinical Studies,
Royal (Dick) School of Veterinary Studies,
The University of Edinburgh, Scotland

Key words Mast cells · Whole-cell currents · K^+ channels · Cl^- channels · Inward rectifier

Introduction

Recent electrophysiological studies have suggested that mast cells can possess two types of ion channel that regulate the resting membrane potential: an inwardly rectifying K^+ (IR_K) current [18, 22, 28] and an outwardly rectifying Cl^- (OR_{Cl}) current [14]. The presence or absence of these currents depended on the phenotype of the mast cell (connective tissue or mucosal), and on the species from which the cells were derived. In mouse bone-marrow-derived mast cells (BMMCs), which can differentiate into different phenotypes, both currents were observed either concurrently or individually [14]. Rat BMMCs [22] and RBL-2H3 cells [18, 28], both mucosal phenotypes, only possessed the IR_K current in the resting state. In contrast, neither the IR_K nor the OR_{Cl} currents were present in resting rat peritoneal mast cells, an example of the connective tissue type [18, 22].

Other membrane currents have been described to occur in rat mast cells but only when various second messengers were included in the pipette solution or when the cell was stimulated with secretagogues. These messenger or ligand-activated channels include: Ca^{2+}-permeable channels [13, 20]; cation-selective channels [3, 13, 20]; outwardly rectifying K^+ channels [22, 28]; and outwardly rectifying chloride channels [2, 21, 27, 30]. These channels have been implicated in the process of degranulation, because their activity was only detectable following stimulation of the cells and not in the resting state.

The conventional whole-cell recording configuration, as used in the previous studies, causes dialysis of the intracellular milieu and loss of many cytoplasmic components including solutes and messengers [10, 26]; in addition the above-described experiments were performed at room temperature. To determine if these factors influenced the electrophysiological properties of mast cells, we measured whole-cell currents of mucosal and con-

nective tissue type rat mast cells at various temperatures using the amphotericin-B-perforated-patch technique. We report that an outwardly rectifying chloride current, previously described to occur only in rat mast cells stimulated with secretagogues, is present in both mucosal and connective tissue type mast cells in the resting state.

Materials and methods

Cell preparation

Male Wistar rats between 175 g and 200 g (Moredun Research Institute, Edinburgh, UK) were exsanguinated whilst deeply anasthetized with halothane and used as donors of bone marrow, peritoneal cells and for preparation of lymph node conditioned medium (LNCM). The preparation of bone-marrow-derived cultured mast cells and the production of LNCM have been described [6]. Briefly, femoral bone marrow cells from healthy rats were cultured at 2.5×10^5 to 5×10^5 cells/ml in Iscove's Modified Dulbecco's Medium (IMDM, Gibco-BRL, Paisley, UK) supplemented with 20% horse serum (Advanced Protein Products, Brierley Hill, UK), penicillin (100 IU/ml), and streptomycin (100 µg/ml). The cells were stimulated with batch-tested LNCM at 10–25% v/v, and re fed every 2–5 days. The percentage of mast cells was determined by differential counts (400 cells) of Leishman's stained cytocentrifuge preparations. Mature cultures (n = 12) ranging in age from 13 to 37 days and each containing more than 85% mast cells were used for these experiments, with consistent results. Cells taken at this stage of culture can be regarded as mature as judged by the degree of cytoplasmic granularity and in their content of the mucosal mast-cell-specific protease, rat mast cell protease-II [8].

Peritoneal mast cells were collected by peritoneal lavage with Hanks Balanced Salt Solution (HBSS) containing 2% fetal calf serum (FCS), penicillin/streptomycin and 10 units/ml heparin. Cells were washed twice, re suspended in 30% Percoll and layered on top of a two-stage Percoll density step gradient consisting of 4 ml of 1.09 g/ml over 2 ml of 1.1 g/ml. After centrifugation at 500 g for 20 min, a pellet containing >95% mast cells was obtained. The cells were washed three times in HBSS and re-suspended at a concentration of 2×10^5 to 4×10^5 cells/ml in RPMI medium (Gibco-BRL) containing 10% FCS. Peritoneal mast cells were either used on the day of collection, or were incubated for 24–48 h in the presence or absence of 10 ng/ml recombinant rat stem cell factor ($rrSCF^{164}$), an important mast cell survival, growth and differentiation factor [5].

Solutions and reagents

For amphotericin-B-perforated-patch recording, the pipette solutions contained (in mM): 137 KCl or KCH_3SO_4, 2.7 NaCl, 1 $CaCl_2$, 3 $MgCl_2$, 10 HEPES (pH 7.3) and for conventional whole-cell recording (in mM): 137 KCl or KCH_3SO_4, 2.7 NaCl, 0.1 $CaCl_2$, 1 $MgCl_2$, 10 HEPES, 1 EGTA (pH 7.3). Mast cell Ringer was used as the extracellular solution and contained (in mM): 137 NaCl, 2.7 KCl, 2 $CaCl_2$, 5 $MgCl_2$, 10 HEPES, 5.6 glucose (pH 7.3). In some experiments, NaCl was replaced with KCl to make extracellular solutions containing 10, 50, 90, 137 or 165 mM KCl. Low Cl^- solutions containing 51 and 14 mM Cl^- were made by substituting Na acetate and K acetate for NaCl and KCl respectively, and a low Cl^- solution containing 16.7 mM Cl^- was prepared by substituting Na-isethionate for NaCl. Amphotericin B was obtained from Calbiochem, UK, and the channel blockers 4,4'-diisothiocyanato 2,2' stilbenedisulphonate (DIDS), 4 aminopyridine, and tetraethylammonium chloride (TEA) were obtained from Sigma, Poole, UK. $rrSCF^{164}$ was kindly provided by Dr. Keith Langley of Amgen, Thousands Oak, Calif., USA.

Whole-cell recordings

For electrophysiological recording, mast cells were re-suspended in mast cell Ringer, plated onto glass coverslips, and incubated at 37°C for up to 7 h before being placed in the recording chamber. Both mast cell phenotypes adhered to untreated glass without need for further immobilization. Any contaminating macrophages in the preparations could be discerned by their large size and lack of cytoplasmic granularity. Perforated-patch recordings were performed using amphotericin B to permeabilize the membrane as described elsewhere [29]. Briefly, 2 µl of a 50 mg/ml stock solution of amphotericin B in dimethylsulphoxide (DMSO) (Sigma) was added to 0.5 ml of pipette solution to yield a final concentration of 200 µg/ml. Sylgard-coated pipettes were heat polished to resistances between 0.5 and 2.5 MΩ and their tips were filled to ~150 µm with pipette solution free of amphotericin B. Pipettes were then back filled with the amphotericin B/pipette solution before being used immediately to obtain a gigaohm seal. Perforation of the membrane patch, as revealed by the appearance of slow capacitance transients, occurred within 5–25 min and recordings were only made when the access resistance fell to less than 25 MΩ. Capacitance transients were cancelled using capacitive cancellation circuitry on the amplifier which yielded the whole-cell capacitance and access resistance. Conventional whole-cell voltage-clamp recordings were performed as described [7], and the results were compared to those obtained with the perforated patch technique.

Whole cell voltage clamp recording (in both configurations) was performed with a patch clamp amplifier (EPC 7, List). The reference electrode was an Ag-AgCl wire which, in ion substitution experiments, was connected to the bath solution through an agar bridge containing 150 mM KCl. In control experiments, junctional potentials that developed at this interface were less than 1 mV and no corrections were made. When the KCl in the pipette solutions was replaced with KCH_3SO_4, large junctional potentials developed at the pipette solution/pipette electrode interface. These could not be cancelled using the pipette offset potential circuitry on the amplifier. To overcome this problem, a fine open-ended plastic tube containing 150 mM KCl in 5% agar was placed over the pipette electrode which acted as an agar bridge between the electrode and the pipette solution (modified from [1]). The zero-current potential before formation of the gigaohm seal was set to 0 mV. Voltage pulses of 200 ms duration were applied every second from –100 mV to +40 mV in 10-mV steps from the holding potential of –40 mV. In some experiments, this protocol was extended from –140 mV to +100 mV to accentuate the currents (see Results and legends). The voltage pulses and membrane currents were stored digitally on video tape and on a continuous pen recording. Currents were filtered at 2 kHz by an 8-pole Bessel filter, digitized with an analogue–digital converter (CED 1401, Cambridge, UK), and stored with the voltage pulses on a personal computer for later analysis. Current/voltage (I/V) relationships were generated and analysed with the CED voltage-clamp software in which currents were sampled at 1 kHz and averaged over a 20-ms period. In most cases, the currents were sampled in the middle of the 200-ms pulse. However, if there was evidence of time-dependent inactivation, the currents were sampled in the region of the peak. Leak currents determined from the linear range of the I/V curve were subtracted before calculating slope conductances using a least squares fit to data points between –140 mV to –100 mV and +80 mV to +100 mV. Due to the magnitude of inward currents in high-K^+ buffers, conductances in these conditions were calculated in the range –100 mV to –80 mV.

Bath temperature was varied between room temperature (16–20°C) and 37°C with a Peltier device (Firbank Electronics, UK). We found that, at 37°C, the stability of the pipette membrane seal was unreliable, often resulting in breakdown of the preparation. We therefore increased the temperature of the extracellular solution in the recording chamber in approximately 5°C increments, and recorded the whole-cell currents at 25°C, 30°C and 37°C if possible. Each temperature change took approximately 2 min. For some of the statistical analysis, data acquired at the

three temperatures have been grouped and results reported for the range 25–37°C. Solution changes were made by perfusion and aspiration of the bath (chamber volume 4 ml) which took from 30 s to 2 min depending on flow rate. During solution exchange, the perfusate passed over the activated Peltier element before reaching the cells; the bath temperature typically decreased by 2–3 °C during this time but this did not affect the current recordings described here.

Statistical analysis

Conductances are expressed as mean ± SD. Comparisons between conventional whole-cell recordings and perforated-patch recordings were made by unpaired Student's *t*-tests. Conductances at room temperature (16–20°C) were compared to those in the range 25–37°C by paired or unpaired Student's *t*-tests, depending on whether recordings were obtained in both ranges from the same cell. Because of small group sizes with non-parametric distributions, conductances at each temperature increment were compared using Kruskal-Wallis and Mann-Whitney tests.

Results

Whole-cell currents in rat BMMCs

I/V relationships obtained from 79 rat BMMCs perforated with amphotericin B and warmed to temperatures between 25 and 37°C showed two types of voltage-dependent current. An inwardly rectifying (IR) current was rapidly activated by hyperpolarizing potential steps (Fig. 1A), and an outwardly rectifying (OR) current was seen in cells depolarized to positive potentials (Fig. 1B). At potentials between –100 mV and +40 mV, the OR currents were instantaneous and sustained, but at higher potentials the current exhibited time-dependent inactivation (see later). A total of 37 cells (47%) showed the inwardly and outwardly rectifying currents concurrently (Fig. 1C). An additional 15 cells (19%) showed only the outward current, and in 14 cells (18%) only the inward current was observed. In some cells (16%), no voltage-dependent currents were observed and the *I/V* relationship represented a basal leak conductance. Both the IR and OR currents were observed when recording with pipette solutions containing either KCl or KCH_3SO_4, suggesting that movement of Cl^- from the pipette into the cell was not responsible for induction of the currents.

The IR and OR conductances in the range of 25–37°C were 1.74 ± 1.1 nS (n = 41) and 2.21 ± 1.4 nS (n = 31) respectively. The capacitance of rat BMMCs was 4.8 ± 1.5 pF (mean ± SD, n = 116), but this did not correlate with the IR or OR conductances, suggesting that the currents were not directly dependent on membrane area. The mean leak conductance in the range of 25–37°C was 0.75 ± 0.62 nS (n = 53).

Ionic selectivity of the currents

The IR currents observed to occur in our rat BMMCs were very similar in appearance to those described to be present in RBL-2H3 cells [18, 28], rat BMMCs grown in the presence of interleukin-3 (IL-3) [22], and cultured mouse BMMCs [14], in which the currents were characterized as a K^+-selective inward rectifier. Our *I/V* curves were characterized by inward currents at potentials more negative

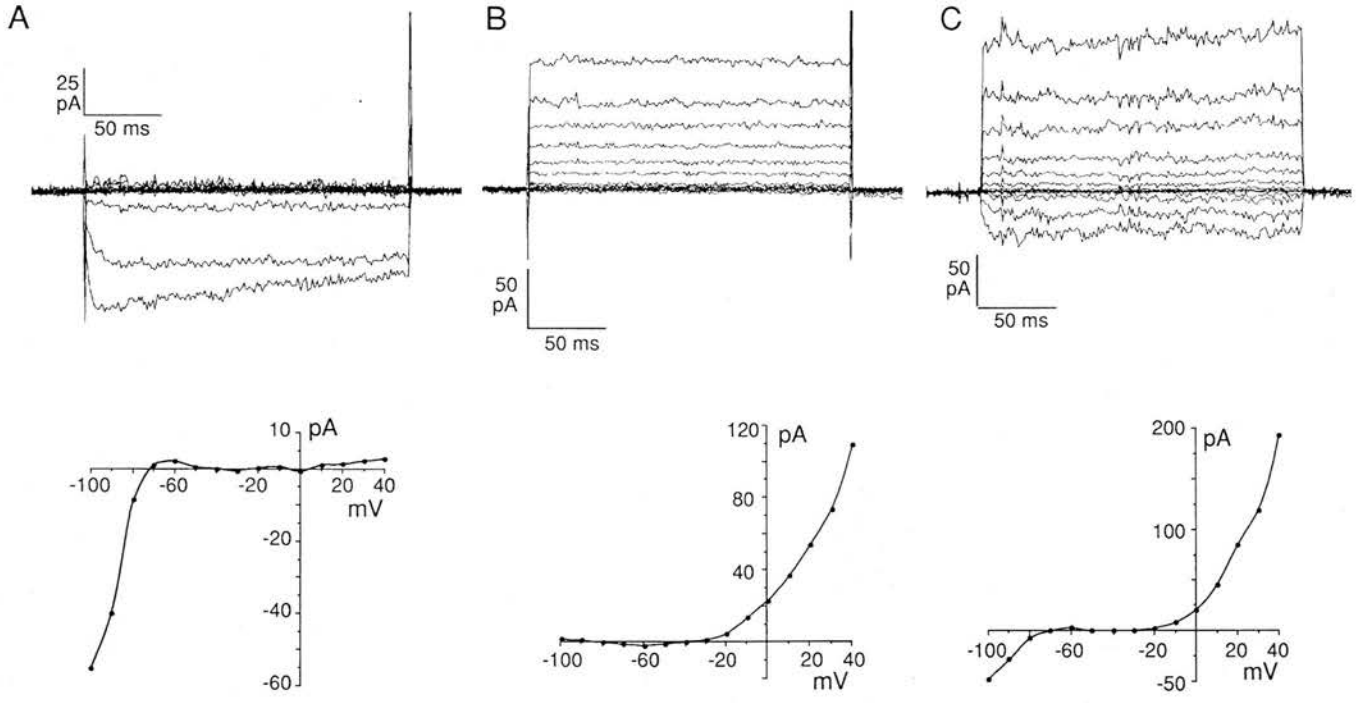

Fig. 1A–C Whole-cell membrane currents recorded from amphotericin B perforated rat bone marrow derived mast cells (BMMCs) with accompanying leak-subtracted current/voltage (*I/V*)relationships. Cells were clamped at a holding potential of –40 mV and voltage pulses of 200 ms duration were applied from –100 mV to + 40 mV in 10-mV steps at 1-s intervals. **A** Inwardly rectifying current. **B** Outwardly rectifying current. **C** Concurrent inwardly and outwardly rectifying currents

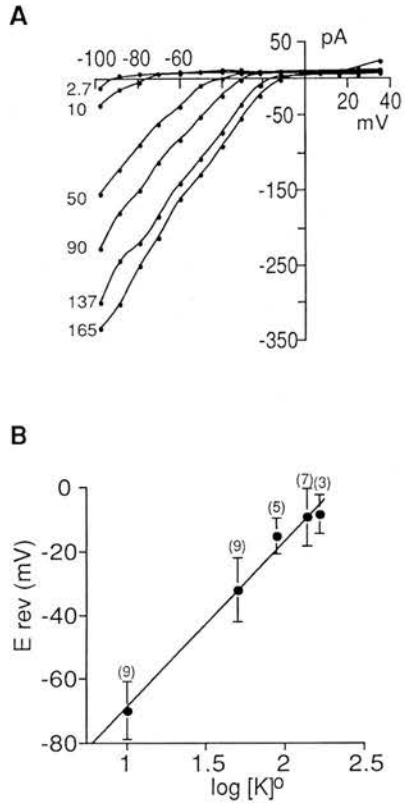

Fig. 2A, B Effect of extracellular K^+ concentration on inwardly rectifying currents. **A** Whole-cell *I/V* curves of a BMMC in six different concentrations of extracellular K^+. There is a positive shift in reversal potential as the extracellular K^+ increases from 2.7 mM to 165 mM. **B** Reversal potentials (*E rev*) plotted against $\log_{10}$ extracellular K^+ (mM). The line is a least-squares fit to the data. The slope of 52 mV/decade is close to that predicted for a K^+-selective membrane

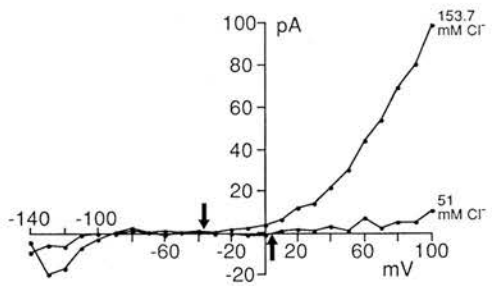

Fig. 3 Effect of extracellular Cl^- concentration on the outwardly rectifying current. When the extracellular Cl^- concentration is decreased from 153.7 mM to 51 mM by substituting Na-acetate for NaCl, the outwardly rectifying conductance is markedly decreased and the reversal potential shifts in a positive direction (*arrows*)

than the K^+ reversal potential and typically contained a region showing a small outward current just positive to the reversal potential, as shown in Fig. 1A. To investigate the proportion of cells showing the IR current, we first examined *I/V* relationships from 21 BMMCs in extracellular solutions containing 2.7 and 10 mM K^+. In mast cell Ringer (2.7 mM K^+) 15 cells (71%) showed the IR current, but when the extracellular K^+ was increased to 10 mM the current was present in all 21 cells (100%). When the extracellular K^+ was increased from 2.7 mM to 165 mM (with a corresponding decrease in the Na^+ concentration), the reversal potential of the *I/V* curves shifted in a positive direction (Fig. 2A). The linear relationship between reversal potential and log extracellular K^+ concentration with a least squares slope of 52 mV/decade indicates that the conductance is essentially K^+ selective (Fig. 2B). The slope conductance measured between –100 mV and –80 mV also increased with extracellular K^+ and was 1.48 ± 0.7 nS in 10 mM K^+(n = 9), 4.27 ± 1.4 nS in 50 mM K^+ (n = 9), 5.50 ± 2.3 nS in 90 mM K^+(n = 5), 6.24 ± 2.8 nS in 137 mM K^+(n = 7), and 5.8 ± 4.0 nS in 165 mM K^+(n = 3). An increase in conductance with increasing extracellular K^+ concentration also indicates that the current is predominantly carried by K^+ ions.

The OR current was not affected by changes in extracellular K^+ concentration. However, when the extracellular Cl^- concentration was reduced to 51 mM by substituting Na acetate for NaCl, the OR conductance decreased by 82 ± 8.5% (Fig. 3), from a mean of 2.7 ± 2.1 nS to 0.51 ± 0.53 nS (n = 5). In three cells bathed in extracellular solution containing 14 mM Cl^- the peak OR conductance was reduced to 0.24 nS in one cell and completely abolished in the other two cells. If cytosolic Cl^- was invariant during solution exchange, the shift in reversal potential predicted by the Nernst equation for a threefold decrease in extracellular Cl^- concentration would be 28 mV for a membrane selectively permeable to Cl^-. Reducing the extracellular Cl^- concentration from 153.7 mM to 51 mM resulted in a positive shift in the reversal potential of the OR current by 31 ± 21 mV (n = 5, Fig. 3 arrows). The deviation from theory resulting in a large standard deviation may reflect changes in intracellular Cl^- concentration occurring during the exchange (cytosolic Cl^- is not known in perforated-patch experiments and varies until a Donnan equilibrium is established between pipette and cell). The OR conductance was also decreased when Na isethionate was substituted for NaCl to yield an extracellular solution containing 16.7 mM Cl^- (3.39 ± 2.3 nS to 0.88 ± 1.2 nS, n = 4), and this effect was reversible on washout of the bath (Fig. 4B).

The OR current was not affected by 100 μM 4-aminopyridine or 25 mM TEA (not shown), but the OR conductance was reversibly decreased by the chloride channel blocker DIDS. Addition of 20 μM DIDS to the extracellular solution reduced the OR conductance by 69 ± 23% from a mean of 2.8 ± 2.0 nS to 1.0 ± 1.3 nS (n = 7). Figure 4C shows a typical experiment in which the OR conductance decreased after addition of 20 μM DIDS to the bath, but partially recovered after the blocker was washed out. All of these observations indicate that the OR currents in rat BMMCs are predominantly carried by Cl^- ions.

Dependence of the OR Cl^- conductance on bath temperature and cytoplasmic integrity

The OR chloride conductance has not been described previously to occur in rat mucosal type mast cells inves-

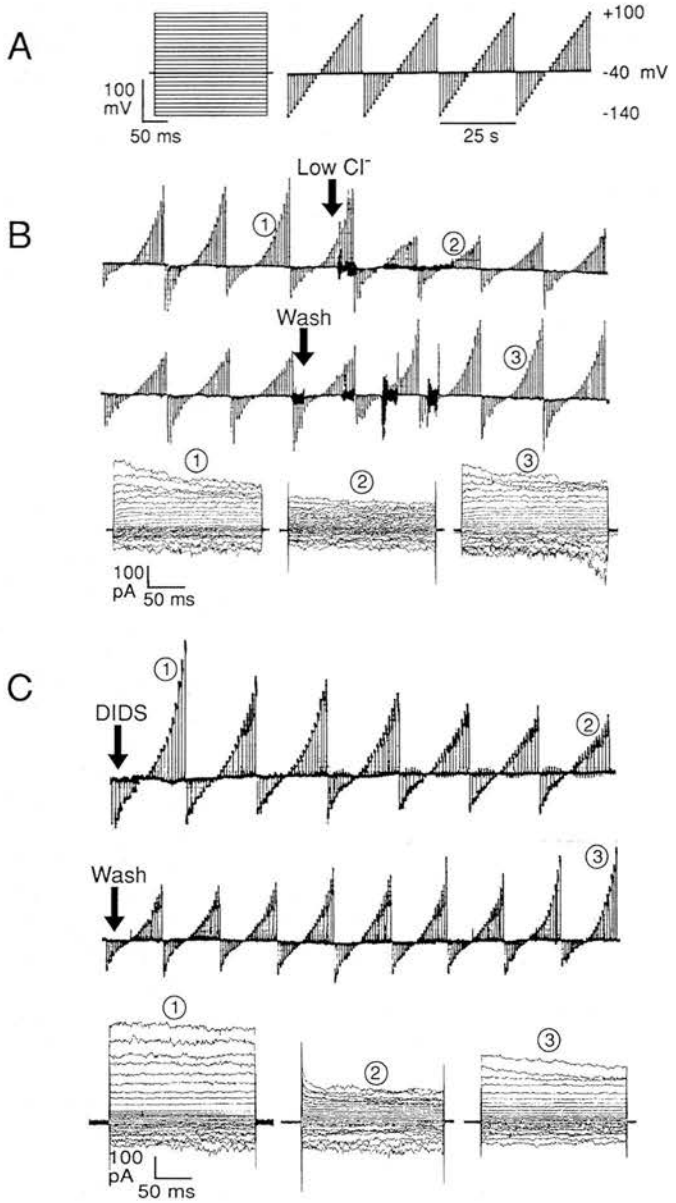

Fig. 4 Effect of extracellular Cl^- concentration and DIDS on whole-cell membrane currents in BMMCs. **A** The voltage step protocol. Cells were held at a holding potential of –40 mV and voltage pulses of 200 ms duration were applied from –140 mV to +100 mV in 10-mV steps at 1-s intervals. **B,C** Typical continuous pen recordings of the *I/V* relationships. Below each *trace* are the original superimposed currents evoked by the 25 voltage steps labelled by each *encircled number*. **B** Whole-cell currents in a BMMC after the mast cell Ringer (153.7 mM Cl^-) was exchanged for an extracellular solution containing Na-isethionate (16.7 mM Cl^-, *first arrow*). The outwardly rectifying (OR) current, showing time-dependent inactivation at potentials above +60 mV, is markedly reduced between *encircled number 1* and *encircled number 2*. At the *second arrow*, the bath was washed out with mast cell Ringer resulting in restoration of the current (*encircled number 3*). Noise indicates the time taken for solution exchange. Pipette solution contained KCH_3SO_4. **C** Effect of DIDS on the OR current. At the *first arrow*, 20 μM DIDS was added to the bath resulting in gradual diminution of the OR current. At the *second arrow*, the DIDS was washed out of the bath resulting in recovery of the OR current. Pipette solution contained KCl

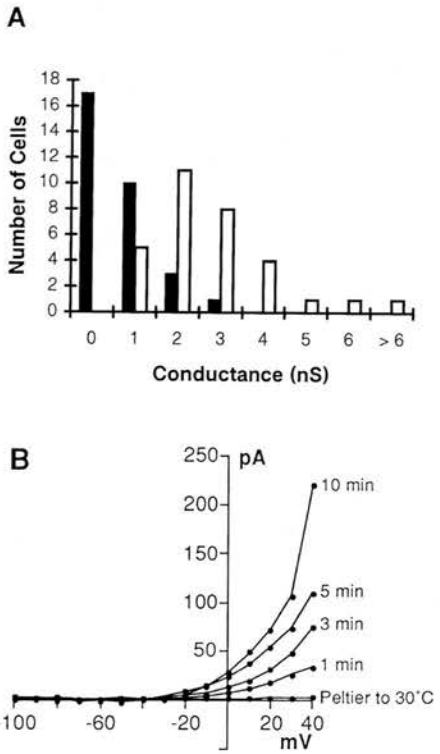

Fig. 5 **A** Perforated-patch experiments showing the effect of increasing bath temperature on 31 BMMCs that showed the OR chloride (OR_{Cl}) current at 25–37°C. The distribution of OR_{Cl} conductances at room temperature (16–20°C) is shown by the *black bars* and those between 25 and 37°C by the *white bars*. The shift of the distribution to the *right* indicates activation of the current by the rise in temperature. **B** Activation of the OR_{Cl} current in a cell warmed from room temperature to 30°C. *I/V* relationships are shown at intervals following activation of the Peltier device. The cell was clamped at a holding potential of –40 mV and voltage pulses of 200 ms duration were applied from –100 mV to + 40 mV in 10-mV steps. Leak currents were subtracted

tigated using conventional whole-cell recording techniques [18, 22]. We wished to determine if our results were influenced by recording conditions, so we compared 117 perforated-patch recordings obtained at room temperature (16–20°C) with our results at the warmer temperatures in the range of 25–37°C. At room temperature, 23% of amphotericin-B-perforated BMMCs displayed both IR_K and OR_{Cl} currents concurrently, with a further 49% showing only IR_K currents. In marked contrast to the results obtained at 25–37°C, only 3% of BMMCs displayed exclusively outward currents. Out of 117 cells, 25% appeared quiescent, displaying neither inward nor outward currents. The IR_K and OR_{Cl} conductances at room temperature were 1.22 ± 0.7 nS (n = 56) and 1.25 ± 0.9 nS (n = 20), respectively, both significantly lower than those recorded at 25–37°C (P<0.005). The difference between these results and those described earlier is primarily attributable to the increased proportion of cells showing OR_{Cl} currents at 25–37°C (26% at room temperature compared to 66% at 25–37°C). This effect is illustrated in Fig. 5A, which shows the effect of warming on the distribution of OR_{Cl}

Table 1 Effect of recording conditions on the OR_{Cl} conductance. The probability of observing the conductance increases as the conditions approach physiological. WCR - Whole cell recording

Parameter	Conventional WCR: cytoplasm disrupted		Perforated-patch recording: cytoplasm preserved	
Temperature	16–20 °C	25–37 °C	16–20 °C	25–37 °C
% Cells showing OR_{Cl}	7%	21%	26%	66%
Number cells showing OR_{Cl}	3/44	3/14	30/117	52/79
Mean conductance ± sd (nS)	0.87 ± 0.6 (n = 3)	0.69 ± 0.1 (n = 3)	1.25 ± 0.9 (n = 30)	2.21 ± 1.4 (n = 52)

conductances in 31 BMMCs that showed the OR_{Cl} current at 25–37°C.

The effect of warming on the OR_{Cl} current was also demonstrated in individual cells by monitoring the *I/V* relationships as BMMCs were warmed. Figure 5B shows the development of the OR_{Cl} current in a typical cell following activation of the Peltier device. The temperature at which the OR_{Cl} current developed varied from cell to cell; in most BMMCs, the current developed at either 25 °C (n = 20) or 30°C (n = 22), but in some cells the current only appeared at 37°C (n = 6). The median OR conductance also increased with each temperature increment but the difference between the three temperatures did not reach statistical significance, probably due to small group sizes. In cells that exhibited the OR_{Cl} current, the time from the start of warming to development of the peak conductance ranged from 132 to 696 s with a mean and SD of 309 ± 132 s (n = 21). These figures indicate that the OR_{Cl} conductance continues to increase even after the elevation of temperature has been completed. This delay would most likely arise if the current was dependent on a cytosolic factor. The OR current was typically stable for long periods, and in one cell it was monitored for 60 min without deterioration. However, we could not determine if the effect of warming was reversible because our Peltier device did not allow rapid cooling of the bath. Taken together, these results clearly indicate that detection of the OR_{Cl} current is more likely if the temperature of the cells is increased towards physiological values.

We then examined conventional whole-cell recordings from BMMCs to determine if maintenance of cytoplasmic integrity was also important for demonstration of the OR_{Cl} current. *I/V* relationships showed that 41 out of 44 BMMCs at room temperature (93%) displayed the IR_K current, with a mean slope conductance of 0.83 ± 0.5 nS (n = 22). A small OR conductance (0.87 ± 0.6 nS) was also present at room temperature in 3 out of 44 cells, but only in those experiments in which KCH_3SO_4 was used in the pipette solution (n = 13). When cells were warmed to 25–37°C, 3 out of 14 BMMCs showed some OR conductance but it was much lower than that measured in perforated-patch recordings (0.69 ± 0.1 nS).

A summary of the effects of temperature and cytoplasmic disruption on the activation of the OR conductance in BMMCs is shown in Table 1. The results clearly indicate that the OR_{Cl} current is dependent both on temperature and the degree of cytoplasmic integrity.

Whole-cell currents in rat peritoneal mast cells

The OR chloride current in rat BMMCs was similar to that described to occur in rat peritoneal mast cells (RPMCs) when cAMP was included in the pipette solution or when the cells were stimulated with secretagogues [2, 11, 21]. To determine if an OR_{Cl} could also be detected in resting RPMCs, we used the perforated-patch technique to obtain *I/V* relationships from cells at room temperature and in the range 25–37°C. Figure 6B shows the development of an OR current in an RPMC warmed to 25°C and the abrupt decrease in current amplitude and slope conductance following addition of 20 μM DIDS to the bath. In five similar experiments, 20 μM DIDS reduced the mean OR conductance by 53 ± 28% from 1.7 ± 0.96 nS to 0.75 ± 0.53 nS (n = 5). A similar effect was observed when RPMCs showing the OR conductance in mast cell Ringer were perfused with an extracellular solution containing 16.7 mM Cl^- (Fig. 6C), again indicating that the conductance was Cl^- selective. As in rat BMMCs, the expression of the OR_{Cl} current was variable and depended on recording conditions. Out of 40 RPMCs, 10 (25%) showed the OR current between 25 °C and 37°C, in contrast to 9 out of 55 cells (16%) from which recordings were made at room temperature. The slope conductance also increased with temperature from 1.15 ± 0.36 nS (n = 9) to 1.51 ± 0.86 nS (n = 10), although the difference did not reach statistical significance. The OR_{Cl} was also more commonly observed in RPMCs that had been incubated for ≥ 24 h with 10 ng/ml $rrSCF^{164}$. From 55 RPMCs recorded at room temperature, 12 cells had been incubated with $rrSCF^{164}$; the OR_{Cl} was present in 5 cells from this subgroup (42%) in contrast to 4 out of the remaining 43 cells (9%). The mean OR conductance was higher in the $rrSCF^{164}$ treated group (1.3 ± 0.4 nS vs 0.96 ± 0.23 nS) but again the difference was not statistically significant.

In accordance with previous reports [18, 22], we could not demonstrate a K^+-selective IR current in RPMCs under our experimental conditions. In three cells bathed in high-K^+ Ringer (50 mM), there was no change in conductance in the range –140 mV to –100 mV.

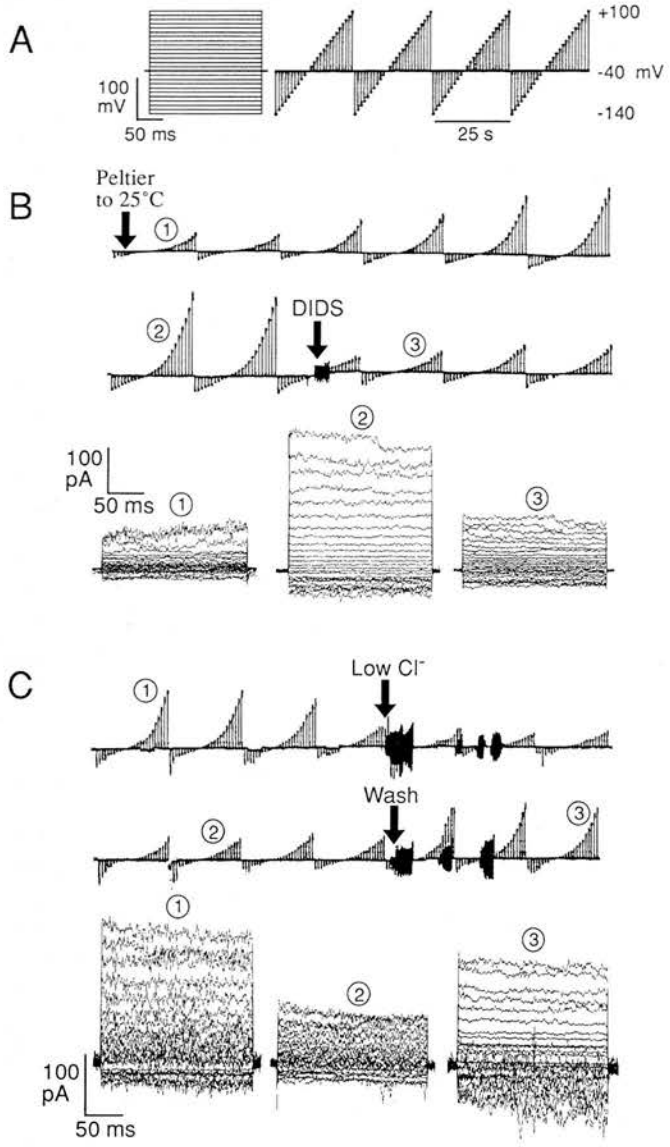

Fig. 6A–C Effect of temperature, DIDS and extracellular Cl^- concentration on whole-cell membrane currents in rat peritoneal mast cells (RPMCs). **A** The voltage step protocol. Cells were held at a holding potential of –40 mV and voltage pulses of 200 ms duration were applied from –140 mV to +100 mV in 10-mV steps at 1-s intervals. **B** After warming the cell to 25 °C (*first arrow*), an outwardly rectifying (OR) current develops that exhibits time-dependent inactivation at potentials greater than +60 mV (*encircled number 2*). At the *second arrow*, 20 μM DIDS was added to the bath resulting in a sudden diminution of the OR current (*encircled number 3*). Pipette solution contained KCH_3SO_4. **C** Whole-cell currents in an RPMC after the mast cell Ringer (153.7 mM Cl^-) was exchanged for an extracellular solution containing Na-isethionate (16.7 mM Cl^-, *first arrow*). The OR current is markedly reduced between (*encircled numbers 1* and *2*). At the *second arrow*, the bath was washed out with mast cell Ringer resulting in restoration of the current (*encircled number 3*). Noise indicates the time taken for solution exchange. Pipette solution contained KCH_3SO_4

Discussion

Activity of the OR_{Cl} in rat mast cells

In this study, we characterized whole-cell currents of rat BMMCs grown in the presence of cytokines derived from concanavalin-A-stimulated T-lymphocytes. These cells have not been studied electrophysiologically but they have been extensively characterized biochemically and immunologically and in all respects so far studied they are identical to intestinal mucosal mast cells [19, 23]. They may, therefore, represent a better model for electrophysiological studies of mucosal mast cells than RBL-2H3 cells [18] or mast cells grown in the presence of rat recombinant IL-3 [22]. In contrast to the latter studies, we report that rat BMMCs possess an OR_{Cl} in addition to the previously described K^+-selective inwardly rectifying (IR_K) current. This discrepancy may result from variations in cell phenotype; the additional growth factors and concanavalin A in the LNCM culture system could be necessary for expression of the outwardly rectifying chloride channel which was not observed to occur in either of the other cell types. However, this explanation seems unlikely because the OR_{Cl} was also present in RPMCs (an example of the connective tissue phenotype) and these cells were not exposed to the aforementioned factors.

A more likely possibility for the discrepancy described is the apparent dependency of the OR_{Cl} conductance on experimental conditions. We found that with the conventional whole-cell recording technique at room temperature (as used in previous studies) only 3 out of 44 BMMCs showed an OR_{Cl} current. However, when the integrity of the cell's cytoplasm was preserved using the perforated-patch technique, the OR_{Cl} current was readily demonstrable both in BMMCs (see Table 1) and RPMCs (Fig. 6). In addition, we found that increasing the bath temperature towards physiological values increased the proportion of cells that possessed the OR_{Cl} current, although the conductances were lower with the conventional whole-cell technique. These findings suggest that the OR_{Cl} may be dependent on an essential intracellular component that is leached out of the cell during conventional voltage-clamp recordings. A similar effect was recently reported for the immunoglobulin E (IgE) receptor-activated calcium conductance in rat mast cells, which could only be detected using perforated-patch recordings performed at 37°C [33].

The OR_{Cl} conductance observed in our experiments is similar to that induced in RPMCs when cAMP is included in the pipette solution [2, 27]. For example, the time course for development of the OR_{Cl} current in RPMCs following "break-in" is similar to that following warming of BMMCs or RPMCs; the shape of the *I/V* curve is similar in both cases; and both currents are blocked by 20 μM DIDS. In previous studies of RPMCs [27], it was concluded that in vivo a rise in intracellular cAMP following stimulation of the cells with secretagogues or antigen was responsible for activation of the OR_{Cl} current.

In our cells, neither secretagogues nor exogenous second messengers were required to elicit the current. This suggests that if cAMP is the "missing" cytosolic factor in conventional whole-cell recordings then only basal levels of the messenger are required to support the OR_{Cl} conductance.

The OR_{Cl} conductance in rat mast cells also shares certain similarities with a volume-regulated Cl^- conductance in T-lymphocytes [17]. In our experiments, the OR_{Cl} conductance was also observed when pipette KCl was replaced with KCH_3SO_4, suggesting that the current was not induced by movement of pipette Cl^- and osmotically obliged water into the cell during perforated-patch recordings. It was also concluded in previous studies that the cAMP-activated Cl^- current in RPMCs was not dependent on changes in cell volume [21].

However, cells subjected to perforated-patch recordings are very susceptible to small osmotic imbalances between cytosol and bath which could lead to activation of volume-regulated Cl^- channels. The effect of osmolarity on the activation of OR_{Cl} in BMMCs and RPMCs, and the relationship between the currents described here and in previous studies, therefore awaits further study.

Variation in expression of whole-cell currents

In the mouse BMMC system, the presence or absence of IR_K and OR_{Cl} currents in individual mast cells was interpreted as heterogeneity of ion channel expression [14]. We also found variation in the presence of the two currents in our cell populations, but we favour an alternative explanation to heterogeneity of ion channel expression. We suggest that a normal rat BMMC possesses the ion channels for both the IR_K and OR_{Cl} currents, and that the heterogeneous distribution of current patterns within the population results from extrinsic factors (i.e. experimental conditions) rather than intrinsic factors (i.e. restricted expression of ion channels). This is highlighted in Table 1, which shows the variation in expression of the OR_{Cl} conductance in BMMCs under different conditions. Likewise, the IR current was not detected in some cells in mast cell Ringer, but when the extracellular K^+ concentration was raised it was present in all cells tested. Hence, with both the OR_{Cl} and the IR_K, the lack of a detectable current did not reflect the lack of the appropriate ion channels. However, although we demonstrated the OR_{Cl} current in both BMMCs and RPMCs, the IR_K was only detectable in BMMCs. This may reflect true heterogeneity between the cell phenotypes as rat BMMCs and RPMCs have distinct biochemical and functional characteristics. However, the possibility still remains that the lack of the IR_K current may be an artefact of the isolation procedure, similar to that affecting IgE responses in freshly isolated RPMCs [32]. RPMCs undergo apoptosis on removal from the abdominal cavity, unless stimulated with the appropriate growth factors [5, 9], and the apparent influence of the cytokine $rrSCF^{164}$ on the OR_{Cl} current lends support to this hypothesis.

Physiological relevance of the IR_K and the OR_{Cl} currents in rat mast cells

Previous studies have shown that the IR_K is involved in regulation of the resting membrane potential [14, 18]. As seen in Fig. 1, the current is rapidly activated in BMMCs by hyperpolarizing potential steps, which in vivo would prevent further hyperpolarization. Note also the presence of the slight outward current "bump" in the IR_K *I/V* curve just positive to the reversal potential. This would tend to restore the resting membrane potential if the cell was slightly depolarized from the K^+ reversal potential. The IR_K current therefore provides a mechanism that would prevent excessive hyperpolarizations, and resist small depolarizations, of the cell. The lack of a detectable IR_K in RPMCs explains why the resting potential of these cells is close to 0 mV [18], but whether this accurately reflects the situation in vivo remains to be determined.

The OR_{Cl} current in our cells was only activated when the cell was depolarized to potentials more positive than –30 mV (Fig. 1B, C). This suggests that in vivo the OR_{Cl} current could be activated by large fluctuations in resting membrane potential or by depolarization, as occurs following stimulation of tumour mast cells following stimulation with antigen [12, 24, 31]. In RBL-2H3 cells, antigen-mediated depolarization is followed by a repolarization towards the resting membrane potential [15, 24], a process considered to be due to efflux of K^+ ions from the cell [16]. We suggest that the influx of Cl^- ions that follows activation of the OR_{Cl} [4] would also tend to repolarize the cell, thus restoring a negative membrane potential. The OR_{Cl} current in rat BMMCs could therefore serve two functions: (1) to regulate the resting membrane potential, as in mouse BMMCs [14] and (2) to counteract the depolarization of the cell during degranulation, thus maintaining the driving force for Ca^{2+} entry [21, 25].

Acknowledgements We thank Drs. A. MacDonald and M. Shipston for helpful advice, and Mrs. J. Vaagenes and Mrs. E. Thornton for technical support. This work was supported by a grant from the Wellcome Trust (038342/Z/93/Z/1.5B/PMC/RF)

References

1. Bormann J, Hamill OP, Sakmann B (1987) Mechanism of anion permeation through channels gated by glycine and gamma-aminobutyric acid in mouse cultured spinal neurones. J Physiol (Lond) 385:243–286
2. Dietrich J, Lindau M (1994) Chloride channels in mast-cells – block by DIDS and role in exocytosis. J Gen Physiol 104:1099–1111
3. Fasolato C, Hoth M, Matthews G, Penner R (1993) Ca^{2+} and Mn^{2+} influx through receptor-mediated activation of nonspecific cation channels in mast-cells. Proc Natl Acad Sci USA 90:3068–3072
4. Friis UG, Johansen T, Hayes NA, Foreman JC (1994) IgE-receptor activated chloride uptake in relation to histamine secretion from rat mast cells. Br J Pharmacol 111:1179–1183
5. Galli SJ, Zsebo KM, Geissler EN (1994) The kit-ligand, stem-cell factor. Adv Immunol 55:1–96
6. Haig DM, McMenamin C, Redmond J, Brown D, Young IG, Cohen SDR, Hapel AJ (1988) Rat IL-3 stimulates the growth

of rat mucosal mast cells in culture. Immunology 65:205–211
7. Hamill OP, Marty A, Neher E, Sakmann B, Sigworth FJ (1981) Improved patch-clamp techniques for high-resolution current recording from cells and cell-free membrane patches. Pflügers Arch 391:85–100
8. Hill PB, MacDonald AJ, Thornton EM, Newlands GFJ, Galli SJ, Miller HRP (1996) Stem-cell factor enhances immunoglobulin E dependent mediator release from cultured rat bone marrow-derived mast-cells – activation of previously unresponsive cells demonstrated by a novel ELISPOT assay. Immunology 87:326–333
9. Horigome K, Bullock ED, Johnson EM (1994) Effects of nerve growth-factor on rat peritoneal mast-cells – survival promotion and immediate-early gene induction. J Biol Chem 269:2695–2702
10. Horn R, Marty A (1988) Muscarinic activation of ionic currents measured by a new whole-cell recording method. J Gen Physiol 92:145–159
11. Janiszewski J, Bienenstock J, Blennerhassett M (1994) Picomolar doses of substance P trigger electrical responses in mast cells without degranulation. Am J Physiol 267:C138-C145
12. Kanner BI, Metzger H (1983) Crosslinking of the receptors for immunoglobulin E depolarizes the plasma membrane of rat basophilic leukemia cells. Proc Natl Acad Sci USA 80:5744–5748
13. Kuno M, Okada T, Shibata T (1989) A patch-clamp study: secretagogue-induced currents in rat peritoneal mast cells. Am J Physiol 256:C560-C568
14. Kuno M, Shibata T, Kawawaki J, Kyogoku I (1995) A heterogeneous electrophysiological profile of bone marrow-derived mast-cells. J Membr Biol 143:115–122
15. Labrecque GF, Holowka D, Baird B (1989) Antigen-triggered membrane potential changes in IgE sensitized rat basophilic leukemia cells: evidence for a repolarizing response that is important in the stimulation of cellular degranulation. J Immunol 142:236–243
16. Labrecque GF, Holowka D, Baird B (1991) Characterization of increased K^+ permeability associated with the stimulation of receptors for immunoglobulin E on rat basophilic leukemia cells. J Biol Chem 266:14912–14917
17. Lewis RS, Ross PE, Cahalan MD (1993) Chloride channels activated by osmotic stress in T lymphocytes. J Gen Physiol 101:801–826
18. Lindau M, Fernandez JM (1986) A patch-clamp study of histamine-secreting cells. J Gen Physiol 88:349–368
19. MacDonald AJ, Haig DM, Bazin H, McGuigan AC, Moqbel R, Miller HRP (1989) IgE-mediated release of rat mast-cell protease-II, beta-hexosaminidase and leukotriene-C4 from cultured bone marrow-derived rat mast-cells. Immunology 67:414–418
20. Matthews G, Neher E, Penner R (1989) Second messenger-activated calcium influx in rat peritoneal mast cells. J Physiol (Lond) 418:105–130
21. Matthews G, Neher E, Penner R (1989) Chloride conductance activated by external agonists and internal messengers in rat peritoneal mast cells. J Physiol (Lond) 418:131–144
22. McCloskey MA, Qian YX (1994) Selective expression of potassium channels during mast cell differentiation. J Biol Chem 269:14813–14819
23. McMenamin C, Haig DM, Gibson S, Newlands GFJ, Miller HRP (1987) Phenotypic analysis of mast cell granule proteinases in normal rat bone marrow cultures. Immunology 60:147–149
24. Mohr FC, Fewtrell C (1987) IgE receptor-mediated depolarization of rat basophilic leukemia cells measured with the fluorescent probe bis-oxonol. J Immunol 138:1564–1570
25. Mohr FC, Fewtrell C (1987) Depolarization of rat basophilic leukemia cells inhibits calcium uptake and exocytosis. J Cell Biol 104:783–792
26. Penner R, Pusch M, Neher E (1987) Washout phenomena in dialyzed mast cells allow discrimination of different steps in stimulus–secretion coupling. Biosci Rep 7:313–321
27. Penner R, Matthews G, Neher E (1988) Regulation of calcium influx by second messengers in rat mast cells. Nature 334:499–504
28. Qian YX, McCloskey MA (1993) Activation of mast cell K^+ channels through multiple G protein-linked receptors. Proc Natl Acad Sci USA 90:7844–7848
29. Rae J, Cooper K, Gates P, Watsky M (1991) Low access resistance perforated patch recordings using amphotericin B. J Neurosci Methods 37:15–26
30. Romanin C, Reinsprecht M, Pecht I, Schindler H (1991) Immunologically activated chloride channels involved in degranulation of rat mucosal mast cells. EMBO J 10:3603–3608
31. Sagi-Eisenberg R, Pecht I (1983) Membrane potential changes during IgE-mediated histamine release from rat basophilic leukemia cells. J Membr Biol 75:97–104
32. Taylor AM, Galli SJ, Coleman JW (1996) Stem-cell factor, the kit ligand, induces direct degranulation of rat peritoneal mast cells in vitro and in vivo: dependence of the in vitro effect on period of culture and comparisons of stem-cell factor with other mast cell-activating agents. Immunology 86:427–433
33. Zhang L, McCloskey MA (1995) Immunoglobulin E receptor-activated calcium conductance in rat mast cells. J Physiol (Lond) 483:59–66

Immunology 1996 **87** 326–333

Stem cell factor enhances immunoglobulin E-dependent mediator release from cultured rat bone marrow-derived mast cells: activation of previously unresponsive cells demonstrated by a novel ELISPOT assay

P. B. HILL,* A. J. MACDONALD,† E. M. THORNTON,† G. F. J. NEWLANDS,‡ S. J. GALLI§ & H. R. P. MILLER† **Department of Preclinical Veterinary Sciences, University of Edinburgh, †Department of Veterinary Clinical Studies, University of Edinburgh, ‡Moredun Research Institute, Edinburgh, UK and §Departments of Pathology, Beth Israel Hospital and Harvard Medical School, Boston, MA, USA*

SUMMARY

Mucosal mast cells (MMC) are important effector cells in the immune response against gastrointestinal nematodes. We used cultured rat bone marrow-derived mast cells (BMMC) as an *in vitro* model of MMC to study the effects of the multifunctional cytokine stem cell factor (SCF) on immunoglobulin E (IgE)-dependent secretion of granule mediators. SCF (≤1000 ng/ml) was not a direct secretagogue for these cells, but it significantly enhanced IgE-mediated secretion of the granule constituents rat mast cell protease-II (RMCP-II) and β-hexosaminidase from mature BMMC in a dose-dependent manner (>10 ng/ml). Maximum up-regulation of secretion occurred after cells were pretreated with SCF (50 ng/ml) for 5 minutes before challenge with anti-IgE, but the effect then declined and was absent in cells incubated with the cytokine for 3 to 24 h. In a novel ELISPOT assay developed to identify individual BMMC secreting RMCP-II, the proportion of mature BMMC responding to anti-IgE was significantly increased by treatment with SCF. To investigate this effect further, the percentage release of RMCP-II and β-hexosaminidase from populations of mature BMMC was directly compared to the proportion of individual cells releasing RMCP-II as detected by ELISPOT. The release of both mediators was enhanced by SCF, and the increased percentage release reflected both an increased proportion of secreting cells, and enhanced mediator release from individual cells. These results suggest that SCF can enhance IgE-dependent mediator release from BMMC not only by augmenting the secretory response from individual cells, but also by activating previously unresponsive cells.

INTRODUCTION

Intestinal mucosal mast cells (MMC) in the rat differ from connective tissue mast cells (CTMC) in their response to secretagogues,[1] and in their content of granule proteases.[2] Unlike rat CTMC, which contain rat mast cell protease-I (RMCP-I), rat MMC contain the granule chymase rat mast cell protease-II (RMCP-II), which is released into the blood-stream and gut lumen during immune expulsion of the intestinal parasites *Nippostrongylus brasiliensis* and *Trichinella spiralis*.[3–5] RMCP-II increases gut epithelial permeability via a paracellular route, possibly by effects on junctional complex proteins.[6]

Isolation of rat MMC from the gut is laborious and can give variable results.[1,7,8] By contrast, rat bone marrow-derived mast cells (BMMC), which exhibit many features of rat MMC,[9,10] can be grown in the presence of an interleukin-3 (IL-3)-rich T-cell-conditioned medium.[11,12] Like MMC *in vivo*, rat BMMC release substantial quantities of RMCP-II when activated immunologically,[13] and accordingly can be considered as an *in vitro* model of rat MMC.

Many aspects of mast cell development and function are influenced by stem cell factor (SCF), the ligand for the c-*kit* tyrosine kinase receptor. This cytokine influences chemotaxis, adhesion, survival, proliferation, differentiation and maturation of mast cells.[14–17] SCF can also induce and/or enhance mediator release from CTMC, including mouse skin,[18] rat[10] or mouse[20] peritoneal, and human lung[21] or skin[22] mast cells.

In this study, we evaluated whether SCF had any effects on the secretory function of rat BMMC. We found that although SCF is not a secretagogue for these cells, it enhances immunoglobulin E (IgE)-dependent mediator release from rat BMMC. Using a novel enzyme-linked immunospot (ELISPOT) assay to identify individual cells releasing RMCP-II, we show for the first time that only a proportion of a BMMC population

Received 8 September 1995; accepted 28 September 1995.

Abbreviations: BMMC, bone marrow-derived mast cells; RMCP-II, rat mast cell protease II; SCF, recombinant rat stem cell factor.

Correspondence: P. B. Hill, Department of Preclinical Veterinary Sciences, Royal (Dick) School of Veterinary Studies, Summerhall, Edinburgh, EH9 1QH, UK.

respond to immunological stimulation. Furthermore, we found that enhancement of mediator release by SCF is associated with an increase in the proportion of individual cells secreting RMCP-II, suggesting that the cytokine functions in part by activating previously unresponsive cells. Our findings also suggest a modulatory role for SCF in gastrointestinal immune responses.

MATERIALS AND METHODS

Cultured bone marrow mast cells (BMMC)

The preparation of bone marrow-derived mast cells and the production of lymph node conditioned medium (LNCM) have been described.[12] Briefly, femoral bone marrow cells from male Wistar rats were cultured at $2{\cdot}5–5 \times 10^5$ cells/ml in Iscove's Modified Dulbecco's medium (IMDM, Gibco-Brl, Paisley) supplemented with 20% horse serum (Advanced Protein Products, Brierley Hill), penicillin (100 IU/ml), and streptomycin (100 μg/ml). The cells were stimulated with LNCM at 10–25% v/v, and refed every 2–5 days. Percentage mast cells was determined by differential counts (400 cells) on Leishman's-stained cytocentrifuge preparations. BMMC proliferated rapidly initially, representing 85% of cells after approximately 15 days. After this, the percentage of BMMC increased slowly to almost 100% before cell viability declined. Before use, BMMC were washed three times by centrifugation (200 *g*) and resuspension, counted using a haemocytometer and assessed for viability by nigrosine exclusion. Unless stated otherwise, cells were used from cultures containing >95% mast cells with >95% viability. Mean RMCP-II concentration in individual mast cells, determined by enzyme-linked immunosorbent assay (ELISA)[23] of freeze/thawed cell pellets, increased from $3{\cdot}4 \pm 0{\cdot}3$ pg/cell at day 4 to $30{\cdot}4 \pm 3$ pg/cell at day 28 (data from two cultures).

Reagents

Cell suspensions were washed and diluted in Tyrode's buffer (TB, containing (in mM): NaCl 137, glucose 5·6, KCl 2·7, NaH_2PO_4 0·4, HEPES 10, bovine serum albumin 0·25% w/v, pH 7·3). SCF and secretagogues were diluted in Tyrode's buffer/1 mM Ca^{2+}/1 mM Mg^{2+} (TB^+). Recombinant rat SCF (2·2 mg/ml) was kindly provided by Dr Keith Langley of Amgen Inc., Thousands Oaks, CA. Preparation of purified RMCP-II, murine monoclonal anti-RMCP-II and sheep anti-RMCP-II for use in ELISA and ELISPOT assays has been described.[23] ELISPOT substrate buffer (AMP buffer) comprised 1·0 M 2-amino-2-methyl-1-propanol (Sigma), 0·7 mM $MgCl_2$ and 0·01% v/v Triton-X-405, pH 10·25. The ELISPOT substrate was 5-bromo-4-chloro-3-indoyl phosphate (BCIP, Sigma). The final substrate solution was prepared as described,[24] and comprised 1 mg/ml BCIP in AMP buffer with 0·6% w/v agarose (Type 1, Sigma).

Immunological stimulation of mediator release from BMMC

Two IgE-mediated stimulation protocols were used. In some experiments, cells were challenged directly with goat anti-rat IgE (provided by Dr E. Hall, Glasgow Veterinary School, UK), because cultured rat BMMC maintained in LNCM are ordinarily exposed to 1–2 μg rat IgE per ml,[25] and binding of this endogenous IgE to BMMC was detected throughout culture by flow cytometry (not shown). In other experiments (see legends), IgE binding was increased (shown by flow cytometry) by passively sensitizing the BMMC with monoclonal mouse IgE anti-dinitrophenyl (DNP) (SPE-7, Sigma). BMMC were washed three times in TB, incubated with 10 μg mouse IgE/10^6 cells in TB/4 mM EDTA for 1 h at 37°, and washed again three times in TB. In these experiments, DNP–bovine serum albumin (BSA) (Calbiochem, Nottingham) was used for challenge.

Percentage mediator release from BMMC populations

Triplicate or quadruplicate aliquots (0·5 ml) containing 0·8–1×10^6 BMMC were incubated with various concentrations of SCF (diluted in TB^+) or TB^+ control for various periods at 37° in a shaking water bath. After the addition of appropriately diluted antibodies or antigen in 0·5 ml TB^+, the cells were incubated at 37° for a further 30 min. Goat anti-rat IgE (αIgE) was used at an optimal dilution of 1 : 250, and DNP–BSA at a concentration of 10 μg/ml. Normal goat serum (NGS, 1 : 250) was used as a control for αIgE, and TB^+ as a control for DNP–BSA. Cells were pelleted by centrifugation (12 000 *g*) at 4° and transferred to an iced water bath. After collection of supernatants, cell pellets were resuspended in 1 ml TB and subjected to three freeze–thaw cycles in methanol/dry ice to fracture plasma membranes and release remaining mediators. Supernatants and pellets were stored at −70° until assayed for RMCP II[23] and β-hexosaminidase.[13]

Enumeration of RMCP-II release from individual BMMC by ELISPOT assay

We developed a modification of the technique originally described by Sedgwick and Holt[24] for the enumeration of antibody-secreting cells. Forty-eight-well cell culture plates (Costar, Cambridge, MA) were incubated overnight at 4° with 150 μl/well mouse monoclonal anti-RMCP II (1 μg/ml) in phosphate-buffered saline (PBS), pH 7·5. After washing twice with PBS/0·05% Tween 20 (PBS/T20), remaining binding sites were blocked by adding 200 μl/well 1% non-fat milk (Marvel, Premier Brands, Stafford) in PBS and incubating for 1 h at 37°. The plate was washed four times in PBS, and 125 μl of a BMMC suspension was added to each well (diluted in TB to provide between 100 and 400 cells/well). Examination of wells under phase contrast microscopy confirmed the presence of a single cell suspension. RMCP II (50 ng/ml) was added to two wells as a positive control, and wells containing no cells were included as negative controls. Cells or controls were incubated with SCF as described above, followed by 125 μl appropriately diluted αIgE, DNP–BSA, NGS, or TB for 30 min at 37°. After four washes in PBS/T20 to remove the cells, plates were sequentially incubated with 150 μl/well 1 : 1000 sheep anti-RMCP-II and 150 μl/well 1 : 10 000 donkey anti-sheep IgG–alkaline phosphatase conjugate (Sigma), both diluted in PBS/T20/4% BSA. Incubations were for 1 hr at 37° and plates were washed four times after each incubation in PBS/T20. Finally, 200 μl ELISPOT substrate (heated to 40°) was added to each well, and the plate was left overnight at room temperature (18–22°) to allow colour development.

Assay sensitivity was assessed by determining the lowest concentration of purified RMCP-II that could be detected in a 1 μl droplet. Twofold serial dilutions of RMCP-II from 500 pg/μl to 0·03 pg/μl were added to plates using a 1 μl pipette, and incubated for 30 min at 37°. Specific binding of RMCP-II

to antibody-coated wells was determined by adding serial dilutions of RMCP-II in 1 μl droplets to wells coated with PBS, rabbit polyclonal anti-RMCP-I, and mouse monoclonal anti-RMCP-II. (The mouse monoclonal anti-RMCP-II used in this assay is specific for RMCP-II, and does not cross-react with RMCP-I.[23]) Plates were then developed as described above.

Bound RMCP-II released from individual BMMC resulted in the development of discrete blue spots in ELISPOT assays. These were counted under a bright light without magnification. Variation in spot size was noted in all assays, but was not quantified.

Positive (50 ng/ml RMCP-II) or negative (no cells) control wells were diffusely blue or clear respectively. The sensitivity of the assay was 1·0 pg RMCP-II/μl, indicating sufficient sensitivity to detect RMCP-II-release from individual cells. Binding of RMCP-II occurred only in wells coated with anti-RMCP-II. No spots developed in wells coated with PBS or anti-RMCP-I, thus confirming that RMCP-II was bound specifically by wells coated with homologous antibody.

Statistical analysis

Analysis of variance (ANOVA) and unpaired Student's *t*-tests were used to compare treatment groups. The data were analysed using Minitab statistical software. Results are reported as mean ± SEM.

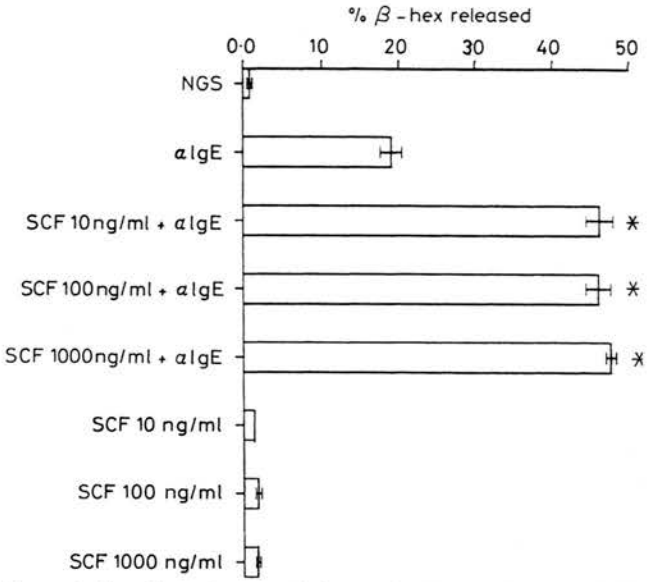

Figure 1. The effect of stem cell factor (SCF) on β-hexosaminidase release from BMMC. The BMMC (10^6 per tube; $n = 3$) were preincubated with SCF at 10, 100, or 1000 ng/ml, or with buffer alone, for 15 min before addition of goat anti-rat IgE (αIgE) or normal goat serum (NGS) at 1/250 final dilution for a further 15 min. Each bar represents the mean ± SEM of triplicate release assay tubes. *Significant difference from cells treated with buffer alone ($P < 0·005$).

RESULTS

SCF enhances IgE-dependent mediator release from mature BMMC

Preincubation of BMMC populations with SCF at 10, 100 or 1000 ng/ml for 15 min resulted in a highly significant ($P < 0·005$) enhancement of IgE-dependent β-hexosaminidase release, from 19% without SCF preincubation to a mean of 47% in cells challenged with αIgE (Fig. 1). In a separate experiment, SCF did not enhance mediator release at concentrations of 0·001 to 1 ng/ml, but again significantly increased secretion when used at 10 and 100 ng/ml (not shown). When mature BMMC were incubated with SCF (50 ng/ml) for 5, 15, or 60 min, or 3 or 24 h before challenge with αIgE, maximal enhancement of RMCP-II or β-hexosaminidase release occurred after a 5 min preincubation, but the effect declined thereafter was not statistically significant in BMMC that had been treated with SCF for 3 or 24 hr (Fig. 2). Incubation with SCF (10, 100, 1000 ng/ml) did not cause direct release of β-hexosaminidase from BMMC in the absence of anti-IgE, suggesting that SCF was not a direct secretagogue for these cells.

SCF enhances the proportion of BMMC that release RMCP-II in response to anti-IgE

We first verified that the number of spots counted in ELISPOT assays were correlated to cell density by assaying twofold dilutions of BMMC from 150 BMMC/well to 10 BMMC/well. The number of spots in wells treated with anti-IgE increased linearly with increasing cell density ($r = 0·99$, $P < 0·001$), with a mean of 21% BMMC releasing RMCP-II, compared to a background release from only 0·3% of BMMC treated with NGS (Fig. 3).

We then used the ELISPOT assay to determine whether preincubation with SCF altered the proportion of BMMC within a population that responded to stimulation with anti-IgE. The proportion of BMMC releasing RMCP-II was increased by preincubation with SCF in a concentration- and time-dependent manner. Concentrations of 50 or 25 ng/ml resulted in the highest proportion of cells responding (35 ± 5 or 36 ± 3% respectively), compared to 4 ± 0·7% of cells treated with anti-IgE alone (Fig. 4a). In subsequent assays, a SCF concentration of 50 ng/ml was used.

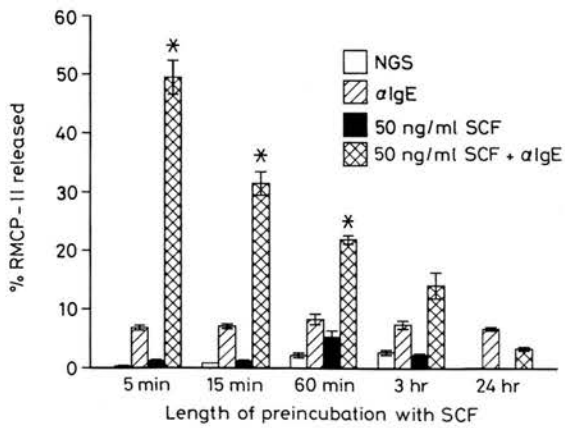

Figure 2. Time course of the effect of SCF on IgE-dependent RMCP-II release from BMMC. The BMMC (10^6 per tube) were preincubated with 50 ng/ml SCF or buffer alone for various times followed by αIgE or NGS at 1/250 final dilution for 30 min. Each bar represents the mean ± SEM of triplicate release assay tubes. *Significant difference from cells treated with αIgE for equivalent time periods ($P < 0·05$). β-hexosaminidase release (not shown) was highly correlated with RMCP-II release ($r = 0·976$, $P < 0·001$).

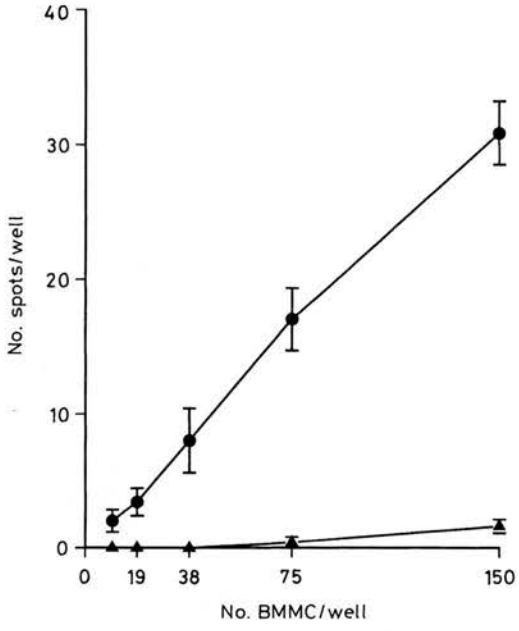

Figure 3. Relationship between cell density and number of spots/well determined by assaying serial dilutions of cell suspensions from 150 cells/well to 10 cells/well. BMMC from a culture containing 38% mast cells were challenged with goat anti-rat IgE (solid circles) or normal goat serum (solid triangles). Each point represents the mean ± SEM of individual spot counts in five wells. Correlation coefficient between cell density and number of spots in wells challenged with anti-rat IgE = 0·99, $P < 0·001$.

The effect of SCF was shown to be time dependent by incubating BMMC with 50 ng/ml SCF for 5, 15, 30, 60, or 120 min before challenge with anti-IgE (Fig. 4b). A 30-min incubation resulted in the highest proportion of cells releasing RMCP II (34 ± 2%), but this was not significantly different from the results obtained after a 5-min incubation (26 ± 3%); both values were highly significant when compared to results for cells treated with anti-IgE alone (8 ± 1%, $P < 0·01$ for either comparison). SCF therefore increased the proportion of BMMC that detectably responded to anti-IgE at concentrations and incubation times similar to those that enhanced total mediator release as described in the initial experiments. For all subsequent assays, BMMC were incubated with SCF for 5 min before addition of the secretagogue (anti-IgE or antigen) or control.

Effects of SCF on mediator release from BMMC populations at various stages of culture

ELISPOT assays (100 cells/well) were performed throughout the course of two BMMC cultures to determine whether the response to SCF might be related to maturity of the culture. The response of BMMC to anti-IgE and SCF fell into two categories. In four experiments performed using cultures containing 8, 36, 41, or 64% BMMC, a highly significant ($P < 0·001$) proportion of BMMC responded to anti-IgE alone when compared to NGS controls, but addition of SCF had no significant effect (Fig. 5a). In contrast, SCF significantly increased ($P < 0·001$) the proportion of BMMC responding to anti-IgE in 4 out of 5 experiments performed using cultures containing 85, 87, 92, 94, or 95% mast cells (Fig. 5b).

Mediator release in response to anti-IgE apparently decreased as the cultures matured, but this effect may partially be due to increased spontaneous release of RMCP-II (compare Figs. 5a and 5b); in some experiments, the proportion of BMMC responding to anti-IgE was not significantly different from background release in negative controls (NGS versus αIgE in Fig. 5b). At no stage did SCF alter the response of cells treated with NGS. This finding provided additional evidence that, in isolation SCF had no detectable secretagogue activity in these BMMC populations.

Effects of SCF on release of RMCP-II from individual BMMC compared with percentage mediator release by the entire population of BMMC

We wished to determine whether an SCF-dependent increase in mediator release by a BMMC population as a whole might reflect an increase in the *proportion* of secreting cells as opposed to increased *amounts* of mediator release from the responding BMMC. We therefore compared results from ELISPOT assays to those obtained in conventional mediator release assays, using aliquots of the same cell populations. In addition, we wished to determine whether passive sensitization of cells with IgE would enhance the response of mature BMMC populations to immunological stimulation. Accordingly, we sensitized BMMC from a mature culture with mouse IgE anti-DNP, incubated the sensitized cells with SCF (50 ng/ml for 5 min before challenge) or buffer as a control, and then stimulated the BMMC with DNP–BSA. For each experiment, the percentage release of RMCP-II and β-hexosaminidase from $0·8 \times 10^6$ BMMC was compared to the proportion of BMMC from the same population that released RMCP-II as determined by ELISPOT (Fig. 6). In these experiments, mean specific IgE-dependent release of RMCP-II or β-hexosaminidase (% release from DNP minus % release from control) in the absence of SCF was 9 ± 0·5% and 12 ± 0·3% respectively ($P < 0·01$ vs. results with buffer alone). After pretreatment with SCF, the cells' response to antigen-mediated stimulation increased significantly ($P < 0·001$) to 26 ± 1% or 36 ± 3% for RMCP-II and β-hexosaminidase respectively. In the ELISPOT assays, a mean of 14 ± 1% individual IgE-sensitized BMMC released RMCP-II in response to DNP–BSA alone, and this increased significantly ($P < 0·01$) to 21 ± 1% after pretreatment with SCF. Background release from cells treated with buffer alone was 3 ± 0·3%. These results suggest that SCF enhances mediator release from BMMC both by activating previously unresponsive cells and by augmenting the secretory response in degranulating cells.

DISCUSSION

In all respects so far studied, rat BMMC represent the *in vitro* analogues of rat intestinal MMC. Importantly, BMMC release RMCP-II following IgE-mediated stimulation, and therefore provide a useful model for studying the mechanisms involved in mediator release.[13] We initially explored the effects of SCF on the IgE-mediated secretion of RMCP-II and β-hexosaminidase from populations of mature BMMC (from cultures containing >95% BMMC). We found that, in contrast to mouse[20] or

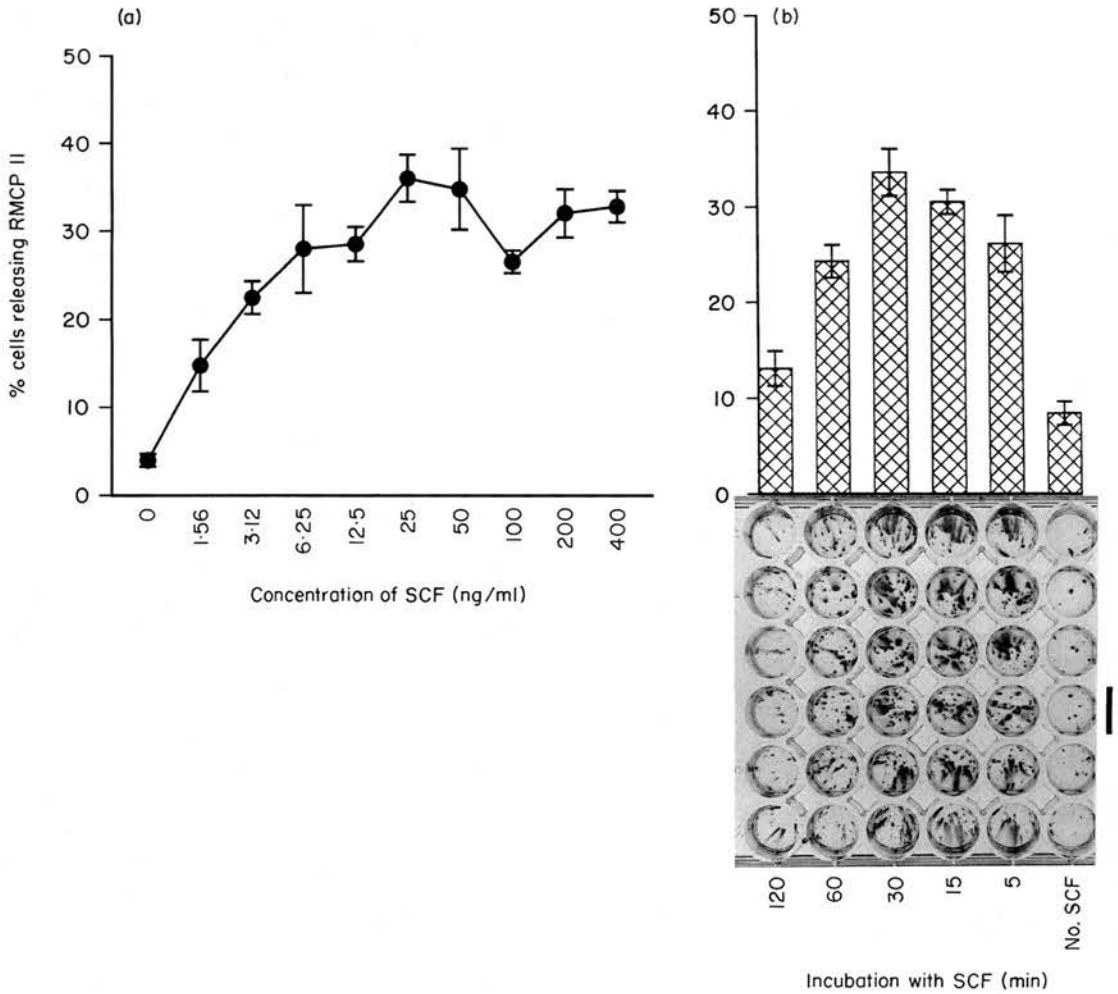

Figure 4. (a) The effect of SCF concentration on RMCP II release from BMMC in response to anti-IgE. Cells from a culture containing >99% BMMC were incubated with varying concentrations of SCF for 5 min before challenge with anti-IgE. Percentage of cells that detectably released RMCP-II was determined by ELISPOT. Each bar represents the mean ± SEM of spot counts from four wells. (b) Release of RMCP-II from anti-IgE treated BMMC (200 BMMC/well, from a culture containing, >99% mast cells) after incubation with SCF (50 ng/ml) for varying periods of time. The graphic illustrates the increased number of spots in wells after 5, 15, or 30 min preincubation with SCF, compared to 60 or 120 min, or control wells (no SCF). Scale marker = 1 cm. Bars represent the mean ± SEM of spot counts from six wells.

rat[19,26] peritoneal mast cells, or mouse[18] or human[22] skin mast cells, SCF did not directly induce mediator release from rat BMMC under our experimental conditions. However, pretreatment of BMMC with SCF (>10 ng/ml) for 5 min before challenge with anti-IgE resulted in an approximately 2·5-fold increase in mediator release (from 19% to 47%). Enhancement of IgE-dependent mediator release by SCF was maximal after short preincubations (5 min) and was not evident after incubations over 3 hr. This effect has also been reported for human skin[22] and lung[21] mast cells, and is most likely due to internalization of c-*kit* receptor/SCF complexes following ligand binding.[27]

In studies of mast cell function, it is customary to report the effects of secretagogues or cytokines on mast cell secretion in terms of percentage release of various mediators.[13,20,22,28–31] Typically, in accord with our own findings, secretagogue-activated mast cell populations specifically release 10–50% of the stored mediators present in the cells. We were interested in how values for specific mediator release might reflect the extent to which *individual* BMMC within a population respond to IgE-dependent stimulation, and whether SCF-dependent enhancement in mediator release reflected individual cells releasing more mediator, or increased numbers of cells responding to stimulation.

Using the ELISPOT assay, we demonstrated for the first time that the majority (80–90%) of the BMMC populations were refractory to stimulation by either anti-IgE or specific antigen, but the proportion of responding cells was significantly increased by pretreatment with SCF. However, when the results of ELISPOT assays and conventional mediator release assays were directly compared (as in Fig. 6), the increase in percentage total mediator release (approximately threefold) was greater than the increase in the proportion of responding cells (approximately 1·5-fold). Our results suggest that SCF up-regulates secretion from mature BMMC in two ways: first, by activating previously unresponsive cells as clearly shown by

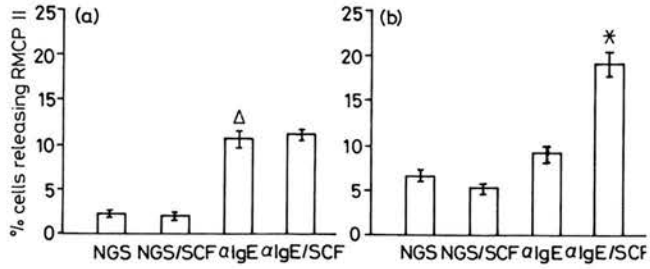

Figure 5. The effect of SCF on IgE-dependent RMCP-II release from individual BMMC derived from cultures at different stages of maturity. Cells were incubated in the presence (50 ng/ml for 5 min) or absence of SCF before challenge with anti-IgE. (a) Representative result from a culture containing less than 85% (i.e. 64%) mast cells. There was a significant effect of anti-IgE (αIgE) compared to normal goat serum (NGS, Δ, $P < 0{\cdot}001$), but SCF had no significant effect on the release of RMCP-II either with or without anti-IgE challenge. Similar results were obtained with cultures containing 8, 36, and 41% mast cells. (b) Representative result from a culture containing more than 85% (i.e. 94%) mast cells. The number of cells responding was significantly increased after incubation with SCF (*$P < 0{\cdot}001$). Similar results were obtained from cultures containing 85, 87, 92, and 94% mast cells. In this experiment, the responses of BMMC to anti-IgE or normal goat serum were not significantly different. Each bar represents the mean ± SEM of the spot counts from nine wells from each of two separate ELISPOT assays.

the ELISPOT assays; and second, by enhancing mediator release from individual cells. The latter conclusion was also suggested by an increase in spot size from cells treated with SCF, but we did not attempt to quantify this effect.

We also used the ELISPOT assay to investigate the effect of SCF on the secretory pattern of individual BMMC at various stages during culture. Pretreatment of BMMC with SCF enhanced IgE-dependent mediator release from mature

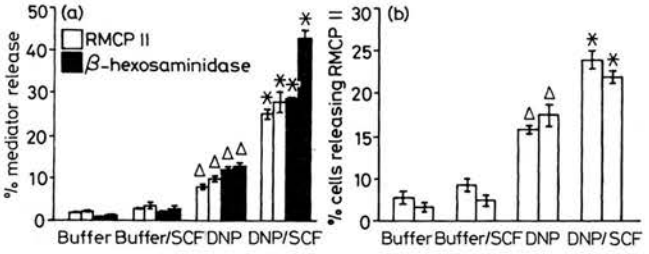

Figure 6. (a) Conventional mediator release assay showing percentage release of β-hexosaminidase and RMCP-II from entire populations of BMMC (from a culture containing >99% mast cells) tested in two separate experiments. BMMC were sensitized with mouse monoclonal IgE anti-DNP and then stimulated with DNP–BSA in the presence (50 ng/ml for 5 min before challenge) or absence of SCF. Each bar represents the mean ± SEM from quadruplicate aliquots of $0{\cdot}8 \times 10^6$ BMMC. (b) ELISPOT assays measuring the proportion of BMMC that released RMCP-II, performed in parallel to the experiments in (a) using aliquots of the same cell populations. Each bar represents the mean ± SEM of spot counts from nine wells from each of two separate ELISPOT assays. The increased mediator release in the conventional assay (a) is clearly associated with an increase in the number of cells responding to immunological stimulation as demonstrated in the ELISPOT assay (b). Δ, significant difference from buffer or buffer/SCF ($P < 0{\cdot}01$); *significant difference from cells stimulated with DNP alone ($P < 0{\cdot}05$).

BMMC (i.e. from cultures containing at least 85% mast cells), but did not up-regulate secretion from cells derived from immature cultures containing less than 85% mast cells. The lack of an effect of SCF on IgE-dependent mediator release from immature populations of BMMC might have reflected effects of 'contaminating cells' in these preparations. Immature cultures contain other bone marrow-derived cells (especially macrophages), which could potentially influence the effects of cytokines on mast cells. Alternatively, lower expression of the SCF receptor (c-*kit*) in developing cells, or differences between mature and immature BMMC in the intracellular mechanisms necessary for transducing the signal, may have contributed to the apparent lack of SCF responsiveness in these populations. Whether the different effects of SCF on BMMC at various stages of growth/maturation *in vitro* reflect a similar phenomenon *in vivo* remains to be determined.

Activation of the FcεR1 receptor in mast cells leads to extensive tyrosine phosphorylation of intracellular intermediates which are critically involved in signal transduction.[32–35] Activation of the c-*kit* receptor by SCF also leads to tyrosine phosphorylation of multiple cytosolic proteins,[36] and overlap between the two signalling pathways has already been demonstrated in mouse bone marrow-derived cultured mast cells[37,38] and rat peritoneal mast cells,[26] suggesting some overlap in the mechanisms by which degranulation can be triggered via the FcεR1 or the c-*kit* receptor. Our results suggest that, in rat BMMC, SCF can prime the cell for subsequent activation via the IgE receptor, but cannot directly induce degranulation. To address the possibility that SCF was in some way compensating for sub-optimal binding of endogenous IgE, the BMMC were sensitized with IgE anti-DNP and challenged with DNP. In these experiments (Fig. 6), pretreatment with SCF resulted in similar increases in both the proportion of cells responding to antigen and in the total amount of released granule mediators as was previously observed in cells stimulated with anti-IgE without prior addition of exogenous IgE. These results suggest that the effect of the cytokine was not dependent on the degree of IgE binding.

Why do some cells remain refractory to IgE-dependent stimulation even after preincubation with SCF? Failure of a cell to respond to IgE-mediated stimulation could result from a deficiency at any stage of the signal transduction pathway, including inadequate FcεR1 expression, insufficient IgE, lack of intracellular transduction proteins, reduced intracellular calcium stores and/or reduced ion channel expression. Expression of FcεR1 in mouse bone marrow-derived mast cell cultures coincides with granule formation,[39] suggesting that cultured mast cells possess IgE receptors at the onset of maturation. In addition, rat BMMC have surface bond endogenous IgE throughout culture (confirmed by flow cytometry), and therefore FcεR1 receptors, but these could be sub-optimal in some cells. However, when cells were passively sensitized with exogenous IgE, which increased occupancy of the IgE receptors, a refractory population still remained indicating that failure to respond was not related to the degree of IgE binding. In rat basophil leukemia (RBL-2H3) cells[40,41] and human basophils and mast cells,[42,43] stimulation of populations of cells via the FcεR1 resulted in variable intracellular calcium fluxes and oscillations. In addition, correlation of intracellular calcium fluxes with mediator release from individual cells indicated that a sustained rise in intracellular calcium, seen only

in a proportion of the cells, was required to initiate secretion (T. D. Kim, personal communication). Similar heterogeneity in intracellular calcium responses could explain the large proportion of BMMC that fail to respond to immunological stimulation in our study.

In summary, we showed that the cytokine, SCF, enhanced mediator release from a population of mature BMMC, and this up-regulation was shown to be due to both activation of previously unresponsive cells and augmentation of the secretory response in individual cells. The many similarities between rat BMMC and rat MMC suggest that SCF may also be involved in regulation of mast cell responses in the gut, acting as a modulator of gastrointestinal immune responses.

ACKNOWLEDGMENTS

This work was supported by a grant from the Wellcome Trust (038342/Z/93/Z/1.5B/PMC/RF), by United States Public Health Service grants AI-22674 and AI-23990, and by AMGEN, Inc. Dr Galli has performed research funded by AMGEN, Inc., and consults with AMGEN, Inc. under terms that are in accord with Beth Israel Hospital and Harvard Medical School conflict of interest guidelines.

REFERENCES

1. Befus A.D., Pearce F.L., Gauldie J., Horsewood P. & Bienenstock J. (1982) Mucosal mast-cells. 1. Isolation and functional-characteristics of rat intestinal mast cells. *J Immunol* **128,** 2475.
2. Gibson S. & Miller H.R.P. (1986) Mast cell subsets in the rat distinguished immunohistochemically by their content of serine proteinases. *Immunology* **58,** 101.
3. Miller H.R.P., Woodbury R.G., Huntley J.F. & Newlands G.F.J. (1983) Systemic release of mucosal mast cell protease in primed rats challenged with *Nippostrongylus brasiliensis*. *Immunology* **49,** 471.
4. Woodbury R.G., Miller H.R.P., Huntley J.F., Newlands G.F.J., Palliser A.C. & Wakelin D. (1984) Mucosal mast cells are functionally active during spontaneous expulsion of intestinal nematode infections in rat. *Nature* **312,** 450.
5. King S.J. & Miller H.R.P. (1984) Anaphylactic release of mucosal mast cell protease and its relationship to gut permeability in *Nippostrongylus*-primed rats. *Immunology* **51,** 653.
6. Scudamore C.L., Thornton E.M., McMillan L., Newlands G.F.J. & Miller H.R.P. (1995) Release of the mucosal mast cell granule chymase, rat mast cell protease-II, during anaphylaxis is associated with the rapid development of paracellular permeability to macromolecules in rat jejunum. *J Exp Med* (in press).
7. Pearce F.L., Befus A.D., Gauldie J. & Bienenstock J. (1982) Mucosal mast cells. 2. Effects of anti-allergic compounds on histamine-secretion by isolated intestinal mast-cells. *J Immunol* **128,** 2481.
8. Lee T.D.G., Shanahan F., Miller H.R.P., Bienenstock J. & Befus A.D. (1985) Intestinal mucosal mast cells — isolation from rat lamina propria and purification using unit gravity velocity sedimentation. *Immunology* **55,** 721.
9. McMenamin C., Haig D.M., Gibson S., Newlands G.F.J. & Miller H.R.P. (1987) Phenotypic analysis of mast cell granule proteinases in normal rat bone-marrow cultures. *Immunology* **60,** 147.
10. Enerback L. (1987) Mucosal mast cells in the rat and in man. *Int Arch Allergy Appl Immunol* **82,** 249.
11. Haig D.M., McKee T.A., Jarrett E.E.E., Woodbury R. & Miller H.R.P. (1982) Generation of mucosal mast cells is stimulated *in vitro* by factors derived from T-cells of helminth-infected rats. *Nature* **300,** 188.
12. Haig D.M., McMenamin C., Redmond J. *et al.* (1988) Rat IL-3 stimulates the growth of rat mucosal mast cells in culture. *Immunology* **65,** 205.
13. MacDonald A.J., Haig D.M., Bazin H., McGuigan A.C., Moqbel R. & Miller H.R.P. (1989) IgE-mediated release of rat mast cell protease-II, beta-hexosaminidase and leukotriene-C4 from cultured bone marrow-derived rat mast cells. *Immunology* **67,** 414.
14. Galli S.J., Zsebo K.M. & Geissler E.N. (1994) The kit-ligand, stem-cell factor. *Adv Immunol* **55,** 1.
15. Haig D.M., Huntley J.F., Mackellar A. *et al.* (1994) Effects of stem-cell factor (kit-ligand) and interleukin-3 on the growth and serine proteinase expression of rat bone-marrow-derived or serosal mast cells. *Blood* **83,** 72.
16. Tei H., Kasugai T., Tsujimura T. *et al.* (1994) Characterization of cultured mast-cells derived from Ws/Ws mast cell deficient rats with a small deletion at tyrosine kinase domain of c-kit. *Blood* **83,** 916.
17. Tsai M., Shih L.S., Newlands G.F.J. *et al.* (1991) The rat c-*kit* ligand, stem-cell factor, induces the development of connective-tissue type and mucosal mast cells *in vivo* — analysis by anatomical distribution, histochemistry, and protease phenotype. *J Exp Med* **174,** 125.
18. Wershil B.K., Tsai M., Geissler E.N., Zsebo K.M. & Galli S.J. (1992) The rat c-*kit* ligand, stem-cell factor, induces c-*kit* receptor-dependent mouse mast cell activation *in vivo* — evidence that signaling through the c-*kit* receptor can induce expression of cellular function. *J Exp Med* **175,** 245.
19. Nakajima K., Hirai K., Yamaguchi M. *et al.* (1992) Stem-cell factor has histamine releasing activity in rat connective tissue-type mast cells. *Biochem Biophys Res Commun* **183,** 1076.
20. Coleman J.W., Holliday M.R., Kimber I., Zsebo K.M. & Galli S.J. (1993) Regulation of mouse peritoneal mast cell secretory function by stem-cell factor, IL-3 or IL-4. *J Immunol* **150,** 556.
21. Bischoff S.C. & Dahinden C.A. (1992) c-*kit* ligand — a unique potentiator of mediator release by human lung mast cells. *J Exp Med* **175,** 237.
22. Columbo M., Horowitz E.M., Botana L.M. *et al.* (1992) The human recombinant c-*kit* receptor ligand, rhscf, induces mediator release from human cutaneous mast cells and enhances IgE-dependent mediator release from both skin mast cells and peripheral blood basophils. *J Immunol* **149,** 599.
23. Huntley J.F., Mackellar A., Newlands G.F.J., Irvine J. & Miller H.R.P. (1990) Mapping of the rat mast cell granule proteinases RMCP-I and RMCP-II by enzyme-linked-immunosorbent-assay and paired immunofluorescence. *Apmis* **98,** 933.
24. Sedgwick J.D. & Holt P.G. (1983) A solid-phase immunoenzymatic technique for the enumeration of specific antibody-secreting cells. *J Immunol Methods* **57,** 301.
25. Haig D.M., McMenamin C., Gunneberg C., Woodbury R. & Jarrett E.E.E. (1983) Stimulation of mucosal mast cell growth in normal and nude rat bone-marrow cultures. *Proc Natl Acad Sci USA* **80,** 4499.
26. Koike T., Hirai K., Morita Y. & Nozawa Y. (1993) Stem-cell factor-induced signal-transduction in rat mast-cells — activation of phospholipase-D but not phosphoinositide-specific phospholipase-C in c-*kit* receptor stimulation. *J Immunol* **151,** 359.
27. Yee N.S., Langen H. & Besmer P. (1993) Mechanism of kit-ligand, phorbol ester, and calcium-induced down-regulation of c-*kit* receptors in mast cells. *J Biol Chem* **268,** 14189.
28. Razin E., Menciahuerta J.M., Stevens R.L. *et al.* (1983) IgE-mediated release of leukotriene C-4, chondroitin sulfate E-proteoglycan, beta-hexosaminidase, and histamine from cultured bone marrow-derived mouse mast-cells. *J Exp Med* **157,** 189.
29. Levi-Schaffer F., Dayton E.T., Austen K.F. *et al.* (1987) Mouse bone marrow-derived mast cells co-cultured with fibroblasts — morphology and stimulation-induced release of histamine,

leukotriene-B4, leukotriene-C4, and prostaglandin-D2. *J Immunol* **139,** 3431.

30. Levi-Schaffer F., Austen K.F., Caulfield J.P., Hein A., Gravallese P.M. & Stevens R.L. (1987) Co-culture of human lung-derived mast cells with mouse-3T3 fibroblasts — morphology and IgE-mediated release of histamine, prostaglandin-D2, and leukotrienes. *J Immunol* **139,** 494.
31. Broide D.H., Metcalfe D.D. & Wasserman S.I. (1988) Functional and biochemical characterization of rat bone-marrow derived mast cells. *J Immunol* **141,** 4298.
32. Sagi-Eisenberg R. & Foreman J.C. eds. (1993) Signal-transmission pathways in mast cell exocytosis. In: *Immunopharmacology of Mast Cells and Basophils*, p. 71. Academic Press, London.
33. Fukamachi H., Yamada N., Miura T. *et al.* (1994) Identification of a protein, spy75, with repetitive helix-turn-helix motifs and an SH3 domain as a major substrate for protein-tyrosine kinase(s) activated by FcεRI cross-linking. *J Immunol* **152,** 642.
34. Benhamou M., Ryba N.J.P., Kihara H., Nishikata H. & Siraganian R.P. (1993) Protein-tyrosine kinase p72(syk) in high-affinity IgE receptor signaling — identification as a component of pp72 and association with the receptor gamma-chain after receptor aggregation. *J Biol Chem* **268,** 23318.
35. Kinet J.P. (1992) The gamma-zeta dimers of Fc receptors as connectors to signal transduction. *Eur J Immunol* **4,** 43.
36. Welham M.J. & Schrader J.W. (1992) Steel factor-induced tyrosine phosphorylation in murine mast cells — common elements with IL-3-induced signal transduction pathways. *J Immunol* **149,** 2772.
37. Tsai M., Tam S.Y. & Galli S.J. (1993) Distinct patterns of early response gene-expression and proliferation in mouse mast cells stimulated by stem-cell factor, interleukin-3, or IgE and antigen. *Eur J Immunol* **23,** 867.
38. Tsai M., Chen R.H., Tam S.Y., Blenis J. & Galli S.J. (1993) Activation of map kinases, pp90(rsk) and pp70-s6 kinases in mouse mast cells by signaling through the c-*kit* receptor tyrosine kinase or FcεRI — rapamycin inhibits activation of pp70-s6 kinase and proliferation in mouse mast cells. *Eur J Immunol* **23,** 3286.
39. Lantz C.S. & Huff T.F. (1995) Murine kit+ lineage(−) bone-marrow progenitors express FcγRII but do not express FcεRI until mast cell granule formation. *J Immunol* **154,** 355.
40. Millard P.J., Gross D., Webb W.W. & Fewtrell C. (1988) Imaging asynchronous changes in intracellular Ca^{2+} in individual stimulated tumor mast cells. *Proc Natl Acad Sci USA* **85,** 1854.
41. Millard P.J., Ryan T.A., Webb W.W. & Fewtrell C. (1989) Immunoglobulin-E receptor cross-linking induces oscillations in intracellular free ionized calcium in individual tumor mast cells. *J Biol Chem* **264,** 19730.
42. MacGlashan D. & Guo C.P. (1991) Oscillations in free cytosolic calcium during IgE-mediated stimulation distinguish human basophils from human mast cells. *J Immunol* **147,** 2259.
43. MacGlashan D. & Botana L.M. (1993) Biphasic Ca^{2+} responses in human basophils — evidence that the initial transient elevation associated with the mobilization of intracellular calcium is an insufficient signal for degranulation. *J Immunol* **150,** 980.